

©2007

Gwangyong Choi

ALL RIGHTS RESERVED

CLIMATOLOGY AND VARIABILITY OF NORTHERN HEMISPHERE SEASONS

by

GWANGYONG CHOI

A Dissertation submitted to the  
Graduate School-New Brunswick

Rutgers, The State University of New Jersey

in partial fulfillment of the requirements

for the degree of

Doctor of Philosophy

Graduate Program in Geography

written under the direction of

Professor David A. Robinson

and approved by

---

---

---

---

New Brunswick, New Jersey

October, 2007

## **ABSTRACT OF THE DISSERTATION**

Climatology and Variability of Northern Hemisphere Seasons

By GWANGYONG CHOI

Dissertation Director:

Professor David A. Robinson

This dissertation is the first comprehensive study to define climatological seasons for temperature, snow, vegetation, and carbon dioxide on a hemispheric scale. The spatial propagation of climatological seasonal onsets and offsets as defined in this study differentiates the dynamical characteristics of empirical floating seasons from conventional static seasons such as the three month interval meteorological seasons. Spatial patterns of dynamical seasonal progression and its association with static and dynamic geographical factors are examined. Long-term trends and spatial patterns of identified changes in the dynamical floating onsets/offsets and durations are also discussed based on the past 40 years of observational data. The coherences and/or differences amongst various floating seasons and their potential linkages with large scale atmospheric circulation patterns are examined to develop seasonal prediction models. Finally, directions of future changes in seasonal onset/offset and duration are predicted

by comparing current (1981-2000) and future (2081-2100) seasons derived from climate models.

Various temporal and spatial patterns of floating climatological seasons - thermal, snow, vegetation, and carbon dioxide - show significant associations with dynamic factors such as oceanic and atmospheric circulation, as well as static factors such as latitude, elevation, topography, surface condition, and proximity to water bodies. Various floating seasonal onsets/offsets and durations show coherences at mid-latitudes but differences in the circumpolar regions or in lower mid-latitude regions. A consistent temporal trend exhibited in time series analyses of various floating seasons is the reduction of winter duration, primarily due to an earlier spring onset. In particular, the earlier spring onset observed in Europe, East Asia, and the southwestern United States shows significant associations with the hemispheric circulation pattern driven by a positive winter AO phase. Observed and modeled seasonal data suggest that the reduction of thermal winter duration is predicted to continue in the future over continents mainly due to an earlier winter offset. It is also predicted that, primarily due to an earlier summer onset, thermal summer duration will continue to increase along 30°N over oceans, suggesting potential changes in low latitude atmospheric circulation.

## ACKNOWLEDGEMENTS

This dissertation could not be accomplished without the financial support mainly through teaching assistantships from Department of Geography at Rutgers, The State University of New Jersey over the past four years. Partially, the American Association of Geographers (AAG) also supported this research through the 2006 AAG Dissertation Grant program. I would like to express my sincere gratitude to both organizations for their encouragement as well as financial aid. Neither would it be possible to proceed with this dissertation without valuable climatic data provided by various research centers. They include Rutgers University's Global Snow Lab., NASA Goddard Earth Sciences Data and Information Services Center, NOAA Earth System Research Laboratory Physical Sciences Division, NOAA National Weather Service Climate Prediction Center, NOAA Climate Monitoring and Diagnostic Laboratory Carbon Cycle Greenhouse Group, and the Geophysical Fluid Dynamics Laboratory. I thank all these organizations for their effort to collect and disseminate the exact data. In particular, I would like to thank Dr. Peter Smith at NASA and Dr. Kirk Thoning at NOAA for their discussion and advice regarding data conversion. I would also like to express my gratitude to Dr. Katarzyna Piotrowicz at Jagiellonian University in Poland, Dr. Annette Menzel at Technical University Munich in Germany, Dr. Tomoshige Inoue at University of Tokyo in Japan, Dr. Ewa Bednorz at Adam Mickiewicz University in Poland, Dr. Jörg Rapp at University of Frankfurt in Germany, Chinese Geographical Journal Society, and the Library at University of Wisconsin-Madison for the copies of journal articles that were not available at Rutgers University's library.

I would like to express my enormous appreciation for help and advice to my dissertation director, Professor David A. Robinson. Since the time I joined Rutgers Geography program in the fall 2002, Dr. Robinson has mentored me with continuous support and priceless encouragement. In spite of his tremendously busy daily schedule, Dr. Robinson gave priority to his graduate student, which allowed me to grow into a dedicated teacher and a passionate researcher. Moreover, three other committee members Dr. Daniel Leathers, Dr. Ming Xu, and Dr. Laura Schneider, offered their valuable advice and comments that enhanced the quality of my dissertation. I extend my great thanks to all of those dissertation committee members.

I am very much grateful to all other members of the faculty and staff in Department of Geography at Rutgers for their unlimited support in many ways. In particular, Betty Ann Abbatemarco, Elaine Gordon, Michael Siegel, Michelle Martel, and Theresa Kirby for their help with academic administrative matters, mapping, and computing. I also thank the staff of the Rutgers Climate Research Lab including Chad Shmukler, Thomas Estilow and all others for their computing and data handling service. In terms of teaching, I would especially like to thank Dr. Roger Balm for his mentoring, which taught me to be a better teacher. In addition, I cannot forget a group of my colleagues in the department because of their warmhearted friendship in every day life in the department. They are David Gwynn, Alexis Buckley, Nelun Dinali Fernando, and many others. With a special emphasis on my gratitude to Nelun Dinali Fernando who helped to enhance the quality of my dissertation through proof-reading and valuable discussion.

Other colleagues at other departments or institutions also contributed a lot to my dissertation. I would like to give special thanks to Dr. Seok-Woo Son at Columbia

University and Mr. Junsu Kim at University of Utah. I have known these two friends since my time at college. They helped me to understand the principles of atmospheric science through numerous discussions and technical support. I also extend sincere thanks to Patricia Alvarez, Nancy N. Moinde-Fockler, and Seunghun Lee for their encouragement and friendship. I am also thankful to Mr. William M. Winger and Ms. Irene Zhylin for their editing help.

Finally, I would like to thank my family for their enormous love and support. My father and mother sacrificed tremendously to educate me. I also express heartfelt gratitude for my two siblings; my sister, Dr. Gyeong-Hwa and my brother, Eun-Yong for their continuous love and support. To date, there have been many important mentors in my life, but my grandfather's influence has been most significant. From time to time, I reflect on my childhood memory. On a cold winter day, a small boy who was born into a farmer's family in the countryside was learning how to write Korean letters from his grandfather, who surprisingly did not have any formal education himself. Every day, my grandfather taught me to look to the gigantic oceans beyond a small creek. Now, the boy has grown up to be a scholar with a Ph.D. from an internationally renowned institution in the United States. My grandfather is smiling at me from the heaven. I still can feel his love and encouragement. Thus, I really would like to tribute this dissertation to my grandfather. I hear his voice, "This is only a commencement. Find many other ways to contribute to people in this world"

**TABLE OF CONTENTS**

ABSTRACT ..... ii

ACKNOWLEDGEMENTS ..... iv

LIST OF TABLES ..... xi

LIST OF FIGURES ..... xiv

I. INTRODUCTION ..... 1

    1.1. Overview ..... 1

    1.2. Objectives of the study ..... 8

II. THEORETICAL BACKGROUND ..... 10

    2.1. Methodologies of demarcating traditional four seasons ..... 10

        Fixed season versus floating season ..... 13

    2.2. Detection of changes in seasonal cycles ..... 38

        Changes in phenological cycles ..... 39

        Changes in hydrological cycles ..... 43

        Changes in geographical season cycles ..... 45

III. DATA AND METHODOLOGY ..... 48

    3.1. Data and pre-processing ..... 48

        NCEP-DOE reanalysis II 2-m daily mean temperature ..... 49

        NOAA AVHRR visible snow cover ..... 52

        NOAA AVHRR Normalized Difference Vegetation Index (NDVI) ..... 54

Atmospheric carbon dioxide (CO <sub>2</sub> ) concentration data .....	56
Large scale atmospheric circulation indices and pressure data .....	57
3.2. Methods to define floating seasons.....	59
Demarcating thermal seasons using surface air temperature data .....	59
Demarcating snow seasons using snow cover data.....	66
Demarcating vegetation seasons using NDVI data.....	69
IV. GEOGRAPHICAL THERMAL SEASONS IN THE NORTHERN HEMISPHERE	76
4.1. Introduction.....	76
4.2. Climatologies of thermal seasonal onset and duration in the Northern Hemisphere .....	77
Temporal and spatial ranges of hemispheric thermal seasons .....	77
Regional variations of thermal seasons.....	87
4.3. Thermal seasonal cycles in the Northern Hemisphere.....	92
4.4. Inter-annual variability and temporal trends of thermal seasonal onsets and durations.....	94
4.5. Summary and conclusion.....	102
V. SNOW SEASONS IN THE NORTHERN HEMISPHERE .....	104
5.1. Introduction.....	104
5.2. Progression of snow seasons in the Northern Hemisphere .....	106
Definition of the Full Snow Season (FSS) and the Core Snow Season (CSS)...	106
Patterns of the Full Snow Season (FSS).....	110

Patterns of the Core Snow Season (CSS) .....	115
Relationships between the FSS and the CSS .....	118
5.3. Inter-annual variations in snow season cycles .....	120
Trends of the Northern Hemisphere average FSS and CSS .....	120
Changes in spatial patterns of the FSS and the CSS .....	125
5.4. Summary and conclusion .....	131
VI. VEGETATION SEASON AND CARBON DIOXIDE SEASON IN THE NORTHERN HEMISPHERE .....	133
6.1. Introduction .....	133
6.2. Spatial patterns of the vegetation season .....	137
6.3. Zonal, longitudinal, and vertical gradients of the vegetation season .....	140
6.4. Defining the carbon dioxide season .....	145
6.5. Changes in the vegetation and carbon dioxide seasons .....	149
6.6. Summary and conclusion .....	156
VII. RELATIONSHIPS BETWEEN VARIOUS SEASONS AND SEASONAL PREDICTABILITY BASED ON ATMOSPHERIC CIRCULATION INDICES .....	158
7.1. Introduction .....	158
7.2. Comparison of thermal, snow, vegetation, and carbon dioxide seasons .....	160
Correlations among hemispheric average onsets and durations .....	160
Spatial lead-lag relationships in the seasonal progression .....	164

7.3. Linkages of thermal seasonal onsets and durations with atmospheric circulation indices .....	173
7.4. Development of seasonal prediction models .....	179
7.5. Summary and conclusion.....	186
VIII. EXPLORING DIRECTIONS OF FUTURE CHANGES IN NORTHERN HEMISPHERE THERMAL SEASONS .....	189
8.1. Introduction.....	189
8.2. Temporal changes in thermal seasonal durations at the end of the 21 <sup>st</sup> century .....	190
8.3. Spatial patterns of future changes in thermal summer and winter durations... ..	194
8.4. Climate model performance in simulating thermal seasons .....	197
8.5. Summary and conclusion.....	200
IX. CONCLUSION AND FUTURE DIRECTIONS.....	202
X. REFERENCES.....	208
CURRICULUM VITAE.....	226

## LIST OF TABLES

### Chapter 2

Table 2.1 Conventional fixed seasons .....	15
Table 2.2. Levick's (1949) air mass classification for NE Atlantic region, which is used to demarcate synoptic seasons for the British Isles (reproduced from Lamb 1950).....	19
Table 2.3. Synoptic seasons based on air masses (Lamb 1950, 1972) .....	21
Table 2.4. Phenological indicators defining four seasons in Germany (Schröder et al. 2006) .....	33
Table 2.5. Definitions of growing seasons (Menzel et al. 2003) .....	34

### Chapter 3

Table 3.1. Data sets used in this study .....	49
Table 3.2. Seasonal temperature indices used in previous studies to demarcate four thermal seasons in different parts of the world.....	62
Table 3.3. Geographical thermal seasons in the Northern Hemisphere employed in this study .....	66

### Chapter 4

Table 4.1. Types of thermal seasonal climate cycles in the Northern Hemisphere .....	93
--------------------------------------------------------------------------------------	----

### Chapter 5

Table 5.1. Pearson correlation coefficients (r) amongst the Northern Hemisphere averaged snow season onsets, ends, and durations during the 1972/1973-2004/2005 period .....	124
------------------------------------------------------------------------------------------------------------------------------------------------------------------------------	-----

## **Chapter 6**

Table 6.1. Stations, data, and onsets/offsets of carbon dioxide seasons analyzed in this study .....	148
------------------------------------------------------------------------------------------------------	-----

## **Chapter 7**

Table 7.1. Pearson correlation coefficients (r) between Northern Hemisphere average thermal seasons and snow seasons for the period 1979-2005.....	161
----------------------------------------------------------------------------------------------------------------------------------------------------	-----

Table 7.2. Pearson correlation coefficients (r) between Northern Hemisphere average thermal seasons and vegetation season (V) for the period 1982-2001, or between thermal seasons and carbon dioxide (CO <sub>2</sub> ) seasons at Barrow, Alaska (B) and at Mauna Loa, Hawaii (M) for the period 1979-2005.....	162
-------------------------------------------------------------------------------------------------------------------------------------------------------------------------------------------------------------------------------------------------------------------------------------------------------------------	-----

Table 7.3. Pearson correlation coefficients (r) between Northern Hemisphere average vegetation season (V) and carbon dioxide (CO <sub>2</sub> ) seasons at Barrow, Alaska (B) and at Mauna Loa, Hawaii (M) for the period 1979-2005 .....	163
-------------------------------------------------------------------------------------------------------------------------------------------------------------------------------------------------------------------------------------------	-----

Table 7.4. Pearson correlation coefficients (r) between Northern Hemisphere average snow seasons and vegetation season (V) for the period 1982-2001, or between snow seasons and carbon dioxide (CO <sub>2</sub> ) seasons at Barrow, Alaska (B) and at Mauna Loa, Hawaii (M) for the period 1979-2005.....	163
-------------------------------------------------------------------------------------------------------------------------------------------------------------------------------------------------------------------------------------------------------------------------------------------------------------	-----

Table 7.5. Statistically-significant Pearson correlation coefficients (r) between thermal seasons and atmospheric circulation indices in the Northern Hemisphere for the period 1979-2005 .....	175
Table 7.6. Statistically-significant Pearson correlation coefficients (r) between snow seasons and atmospheric circulation indices in the Northern Hemisphere for the period 1972-2005 .....	177
Table 7.7. Statistically-significant Pearson correlation coefficients (r) between vegetation (1982-2001) or carbon dioxide season (1974-2004) and atmospheric circulation indices in the Northern Hemisphere.....	178
Table 7.8. Canonical correlation coefficients between thermal seasons and atmospheric circulation indices .....	180

## **Chapter 8**

Table 8.1. Changes in Northern Hemisphere average thermal seasonal onsets and durations between the current (1981-2000) and future (2081-2100) periods.....	192
Table 8.2. Pearson correlation coefficients (r) amongst Northern Hemisphere average thermal seasonal onsets and durations; Modeled future (2081-2100) and current (1979-2005) based on GFDL 2.1.....	193

## LIST OF FIGURES

### Chapter 2

Figure 2.1. Taxonomy of ways of defining seasons .....	12
Figure 2.2. Examples of synoptic seasons based on intra-annual frequencies of air masses. Source: Alpert et al. (2004) and Argiriou et al. (2004).....	22
Figure 2.3. An example of how to demarcate thermal seasons using air temperature. Source: Choi et al. (2006).....	25
Figure 2.4. Spatial patterns of thermal seasonal onsets (or offsets): Winter ends (or spring onsets) in the United States based on monthly temperature data (a) and daily temperature data (b). Source: Jefferson (1938) and Visher (1943).....	27
Figure 2.5. Spatial patterns of human bioclimatological seasons. Source: Tuller (1975)	36
Figure 2.6. An example showing the relationships between human bioclimatological seasons and climatic factors such as latitude. Source: Tuller (1990) .....	37

### Chapter 3

Figure 3.1. The centroids of grid cells for the NCEP-DOE reanalysis daily 2-m temperature data in the Northern Hemisphere .....	50
Figure 3.2. A sample Excel file that shows the X- and Y-dimensions of the final data. X- dimension denotes the day during the year, and Y-dimension denotes the ID for each grid cell introduced in Figure 3.1 .....	51
Figure 3.3. The centroids of 89×89 grid cells for Northern Hemisphere snow cover derived from the NOAA AVHRR visible imagery.....	53

Figure 3.4. The centroids of 360×90 grid cells for the Northern Hemisphere NDVI derived from the NOAA AVHRR imagery .....	55
Figure 3.5. Intra-annual progression of raw daily mean temperature data and 11 day moving average data in Washington DC and Fairbanks, Alaska in 2005 .....	59
Figure 3.6 . Intra-annual progression of long-term (1979-2005) average daily temperature in the Northern Hemisphere.....	61
Figure 3.7. Variations of annual average values of diurnal temperature range over land masses and oceans with respect to latitude in the Northern Hemisphere derived from the NCEP/DOE reanalysis II 2-m daily maximum and minimum temperature data sets (1979-2005) .....	65
Figure 3.8. Weekly snow-covered areas (km <sup>2</sup> ) in the Northern Hemisphere (1972-2005) .....	68
Figure 3.9. Intra-annual variability of the ten-day composite of NDVI by vegetation types (1982-2000): (a) tundra, (b) taiga, (c) mixed forest at mid-latitudes, (d) mid-latitude deciduous forest, (e) mid-latitude desert, (f) subtropical desert, and (g) tropical savanna. ....	75

#### **Chapter 4**

Figure 4.1. Spatial patterns of thermal winter onset (top) and thermal spring onset (bottom) in the Northern Hemisphere, 1979-2005 .....	78
Figure 4.2. Spatial patterns of thermal winter duration in the Northern Hemisphere, 1979-2005.....	79

Figure 4.3. Latitudinal gradients of thermal winter onset (top) and thermal spring onset (bottom) dates over land masses (open symbols) and over oceans (filled symbols) in the Northern Hemisphere.....	81
Figure 4.4. Spatial patterns of thermal summer onset (top) and thermal fall onset (bottom) dates in the Northern Hemisphere, 1979-2005 .....	82
Figure 4.5. Spatial patterns of thermal summer duration in the Northern Hemisphere, 1979-2005 .....	83
Figure 4.6. Latitudinal gradients of thermal summer onset (top) and thermal fall onset (bottom) dates over land masses (open symbols) and over the oceans (filled symbols) in the Northern Hemisphere.....	85
Figure 4.7. Spatial patterns of thermal spring duration (top) and thermal fall duration (bottom) in the Northern Hemisphere, 1979-2005 .....	86
Figure 4.8. Impacts of high elevation on thermal spring onset in the Tibetan Plateau and the Himalayas (top) and thermal fall onset in central Ethiopia (bottom) .....	89
Figure 4.9. Impacts of the cold California Currents and the high elevation of the Rockies on thermal summer onset.....	90
Figure 4.10. Impacts of water bodies on delay of thermal winter onset over the Black Sea and the Caspian Sea .....	90
Figure 4.11. 1000hPa geopotential height (1979-2005) and sea surface temperature (1982-2005) during the meteorological winter (DJF) (top) and during the meteorological summer (JJA) (bottom).....	91
Figure 4.12. Spatial distribution of various thermal seasonal cycle types in the Northern Hemisphere. ....	94

Figure 4.13. Inter-annual variability (one standard deviation) of the Northern Hemisphere averages of thermal summer (top) and winter (bottom) durations, 1979-2005 .....	95
Figure 4.14. Fluctuations of the Northern Hemisphere average of the spatially-varying thermal summer and winter durations, 1979-2005 .....	96
Figure 4.15. Variations of significance level and Z-value in the Mann-Whitney U-test which show statistical significance of differences in Northern Hemisphere averages of thermal winter and summer durations before and since each dividing year.....	97
Figure 4.16. Changes in thermal winter duration between the pre-1988 years (1979-1987) and the post-1987 years (1988-2005) .....	98
Figure 4.17. Changes in thermal spring onset (top) and thermal winter onset (bottom) between the pre-1988 (1979-1987) and post-1987 (1988-2005) periods .....	99
Figure 4.18. Changes in thermal summer duration between the pre-1988 (1979-1987) and the post-1987 (1988-2005) periods .....	100
Figure 4.19. Changes in thermal summer onset (top) and thermal fall onset (bottom) between the pre-1988 (1979-1987) and post-1987 (1988-2005) periods .....	101

## **Chapter 5**

Figure 5.1. Percentage of years with snow cover for at least one week between 1967/1968 and 2004/2005 snow seasons.....	107
Figure 5.2. Temporal discontinuities of snow cover appearances detected along 50°N during the 2004/2005 cold period.....	108
Figure 5.3. Long-term (1967-2005) average onset (FAD; top) and offset dates (LDD; bottom) of the Full Snow Season (FSS) in the Northern Hemisphere. The boxes denote	

the regions where percentage of snow seasons is less than 100% between 1967/1968 and 2004/2005 as shown in Figure 5.1.....	111
Figure 5.4. Long-term (1967/68-2004/05) average duration (weeks) of the Full Snow Season (FSS) in the Northern Hemisphere.....	112
Figure 5.5. The earliest onset of the FSS (top) and its departure from normal (bottom) at different locations in the Northern Hemisphere during the 1967-2005 period. Extreme changes within high mountain areas should be considered too large. Details of this unrealistic result are provided in Chapter 3.....	113
Figure 5.6. The latest offset of the FSS (top) and its departure from normal (bottom) at different locations in the Northern Hemisphere during the 1967-2005 period. Extreme changes within high mountain areas should be considered too large. Details of this unrealistic result are provided in Chapter 3.....	114
Figure 5.7. Long-term (1967-2005) average onset (FCD) and offset (FFD) of the Core Snow Season (CSS) in the Northern Hemisphere.....	116
Figure 5.8. Long-term (1967-2005) average duration of the Core Snow Season (CSS) in the Northern Hemisphere.....	117
Figure 5.9 Snow seasonal cycle zones classified by relationships between Full Snow Season (FSS) and Core Snow Season (CSS) in the Northern Hemisphere, 1967-2005.	119
Figure 5.10. Inter-annual variations in the onsets of the Full Snow Season (FSS) and the Core Snow Season (CSS), 1972-2005 .....	121
Figure 5.11. Inter-annual variations in the offsets of the Full Snow Season (FSS) and the Core Snow Season (CSS), 1972-2005 .....	122

Figure 5.12. Inter-annual variations in the durations of the Full Snow Season (FSS) and the Core Snow Season (CSS), 1972-2005 .....	123
Figure 5.13. Changes (the post-1987 period minus the pre-1988 period) in the Full Snow Season (FSS) onset (top) and offset (bottom) in the Northern Hemisphere, 1972-2003. Extreme changes within high mountain areas should be considered too large. Details of this unrealistic result are provided in Chapter 3.....	126
Figure 5.14. Changes (the post-1987 period minus the pre-1988 period) in the Full Snow Season (FSS) duration in the Northern Hemisphere, 1972/1973-2003/2004. Extreme changes within high mountain areas should be considered too large. Details of this unrealistic result are provided in Chapter 3.....	127
Figure 5.15. Changes (the post-1987 period minus the pre-1988 period) in the Core Snow Season (CSS) onset (top) and offset (bottom) in the Northern Hemisphere, 1972-2003	129
Figure 5.16. Changes (the post-1987 period minus the pre-1988 period) in the Core Snow Season (CSS) duration in the Northern Hemisphere, 1972/1973-2003/2004.....	130

## **Chapter 6**

Figure 6.1. Duration of the vegetation season derived from NDVI data in the Northern Hemisphere, 1982-2001 .....	137
Figure 6.2. Onset (top) and offset (bottom) of the vegetation season derived from NDVI data in the Northern Hemisphere, 1982-2001 .....	138
Figure 6.3. Latitudinal gradients of vegetation season onset in eastern Asia at 110°E (top) and in central North America at 100°W (bottom), 1982-2001 .....	141

Figure 6.4. Latitudinal gradients of vegetation season offset in eastern Asia at 110°E (top) and in central North America at 100°W (bottom), 1982-2001 .....	142
Figure 6.5. Zonal gradients of vegetation season onset in Eurasia (top) and in North America (bottom) along 45°N, 1982-2001 .....	143
Figure 6.6. Zonal gradients of vegetation season offset in Eurasia (top) and in North America (bottom) along 45°N, 1982-2001 .....	144
Figure 6.7. Time series of daily carbon dioxide, double moving average, and its second derivative in Barrow, Alaska in 2003 .....	146
Figure 6.8. Trends of onset (a), offset (b), and duration (c) of spatially-averaged vegetation season in the Northern Hemisphere for the period 1982-2000 .....	150
Figure 6.9. Changes in the onset (top) and offset (bottom) of vegetation season: Last five year (1996-2000) average minus first five year (1982-1986) average .....	152
Figure 6.10. Inter-annual variations of the onset and offset of carbon dioxide season in Barrow, Alaska, 1974-2004 .....	154
Figure 6.11. Inter-annual variations of the onset and offset of carbon dioxide season in Mauna Loa, Hawaii, 1973-2003 .....	155

## **Chapter 7**

Figure 7.1. Comparison of long-term average thermal spring onset (1979-2005) with vegetation seasonal onset (1982-2001) in the Northern Hemisphere .....	165
Figure 7.2. Comparison of long-term average thermal winter onset (1979-2005) with vegetation seasonal offset (1982-2001) in the Northern Hemisphere .....	166

Figure 7.3. Differences between the vegetation season (1982-2001) and thermal growing season durations (1979-2005) in the Northern Hemisphere .....	167
Figure 7.4. Differences between vegetation season (1982-2001) and non-Full Snow Season (non-FSS) durations (1967-2005) in the Northern Hemisphere.....	169
Figure 7.5. Comparison of long-term average thermal winter onset (1979-2005) with snow season onset (1967-2005) in the Northern Hemisphere .....	170
Figure 7.6. Comparison of long-term average thermal spring onset (1979-2005) with Full Snow Season (FSS) offset (1967-2005) in the Northern Hemisphere.....	171
Figure 7.7. Differences between vegetation season (1982-2001) and non-Full Snow Season (non-FSS; 1967-2005) durations in the Northern Hemisphere .....	172
Figure 7.8. Differences in both thermal spring onset (red to blue) and 500hPa geopotential height (blue to purple) between AO positive and negative years. The differences denote the AO positive (1989, 1990, 1993, and 2002) minus and negative (1979, 1980, 1985, and 1987) years.....	174
Figure 7.9. Differences in both thermal summer onset (red to blue) and 500hPa geopotential height (blue to purple) between positive and negative years of (May PNA - previous December PNA). The differences denote the positive (1979, 1981, 1993, and 1997) minus and negative (1987, 1998, 2003, and 2004) years. ....	176
Figure 7.10. X EOF scree (a), X spatial loadings (b), Temporal scores (c), and Y spatial loadings (d) of the first mode of canonical correlations (=0.854) between Northern Hemisphere thermal spring onset (Y) and monthly Arctic Oscillation (AO) index from July in previous year to June in corresponding year (X) for the period 1979-2005 .....	181

Figure 7.11. X EOF screens (a), X spatial loadings (b), Temporal scores (c), and Y spatial loadings (d) of first mode of canonical correlations ( $=0.596$ ) between Northern Hemisphere thermal summer duration (Y) and monthly ENSO index from January to December (X) for the period 1979-2005 ..... 182

Figure 7.12. Simple liner regression models to predict thermal spring onset in Europe (top) and East Asia (bottom) based on the average AO index between January and March. .... 184

Figure 7.13. Simple linear regression models to predict thermal summer duration in central Pacific (top) and Atlantic (bottom) based on the average ENSO index between October and November. .... 185

## **Chapter 8**

Figure 8.1. Time series of current (1981-2000) and future (2081-2100) Northern Hemisphere average thermal seasonal durations derived from the GFDL 2.1 model output surface air temperature data: summer and winter (a), and spring and fall (b) ..... 191

Figure 8.2. Current (1979-2005) observed climatology (color lines) and predicted future changes (colored shades) in thermal summer duration across the Northern Hemisphere. Changes are calculated from the future average (2081-2100) minus current average (1981-2000) extracted from GFDL 2.1 model output temperature data..... 195

Figure 8.3. Current (1979-2005) observed climatology (color lines) and predicted future changes (colored shades) in thermal winter duration across the Northern Hemisphere. Changes are calculated from the future (2081-2100) average minus current (1981-2000) average extracted from GFDL 2.1 model output temperature data. .... 196

Figure 8.4. Differences (modeled-minus-observed) between modeled (GFDL 2.1) and observed (NCEP- DOE reanalysis II) thermal summer (top) and winter (bottom) durations, 1981-2000. Extreme caution is needed to interpret differences of more than 50 days over oceans. Refer to the text for details. .... 198

Figure 8.5. Comparison of modeled daily mean temperatures with observed daily mean temperature during the first half of the year (top) and during the second half of the year (bottom) for the current period (1981-2000) along 27°N over the Pacific and along 30°N over the Atlantic..... 199

## CHAPTER 1

### INTRODUCTION

#### 1.1. Overview

Climatic phenomena demonstrate periodicities on diurnal, seasonal, and inter-annual time scales and much longer glacial-interglacial time scales. Among these climate cycles, the recurrent phenomenon that influences the intra-annual life and energy cycles of human and environments is a season. A famous American writer, Kurt Vonnegut (1922 - 2007) claims there are six seasons: spring, summer, fall, locking season, winter, and unlocking season, each two months long (Klinkowitz 1998). Traditionally, four seasons such as astronomical seasons and meteorological seasons are recognized as standard seasonal cycles. In the seasonal cycles, seasonal onset and termination dates which demarcate each season play crucial roles as temporal benchmarks in determining the various intra-annual biological cycles of living animals and plants. The flowering and greening of foliage (Fitzjarrald et al. 2001; Schwartz & Chen 2002; Schröder et al. 2006), as well as matching, breeding, migrating, and hibernating of animals (Crick & Sparks 1999; Inouye et al. 2000; Roy & Sparks 2000) exemplify the synchronous phenological cycles of fauna and flora with the seasonal progression. Seasonal transition and duration also significantly influence chemical or physical cycles of air, water, and energy. Intra-annually-recurrent biological cycles are indirectly associated with intra-annual hydrological and geochemical cycles such as carbon dioxide concentration, carbon sink, and sequestration determined by annual life cycles of vegetation (Randerson et al. 1997).

Not only intra-annual cycles in the environment but also human socio-economic activities during a year are shaped by the seasonal rhythm. The role of seasons in human history is also seen in the fact that seasons originate from the Latin term “satiōns”, which means “sowing times” according to the Oxford Dictionary of English (Soanes & Stevenson 2005). The examples of human life cycles affected by seasonal onsets and durations include the selection of clothes, the utilization of energy for heating or cooling, and agricultural activities. The accurate recognition of seasonal cycles, which vary according to locations and years, may help maximize human productivity as well as minimize damage attributable to delayed or advanced seasonal onsets and offsets.

Traditionally, it has been regarded that seasonal onsets recur on the same dates year-to-year, anywhere in the world, based on calendar months or astronomical benchmarks (Trenberth 1983; Pielke et al. 1987). Four three-month fixed seasons, which are demarcated based on calendar months, are called meteorological seasons. The onset and offset of meteorological seasons are fixed on the same dates regardless of geographical locations and years: spring (March, April, and May), summer (June, July, and August), fall (September, October, and November), and winter (December, January, and February). Other conventional fixed seasons that are demarcated based on two solstices and equinoxes are called astronomical seasons.

These conventional fixed seasons conflict with spatially and temporally varying seasons. Inter-annual fluctuations of seasonal onsets and durations cause climatic stress on humans and nature particularly during the seasonal transition periods that could be characterized by unusual early warming or late cooling. An advanced warming in the early spring leads to an earlier flowering of fruit trees, and a subsequent cold event

damages the flowers. Consequently, the advance of flowering leads to the reduction of fruit production during the harvest period (Tao et al. 2006). The earlier melting of snow and ice across the Arctic sea is also recognized as a climate stress to the Arctic ecosystem. For instance, polar bears leave their habitats earlier due to the advanced thawing of ice which subsequently causes low fertility or an extinction of polar bear species (Stirling et al. 1999; Wiig 2005; Pennisi 2007). In addition, the earlier snow melt in alpine regions due to advanced spring onsets results in severe droughts (McCabe & Clark 2005) and more frequent and intensive wildland fires (Westerling et al. 2006).

Nevertheless, to date, most scientists use meteorological seasons in their studies; seasons whose periods are inter-annually fixed and identical everywhere in the same hemisphere based on calendar months. This is because the utilization of the meteorological seasons facilitates the calculation of seasonal averages or departures of different variables in climate research. For instance, the IPCC reports (2001, 2007) state, “global warming is more obvious in winter”. The winter in this statement indicates a fixed three-calendar-month period between December and February according to the meteorological seasons. These seasons, as well as astronomical seasons, represent the hemispheric average seasonal cycles without spatial or inter-annual variations. In other words, the IPCC generalizes about the seasonal evidence of global warming, ignoring the intra-annual variation of the seasonal cycle itself. It overlooks the possibility that climate change can be detected in the seasonality changes themselves such as earlier spring (Hartley & Robinson 2000; Ho et al. 2006; Schwartz et al. 2006; Westerling et al. 2006) and shrinking winter (Abdulla 1999; Piotrowicz 2002-3; Choi et al. 2006). As a result, the dependency on the fixed-three-month demarcation of meteorological seasons causes a

disassociation with the actual empirical seasons perceived by humans and nature. For example, people in Alaska experience a much longer cold weather period during a year than those who reside in Washington DC. These examples clearly suggest that employing fixed seasons such as meteorological ones are fundamentally flawed.

Fixed seasons such as meteorological seasons and astronomical seasons are commonly used as international standard seasons because temporally and spatially varying floating seasons on the global scale have not yet been defined. The empirical seasonal progression varies in different cycles at different locations and in different years. Here it is contended that the calendar-month fixed meteorological seasons be replaced with spatially and temporally floating seasons that are defined based on climate variables; namely climatological seasons. Climatological seasonal onset and offset are not static but dynamic. The offset and onset may propagate spatially as a function of various geographical factors. However, traditional fixed seasons have ignored the dynamical characteristics of the empirical seasons appearing in intra-annual landscape changes.

Various geophysical data such as vegetation and snow have been observed by satellite on a hemispheric scale during the recent several decades. These large scale data support the argument of this dissertation that empirical seasonal onset/offset and duration are not fixed spatially and temporally as opposed to conventionally-used meteorological data which support the calculation of three-month fixed interval averages. The animation of global scale data such as remotely sensed satellite imagery exemplifies the dynamical characteristics of floating climatological seasons. Intra-annual northward or southward fluctuations of snow cover (Robinson 1993; Ueda et al. 2003) and vegetation cover (Bogaert et al. 2002; Schwartz et al. 2002) are indicators of the dynamical propagation of

floating seasons. These white or green waves demonstrate that seasonal onsets or offsets vary according to latitude and longitude. On a hemispheric scale, understanding of spatial and temporal fluctuations of seasonal onsets and durations are critically important because the propagation of seasons is a phenomenon of energy redistribution through interactions of atmospheric, hydrological, biophysical, and geophysical variables.

On a local scale, these wavy patterns of hydrological or phenological variables appear in the form of landscape changes when one season transitions into another. For instance, with the arrival of spring, green vegetation covers fields previously occupied by snow due to increases of solar radiation and air temperature. Humans and animals identify the spring onset based in part on these surface landscape changes. Therefore, air temperature, snow cover, and vegetation condition are regarded as crucial indicators that can be used in defining floating climatological seasons.

The disassociation between the conventionally-accepted fixed meteorological seasons and empirical climatological seasons motivated this dissertation project. To date, there has been little effort made to define floating climatological seasons. Recently, the few studies that attempt to define the floating seasons include ones using different climatic (Cheng & Kalkstein 1997; Alpert et al. 2004; Cannon 2005; Choi et al. 2006) or phenological variables (Menzel et al. 2001) at regional scales. These studies can be classified into two categories based on data and methodology adopted. The first category defines floating seasons using climatic or phenological data observed at individual weather stations in a particular country or region (Woś 1981; Inoue & Matsumoto 2003; Ye et al. 2003; Ho et al. 2006). There are many definitions of a floating season at regional scales, but there is no standard definition that can be applied to the demarcation of a

floating season on a global scale. The second category defines regionally-averaged floating seasons based on the intra-annual frequency of air masses or circulation patterns that appear on synoptic or hemispheric scale weather charts (Kalnicky 1987; Cheng & Kalkstein 1997; Alpert et al. 2004). The latter approach provides inter-annual variability in seasonal cycles, but the regionally-averaged definition cannot illustrate spatial variations of the floating seasons within the study regions. For example, Kalnicky (1987) demarcates four distinct seasons in the mid-latitudes of the Northern Hemisphere based on hemispheric average circulation types. This provides a new set of seasonal onsets for each year, but variations of seasonal onset and offset within the mid-latitudes are ignored. In other words, according to this approach, seasonal onset dates in Alaska should coincide with those in Washington, DC every year.

Thus, there remains a necessity to define floating climatological seasons on a global scale, allowing for spatial and temporal fluctuations. From this an understanding of spatial and temporal patterns of seasonal progression is attainable thus helping to optimize inter-annual human life cycles related to seasonal progressions and lessen climatic stresses. For instance, appropriate selection of clothes and the amount of energy to maintain human thermal environment, or plans of agricultural and outdoor activities need accurate information about the seasonal cycles, particularly, temporal fluctuations such as advances or delays of seasonal onset and offset.

Furthermore, analysis of long term trends of floating seasons can provide important information. Recently, a number of studies document that the seasonal phenological events such as the growing seasons (Menzel & Fabian 1999; Tucker et al. 2001; Menzel et al. 2003), the timing of bird or butterfly migration (Crick et al. 1997; Roy & Sparks

2000; Roy & Asher 2003), or flowering (Schwartz & Reiter 2000; Menzel et al. 2001; Fitter & Fitter 2002) have changed in recent decades. These changes in fauna and flora phenological cycles indicate the possibility that there might also be changes in climatological seasonal onset and duration (Choi et al. 2006). To date, however, the spatial coverage of these studies is fragmented and based on one particular country or region. In addition, the indicator used to define phenological seasons varies from one study to another (Walther et al. 2002; Parmesan & Yohe 2003; Root et al. 2003). Thus, it is not easy to understand hemispheric or global scale trends of seasonal cycle change from these heterogeneous and regionally-fragmented analyses. The phenological data used in a few large scale studies (Schwartz et al. 2006) is also heterogeneously distributed and has an urban bias because many observation sites have experienced growing urbanization. Moreover, the studies based on phenological data focus mainly on spring onset phenomena (Sparks & Menzel 2002). Thus, changes in other seasons have not yet been examined.

These circumstances motivated this dissertation to undertake the first attempt to define hemispheric scale floating climatological seasons based on multiple observational data sets. This dissertation examines the long-term climatology or variability of the northern hemispheric seasonal onsets and durations. Potential linkages between seasonal onsets and durations and atmospheric circulation are also investigated. Those lead or lagged linkages are used to develop statistical models that can predict seasonal onset and durations. Potential changes in Northern Hemisphere seasonal onsets and durations by the end of the 21<sup>st</sup> century based on climate model output data are also examined.

## 1.2. Objectives of the study

This is the first study to define and examine various floating climatological seasons on a hemispheric scale based on multiple climatic variables available for a relatively long term period. Surface air temperature over continents and oceans (1979-2005; 2081-2100), continental snow extent (1967-2005), vegetation seasonality (1982-2001), as well as atmospheric carbon dioxide concentrations at Barrow, Alaska (1974-2004) and at the Mauna Loa Observatory in Hawaii (1973-2003) are used to derive the various floating climatological seasons. The following are key study objectives:

- 1) Define onset and offset dates, and durations of various floating seasons for variables including temperature, snow, vegetation, and carbon dioxide on a hemispheric and regional scales.
- 2) Examine spatial extents of onsets, offsets, and durations, and characterize them by latitude, altitude, and land or oceans.
- 3) Define inter-annual variability and long-term trends in seasonal onset/offset and duration and examine changes in spatial patterns.
- 4) Compare and contrast inter-annual fluctuations amongst hemispheric and regional onset/offset and durations of thermal, snow, vegetation, and carbon dioxide seasons.
- 5) Explore lead and lag relationships between thermal seasonal onset, offset, duration, and atmospheric circulation indices such as the Arctic Oscillation, El Niño Southern Oscillation, North Atlantic Oscillation, and the Pacific North American pattern.
- 6) Develop simple statistical seasonal prediction models to forecast thermal onsets,

offsets, and durations where regional associations with atmospheric circulation indices are recognized.

7) Investigate model projections of temporal and spatial changes in thermal seasonal onsets, offsets, and durations at the end of the 21<sup>st</sup> century.

## CHAPTER 2

### THEORETICAL BACKGROUND

#### 2.1. Methodologies of demarcating traditional four seasons

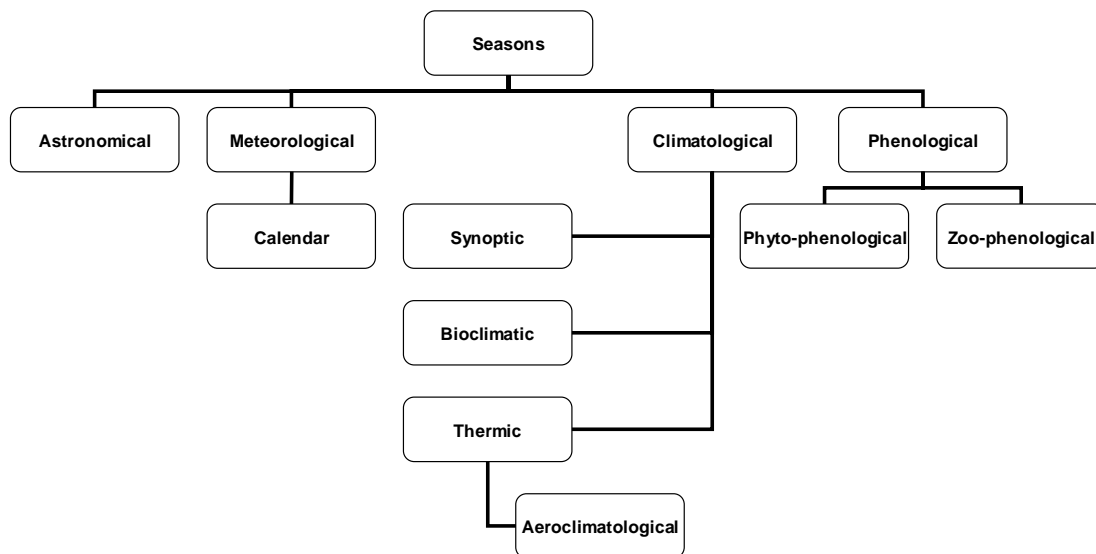
To date, various seasonal conceptualizations have been used to understand recurrent perennial cycles of meteorological and ecological phenomena. For instance, dry or drought seasons versus wet or rainy seasons (Visher 1947, 1949, 1950a; Blochman 1925), and winter or summer monsoon seasons (Mooley 1971) have defined seasonal hydrological events. Phenological seasons such as growing seasons (Abbe 1899), flowering seasons (Robertson 1922), and pollen seasons (Emberlin et al. 2002, 2007) have also been widely used. Similarly, socio-economic seasons such as agricultural seasons, tourism seasons, and sports seasons have been commonly used. The employment of these various seasonal concepts help humans follow optimal life cycles in harmony with climatological seasonal cycles.

Within those seasonal concepts, four distinct seasons - spring, summer, fall, and winter - are globally accepted as representative of standard intra-annual climate cycles. Intra-annual cyclic patterns of thermal conditions in the surface atmosphere are closely associated with transitions of the standard four seasons. Thus, surface air temperature has been most commonly used in defining standard four seasons (White 1925; Jefferson 1938; Trenberth 1983). The accumulations of long term temperature data at numerous weather stations around make it possible to investigate decadal fluctuations of thermal seasons on a hemispheric or global scale. The homogenous spatial consistency with respect to latitude and altitude and periodic occurrences at similar times of a year

facilitate the use of temperature in defining seasons. In contrast, rainfall shows heterogeneous spatial patterns across regions as well as considerable inter-annual variations at individual weather stations. The complexity of rainfall limits its utilization to just the demarcation of regional scale rainy seasons. Hydrological seasons derived from rainfall include wet/dry spells in the tropics (Tyson 1981; Krishnamurti et al. 1995) and monsoon seasons in Asia (Maejima 1967; Lee 1979). Snow cover extends or retreats in association with intra-annual variations of air temperature on a hemispheric scale (Groisman et al. 1994; Frei & Robinson 1999). Thus, snow cover may be applicable to examining the spatial progression of the cold winter season.

To date, only a few studies (Barry & Perry 1973; Piotrowicz 2000; Weston 2006) have documented a systematic overview of how to define seasons using various climatic indicators. Barry and Perry (1973) summarized studies from different parts of the world regarding the classification of synoptic seasons based on displacement types of air masses. Recently, Piotrowicz (2000) provided a more systematic diagram that summarizes comprehensive methods to demarcate seasons (Figure 2.1(a)). Seasons were categorized as astronomical, meteorological, climatological, or phenological. He subsequently introduced climatological seasons as synoptic, thermic, and bioclimatic seasons, and phenological seasons as phyto-phenological and zoo-phenological seasons. Weston (2006) reviewed some previous studies regarding how to define seasons, but the methodologies of defining seasons were not systematically classified in his thesis. In this study, an improved version of Piotrowicz's (2000) taxonomy of ways of defining seasons is provided (Figure 2.1(b)). Compared with the earlier classification, the taxonomy suggested in this dissertation provides a more hierarchical overview and

(a) Piotrowicz (2000)



(b) This study

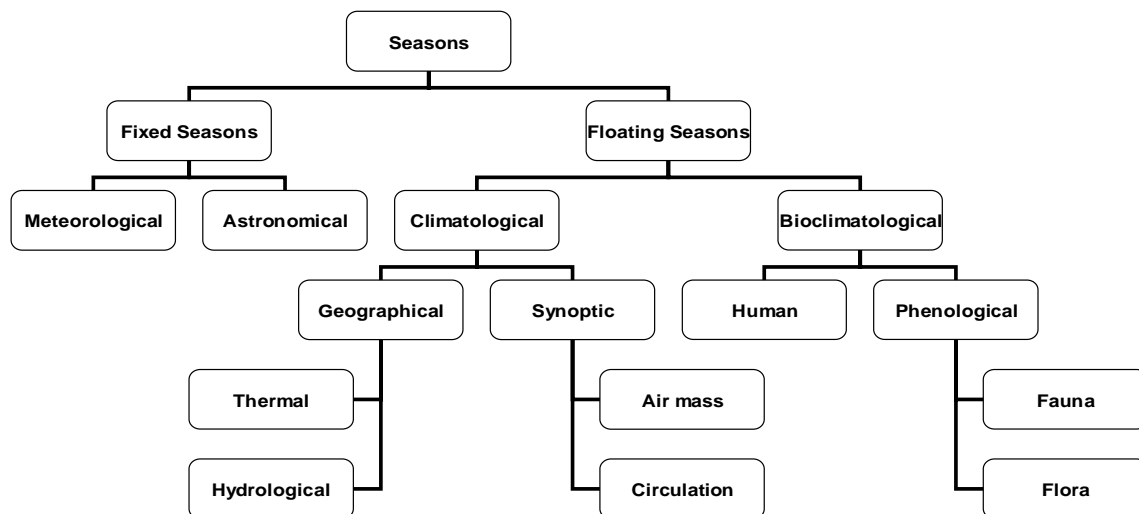


Figure 2.1. Taxonomy of ways of defining seasons

detailed subtypes of seasons with respect to variables and methods. Criteria used in the new taxonomy include fixed and floating seasons. Meteorological and astronomical seasons ignore the spatial and temporal variations of seasons, while climatological and bioclimatological seasons take them into account. Subcategories and their hierarchies are

also introduced. Piotrowicz (2000) classified bioclimatic seasons as a climatological season. In the new taxonomy, a bioclimatological season is classified as an independent category. This is because bioclimatology or biometeorology is recognized as an independent field of study under a climatology umbrella encompassing human bioclimatology as well as phenology of flora and fauna (Tromp 1980). Geographical seasons are classified into thermal and hydrological seasons; and synoptic seasons are classified into air mass-based and air circulation-based seasons in the new taxonomy. Phenological seasons are classified into flora and fauna seasons. An overview of the characteristics of each subtype of seasons follows.

### **Fixed season versus floating season**

In a fixed seasonal cycle, seasonal arrival dates and lengths are unchangeable within the same hemisphere regardless of the year. Traditional fixed seasons such as meteorological seasons and astronomical seasons assume that a year is divided into fixed four quarters based on either calendar months or astronomical benchmarks (Trenberth 1983; Pielke et al. 1987). In contrast, floating seasonal onset and offset vary depending on region and year. They have been derived from climatic variables such as temperature (Jefferson 1938) and atmospheric pressure (Lamb 1950), or from bioclimatic variables such as flowering dates (Schröder et al. 2006) observed at individual locations. Descriptions of the subtypes of fixed and flexible seasons are provided below.

## 1) Types of fixed seasons

Meteorological and astronomical seasons are examples of traditional fixed seasons. Both commonly premise that seasonal onset and termination dates are fixed on the same date according to solar calendar or spatial position of the Earth. For instance, regardless of the geographical location and the year, meteorological summer begins on June 1<sup>st</sup> everywhere in the Northern Hemisphere, and astronomical summer begins on June 22<sup>nd</sup> or 23<sup>rd</sup> every year. Both meteorological and astronomical seasons represent hemispheric average seasonal cycles. They have advantages that the hemispheric average fixed seasonal cycles allow people to share one standard set of four seasons without confusion all over the world. On the other hand, utilization of fixed seasons requires people to understand different states of each season in different regions of the globe because these fixed seasons ignore the spatial and temporal variations of seasonal cycles within the same hemisphere. For instance, air temperature in meteorological summer (June, July, and August) is below 15°C in Barrow, Alaska, which is spring-like weather at mid-latitudes. On the contrary, air temperature in meteorological winter exceeds 20°C in Hawaii, which is summer-like weather at mid-latitudes. The disassociation between thermal seasonal conditions and fixed seasons is demonstrated in surface landscape changes. According to meteorological seasons, March belongs to the spring season even when Alaska is covered with snow. On the contrary, Florida is covered with green vegetation in February.

### a. Meteorological seasons

Meteorological seasons are most popularly used in climate studies such as the IPCC reports (2001, 2007). In defining meteorological seasons, the period of a year is

demarcated into four periods, each of which lasts three calendar months: spring (March, April, and May), summer (June, July, and August), fall (September, October, and November), and winter (December, January, and February) (Table 2.1). This division is used in the Northern Hemisphere, but seasonal cycles of three months are the opposite in the Southern Hemisphere: spring (September, October, and November), summer (December, January, and February), fall (March, April, and May), and winter (June, July and August). The coldest (January) and hottest (July) months in the Northern Hemisphere are pivotal months of boreal meteorological winter and summer, respectively. Trenberth (1983) pointed out a lagged difference between meteorological seasons or astronomical as well as thermal climatological seasons derived from monthly temperature. He concluded that meteorological seasons reasonably agree with empirical thermal conditions in the Northern Hemisphere but not in the Southern Hemisphere.

Three month intervals based on the solar calendar facilitates the calculation of seasonal averages of monthly-based climate variables. However, these three month

Table 2.1 Conventional fixed seasons

Seasons	Meteorological (Calendar) Seasons	Astronomical seasons (solstices and equinoxes)	
		Western* (Starting points in solar calendar)	East Asia** (Middle points in solar calendar)
Spring	March April May	Vernal equinox (March 22) to summer solstice (June 21)	February 4 – May 5
Summer	June July August	Summer solstice (June 22) to Autumnal equinox (September 21)	May 6 – August 6
Fall	September October November	Autumnal equinox (September 22) to winter solstice (December 21)	August 7 –November 6
Winter	December January February	Winter solstice (December 22) to Vernal equinox (March 21)	November 7 –February 3

\*North America and most European countries

\*\* China, Korea, Japan, and Vietnam

intervals are identically applied to seasons within the same hemisphere. Furthermore, the monthly-based consideration of thermal distribution ignores the shorter daily-scale flexibility. For instance, seasons can advance or delay by several days year-to-year. In addition, meteorological seasons do not allow the spatial and temporal variations of seasonal onset and duration within the same hemisphere. Thus, they deviate from climatological seasons which vary in different regions and in different years. Meteorological seasons provide an arithmetic facilitation for scientists studying the atmosphere to calculate seasonal values using three month averages.

b. Astronomical seasons

Astronomical seasons are another type of fixed season. Solar astronomical seasons divide the period of a year on a hemispheric basis according to two solstices and equinoxes that are associated with the declination of the earth. The position of the Earth around the sun determines intra-annual variations of solar energy arriving at the top of Earth's atmosphere within a given region. The two solstices and equinoxes are determined by a relative geometrical position of the tilted Earth to the Sun along the elliptic as the Earth revolves around the Sun once a year. The rotating axis of the Earth connecting the North and the South poles is tilted by  $23.5^\circ$  relative to the elliptic. Thus, on the boreal summer solstice (June 22<sup>nd</sup>), the most intense solar energy with highest solar angle sits at  $23.5^\circ\text{N}$  and the Northern Hemisphere receives the largest amount of solar energy. In contrast, on the boreal winter solstice (December 22<sup>nd</sup>) the regions with the highest solar angle are reversed toward  $23.5^\circ\text{S}$  and the least amount of energy arrives in the Northern Hemisphere. Spring (March 22<sup>nd</sup>) and autumnal (September 22<sup>nd</sup>) equinoxes are transitional benchmarking dates during the year between the two extremes.

On equinoxes, both hemispheres receive equal amount of solar energy at the top of the Earth's atmosphere.

Trenberth (1983) found that there is approximately a one-month lag between astronomically-determined solar energy and the actual hottest or coldest times of the year on the surface. These lag effects are caused by various internal climate constituents and feedbacks in the climate system such as the heat capacity of land masses and oceans. He claimed astronomical seasons to be reasonably acceptable in oceanic regions of the Southern Hemisphere but not in the land masses of the Northern Hemisphere.

Long ago in Eastern civilizations the lunar calendar was used for agricultural cycles. Later, it was realized that the lunar calendar does not match very well with thermal seasons. Thus, approximately 3000 years ago, the Chu dynasty in China developed 24 seasonal cycles based on a solar calendar appropriate to the climate in northern China (Chang 1934). 24 seasonal cycles, which are divided at every 15° in the elliptic including two solstices and equinoxes, have used for solstices and equinoxes to demarcate four distinct seasons. Mid-points of the benchmarking solstice and equinox are used as onset dates of astronomical seasons in East Asia while they are used as arrival dates of seasons in Europe and North America. Astronomical spring begins on November 7 and ends on February 3 in East Asia (Table 2.1). However, this convention in East Asia is also flawed because astronomical seasonal onset has lags with empirical thermal dates. Astronomical seasons ignore internal feedbacks in the climate systems that create various spatial and temporal variations in seasonal cycles.

## 2) Types of floating seasons

Floating seasons such as climatological and bioclimatological overcome the shortcomings of fixed seasons. Nevertheless, relatively few efforts to devise the appropriate ways of demarcating empirical floating seasons on a continental scale have been made (White 1925; Jefferson 1938; Hartshorne 1938). In addition, it is not until recently that changes in the timing of four floating seasons, such as early spring arrivals and winter shortening (Choi et al. 2006; Schwartz et al. 2006) were examined.

### a. Climatological seasons

Floating seasons are classified into climatological and bioclimatological seasons according to the indicator used to define them (Figure 2.1(b)). Climatological floating seasons are defined based on intra-annual periodicity of climate variables in the seasonal variations of the Earth's surface landscapes. The climatological seasons are classified into synoptic and geographical seasons according to the types of climate variables used in their demarcation. Synoptic seasons are the regionally-averaged climatological seasons derived from synoptic weather charts. Synoptic scale growth and decay of seasonally-common air masses (Lamb 1950; Moon & Um 1980; Pielke et al. 1987; Cheng & Kalkstein 1997; Alpert et al. 2004) or atmospheric circulation (Bryson & Lahey 1958; Kalnicky 1987) are analyzed to determine the commencement and duration of surface climatological seasons. In contrast, geographical seasons are the spatially-varying climatological seasons derived from surface climate variables observed at individual weather stations. Critical thresholds of surface climate variables such as air temperature (Jaagus & Ahas 2000; Ivanova et al. 2004; Choi et al. 2006) and sunshine (Inoue & Matsumoto 2003; Weston 2006) are used to demarcate seasons. These thresholds are

associated with geographical landscape changes that appear during seasonal transition periods.

### (1) Synoptic seasons

Synoptic seasons are divided by the appearance of a typical air mass or an atmospheric circulation pattern related to seasonal changes in weather. Synoptic scale high and low pressure systems in daily weather charts are the indicators popularly used in demarcating synoptic seasons. Levick's (1949) air mass classification for the northeastern Atlantic region (Table 2.2) and Dzerdzeevskii's (1968) atmospheric circulation classification for the Northern Hemisphere extratropical latitudes are those examples.

Synoptic seasons are classified into two groups: air mass-based seasons and atmospheric circulation-based seasons. The appearance or the displacement of air masses

Table 2.2. Levick's (1949) air mass classification for NE Atlantic region, which is used to demarcate synoptic seasons for the British Isles (reproduced from Lamb 1950)

Synoptic types	Displacement of air pressure (Based on the British Isle)	Weather conditions
AC (Anticyclonic)	Anticyclones center over or extending over	Usually warm in summer; cold or very cold in winter; mist and fog frequent in autumn
C (Cyclonic)	Depression stagnating over or frequently passing across	Usually mild in autumn and early winter; cool or cold in spring; summer and in later winter, both gales and thunderstorms occur
W (Westerly)	South-High and north-Low	Changeable weather, wind shifting rapidly; cool summer, mild in winter with frequent gales
NW (North-westerly)	Azores High displaced northeastward or north over the Atlantic west	Changeable weather, sometimes fresh or gale force wind; cooler than the westerly type and milder than the northerly type
N (Northerly)	High pressure to Greenland; Low over the Baltic, Scandinavia, and the North Sea	Cold, disturbed weather at all seasons. Snow and sleet common in winter
E (Easterly)	Anticyclones over or extending over Scandinavia or Iceland; Depression circulating over the western North Atlantic	Cold in autumn, winter and spring; warm in summer, sometimes thundery; Very dry weather in western districts
S (Southerly)	High pressure covering central and northern Europe; Atlantic depression blocked west	Warm and thundery in spring and summer, mild in autumn; in winter mild or cold

such as Arctic highs and sub-Polar lows demarks synoptic seasons. The advent of synoptic charts during the World War II period made it possible to define synoptic seasons based on air masses. Arrival dates and durations of synoptic seasons can vary inter-annually. The basic frame of synoptic seasons consists of spring, summer, fall, and winter. More than four seasons such as early spring and late spring in addition to spring are defined (Takahasi 1942; Lamb 1950; Yoshino & Kai 1977).

In East Asia, Takahasi (1942) was the first to define natural seasons for Japan based on intra-annual variation of pressure patterns and precipitation. According to Takahasi's (1942) classification, natural seasons in Japan are classified into early winter, winter, early spring, spring, early summer, plum rain period, summer, early fall, frost rain period, and fall. Similarly, Yoshino and Kai (1977) classified fourteen natural seasons for Japan based on intra-annual prevailing times of typical pressure patterns: early spring, spring, late spring, early summer, Bai-u, summer, late summer, early autumn, autumnal rainy period, autumn, late autumn, early winter, winter, and late winter. In Korea, Moon and Um (1980) defined eleven synoptic seasons based on the frequency of typical displacement of air masses around the Korean Peninsula: early spring, spring and late spring, early summer, summer and late summer, early autumn, autumn and late autumn, and early winter and winter. Moon and Um (1980) compared divisions of seasonal cycles for China, Korea, and Japan carried out in previous papers (Xu & Gao 1962; Kawamura 1973; Yoshino & Kai 1977) with their demarcation of synoptic seasons.

In Europe, Lamb's (1950) "types and spells of weather around the year in the British Isles" is a pioneering work that introduced more systematic divisions of synoptic seasons based on air masses. He examined intra-annual frequency curves for seven typical

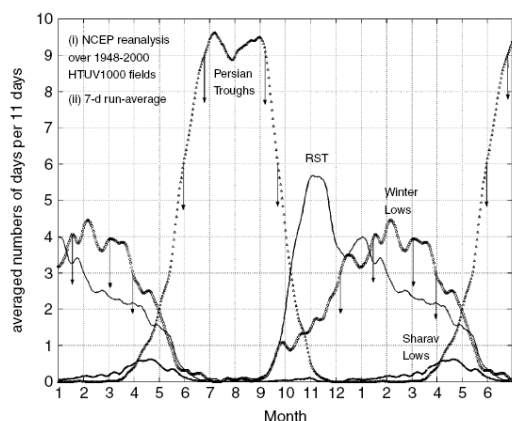
weather types summarized by Levick (1949), and demarcated five dominant synoptic seasons for Britain based on the singularities of a prevailing pressure displacement: high summer, autumn, for-winter, late-winter or early spring, and spring or early summer (Table 2.3). Similarly, Bradka (1966) classified synoptic seasons based on winter-pattern types and frequency of low/high pressure systems at mid-latitudes and high latitudes of the Northern Hemisphere.

Alpert et al. (2004) also defined four synoptic seasons for the Eastern Mediterranean based on the annual frequency distribution of seasonally-prevailing synoptic systems (Figure 2.2(a)). Argiriou et al. (2004) used a fuzzy clustering method with isobaric thickness between 500hPa and 1000hPa over the northeastern Mediterranean to identify

Table 2.3. Synoptic seasons based on air masses (Lamb 1950, 1972)

Seasons	Calendar Period	Synoptic conditions
Spring (Sometimes early summer)	April to early June	Period of consistently low frequency of long spells, apart from the year's maximum of northerly
High summer	Late June to about the end of August	Clear maxima and minima of all types of air masses in the occurrence of long spells
Autumn	Early September to mid November (Indian summer and early autumn until mid October)	Clear maxima and minima in the occurrence of long spells. The final minimum is less sharp than the initial
Early winter (Or fore- winter)	Late November to mid January	Moderate maxima and minima of all types of air masses in the total frequency curve, composed of unlike trends in the individual frequency curves in each types of air mass within these dates
Late winter (Sometimes early spring)	Late January to late March	Unlike trends in the total frequency curves and distinctly changed trends from the period before January 20. A modest maximum in the total frequency curve

(a) Alpert et al. (2004)



(b) Argiriou et al. (2004)

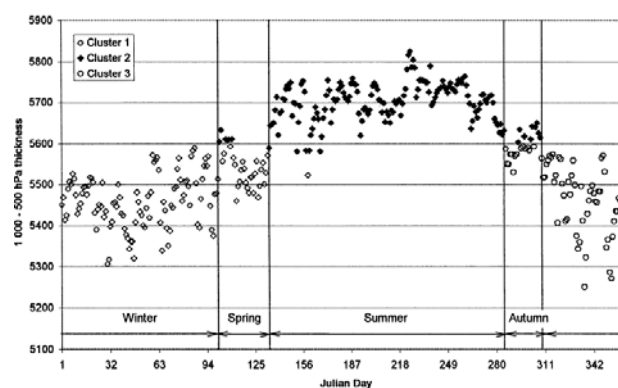


Figure 2.2. Examples of synoptic seasons based on intra-annual frequencies of air masses. Source: Alpert et al. (2004) and Argiriou et al. (2004)

four synoptic seasons (Figure 2.2(b)). Both studies exemplify how to demarcate synoptic seasons based on breaking points or clustering patterns that appear in the time series of intra-annual frequency of synoptic parameters.

In North America, a definition of synoptic seasons based on air masses classification was carried out by Pielke et al. (1987). According to the intra-annual distribution of five synoptic categories, they defined the arrival and termination of four synoptic seasons for nine different regions along the Gulf and the eastern coasts of the United States, and showed that synoptic season cycles vary regionally. Similarly, Cheng and Kalkstein (1997) defined four synoptic seasons over the east coast of the United States based on the frequency of seasonal air masses at fourteen sites. They also showed variations in seasonal lengths according to latitude. They observed winter length in northern locales to be 2.5 months longer than further south.

Four synoptic seasons based on large scale atmosphere circulation types have been rarely defined. Bryson and Lahey (1958) defined four synoptic seasons based on various

circulation indices in the Northern Hemisphere. Circulation indices used in their study include storminess, anti-cyclonicity, baroclinicity, standard deviation of circulation indices, etc. Similarly, Kalnicky (1987) defined four synoptic seasons for extratropical regions of the Northern Hemisphere based on daily frequencies of Dzerdzevskii's circulation types for the years 1899-1969. He pointed out that hemispheric scale season cycles such as starting date and lengths vary inter-annually. A factor analysis of daily frequency of thirteen circulation types, including zonal and disrupted zonal, was performed to cluster circulation patterns that typically occur in the transitional period between seasons.

To date, it has been regarded that arrival dates and durations of synoptic seasons are identical within the study areas without spatial variations. Pielke et al. (1987) and Cheng and Kalkstein (1997) illustrates by comparing multi-regional scale synoptic seasons that the onset and duration of synoptic seasons also vary spatially according to latitude. However, the selection of dominant synoptic conditions to define each season is likely to rely on a researcher's subjectivity. The synoptic conditions vary from one region to another so that a classification scheme appropriate to one region cannot be used in different regions. In addition, relative displacements of air masses are commonly used to define synoptic seasons. Thus, it is difficult to make an objective assessment as to what extent air masses should be close to a particular study area in order to define the arrival of seasons. The arrival and end of synoptic seasons vary year-to-year but there is no spatial variation. Thus, synoptic seasons are regarded as semi-floating seasons because air mass or circulation patterns explain the mechanism of synoptic seasonal transitions.

## (2) Geographical seasons

Geographical seasons are spatially and temporally-floating climatological seasons derived from surface climate variables such as temperature and precipitation. As floating seasons, geographical seasons using surface air temperature as well as phenology have been most popularly demarcated. Surface climate variables such as air temperature, snow, and stream discharge show spatial variations. Compared with fixed seasons such as astronomical and synoptic seasons, geographical seasons can display spatial variations of empirical seasonal onset and offset with respect to latitude, altitude, and proximity to oceans. Atmospheric feedbacks are so complex that the amount of the incoming solar energy at the top of the atmosphere is not identical to that of the Earth's surface (Trenberth 1983). The amount of incoming solar radiation absorbed by the surface varies with respect to the types of surface features. For instance, snow covered regions may reflect more than 85% of incoming solar radiation so that temperature in snow covered areas is at least 5°C lower than that over the snow-free areas at similar latitudes (Dewey 1977; Baker et al. 1992; Leathers & Robinson 1993). As a result, the albedo effect modifies climate in snow covered areas compared with the snow-free areas.

According to the types of variables used to divide seasons, geographical seasons are largely classified into thermal (Jaagus & Ahas 2000; Ivanova et al. 2004; Choi et al. 2006) and hydrological (Cayan et al. 2001; Cannon 2005). Thermal seasons consist of the traditional four seasons, while snow or rainy period is defined as hydrological seasons. There are also several studies (Piotrowicz 1996, 2002-3) focusing on only winter duration or spring onset based on temperature. Intra-annual progression of daily temperature and stream flow forms bell-shape curves so that the inflection points showing abrupt change

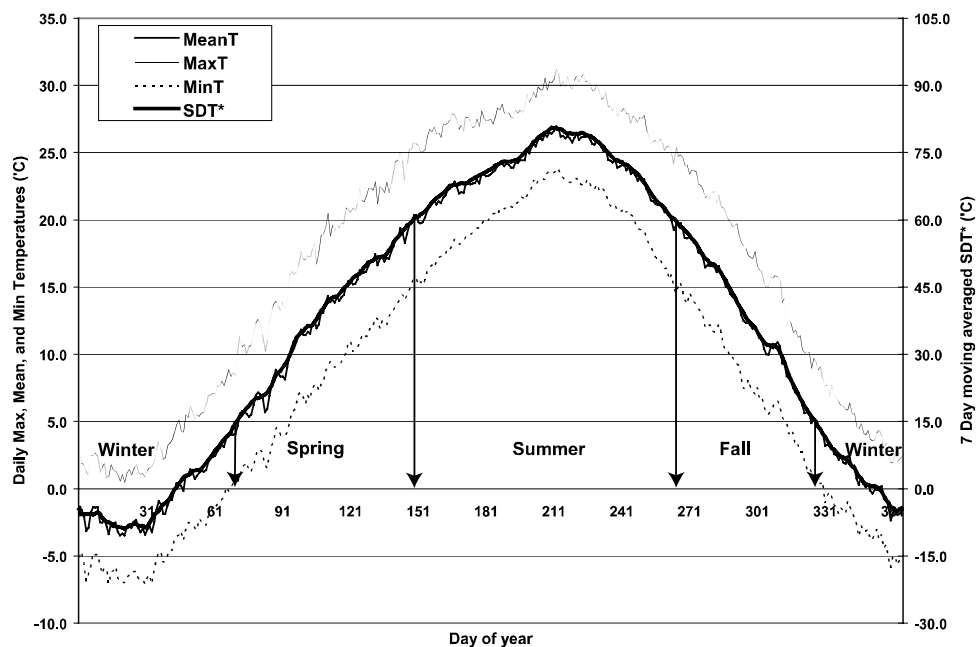


Figure 2.3. An example of how to demarcate thermal seasons using air temperature.  
Source: Choi et al. (2006)

or the events above particular thresholds are regarded as signals of seasonal transition (Figure 2.3). In particular, the Warmth Index ( $T_{\text{mean}} \geq 5^{\circ}\text{C}$ ) and the last freezing ( $0^{\circ}\text{C}$ ) minimum temperature affecting phenology of flora are popularly utilized to differentiate cold seasons against warm seasons (Kira 1949).

In East Asia, Chang (1934) first defined Chinese thermal seasons using air temperature. He used  $10^{\circ}\text{C}$  and  $22^{\circ}\text{C}$  thresholds to separate winter and summer periods. Recently, Ye et al. (2003) used varying thresholds for Beijing, Hailar, and Lanzhou to define four seasons: two of them being  $-1 - -20^{\circ}\text{C}$  for winter and  $13 - 19^{\circ}\text{C}$  for summer. In Japan, Kawamura (1973) divided thermal seasons based on  $10^{\circ}\text{C}$  and  $20^{\circ}\text{C}$  thresholds. Inoue and Matsumoto (2003) used intra-annual sunshine records to define seasons. In Korea, Lee (1979) was the pioneer who defined four thermal seasons using daily

maximum, average, and minimum temperatures observed at three representative sites. He delimited winter when the daily minimum temperature was below 0°C and the daily mean temperature was below 5°C. He demarcated summer when daily average and maximum temperatures exceeded 20°C and 25°C, respectively. Oh et al. (2004) used irregular thresholds to define onset and termination of winter and summer with daily mean temperature observed at one site in Korea. Recently, Choi et al (2006) in Korea improved Lee's (1979) method by introducing the Summed Daily Temperature (SDT), which is the seven day moving average of the combined values of daily maximum, mean, and minimum temperatures. Choi et al. (2006) used 15°C of SDT and 60°C of SDT to identify winter and summer, respectively (Figure 2.3).

In Europe, different thresholds of air temperature have been used to demarcate thermal geographical seasons. According to Piotrowicz (2000), the tradition of defining Polish thermal seasons based on daily air temperature dates back to the early 19<sup>th</sup> century (Jastrzebowski 1829). Similar approaches were used by Polish climatologists such as Romer (1904, 1949), Merecki (1914), Wiszniewski (1960), Hess (1965), and Makowiec (1983). Generally, in those studies 0°C and 15 °C daily mean temperatures were used to define Polish winter and summer, respectively. In recent decades, long-term variations of winter duration in Poland were examined using the same thresholds (Piotrowicz 1996; Kwaśniewska & Pereyma 2004; Kozuchowski & Degirmendzić 2005). Similar thresholds were used for Estonia (Jaagus & Ahas 2000; Ahas et al. 2005; Jaagus 2006), Lithuania (Pempaite 1997; Markevičienė 1996), Scandinavia (Tveito et al. 2000), and eastern Europe (Jaagus et al. 2003). In these studies, the threshold for demarcating winter is 0°C

(a) Jefferson (1938)

(b) Visher (1943)

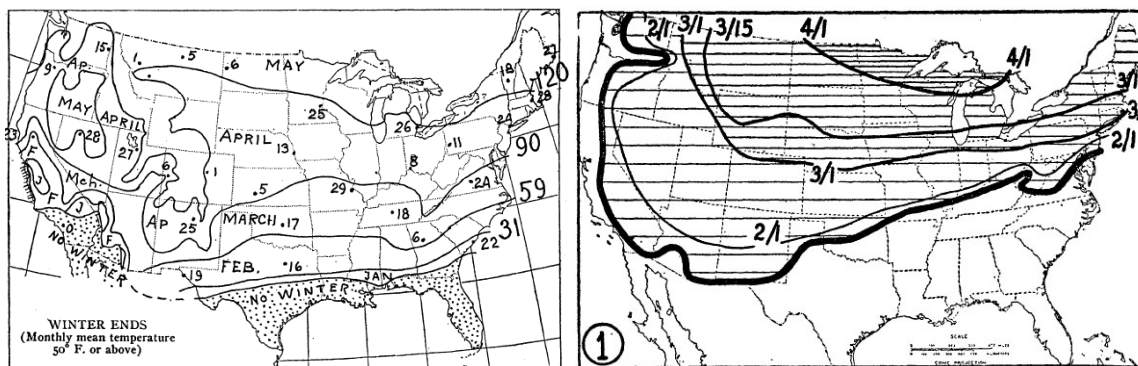


Figure 2.4. Spatial patterns of thermal seasonal onsets (or offsets): Winter ends (or spring onsets) in the United States based on monthly temperature data (a) and daily temperature data (b). Source: Jefferson (1938) and Visher (1943)

of temperature, but there are many thresholds used to delimit summer, including 2.5°C, 10°C, 13°C, and 15°C. In particular, Jaagus et al. (2003) demonstrated spatial variations of seasonal onset dates and duration in the eastern European plain. They found that latitude and proximity to oceans determine the direction of the progression of the early spring. In Germany, Rapp and Schönwiese (1994) used three varying thresholds dividing the range between annual maximum and minimum temperatures into three equal temperature intervals to demarcate four thermal seasons.

In North America, Jefferson (1938) reported four thermal seasons based on monthly air temperature. He used 10°C and 20°C of monthly mean temperature to separate winter and summer for the United States, respectively. He demonstrated that three types of seasonal cycles such as spring-fall-winter, spring-summer-fall- winter, spring-summer-fall cycles- can be identified in landmasses of the United States. Visher (1943, 1944, 1950b) demarcated thermal seasons based on 0°C and 20°C of daily mean temperature.

Compared with Jefferson's (1938) classification, regions without either winter or summer are larger in Visher's classification.

Visher's (1943) method is more sophisticated than Jefferson's (1938) because he used daily data (Figure 2.4). On the other hand, he selected the last day when daily mean temperature below 0 °C continued, but inter-daily fluctuations in intra-annual progression of daily temperatures were not considered. As a result, the no-winter line (a thick black line in Figure 2.4(b)) retreats northward from the southern Gulf Coast. The size of the no-winter region is larger than most would expect. On the contrary, in Visher's (1943) summer duration map (not given) the no-summer limit line advances more southward in the northern contiguous United States.

In North America, the demarcation of seasons based on statistical analyses such as principle components (Green et al. 1993) and clustering (Alsop 1989; Cannon 2005; Weston 2006) has been carried out since the late 1980s. Green et al. (1993) pre-grouped monthly precipitation, temperature, and wind vector data for the meso-scale areas of Southern California to delimit four seasons. He concluded that principal component analyses of monthly climatic variables can be used to define preliminary floating seasons on a meso-scale. Similarly, Alsop (1989) conducted clustering analyses of weekly maximum and minimum temperature and used the dissimilarities among clustered groups to define seasons in Western Oregon. Canon (2005) also applied radially-constrained clustering to separate hydroclimatological seasons based on stream flow data from British Columbia. Canon (2005) claimed that the proposed clustering methods can be universally applied to other cases. Weston (2006) used the K-mean cluster analysis, which is a statistical method of clustering objects based on attributions on K partitions, in order to

demarcate seasons using weekly temperature, albedo, and solar radiation observed at several sites in the Canadian Arctic. Commonly, however, criteria derived for these statistical analyses do not indicate the transitional dates of empirical seasons. Thus, dependency solely on values derived from these statistical analyses may not be an ideal methodology of demarcating empirical seasons.

To date, only a few studies have delimited spatially-varying geographical seasons on greater than regional scales (Hartshorne 1938; Woś 1981; Trenberth 1983; Ivanova et al. 2004). Hartshorne (1938) is the only extensive study demonstrating the distribution of the seasonal cycle based on regional monthly temperature at the global scale. He used 0°C, 10°C, and 20°C thresholds to divide cold, cool, warm, and hot seasons which are equivalent to winter, early spring (or autumn), early (or late) summer, and summer, respectively. He concluded that there are ten seasonal cycles in the world: hot continuously, warm continuously, cool continuously, cold continuously, warm-hot, cool-warm, cold-cool, cool-warm-hot-warm, cold-cool-warm-cool, and cold-cool-warm-hot-warm-cool. The seasonal cycles found in Hartshorne (1938) are comparable to each of Koeppen's climatic types. Woś (1981) demarcated four seasons for seven sites in Asia and one site in tropical South America. Woś (1981) clustered pentads during a year into four seasonal periods according to the types of weather (frosty, transitional, and warm), various temperature thresholds, and occurrence/non-existence of precipitation. Recently, Ivanova et al. (2004) used surface temperature statistics to demarcate geographical seasons in the Arctic Basin.

Compared with these studies introduced above that allow seasonal lengths to float, Trenberth (1983) divided a year into four equal length (91.25 days) periods based on the

sine curves of monthly air temperature. He defined crests and troughs as mid-summers and mid-winters in time series of air temperatures. He showed regionally-varying lag effects between astronomical seasons and temperature-defined seasons. Spatial patterns of the seasonal onset and termination were determined to be affected more by the proximity to ocean than by any other factor. However, empirical thermal seasons are expected to vary more depending on latitude. Trenberth (1983) contributed to the revelation of the difference between thermal seasons and astronomical or meteorological seasons on the global scale. He concluded that over the Northern Hemisphere continents, meteorological seasons are similar to thermal seasons, while over the Southern Hemisphere ocean regions, astronomical seasons are similar to thermal seasons.

Hydro-geographical seasons have been defined in only a few studies based on intra-annual hydrological cycles in eastern or western mountainous areas of the United States. Czikowsky and Fitzjarrald (2004) derived hydrological spring onset dates from stream flow data by using a Precipitation minus Runoff (P-R) method, a recession time constant method, and a diurnal stream flow amplitude method. P-R methods determine spring dates as occurring when the P-R curve returns to the annual dominant point after snowmelts. Recession time which indicates the lapse time for stream flow after a precipitation event to reach an e-folding time of the peak value is a key variable in the recession time constant method. A diurnal stream flow amplitude method and amplitudes of daily and seasonal progression of the diurnal stream flow signal and watershed effects were used. These three methods are commonly based on diurnal or seasonal changes of hydrological balance in streams due to a start of spring phenology in forests. Regonda et al. (2005) used peak timing in stream flow as a mid-point of a broad spring season

without the definition of spring onset or termination dates. Hydro-geographical seasons have many limitations compared with thermal geographical seasons. They include complicated local hydrological processes and limited geographical coverage where hydrological data are available. For instance, study areas for both Czikowsky et al. (2004) and Regonda et al. (2005) are confined to mountainous areas where snow/melt is the primary source of spring stream flow.

Snow cover and snow/rain ratio are better indicators than stream flow records to demarcate the onset/offset of winter season because they are available across large areas. Stankūnavičius and Rimkus (1998) showed the possibility of using the first snowy and last snowy dates in determining the winter season. This is clearly linked with atmospheric thermal conditions locally and regionally.

In conclusion, geographical thermal seasons based on temperature are more reliable compared with geographical hydrological seasons based on rainfall and stream flow. Geographical thermal seasons can depict the spatially and temporally-varying floating four seasons in more detail across large areas. However, care must be taken when using temperature observatories. Changes in a station's environment due to urbanization can lead to overestimates of seasonal arrival dates or lengths when applied regionally or over even broader areas. As the surface in regions surrounding the weather station are changed to asphalt and concrete, local urban heat island effects distort temperature. Thus, individual weather station data should be scrutinized before using those station data in order to select appropriate sites. Choi et al. (2006) found that urbanization effects in large cities can shorten winter by as much as 20 days compared with the surrounding regions in

South Korea. They also asserted that summer can be 20 days longer than in urbanized areas.

b. Bioclimatological seasons

Bioclimatological seasons refer to floating seasons according to indicators related to phenology of flora and fauna as well as human physiology or societal activities. Seasonal phenology of flora includes leaf sprouting, budding, and flowering in spring, and fruiting and foliage in autumn. Seasonal phenology of fauna encompasses appearances of insects and animals, mating, laying eggs, or giving birth in spring as well as migration. Bioclimatological seasons defined by phenological indicators are called phenological seasons. Seasonal progression affects human bioclimatological cycles. Human bioclimatic responses with respect to seasonal fluctuations include limitation of human socioeconomic activities due to earlier or later cold or heat stress. These phenological or human responses are closely associated with the progression of climatological seasons. Similar to climatological seasons, both phenological and human seasons allow arrivals and lengths of seasons to vary spatially and inter-annually.

(1) Phenological seasons

Most studies regarding demarcation of seasons based on phenological data concentrate on spring events such as leaf unfolding and flowering (Menzel 2000; Menzel et al. 2001; Schwartz et al. 2006, Schröder et al. 2006). These spring phenological phenomena are clearly associated with seasonal arrival or climax. However, most studies utilize phenological data without specified definition of spring to examine relationships with other climate variables (Thórhallsdóttir 1998; Sparks et al. 2000; Ahas et al. 2000; Scheifinger et al. 2003; Ho et al. 2006; Zheng et al. 2006). In addition, most of

Table 2.4. Phenological indicators defining four seasons in Germany (Schröder et al. 2006)

Phenological seasons	Species	Phenological phases
Spring	<i>Forsythia suspensa</i>	Blooming
Summer	<i>Sambucus nigra</i>	Blooming
Fall	<i>Sambucus nigra</i>	Fruiting
Winter	<i>Triticum aestivum</i>	Sprouting

these studies use different species in different regions (Schwartz & Reiter 2000; Defila & Clot 2001; Menzel et al. 2001; Schwartz & Chen 2002; Zhao & Schwartz 2003), thus making it difficult to discern global scale patterns of seasonal transitions. Schwartz et al. (2006) were the first to aggregate phenology data of lilac (*Syringa*) species for mid-latitude regions of the Northern Hemisphere to examine the spring onset trends for the period 1961-2000. However, their data are not homogeneously distributed and are unavailable at most high altitudes and latitudes.

Several studies utilize records of harvesting time, leaf coloring, and leaf fall to delimit autumn season. Menzel and Fabian (1999) used leaf unfolding as a spring onset signal and leaf fall as an autumnal termination signal to examine growing seasons in Europe. Furthermore, Schröder et al. (2006) defined four distinct phenological seasons by using phenology of representative species of plants (Table 2.4). Blooming of *forsythia suspensa* and sprouting of *triticum aestivum* were used to define spring onset and winter onset, respectively. Blooming and fruiting of *sambucus nigra* were used as indicators to define the summer period.

Table 2.5. Definitions of growing seasons (Menzel et al. 2003)

Frost day	Daily minimum Temperature	Growing season	Daily mean Temperature
Last frost date in the first half of the year	Last record of $T_{min} < 0^{\circ} C$	Winter end (or spring onset)	First record of $T_{mean} \geq 5^{\circ} C$ continuously
First frost date in the second half of the year	First record of $T_{min} < 0^{\circ} C$	Fall end (or winter onset)	Last record of $T_{mean} \geq 5^{\circ} C$ continuously
Frost free period	Duration without $T_{min} < 0^{\circ} C$ continuously	Growing season	Duration of $T_{mean} \geq 5^{\circ} C$ continuously

In addition, many thresholds of temperature that are related to the seasonal phenology of plants define phenological growing seasons. Temperature thresholds for a frost day or warmth Index (Kira 1949) as summarized in Table 2.5 are used to define phenological growing season (Menzel et al. 2003). Growing seasons are also defined based on the Normalized Difference Vegetation Index (NDVI) satellite data (Myneni et al. 1997; Tucker et al. 2001) as well as CO<sub>2</sub> concentration data (Keeling et al. 1996; Randerson et al. 1997)

In particular, Keeling et al. (1996) suggested that the beginning of the intra-annual downward CO<sub>2</sub> concentration due to onset of springtime photosynthesis of plants can be used as a spring onset signal. Myneni et al. (1997) also addressed offsetting relationships between increasing NDVI and downward CO<sub>2</sub> concentration, implying the possibility that the timing of increasing NDVI can be used as a spring onset signal. Tucker et al. (2001) were the first to derive the floating start and termination dates of the growing season from NDVI temporal profiles using a log nonlinear technique that was developed by Badhwar et al. (1982) and Badhwar (1984). However, they only calculated five zonal averages by continents for three different periods so that coarse resolution information is documented without explanation of spatial patterns of the changes. Schwartz et al. (2002)

also calculated the start of spring season based on White et al.'s (2002) method of how to derive the start of the growing season from the NDVI. In their methodology, dates of the start of spring season are defined based on the phenology of one particular species such as lilac, but it can be debated whether one particular species can be used as a standard indicator in defining climatological seasonal onset. It is because the species as a spring onset indicator can vary depending on countries. The middle point of spring NDVI may not be the onset point of spring but the centroid of spring period. Shabanov et al. (2002) also tried to reveal the changes in spring and autumnal dates by using the intra-annual variations of NDVI. They subjectively selected fixed values of Day 120 as the spring time onset of greenness and Day 270 as the decline of autumnal greenness.

Fitzjarrand et al. (2001) used daily mean temperature and humidity to identify a sudden decreasing point of the Bowen Ratio, which is defined as the ratio of latent heat to sensible heat. The sudden decrease of the ratio is associated with an increase of evapotranspiration due to springtime leaf burst, which indicates spring onset timing. Based on the Bowen Ratio method, Fitzjarrand et al. (2001) illustrated spatially-floating spring onset patterns for the eastern United States.

Overall, studies on the demarcation of four distinct phenological seasons are rare (Schröder et al. 2006) due to the difficulties in determining proper indicators for separating all seasons (Sparks & Menzel 2002). In addition, urbanization effects (Neil & Wu 2006), irregular coarse distribution of phenological monitoring networks (Beaubien & Hall-Beyer 2003), different species and ages, and micro-environments are challenges to collect reliable phenological data. Nevertheless, traditional phenological data in spring

are invaluable, as at some sites, phenological records date back to the early 1400s (Sparks & Carey 1995; Menzel 2005; Menzel & Dose 2005).

## (2) Human bioclimatological seasons

Human bioclimatological seasons refer to floating seasonal cycles that represent intra-annual physiological or socio-economic activity cycles in response to seasonal thermal or hydrological climate cycles. Trading, tourism, agriculture, gardening, energy consumption, pollution, clothing, human disease, and mortality exemplify those activities that are affected by human bioclimatic seasons.

To date, few efforts have been made to define human bioclimatological seasons. Tuller (1975) defined bioclimatological seasons in Canada based on a climatic index developed by Terjung (1968), which is a combined index of the comfort index derived from temperature and humidity for hot weather and a wind-chill index derived from

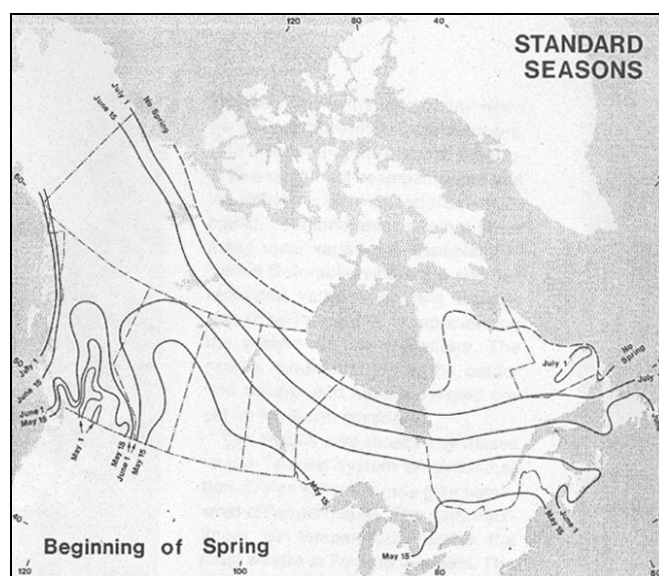


Figure 2.5. Spatial patterns of human bioclimatological seasons. Source: Tuller (1975)

temperature, wind speed, and available solar energy for cold weather. Tuller (1990) showed spatial advances or delays of seasonal arrivals attributable to latitude and proximity to an ocean. A spring onset date map, as shown in Figure 2.5, illustrates a mid-May start in Southern Canada which is a consistent continuation of Jefferson's (1938) spring onset for the United States (Figure 2.4(a)).

Tuller (1977) defined human comfort standard seasons for New Zealand using the same indices, showing that the arrival and the length of human comfort seasons vary

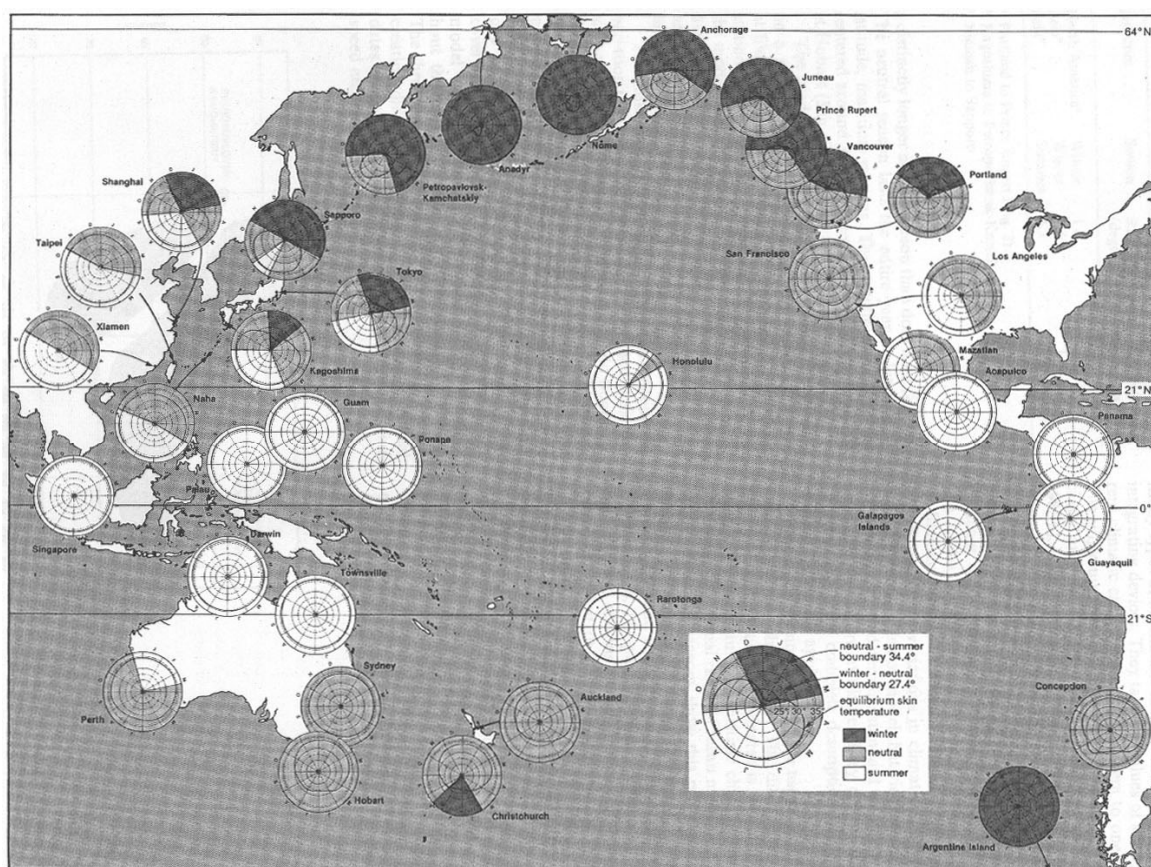


Figure 2.6. An example showing the relationships between human bioclimatological seasons and climatic factors such as latitude. Source: Tuller (1990)

regionally. Tuller (1990) examined annual cycles of human thermal standard seasons for the Pacific Basin using equilibrium skin temperature (Figure 2.6). According to this analysis, only summer exists at stations below 21°N, while only winter exists at stations above 64°N. He also revealed that the northward propagation of winter and summer occurs fast over interior regions of Asia due to high continentality.

Definitions of various human bioclimatological seasons are needed to maximize the efficiency of various human socio-economic activities, and reduce climatic stress. Potential indicators that can be used in defining such seasons include biothermal indices such as Effective Temperature (ET), Wind-chill index (WCI), Apparent Temperature (AT), Heat Index (HI), and Potential Equivalent Temperature (PET).

## **2.2. Detection of changes in seasonal cycles**

To date, studies about fluctuations of seasonal climate have been carried out largely focusing on the following three topics: 1) trends in averaged climatic values during fixed meteorological seasons, 2) trends in intensity or frequency of extreme events during fixed meteorological seasons, and 3) changes in floating timing of seasonal phenomena.

Studies about changes in the timing of seasonal climatic phenomena are mainly summarized into three topics in terms of utilized variables: 1) changes in seasonal phenological cycles of flora and fauna, 2) changes in seasonal hydrological cycles, and 3) changes in seasonal cycles derived from climate variables. Studies on changes in seasonal phenological cycles concentrate on spring phenomena such as leaf unfolding and flowering (Sparks & Menzel 2002) as well as the appearance and egg-laying of animals and insects (Brown et al. 1999; Crick & Sparks 1999; Roy & Sparks 2000; Roy & Asher

2003). Remote sensing data such as NDVI (Myneni et al. 1997; Tucker et al. 2001) and CO<sub>2</sub> concentration (Keeling et al. 1996) are also used in detecting changes in phenological seasons (Schwartz et al. 2006). Only a few studies examined changes in autumnal phenology (Menzel & Fabian 1999, 2001; Menzel 2000).

Studies focusing on changes in seasonal hydrological cycles examine snow appearance/disappearance (Stone et al. 2002), ice or snow melting (Belchansky et al. 2004), spring peak stream flow (Hodgkins & Dudley 2006) and drought (Westerling et al. 2006). In contrast, studies on changes in seasonal cycles derived from climate variables such as air masses, atmospheric circulation, and surface atmospheric temperature examine the start and the length of synoptic seasons and geographical thermal seasons. Such studies uncovered the following regarding changes in seasonal cycles from the 20<sup>th</sup> century to the present.

### **Changes in phenological cycles**

From a global standpoint, Peñuelas & Filella (2001), Walther et al. (2002), Parmesan and Yohe (2003), Root et al. (2003), and Parmesan (2006) reviewed many case studies focusing on the topic of changes in phenological cycles in recent decades. Peñuelas and Filella (2001) also reviewed previous papers showing the influence of ecological consequences of global warming on plants and animals. Walther et al. (2002) concluded that the phenological spring onset has advanced and migrated northward and toward highlands in the recent several decades. Similarly, Parmesan and Yohe (2003) concluded that aggregated impacts of climate change manifest a shift in a poleward systematic range at the rate of 6.1km per decade spatially and in an earlier shift of spring events at the rate

of 2.3 days per decades temporally. Root et al. (2003) concluded that a 0.6 °C warming during the 20<sup>th</sup> century influenced the advancement of spring events by 5.1 days per decade in 80% of species showing changes in the Northern Hemisphere according to their mega-data analyses. Parmesan (2006) concluded that habitat ranges for polar or alpine ecological species as well as coral reefs and amphibians in the tropics have contracted due to climate change, which may be driving them toward extinction. These reviews commonly addressed the point that both the advanced onset of spring and slightly delayed termination of fall caused the lengthening of growing seasons (Menzel & Fabian 1999). Numerous regional scale studies about phenological cycles addressed the changes in spring onset or growing seasons.

#### 1) Europe

In the case of spring flora phenology, Menzel and Fabian (1999) documented that 6 days of advancement of spring phenology and 4.8 days of delay of fall phenology have increased the growing season by 10.8 days in Europe during the last 30 years. Sheifinger et al. (2003) reported that in central Europe, flora phenological events advanced at the rate of -2.0 days/decade during the 1951-1997 period. Fitter and Fitter (2002) also identified that flowering timing in Britain has shifted earlier by 4.5 days in the 1990s compared with the 1954-1990 period. According to an analysis of leaf burst and coloring data by Defila and Clot (2001), phenological spring onset of -11.6 days (-2.8 days/decade) and autumnal ends of +1.7 days (+0.34 days/decade) led to expansion of vegetation period of 13.3 days over the period 1951-2000 in Switzerland. Menzel et al. (2001) also showed that both an obvious advancement of spring phenology of plants at the rate of -1.6 – -2.3 days/decade and a weaker delay of autumnal phenology at the rate

of +1.0 – +0.8 days/decade resulted in a 5 day increase of phenological season in Germany during 1951-1996. Schröder et al. (2006) revealed that the timing of German spring phenology of plants has advanced by 15 days in the 1990s compared with the past 30 years (1961-1990). In case of spring fauna phenology, Roy and Asher (2003) reported that sighting dates of butterflies delays at the rate of 3-4 days/100km with increases of latitude in the Britain. In addition, Crick et al. (1997) found that the date of egg laying of birds shows an advancement of -3.5 days/ decade over the 1971-1995 period.

## 2) East Asia

Ho et al. (2006) revealed that first bloom dates for five species have advanced at the rate of -1.4 – -2.4 days/decade in Seoul, Korea for the period 1922-2004. Schwartz and Chen (2002) concluded that the timing of blooming and leafing in spring does not show any particular trends in China, while spring frost dates derived from the time series of air temperature have advanced by 6 days over the 1959-1993 period. Zheng et al. (2006) found that the early spring phenophases such as first bloom and leaf unfolding have advanced by -1.1– -5.4 days/decade in the northern region at 33°N of latitude between 1963 and 1996, while the late occurrences of spring phenophase at the rate of +2.4 – +6.9 days per decade are observed in eastern China. According to analyses of long term cherry blossom data during the last six centuries in Kyoto Japan, Menzel and Dose (2005) concluded that an increasing trend begins to appear since the early 20<sup>th</sup> century, showing more increases in recent decades.

## 3) North America

Schwartz and Reiter (2000) revealed that spring phenological timing has advanced by -4.2 – -5.4 days in North America over a recent 35 year period (1959-1993) which is

equivalent to a rate of -1.4 – -1.8 days/decade. Zhao and Schwartz (2003) demonstrated that the blooming of several species has increased at the rate of -2.3 – -7.0 days/decade in Wisconsin between 1965 and 1998. Cayan et al. (2001) showed that bloom dates of lilacs and honeysuckle between 1957 and 1994 have advanced in the western United States at the rate of 2 days/decade and 3.8 days/decade, respectively. Beaubien and Freeland (2000) demonstrated that spring blooming in western Canada has advanced at the rate of 2.6 days/decade based on the flowering data for the period 1901-1997.

#### 4) Northern Hemisphere

Tucker et al. (2001) documented that the onset dates of the growing season based on the NDVI above 35°N began 5.6 days earlier between 1982 and 1991, was 3.9 days later in 1991 and 1992, and 1.7 days earlier from 1992 to 1999. They concluded that the volcanic eruption of Mt. Pinatubo temporarily delayed the onset of growing seasons during 1992 and 1993. Shabanov et al. (2002) compared the 45°N NDVI values on day 120 and on day 270 of 1981-1982 and 1993-1994 in bi-yearly curves. They found that spring onset has advanced by 6 days in the 1993-1994 period compared with the 1981-1982, while the timing of autumnal greenness decline have been delayed by 4 days. However, the meaning of Day 120 and Day 270 selected by Shabanov et al. (2002) is not specified. Thus, it is not clear whether Day 120 and Day 270 indicate spring and autumnal onset dates or centroid dates or end dates. Moreover, what they quantified as changed days of spring and autumnal greenness is vague because the daily differences between two biannual averaged annual curves of the NDVI at 45°N vary depending on what day of the year it is. According to Schwartz et al.'s (2006) analyses of a lilac phenology network data, early spring events such as leaf burst have advanced at the rate

of -1.2 days/decade across the Northern Hemisphere land masses for the period 1955-2002.

### **Changes in hydrological cycles**

Most studies about changes in hydrological cycles have mostly focused on western or eastern North America, or on the Arctic regions. Burn (1994) reported that spring stream flow had advanced in western Canada over the past several decades. Zhang et al. (2001) also documented that spring hydrological events such as dates of annual maximum daily stream flow, the centroid of annual stream flow, and river freeze-up were increasingly earlier in western Canada over the past several decades.

Cayan et al. (2001) revealed that the spring pulse date, which is the peak timing of stream flow, has advanced at the rate of 2 days/decade in the western United States over the 1948-1995 period. Similarly, Stewart et al. (2005) reported that the timing of springtime snowmelt and stream flow has advanced by 1-4 weeks (-1.3 - -5.3 days/decade) for the period 1948-2002 in western United States. In addition, Hartley and Robinson (2000) found that the center date of winter, which is defined from heating degree days, shows an earlier trend at the rate of 1.6 days per decade in the Northern Plains of the United States over the 1895-1996 period. Regonda et al. (2005) pointed out that the peak flow timing of the spring season above 2500m-elevation has advanced by 10-20 days during the past 50 years in the western United States. McCabe and Clark (2005) claimed that this earlier snow melting appeared suddenly in the mid-1980s in the western United States. Cannon (2005) also showed through comparison of critical dates

derived from clustering analysis that earlier stream flow patterns are identified in the rivers in British Columbia over the 1951-2000 period.

In addition, Westerling et al. (2006) claimed, through analyses of fire and climatic data since 1970, that the dry wildfire season in the western United States had expanded and that fires were more intense and frequent in the first few years of the 21<sup>st</sup> century due to earlier spring onsets since the mid-1980s. They attributed the early spring onset to advanced snow melting dates.

Hodgkins et al. (2003) documented that the timing of spring stream flow shows an advanced tendency by 1-2 weeks (-2.3 - -4.7 days/decade) in New England in the last three decades. Czirkowsky and Fitzjarrald (2004) found that earlier spring onset by -5 - -6.6 days occurs in New England - New York and Virginia in the 1976-2000 period compared with 1951-1975. Hodgkins and Dudley (2006) found that the timing of spring stream flow has advanced by -0.7 - -1.2 days/decade during the last 80 year period in eastern North America. Hayhoe et al. (2006) predicted that under the lower greenhouse emission scenario (B1), peak spring streamflow in the northeastern United States will be advanced by 10 days at the end of the 21<sup>st</sup> century.

For the Arctic regions, Foster (1989) and Foster et al. (1992) found that the disappearance date of snow has advanced in the Arctic tundra during the 1980s. Stone et al. (2002) reported that the trend toward earlier snow melt began in the mid-1960s and the rate of earlier spring onset is 1.3 days/decade ( $\pm 0.8$  days) in northern Alaska. Comiso (2003) used satellite thermal infrared data to show that the ice melting season in pan-Arctic regions has lengthened at the rate of 10-17 days/decade over the 1981-2001 period due to a recent warming. Belchansky et al. (2004) also documented that the Arctic ice

melting season increased 2-3 weeks in length over the 1979-2001 period.

### **Changes in geographical season cycles**

Analyses of changes in geographical thermal seasons have been carried out in a few studies. In Europe, Markevičienė (1996) documented that there were fluctuations in seasonal onsets and durations in Lithuania over the last 200 years. According to Markevičienė's (1996) summary, spring and summer began late during the 19<sup>th</sup> century, while they began earlier during the 20<sup>th</sup> century by 3-4 days. Also, the timing of autumn onset changed from earlier to later dates. In particular, Markevičienė (1996) found that spring and summer seasons were arriving earlier and lasting longer in urban areas compared with rural areas, while autumn and winter began later and lasted for shorter periods in urban areas. Jaagus and Ahas (2000) revealed that winter duration shortened by 30 days in Estonia over the 1891-1998 period, while summer lengthened by 11 days. Piotrowicz (2002/2003) reconstructed long-term (1792-2002) time series of thermal winter ( $T_{\text{mean}} < 0^{\circ}\text{C}$ ) cycles for Krakow, Poland based on monthly and daily mean temperature. According to the reconstructed time series graph, it is revealed that thermal winter has shortened by approximately 30 days during 1960-2000 compared with the period 1830-1870. Jaagus et al. (2003) documented that spring onset in the eastern European plain has advanced by 6-25 days, resulting in 10-30 days of reduction of winter length over the 1881-1995 period. Jaagus (2006) updated that spring onset in Estonia has been advanced by 20-45 days over the 1951-2000 period.

In Asia, Choi and Kwon (2001) found through an analysis of daily temperatures observed at six weather stations in South Korea that winter duration shortened by 22-49

days, while spring and summer durations lengthened by 6-16 days between 1920 and 1999. Oh et al. (2004) observed that winter duration decreased by 27 days in Busan, Korea between the 1910s and the 1990s, while summer and fall duration lengthened by 22 days and 6 days, respectively. Choi et al. (2006) examined changes in both temporal trends and spatial patterns of seasonal onset date and duration across South Korea for the period 1973-2004. They found that winter duration has shortened by 10 days since 1988 compared with the pre-1987 period due to spring arriving 6 days earlier and winter beginning 4 days later. In particular, they showed that the earlier spring onset pattern began in southern areas in the mid-1980s and spread northward in the 1990s. In China, Ye et al. (2003) found that winter period has shortened by 32-34 days in Beijing, Hailar, and Lanzou over the last half of the 20<sup>th</sup> century, while summer has lengthened by 12-27 days.

In North America, Weston (2006) employed radiation, albedo, and air temperature observations and found that summer duration increased approximately at the rate of 6 days/decade due to an earlier summer onset in Canadian high arctic regions over the 1957-2003 period.

There are also studies on changes in growing seasons that are derived from climate variables based on the knowledge of phenological response of flora to climatic variations. For instance, Menzel et al. (2003) documented that over the 1951-2000 period, the spring frost ( $T_{min} < 0^{\circ}\text{C}$ ) date has advanced by 2.4 days/decade, while autumnal frost date has delayed by 2.5 days/decade. Palecki (1994) found an advanced pattern of spring onset (last record of  $T_{min} < 0^{\circ}\text{C}$ ) date by more than 12 days in the 1980s in the northern and northeastern United States excluding New England compared with that in the 1910s. He

also found that autumnal freezing date did not show any apparent change during the 20<sup>th</sup> century. Fitzjarrald et al. (2001) revealed that changes in spring onset date, which are extracted based on the Bowen ratio method, are not clear since 1880, except for 6-8 days earlier trend in the northeast United States only since the 1960s. In addition, Sheifinger et al. (2003) reported that in central Europe frost days decreased at the rate of -2 days per decade during the 1951-1997 period.

In conclusion, to date, most studies on changes in seasonal cycles have examined primarily changes in spring onset using phenology of flora and fauna or snow melt and streamflow. In spite of regional noise, most studies agree that spring onset has advanced in recent decades on various regional scales. The spatial coverage of data sets used in earlier studies was confined to the regional scale, indicating the need for hemispheric scale studies to understand seasonal changes. Several studies also suggested coupling between sudden warming in the stratosphere and troposphere-orientated energy flux (Black et al. 2005), or atmospheric circulation such as Northern Atlantic Oscillation (D'Odorico et al. 2002; Scheifinger et al. 2002; Paluš et al. 2005), as a potential mechanism for the fluctuations of spring onset. However, causes of earlier spring onset in recent decades have not been fully studied.

Changes in onsets/offsets and durations of other seasons have rarely been examined. One of the reasons could be the lack of a standard definition of seasons. This dissertation defines four standard floating seasons on a hemispheric scale. This study also investigates whether there have been changes in seasonality in recent decades and the mechanisms of such changes.

## CHAPTER 3

### DATA AND METHODOLOGY

#### 3.1. Data and pre-processing

Four comprehensive data sets are used to define seasons in this dissertation: National Centers for Environmental Prediction-Department of Energy (NCEP-DOE) reanalysis II 2-m daily temperature data, National Oceanic and Atmospheric Administration (NOAA) weekly snow maps, NOAA AVHRR Normalized Differences Vegetation Index (NDVI) data, and GFDL 2.1 model output 2-m daily temperature data (Table 3.1). These gridded data sets consist of 1°-2.5° grid cells and cover the Northern Hemisphere. In addition, atmospheric carbon dioxide (CO<sub>2</sub>) concentration data collected from flask air samples at two sites in the Northern Hemisphere are used to examine intra-annual variations at Point Barrow, Alaska (71.3°N, 157.3°W) and Mauna Loa Observatory, Hawaii (19.5°N, 155.6°W).

Large-scale atmospheric circulation indices, including the Arctic Oscillation (AO), the El Niño Southern Oscillation (ENSO), the Pacific-North America pattern (PNA), and the Northern Atlantic Oscillation (NAO) obtained from NOAA National Weather Service Climate Prediction Center (NOAA 2006), are used to examine linkages between seasonal variations in the observed variables and atmospheric circulation in the Northern Hemisphere. 500hPa geopotential height and sea surface temperature obtained from NOAA Earth System Research Observatory (NOAA 2007a) are also used to examine relationships between seasonal patterns and pressure/oceanic currents.

Table 3.1. Data sets used in this study

DATA		Temporal resolution		Spatial resolution	
Variable	Source	Interval	Span	Pixel size	Coverage
Reanalyzed 2-m temperature	NCEP/DOE reanalysis II	Daily mean	1979-2005	Gaussian Grid 1.88°×1.87°	Northern Hemisphere
Snow cover	NOAA weekly snow maps (Rutgers Global Snow Lab)	Weekly composite	1967-2005	National Meteorological Center Limited-Area Fine Mesh 89×89 Cartesian grids (16,000km <sup>2</sup> to 42,000km <sup>2</sup> )	Northern Hemisphere
Normalized Difference Vegetation Index (NDVI)	NOAA AVHRR	10-day composite	1982-2001	1°×1°	Northern Hemisphere
Climate model output 2-m temperature	GFDL 2.1 climate model	Daily mean	1981-2000; 2081-2100	2.5°×2.5°	Northern Hemisphere

The detailed characteristics and required pre-processing of the four comprehensive data sets used to demarcate seasons as well as other ancillary data such as CO<sub>2</sub>, atmospheric circulation indices and pressure data are described below.

### **NCEP-DOE reanalysis II 2-m daily mean temperature**

Seasonal onset dates in the Northern Hemisphere are extracted from the NCEP-DOE reanalysis II 2-m daily mean temperature data for the period 1979-2005 (Figure 3.1). The NCEP-DOE reanalysis II product is an improved version of the NCEP/NCAR reanalysis I data. The original NCEP/NCAR reanalysis project was carried out to produce the assimilated atmospheric and surface climate data by aggregating a variety of global scale modern observation data from surface air temperature to satellite imagery (Kalnay et al. 1996). The NCEP/NCAR reanalysis I data go back to 1948, but have various errors in data input procedures and physical processes used in the model (NOAA 2002). For

instance, the 1973 snow cover data are used to reanalyze 2-m daily mean temperature data for the 1973-1994 period. Thus, the NCEP-DOE reanalysis II data, which date back to 1979, are employed in this study. The 2-m daily mean temperature data cover  $88.542^{\circ}\text{N} - 88.542^{\circ}\text{S}$  and  $0^{\circ}\text{E} - 358.125^{\circ}\text{E}$ , and include a  $192 \times 94$  distribution of global T62 Gaussian grid cells. In this study, daily 2-m mean temperature data covering the Northern Hemisphere are used to extract seasonal onset data for the period 1979-2005 (Figure 3.1).

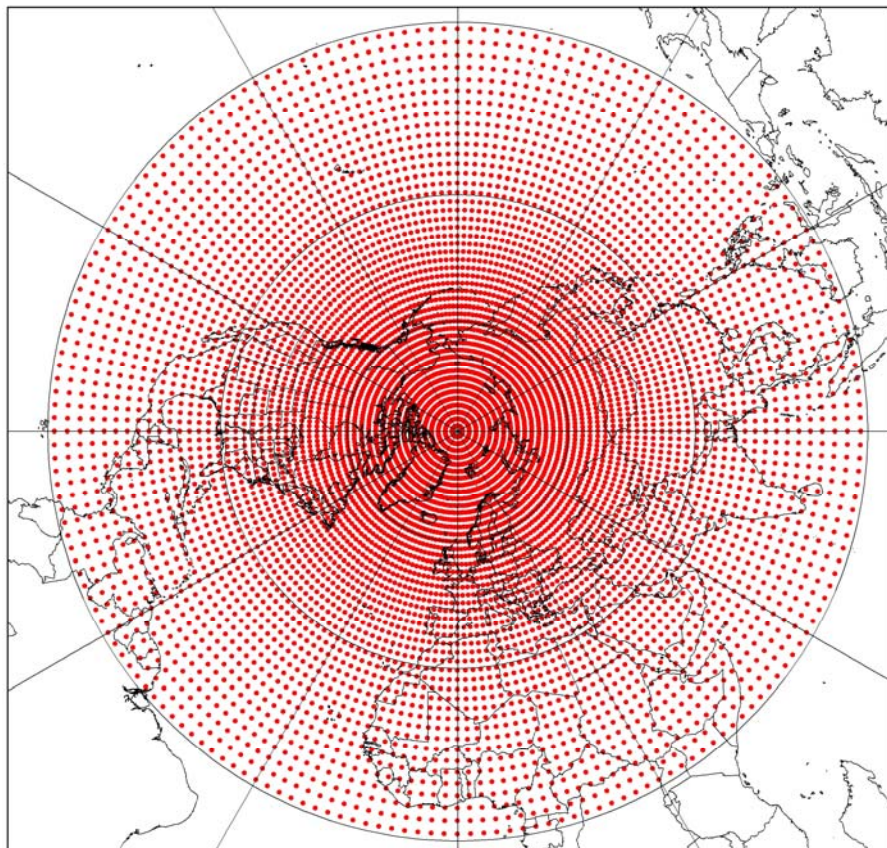


Figure 3.1. The centroids of grid cells for the NCEP-DOE reanalysis daily 2-m temperature data in the Northern Hemisphere

The daily reanalysis data for one full year have been archived as individual binary NetCDF (\*.nc) files. Daily temperature data are extracted from the original archive and converted to ascii data format using the Interface Description Language (IDL). The aggregated data facilitate the calculations of moving averages and the detection of the first or last date when a certain threshold exceeds. In each Excel spreadsheet, X-dimension denotes the Julian date and Y-dimension indicates the cell ID which covers the ranges of 88.542°N, 0°E to 0°N-358.125°E with 9024 grid cells (192×47=9024) (Figure 3.2). The size of each grid cell varies because cells covering the Northern Hemisphere are divided according to a Gaussian grid.

The screenshot shows a Microsoft Excel spreadsheet titled '2005FH\_MA'. The data is organized in a grid with columns labeled A through N and rows numbered 1 through 43. Column A contains 'Calendar' and 'JD' (Julian Date). Columns B through N contain numerical values representing data for different grid cells. The values are arranged in a pattern that suggests a Gaussian grid, with values increasing towards the center of the grid.

	A	B	C	D	E	F	G	H	I	J	K	L	M	N	O
1	Calendar	1/1/2005	1/2/2005	1/3/2005	1/4/2005	1/5/2005	1/6/2005	1/7/2005	1/8/2005	1/9/2005	1/10/2005	1/11/2005	1/12/2005	1/13/2005	1/14/2005
2	JD	1	2	3	4	5	6	7	8	9	10	11	12	13	14
3							250.9609	251.99	252.5282	252.1727	251.5665	252.2018	251.7073	250.0582	249.
4							250.9682	252.0036	252.5445	252.1891	251.5636	252.2	251.7036	250.0273	
5							250.9818	252.0218	252.5655	252.2164	251.5836	252.22	251.7336	250.0536	249.
6							250.9909	252.0355	252.5827	252.2427	251.6018	252.2409	251.7645	250.08	249.
7							250.9991	252.05	252.5991	252.2636	251.6136	252.2545	251.7873	250.0945	249.
8							251.0064	252.0627	252.6145	252.2855	251.6255	252.2736	251.8182	250.1173	249.
9							250.9955	252.0618	252.6155	252.2764	251.5809	252.2327	251.7636	249.9818	249.
10							250.9964	252.0682	252.6245	252.2927	251.5845	252.2455	251.7891	250	249.
11							251	252.0764	252.6355	252.3145	251.5936	252.26	251.8182	250.0218	249.
12							250.9982	252.0791	252.6391	252.33	251.5936	252.2673	251.8391	250.0345	249.
13							250.9927	252.0782	252.6391	252.3409	251.5882	252.27	251.8573	250.0409	249.
14							250.9855	252.0755	252.6373	252.3527	251.5882	252.2764	251.8791	250.0582	249.
15							250.9745	252.0691	252.6336	252.3573	251.5645	252.2591	251.8691	250.0182	249.
16							250.9773	252.0755	252.6409	252.38	251.5845	252.2845	251.9164	250.0809	249.
17							250.9555	252.0591	252.6255	252.3727	251.5464	252.2527	251.8918	250.0145	249.
18							250.9518	252.0591	252.6255	252.3918	251.5618	252.2709	251.9309	250.0527	249.
19							250.9364	252.0464	252.6136	252.39	251.5555	252.2673	251.9427	250.0518	249.
20							250.9182	252.0327	252.6036	252.3918	251.5609	252.2727	251.9673	250.0709	249.
21							250.8973	252.0145	252.5864	252.39	251.56	252.2709	251.9845	250.0845	249.
22							250.8773	251.9864	252.5691	252.3882	251.5664	252.2755	252.01	250.1027	249.
23							250.8473	251.9691	252.5436	252.3791	251.5609	252.2673	252.0209	250.1027	249.
24							250.8145	251.9391	252.5136	252.3709	251.5382	252.2418	252.0182	250.08	249.
25							250.7891	251.9155	252.4909	252.3727	251.5645	252.2636	252.0709	250.13	249.
26							250.7618	251.8909	252.4664	252.3718	251.5873	252.2782	252.1	250.1582	249.
27							250.7318	251.8627	252.4373	252.3655	251.5636	252.2482	252.1091	250.1682	249.
28							250.6918	251.8245	252.3991	252.3482	251.5173	252.2	252.0862	250.1236	249.
29							250.6618	251.7973	252.3709	252.34	251.4891	252.1618	252.0773	250.12	249.
30							250.6309	251.7682	252.3391	252.3236	251.4518	252.1127	252.0562	250.1045	249.
31							250.6009	251.7382	252.3091	252.3091	251.4136	252.0627	252.0373	250.0864	249.
32							250.5618	251.7009	252.2709	252.2836	251.3673	252.0045	252.0255	250.0736	249.
33							250.5309	251.6718	252.24	252.2645	251.3336	251.96	252.0164	250.07	249.
34							250.4945	251.6364	252.2009	252.2409	251.2845	251.8982	251.9927	250.0445	249.
35							250.4509	251.5936	252.1545	252.2082	251.2436	251.8436	251.99	250.0509	249.
36							250.4164	251.56	252.1164	252.1855	251.21	251.7945	251.9382	250.0091	249.
37							250.3809	251.5264	252.0791	252.1609	251.1745	251.7427	251.9182	249.9982	249.
38							250.3418	251.4873	252.0373	252.1309	251.14	251.6927	251.9427	250.0355	249.
39							250.3073	251.4518	252	252.1018	251.1064	251.6418	251.9245	250.0291	249.
40							250.2673	251.4136	252	252.0627	251.0627	251.5827	251.8918	250.0182	249.
41							250.2273	251.3745	252	252.0236	251.0236	251.5436	251.8518	250.0073	249.
42							250.1873	251.3355	252	251.9845	251.0845	251.5045	251.8118	250.0018	249.
43							250.1473	251.2955	252	251.9455	251.1455	251.4655	251.7618	250.0018	249.

Figure 3.2. A sample Excel file that shows the X- and Y-dimensions of the final data. X-dimension denotes the day during the year, and Y-dimension denotes the ID for each grid cell introduced in Figure 3.1

### **NOAA AVHRR visible snow cover**

Weekly snow cover data for the period 1967-2005 are used to define the onset and termination of snow covered winter seasons in this study. The weekly snow cover data consist of binary format codes (0= snow free, 1= snow covered) that trained meteorologists at NOAA mapped and digitized based on photocopies of snow cover derived from AVHRR visible satellite imagery (Robinson et al. 1993). If at least 50% of the cell is covered with snow, it is assigned as snow-covered; otherwise, it is snow-free. The snow data were digitized based on the National Meteorological Center Limited-Area Fine Mesh 89×89 Cartesian grids laid over a polar stereographic projection (Figure 3.3) the size of which varies in the range of 16,000 km<sup>2</sup> to 42,000 km<sup>2</sup>. NOAA snow data have been reprocessed and archived at Rutgers University's Global Snow Laboratory where they were accessed for this study.

The snow cover data between 1967 and 1971 are excluded in the time series analyses because there are missing data of more than two weeks. Since the year 1999, the Interactive Multisensor Snow and Ice Mapping System (IMS) product (Ramsay 1998) is included in the data set. There is an inconsistency between the IMS product (June 1999-present) and the NOAA product (October 1966 - May 1999) on a regional scale (Robinson & Estilow 2006). Caution is required when analyzing highly elevated complex terrains such as the Himalayas and the Tibetan Plateau because the pre-IMS era snow extent in the mountainous areas was overestimated. To examine appearance and disappearance dates of snow-cover, weekly snow cover data for each year are aggregated in individual Excel spreadsheets for the study period. Each data file in the spreadsheet consists of 52 or 53 columns in the horizontal X-dimension which represents the number

of weeks during the year, and  $89 \times 89 = 7921$  rows in the vertical Y-dimension which represents the total grid cells covering the entire Northern Hemisphere as shown in Figure 3.3.

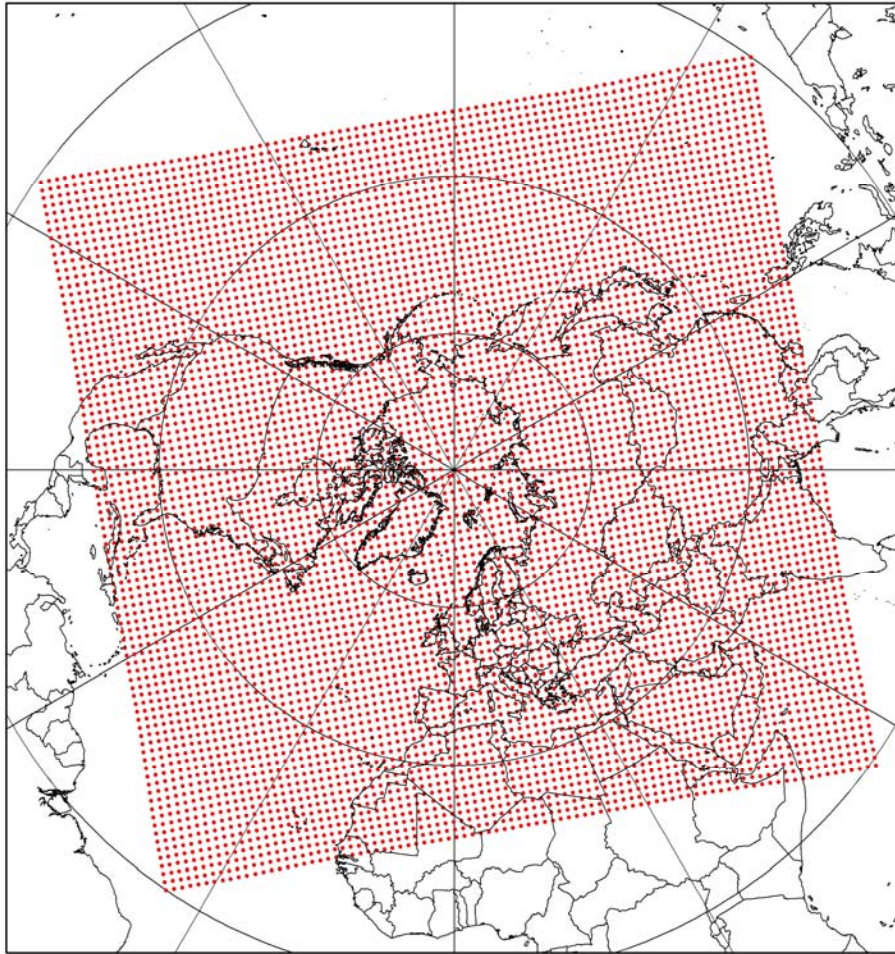


Figure 3.3. The centroids of  $89 \times 89$  grid cells for Northern Hemisphere snow cover derived from the NOAA AVHRR visible imagery

### **NOAA AVHRR Normalized Difference Vegetation Index (NDVI)**

Ten-day composites of NOAA AVHRR Normalized Difference Vegetation Index (NDVI) for the period 1982-2001 are used to detect the onset and offset of the vegetation season. In particular,  $1^{\circ} \times 1^{\circ}$  resolution data, a scale suitable for examining hemispheric scale patterns, are used in this study.  $8\text{km} \times 8\text{km}$  resolution data are also available but they are more useful for local and regional analyses. The NDVI is a ratio value that discriminates vegetation from other types of surfaces (Justice et al. 1985) and is popularly used to indirectly estimate vegetation parameters such as green-leaf biomass and green-leaf area (Asrar et al. 1984; Myneni et al. 1997). NOAA AVHRR NDVI is calculated by comparing the reflectance between visible (V: 0.58-0.68 micrometer) and near-infrared (NIR: 0.73-1.10 micrometer) channels.

$$NDVI = \frac{NIR - V}{NIR + V}$$

The NDVI is a unitless value which varies from -1 to +1. In general, densely vegetated areas show an NDVI of 0.3-0.8, while sparsely vegetated areas have values of 0.05 - 0.1. Water or snow-covered areas have negative values. The quality of NDVI data is enhanced through the elimination of contamination by atmospheric and anisotropic effects such as Rayleigh scattering (NGDC, 1993) and ozone absorption (McPeters et al. 1993) based on Gordon et al.'s (1988) method. Tucker et al. (2001) showed that critical biases related to the drifting of sensors of multi-NOAA satellites series over time (Kaufmann et al. 2000) are not found in the NDVI data set. Moreover, ten-day composites of NDVI remove the cloud cover contamination by selecting the maximum

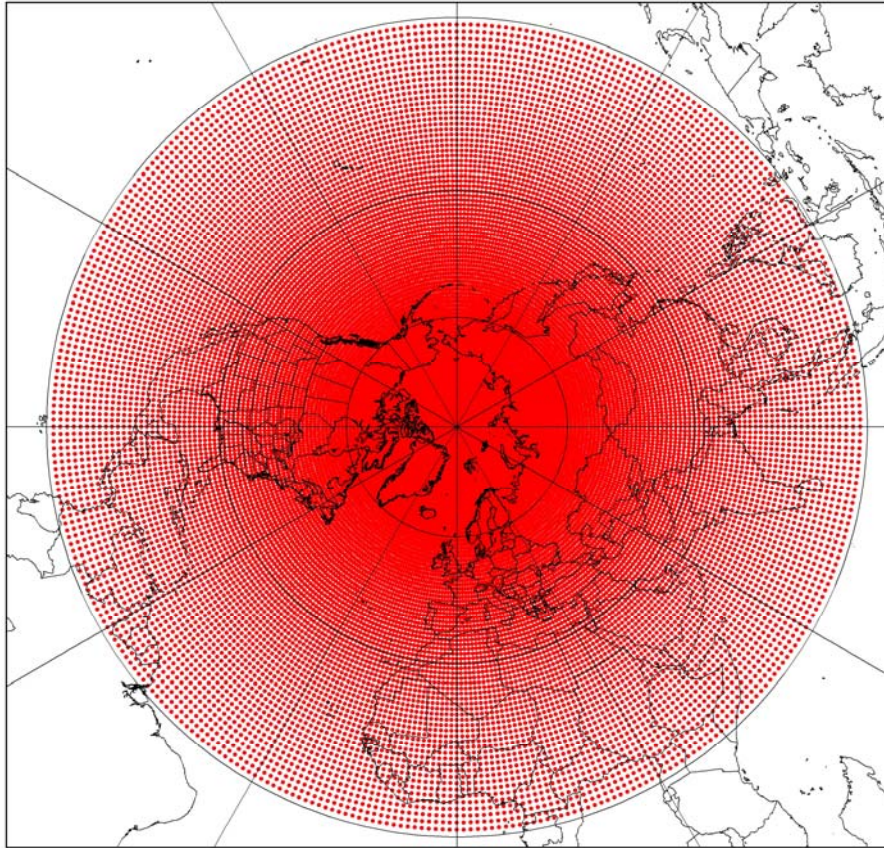


Figure 3.4. The centroids of  $360 \times 90$  grid cells for the Northern Hemisphere NDVI derived from the NOAA AVHRR imagery

NDVI from ten daily values (Holben et al. 1986). Further consideration of cloud effects is needed depending on the purpose of study (NASA 2006). For instance, in monsoon regions (Haque & Lal 1991) and over the Arctic basin (Curry et al. 1996; Walsh & Chapman 1998) persistent cloud cover for more than 10 days can interrupt the detection of NDVI. However, vegetation season onset and offset do not occur during summer monsoon seasons. Analyses of NDVI time series also verify that the critical contamination of NDVI by cloud is not found over land masses around the Arctic sea

during vegetation seasons. The Inter-Tropical Convergence Zone (ITCZ) identified with cloud bands are excluded in this study because the onset and offset of vegetation seasons, if such exist at such low latitudes, are not clearly detected.

Ten-day composite NDVI data consist of  $360 \times 90 = 32,400$   $1^\circ \times 1^\circ$  grid cells encompassing the Northern Hemisphere (Figure 3.4). The NDVI data are extracted as ascii format data (\*.dat) using a FORTRAN program. Similar to the two previously discussed data sets, ten-day composite data are aggregated as annual data sets for the period 1982-2001. Thus, Excel spreadsheets for individual years consist of 36 columns in the X-dimension, which denote the number of ten-days for the year, and 32,400 rows, which indicate the cell ID. The cell ID begins from the Arctic eastern region adjacent to the Prime meridian ( $89.5^\circ\text{N}$ ,  $0.5^\circ\text{E}$ ), rotates counter clockwise moving equator-ward, and ends in the Northern Hemisphere western tropical region at  $0.5^\circ\text{N}$ ,  $79.5^\circ\text{W}$ .

### **Atmospheric carbon dioxide (CO<sub>2</sub>) concentration data**

Various temporal resolution of carbon dioxide concentration data, including daily, ten-day, weekly, and biweekly, have been archived by the Carbon Dioxide Information Analysis Center (CDIAC 2004). The oldest data dates back to 1957 at the Mauna Loa Observatory in Hawaii. In this study, daily atmospheric CO<sub>2</sub> data gathered at Point Barrow, Alaska ( $71.3^\circ\text{N}$ ,  $157.3^\circ\text{W}$ ) and at Mauna Loa ( $19.5^\circ\text{N}$ ,  $155.6^\circ\text{W}$ ) are used to define carbon dioxide seasons. Daily CO<sub>2</sub> data used in this study extends back to the early 1970s: at Barrow (1974-2004) and at Mauna Loa (1973-2003). The Barrow observation site is 11m above sea level, while Mauna Loa is 3397 m above sea level. The

CO<sub>2</sub> data contaminated by Mauna Loa volcanic eruptions in 1975 and 1984 are not included in the analyses.

### **Large scale atmospheric circulation indices and pressure data**

Monthly large scale atmospheric circulation indices such as the Arctic Oscillation (AO), the El Niño Southern Oscillation (ENSO), the Pacific-North American pattern (PNA), and the Northern Atlantic Oscillation (NAO) were obtained from the NOAA National Weather Service Climate Prediction Center (NOAA 2006). Atmospheric pressure data are extracted from the NCEP DOE reanalysis II data set (NOAA 2007a). The definitions, characteristic, and calculation equations of the circulation indices are as follows:

#### 1) AO

The AO is the oscillation index between the Arctic areas and the mid-latitudes (Thompson & Wallace, 1998, 2000). The AO index is calculated by projecting the mean 1000-hPa (700-hPa) height anomalies onto the leading EOF mode, and it is then normalized by the standard deviation of the monthly index from long-term average.

#### 2) ENSO

The ENSO is the planetary-scale seesaw pattern of two dipoles in sea level pressure (SLP) and sea surface temperature between the eastern Pacific and the western Pacific–Indian Ocean region (Troup, 1965). The Oceanic Niño Index (ONI) is the three-month running mean of ERSST.v2 SST anomalies in the Niño 3.4 regions (5°N–5°S, 120°–170°W). The Southern Oscillation Index (SOI) is calculated using the following equation:

$$\text{SOI} = \frac{\frac{(\text{Actual Tahiti (SLP)} - \text{Mean Tahiti (SLP)})}{\text{Standard Deviation Tahiti}} - \frac{(\text{Actual Darwin (SLP)} - \text{Mean Darwin (SLP)})}{\text{Standard Deviation Darwin}}}{\text{Monthly Standard Deviation (MSD)}}$$

### 3) PNA

The PNA is a Rossby wave pattern that spans from the equatorial Pacific through the northwest of North America and down to the southeastern part of North America (Wallace & Gutzler 1981). The positive phase of the PNA pattern features above-average heights in the vicinity of Hawaii and over the intermountain region of North America, and below-average heights south of the Aleutian Islands and over the southeastern United States. The monthly PNA is calculated by the following equations, where  $Z^*$  denotes monthly mean 500 hPa geopotential height anomaly in each month compared with a long-term base period (i.e. 1950-2000).

$$\begin{aligned} \text{PNA} = & Z^*(15^\circ\text{N}-25^\circ\text{N}, 180-140^\circ\text{W}) - Z^*(40^\circ\text{N}-50^\circ\text{N}, 180-140^\circ\text{W}) \\ & + Z^*(45^\circ\text{N}-60^\circ\text{N}, 125^\circ\text{W}-105^\circ\text{W}) - Z^*(25^\circ\text{N}-35^\circ\text{N}, 90^\circ\text{W}-70^\circ\text{W}) \end{aligned}$$

### 4) NAO

The NAO is a north-south dipole of atmospheric pressure anomalies with one center located over Greenland and the other center of opposite sign spanning the central latitudes of the North Atlantic between 35°N and 40°N (Wallace & Gutzler 1981). The loading pattern of the NAO is the first leading mode of Rotated Empirical Orthogonal Function (REOF) analysis of monthly mean 500hPa height during a long-term base period (i.e. 1950-2000).

### 3.2. Methods to define floating seasons

#### Demarcating thermal seasons using surface air temperature data

The aggregated intra-annual time series of daily temperature in one given year forms a bell-shaped curve with fluctuations of small peaks and troughs (Figure 3.5). In this study, the bell-shaped curve is divided by the day of the year based on particular thresholds to demarcate four seasons. The small fluctuations in the curve make it impossible to detect the first or the last dates when specific temperatures continuously exceed or drop below particular thresholds. For instance, after temperatures are high enough to define spring onset, they can drop below the freezing point for several days. The appearances of these

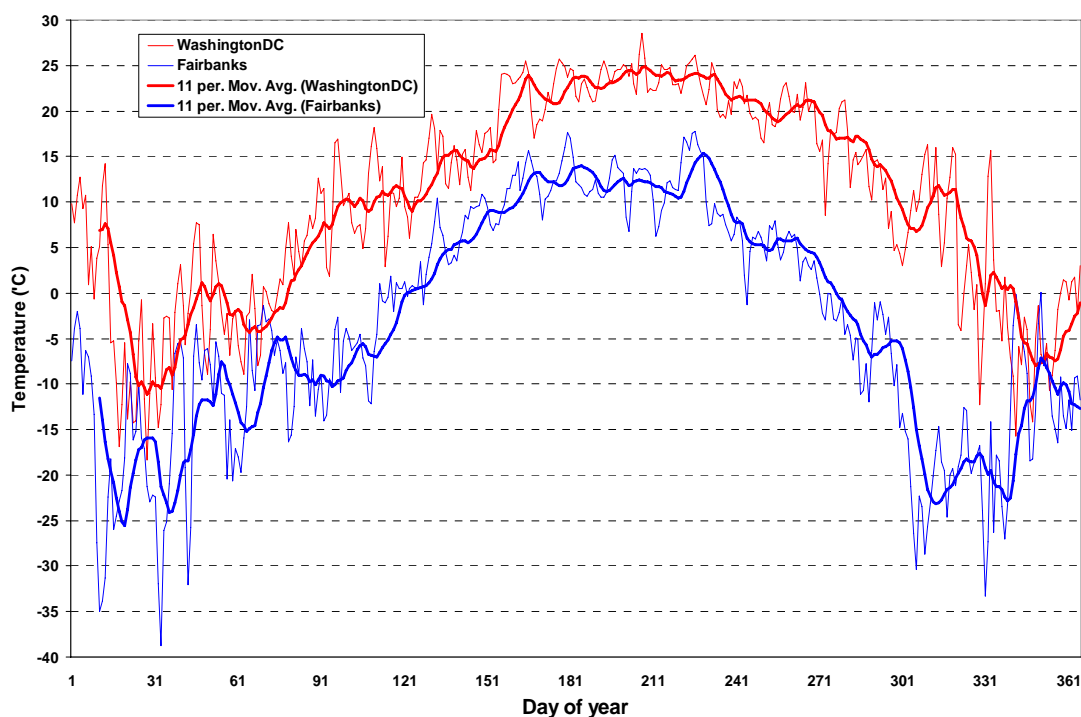


Figure 3.5. Intra-annual progression of raw daily mean temperature data and 11 day moving average data in Washington DC and Fairbanks, Alaska in 2005

peaks and troughs in intra-annual temperature time series are caused by the passing of storms, fronts, and air masses over the region. In particular, blocking pressure systems can cause long-lasting extreme weather patterns related to the high amplitude of these ridges and troughs. According to Barriopedro et al. (2006), the seasonal average duration of blocking system varies between 6.7-10.0 days in the Northern Hemisphere. An odd number of days are required in calculating daily moving average values. Thus, in this study, an 11-day moving average of daily temperatures is carried out for the purpose of detrending these fluctuations. The smoothed curves through the moving average show continuous increasing or decreasing trends which enhance the robustness of demarcating seasons according to the absolute thresholds of temperature.

Figure 3.6 illustrates the intra-annual progression of daily mean temperature during a year in the Northern Hemisphere based on long-term (1975-2005) climatological values of NCEP/DOE reanalysis II 2-m temperature data. According to the climatological curve, it is regarded that extreme cases of spring and summer onsets occur between Day 14 and Day 212 during one calendar year because annual maximum and minimum values of daily mean temperatures occur on these days during this period (Figure 3.6). In the same manner, it is regarded that autumnal and winter onsets occur between Day 212 of the corresponding year and Day 14 of the following year according to the annual range of daily mean temperatures.

In terms of the thresholds used to demarcate seasons, two approaches have been carried out so far: a relative threshold approach and an absolute threshold approach. In a few studies, relative values based on statistics of local climate variables (Rapp & Schönwiese 1994; Ye et al. 2003; Oh et al. 2004) or equal intervals (Trenberth 1983), and

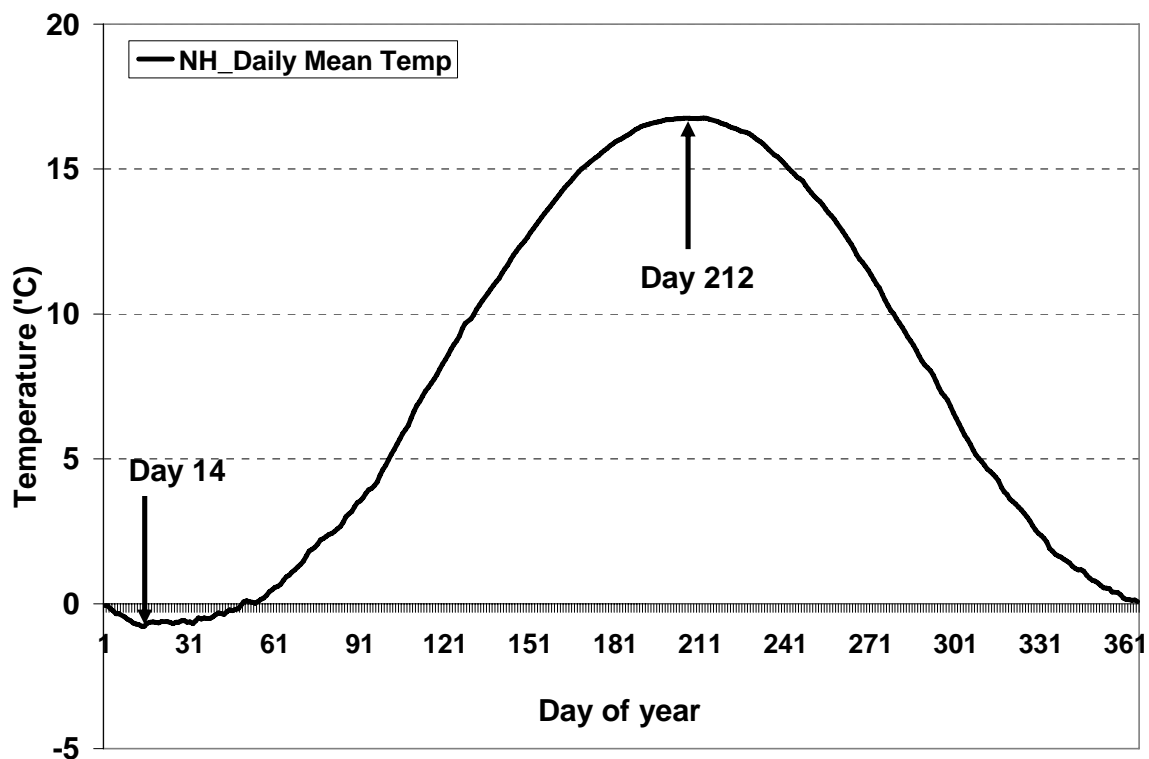


Figure 3.6 . Intra-annual progression of long-term (1979-2005) average daily temperature in the Northern Hemisphere

thresholds derived from principal components or clustering analyses (Alsop 1989; Green 1993; Cannon 2005; Weston 2006) have been used. However, the relative value approach makes it difficult to interpret the physical meaning of the calculated statistical thresholds related to seasonal progressions. This shortcoming leads to most studies employing absolute temperature thresholds related to changes of surface landscape.

Thus, in this study, absolute thresholds of daily mean temperatures related to these surface landscape changes are selected referring to thresholds used in previous studies (Table 3.2). The landscape changes such as appearance or disappearance of vegetation and snow cover are regarded as typical indicators of seasonal onset and end. Table 3.2 (a)-(d) provides a summary of the temperature thresholds used in various earlier studies

Table 3.2. Seasonal temperature indices used in previous studies to demarcate four thermal seasons in different parts of the world

(a) Northern Hemisphere or Globe

Sources	Winter to Spring	Spring to Summer	Summer to Fall	Fall to Winter
Several locations on the Globe	Hartshorne (1938)			
	Monthly mean $\geq 0^{\circ}\text{C}$ (cold season)	Monthly mean $\geq 20^{\circ}\text{C}$ (hot season)	Monthly mean $\leq 20^{\circ}\text{C}$ (hot season)	Monthly mean $\leq 0^{\circ}\text{C}$ (cold season)

(b) Americas

Sources	Winter to Spring	Spring to Summer	Summer to Fall	Fall to Winter
South America	Vincent et al. (2005)			
		Summer days: Daily max $\geq 25^{\circ}\text{C}$		
USA	Conrad & Pollak (1950)			
	Daily mean $\geq 0^{\circ}\text{C}$	Daily mean $\geq 18.3^{\circ}\text{C}$	Daily mean $\leq 18.3^{\circ}\text{C}$	Monthly mean $\leq 0^{\circ}\text{C}$
	Jefferson (1938)			
	Monthly mean $\geq 10^{\circ}\text{C}$	Monthly mean $\geq 20^{\circ}\text{C}$	Monthly mean $\leq 20^{\circ}\text{C}$	Monthly mean $\leq 10^{\circ}\text{C}$
	Visher (1943, 1944, 1950b)			
	Daily mean $\geq 0^{\circ}\text{C}$	Daily mean $\geq 20^{\circ}\text{C}$	Daily mean $\leq 20^{\circ}\text{C}$	Daily mean $\leq 0^{\circ}\text{C}$
	NOAA (2007b)			
	Summer days: Daily max $\geq 25^{\circ}\text{C}$			

(c) Asia

Sources	Winter to Spring	Spring to Summer	Summer to Fall	Fall to Winter
Korea	Choi et al. (2006) used seven-day moving average values of Summed Daily Temperatures (SDT=daily max+mean+min temperatures).			
	Last record of daily min ( $0^{\circ}\text{C}$ ) +mean( $5^{\circ}\text{C}$ )+max( $10^{\circ}\text{C}$ )=SDT $\leq 15^{\circ}\text{C}$	First record of daily min ( $15^{\circ}\text{C}$ ) +mean( $20^{\circ}\text{C}$ )+max( $25^{\circ}\text{C}$ )=SDT $\geq 60^{\circ}\text{C}$	Last record of daily min ( $15^{\circ}\text{C}$ ) +mean( $20^{\circ}\text{C}$ )+max( $25^{\circ}\text{C}$ ) $\geq 60^{\circ}\text{C}$	First record of daily min ( $0^{\circ}\text{C}$ ) +mean( $5^{\circ}\text{C}$ ) +max( $10^{\circ}\text{C}$ ) =SDT $\leq 15^{\circ}\text{C}$
	Oh et al. (2004) used the regional thresholds only for Busan			
	Daily mean $\geq 7.8^{\circ}\text{C}$	Daily mean $\geq 20^{\circ}\text{C}$	Daily mean $\leq 21.8^{\circ}\text{C}$	Daily mean $\leq 11^{\circ}\text{C}$
	Lee (1979)			
First record of daily min $\geq 0^{\circ}\text{C}$	First record of daily max $\geq 25^{\circ}$	Last record of daily max $\geq 25^{\circ}$	First record of daily min $\leq 0^{\circ}\text{C}$	

	and daily mean $\geq 5^{\circ}\text{C}$	C and daily mean $\geq 20^{\circ}\text{C}$	C and daily mean $\geq 20^{\circ}\text{C}$	and daily mean $\leq 5^{\circ}\text{C}$
Japan	Kawamura (1973)			
	Pentad mean $\geq 10^{\circ}\text{C}$	Pentad mean $\geq 20^{\circ}\text{C}$	Pentad mean $\leq 20^{\circ}\text{C}$	Pentad mean $\leq 10^{\circ}\text{C}$
China	Ye et al. (2003) use varying threshold for Beijing, Hailar, and Lanzhou			
	Daily mean $\geq -1 \sim -20^{\circ}\text{C}$	Daily mean $\geq 13 \sim 19^{\circ}\text{C}$	Daily mean $\leq 13 \sim 19^{\circ}\text{C}$	Daily mean $\leq -1 \sim -20^{\circ}\text{C}$
	Chang (1934) and Chang (1946)			
	Daily pentad mean $\geq 10^{\circ}\text{C}$	Daily pentad mean $\geq 22^{\circ}\text{C}$	Daily pentad mean $\leq 22^{\circ}\text{C}$	Daily pentad mean $\leq 10^{\circ}\text{C}$

## (d) Europe

Sources	Winter to Spring	Spring to Summer	Summer to Fall	Fall to Winter
Europe	Alexander et al. (2006)			
		Summer days: Daily max $\geq 25^{\circ}\text{C}$		
Eastern Europe	Jaagus et al. (2003). Early spring is defined when daily mean temperature is above $0^{\circ}\text{C}$			
	Daily mean $\geq 5^{\circ}\text{C}$	Daily mean $\geq 13^{\circ}\text{C}$	Daily mean $\leq 13^{\circ}\text{C}$	Daily mean $\leq 5^{\circ}\text{C}$
Lithuania	Markevičienė (1996) and Pempaitė (1997)			
	Daily mean $\geq 0^{\circ}\text{C}$	Daily mean $\geq 15^{\circ}\text{C}$	Daily mean $\leq 15^{\circ}\text{C}$	Daily mean $\leq 0^{\circ}\text{C}$
Estonia	Jaagus & Ahas (2000) and Ahas et al. (2005)			
	Daily mean $\geq 5^{\circ}\text{C}$	Daily mean $\geq 13^{\circ}\text{C}$	Daily mean $\leq 13^{\circ}\text{C}$	Daily mean $\leq 5^{\circ}\text{C}$
	Jaagus et al. (2003) and Jaagus (2006)			
	Daily mean $\geq 0^{\circ}\text{C}$	Daily mean $\geq 13^{\circ}\text{C}$	Daily mean $\leq 13^{\circ}\text{C}$	Daily mean $\leq 0^{\circ}\text{C}$
Poland	Romer (1904, 1949), Merecki (1914), Wiszniewski (1959), Wiszniewski (1960), Hess (1965), Makowiec (1983), and Kożuchowski & Degirmendzić (2005). Early spring and late fall are defined when daily mean temperature is between $0^{\circ}\text{C}$ and $5^{\circ}\text{C}$			
	Daily mean $\geq 5^{\circ}\text{C}$	Daily mean $\geq 15^{\circ}\text{C}$	Daily mean $\leq 15^{\circ}\text{C}$	Daily mean $\leq 5^{\circ}\text{C}$
	Kwaśniewska & Pereyma (2004)			
	Daily mean $\geq -2.5^{\circ}\text{C}$	Daily mean $\geq 2.5^{\circ}\text{C}$	Daily mean $\leq 2.5^{\circ}\text{C}$	Daily mean $\leq -2.5^{\circ}\text{C}$
	Piotrowicz (1996, 2002-3) defined only winter season			
	Daily mean $\geq 0^{\circ}\text{C}$			Daily mean $\leq 0^{\circ}\text{C}$
Scandinavia (Finland, Sweden, and Norway)	Tveito et al. (2000)			
	Daily mean $\geq 0^{\circ}\text{C}$	Daily mean $\geq 10^{\circ}\text{C}$	Daily mean $\leq 10^{\circ}\text{C}$	Daily mean $\leq 0^{\circ}\text{C}$

to demarcate four seasons in different parts of the world.

These studies have commonly used the thresholds of 0°C or 5°C for daily or monthly mean temperature to define the cold winter period. These values are related to snow and ice melting or the phenological onset of vegetation. In this study, the first or last record of a 5°C daily mean temperature in the intra-annual progression curve is selected to define winter onset and termination dates. A 5°C daily mean temperature threshold has been popularly used to define growing seasons (Menzel et al. 2003) and the Warmth Index (Kira 1949). In several other studies, a daily mean temperature of 0°C is used to define early spring because at the freezing point vegetation can be harmed (Visher 1943; Piotrowicz 1996). However, 0°C should be based on daily *minimum* temperature instead of daily *mean* temperature if the threshold intends to consider the harmful effects of nighttime low temperatures (e.g., frost) on vegetation.

According to the calculation of the difference between the annual average of daily mean temperature and the annual average of daily minimum temperature in the Northern Hemisphere (Figure 3.7), the diurnal temperature range (DTR) varies by latitude and surface type. For example, the DTR on land masses is higher at mid-latitudes between 10°N and 50°N than the Northern hemisphere average. In contrast, the DTR over the ocean is higher at high latitudes above 60°N compared with the average. However, the Northern hemisphere averages of the DTRs over land masses, ocean or both are 9.4°C, 2.4°C, and 5.7°C, respectively. The range between daily minimum or maximum temperatures and daily mean temperature is approximately 5°C over land masses in the Northern Hemisphere. It indicates that 5°C for daily mean temperature can substitute 0°C

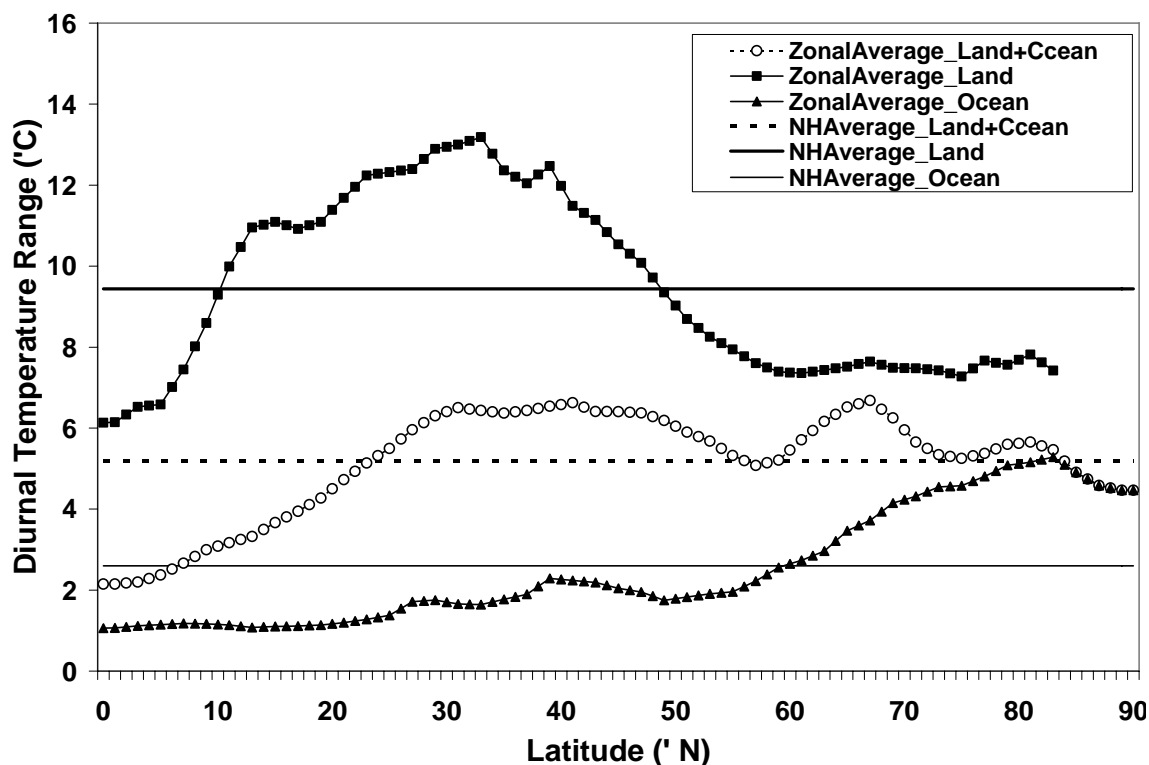


Figure 3.7. Variations of annual average values of diurnal temperature range over land masses and oceans with respect to latitude in the Northern Hemisphere derived from the NCEP/DOE reanalysis II 2-m daily maximum and minimum temperature data sets (1979-2005)

for daily minimum temperature that affects nighttime biogeochemical activities such as freezing vegetation and precipitation type.

Regarding the summer season, a 25°C daily maximum temperature threshold has been popularly used to define “Summer Days” in many regions (Vincent et al. 2005; Alexander et al. 2006). Thus, the first or the last records of a 20°C daily mean temperature in the intra-annual progression curve are defined as hot summer periods based on the hemisphere average range (5°C) between daily maximum and mean temperatures. In several northern European countries, a 15°C daily mean temperature threshold is used to define the summer season. However, this threshold is not the value

based on floating seasons but the value observed at the beginning of June in these regions based on the fixed meteorological summer onset date.

In summary, in this study, 5°C and 20°C daily mean temperatures are used as thresholds to demarcate winter and summer, respectively, after carrying out the 11-day moving average (Table 3.3). The interim periods are defined as transitional spring and fall seasons. Accordingly, the last date that the daily mean temperature is less than 5°C, and the first date that the mean temperature exceeds 20°C between Day 14 and Day 212 are defined as winter termination (vernal onset) and summer onset (vernal termination) dates, respectively. The opposite progression in the second half of the year defines summer termination (autumnal onset) and winter onset (autumnal termination) dates. These absolute thresholds demarcate four standard thermal seasons everywhere in the Northern Hemisphere (Table 3.3).

Table 3.3. Geographical thermal seasons in the Northern Hemisphere employed in this study. An 11-day moving average of daily mean temperatures is used to detrend small peaks and troughs in inter-annual time series

Winter to Spring	Spring to Summer	Summer to Fall	Fall to Winter
Last record of daily mean temperature < 5°C	First record of daily mean temperature $\geq 20^\circ\text{C}$	Last record of daily mean temperature $\geq 20^\circ\text{C}$	First record of daily mean temperature < 5°C

### **Demarcating snow seasons using snow cover data**

Snow cover is another variable that is used to demarcate the cold winter season in this study. It is assumed that the boundary between snow-covered areas and snow-free areas indicates the front of winter onset or offset. In this study, two types of snow seasons are

defined: the Full Snow Season (FSS) and the Core Snow Season (CSS). The interval between the First Appearance Date (FAD) of snow cover during the second half of the year and the Last Disappearance Date (LDD) of snow cover during the first half of the year is defined as the Full Snow Season (FSS). The interval between the First snow-Covered Date of the Longest-lasting snow cover event (FCD) and the First snow-Free Date after the longest-lasting snow cover event (FFD) is defined as the Core Snow Season (CSS)

According to monthly statistics of snow-covered areas (Robinson & Frei 2000), it is estimated that both January and February are the months with maximum extent ( $46 \times 10^6$  km<sup>2</sup>), while August is the month with minimum extent ( $4 \times 10^6$  km<sup>2</sup>). Based on weekly snow cover data (Figure 3.8), the maximum winter extent in the Northern Hemisphere occurs in the 5<sup>th</sup> week of the year ( $47.2 \times 10^6$  km<sup>2</sup>), while the minimum extent occurs in the 33<sup>rd</sup> week ( $3.4 \times 10^6$  km<sup>2</sup>). Therefore, in this study, it is assumed that winter termination based on snow cover occurs between the 5<sup>th</sup> and 33<sup>rd</sup> weeks during the year, while winter onset occurs between the 33<sup>rd</sup> and 5<sup>th</sup> weeks in the following year.

Snow covered periods vary spatially according to latitude and altitude as the year progresses. In addition, there are inter-annual differences in the spatial range of snow cover on the same dates of the year. In some lower mid-latitude regions, snow cover is not detected every year. For example, snow cover is rarely, if ever, observed in most of Florida and southern Texas. In addition, over much of the mid-latitudes, snow cover frequently disappears and re-appears during the winter. Therefore, in this study, winter onset and termination dates are defined only for the regions where snow cover is detected

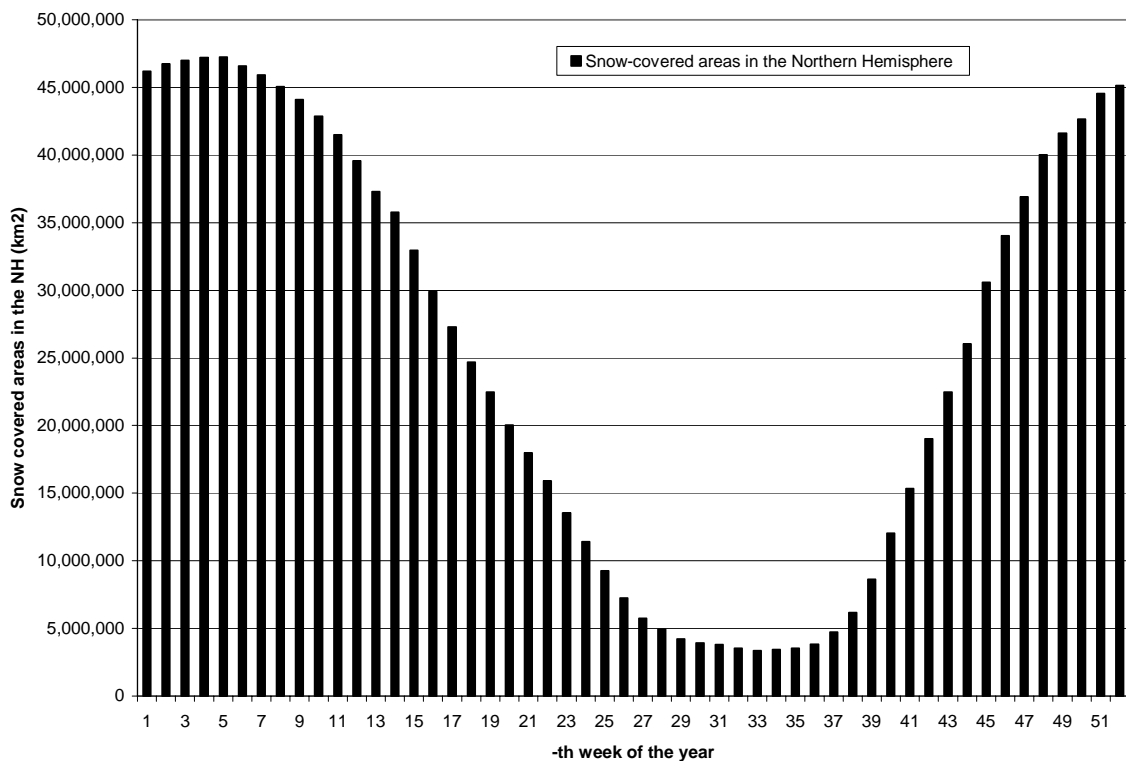


Figure 3.8. Weekly snow-covered areas (km<sup>2</sup>) in the Northern Hemisphere (1972-2005)

at least once throughout each year for more than 75% of the years in the study period.

In summary, the first snow-covered events between the 33<sup>rd</sup> and 5<sup>th</sup> weeks in the following year are defined as the onset of FSS, while the disappearance of the last snow cover events between the 5<sup>th</sup> and 33<sup>rd</sup> weeks is defined as the offset of FSS for the regions where snow events usually occur year-to-year. The onset and offset of CSS are defined as the first and the last dates of continuous long-lasting snow-covered period close to weeks 4-5 (late January-early February).

### **Demarcating vegetation seasons using NDVI data**

In this study, intra-annual time series of ten-day composites of NDVI are used to define onset and offset dates of vegetation seasons. With the beginning of spring, the land surface vegetation begins to green up. In contrast, the greenness of vegetation is quickly reduced due to cold temperatures with the arrival of winter. Thus, sudden changes in the NDVI during seasonal transition periods can be used as indicators to demarcate vegetation seasons.

Methods employed in earlier studies to demarcate phenological growing seasons using the NDVI are largely categorized into two approaches: absolute threshold and relative threshold. Absolute threshold approaches use fixed values derived from regional statistics of the NDVI in several studies (Fischer 1994; Markon et al. 1995; Lloyd 1990; Hogda et al. 2001; Jia et al. 2004). For example, Jia et al. (2004) used a 0.9 NDVI as the fixed threshold to define spring onset for Arctic areas. In contrast, relative threshold approaches are based on floating values such as inflection points derived from statistical distribution curves (Badhwar 1984; Myneni et al. 1997; Tucker et al. 2001; Yu et al. 2004) and the midpoints of increasing curves (White et al. 2002; Schwartz et al. 2002). For example, Badhwar (1984) used the inflection points determined statistically from Weibull's distribution curve. There are also several studies (Myneni et al. 1997; Shabanov et al. 2002) that, without clear definition of NDVI seasons, compared the dates in later periods with the same NDVI with the dates subjectively selected in the earlier period.

The absolute threshold approach makes it less complicated to demarcate seasons, but the threshold values vary according to regions and types of vegetation (Reed et al. 1994).

The relative threshold approach using complicated statistical methods is less effective in calculating the values for more than 9000 grid cell data during the entire study period. In most previous studies, the spatial resolution of one pixel for the AVHRR NDVI imagery used to examine regional scale seasons is 1km or 8km. Cloud contamination in high resolution imagery is one of the critical issues that degrade the quality of the NDVI data. In contrast, a  $1^{\circ} \times 1^{\circ}$  coarse grid cell, the size of which is equivalent to approximately  $100\text{km} \times 100\text{km}$  at mid-latitudes, is less affected by cloud contamination, except for synoptic scale clouds that stay for more than 10 days such as monsoon cloud bands.

Figure 3.9 illustrates long-term (1982-2000) average NDVI curves for each vegetation region and the standard deviation of NDVI values across sampled multiple  $1^{\circ} \times 1^{\circ}$  grid cells. Intra-annual time series of ten-day NDVI composites, even in the coarse resolution imagery, do not always show clear inflection points at which vegetation rapidly increases or decreases. Time series of NDVI in tundra or grassland regions form bell-shaped curves with clear inflection points (Figure 3.9(a)). In contrast, the inflection points are less clear in taiga and coniferous- or deciduous-mixed forests which have complicated fluctuations between the cold and growing periods (Figure 3.9(b)-19(d)). Thus, filtering methods, such as moving averages, are needed to distinguish the steadily increasing or decreasing trend from temporary noisy peaks and troughs in the time series.

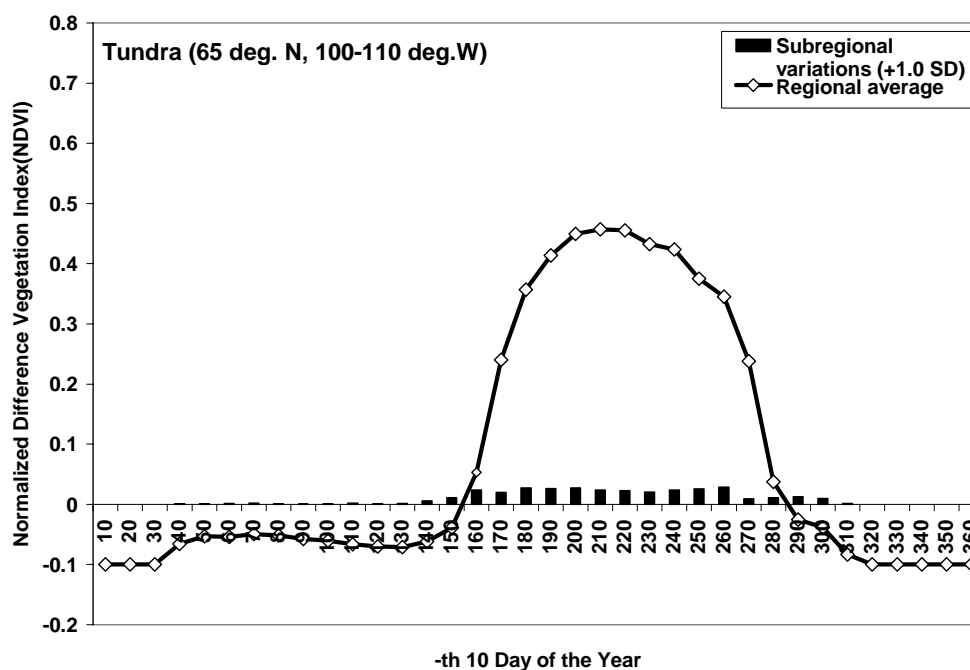
In the mid-latitude deserts of northeastern China, NDVI is less than 0.15 during the year (Figure 3.9(e)). Similarly, the NDVI values in subtropical deserts such as the African Sahara are lower than 0.1 all year round (Figure 3.9(f)). In addition, desert inflection points are more affected by intra-annual progression of precipitation than by temperature. As a result, vegetation index values are less sensitive to variations in

thermal energy during the seasonal transitional periods, and seasonal onsets based on the NDVI are not undertaken for desert regions. Similarly, the intra-annual curve of NDVI for tropical shrubs and everglades are more affected by the timing of wet-dry seasons. In tropical regions below 30°N, the NDVI difference between July and December (July minus December) is less than 0.17 (Figure 3.9(g)) because according to the spatial distribution of thermal seasons there are only summer periods without seasonal change. Inflection points indicating onsets and terminations of thermal growing seasons are not observed in the tropical regions. Thus, the thermally-driven vegetation seasonal onset and offset are defined in this study.

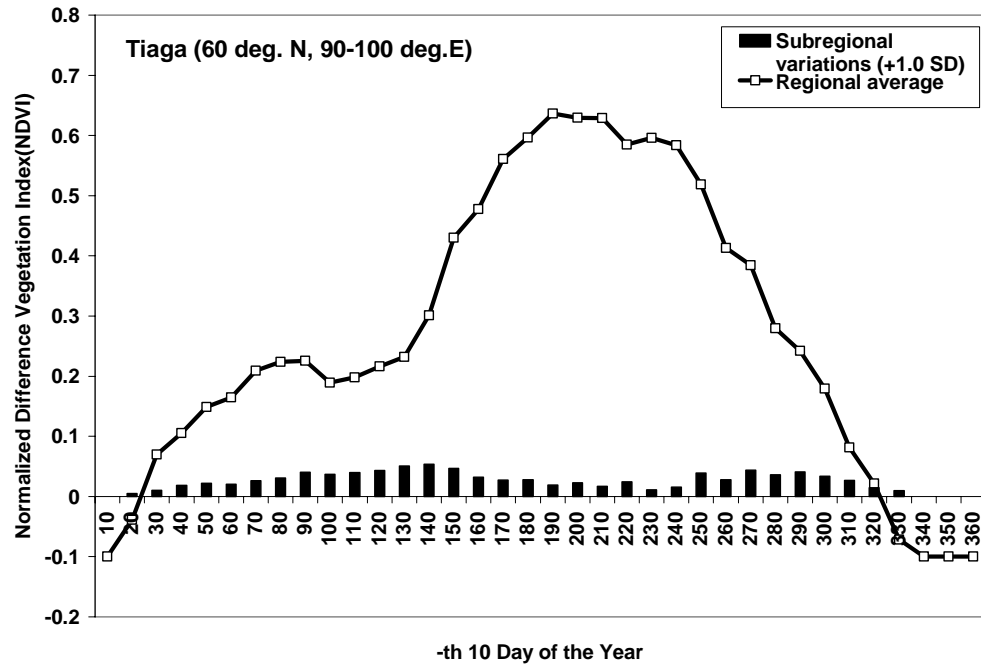
Based on the characteristics of the intra-annual NDVI variations for various forest types, the following criteria are used to define the onset and offset of vegetation seasons. First, those pixels with an NDVI of less than 0.15 are excluded because they are regarded as deserts. Similarly, those pixels where the NDVI difference between July and December is less than 0.17 are also excluded because they are taken as tropical regions where thermal summer is year round. Second, 30 day moving average NDVI is employed. This should show a continuous increasing trend for more than one month following an onset date, while the moving average NDVI before the offset date should show a continuous decreasing trend for more than one month. Continuity detection based on a 30 day moving average time series eliminates temporary peaks and troughs caused by snow events and other noise. Third, to eliminate temporary troughs caused by agricultural crop harvesting, the NDVI value on the onset date should be greater than the previous 30 day moving averages, while the NDVI value on the offset date should be greater than the following 30 day moving averages. Fourth, the onset or offset date is selected based on

an inflection point showing a sudden increase or decrease of the NDVI which is recognized by the date with the maximum value in the time series of the second derivatives of NDVI. Fifth, the onset date occurs between Day 50 and Day 210, while the offset date occurs between Day 250 and Day 20 in the following year. This method is applied to each Northern Hemisphere pixel based on intra-annual NDVI time series for the period 1982-2001.

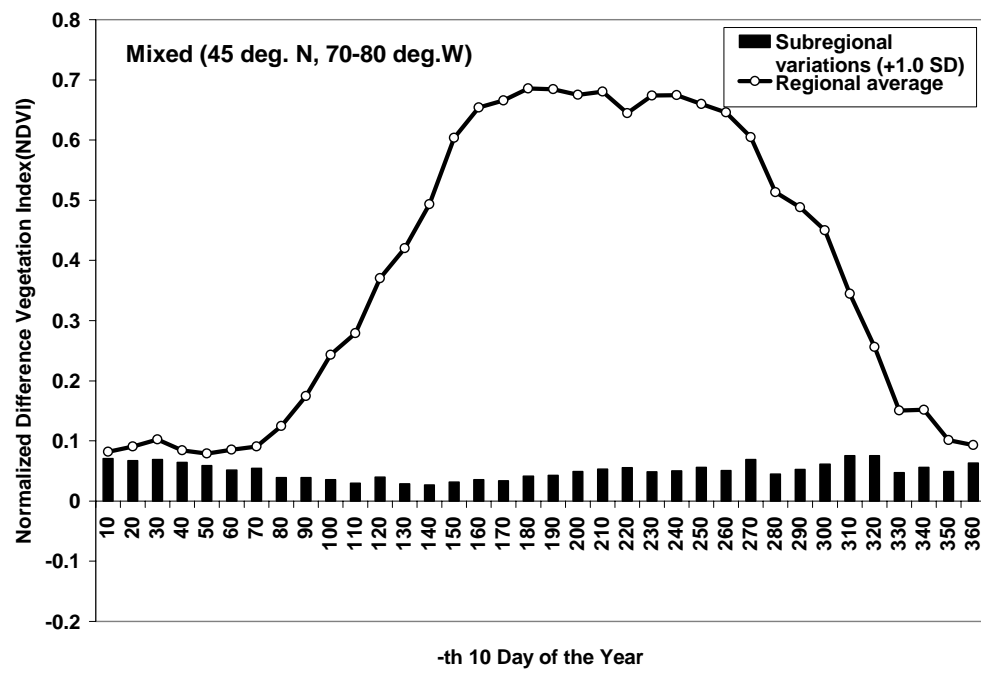
(a) Canadian tundra



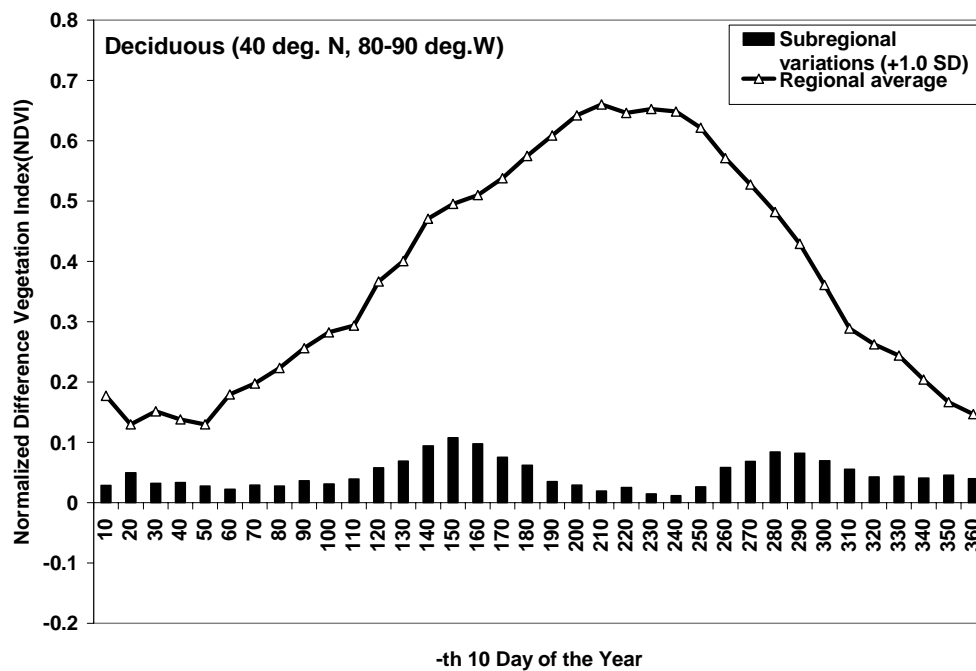
(b) Siberian taiga



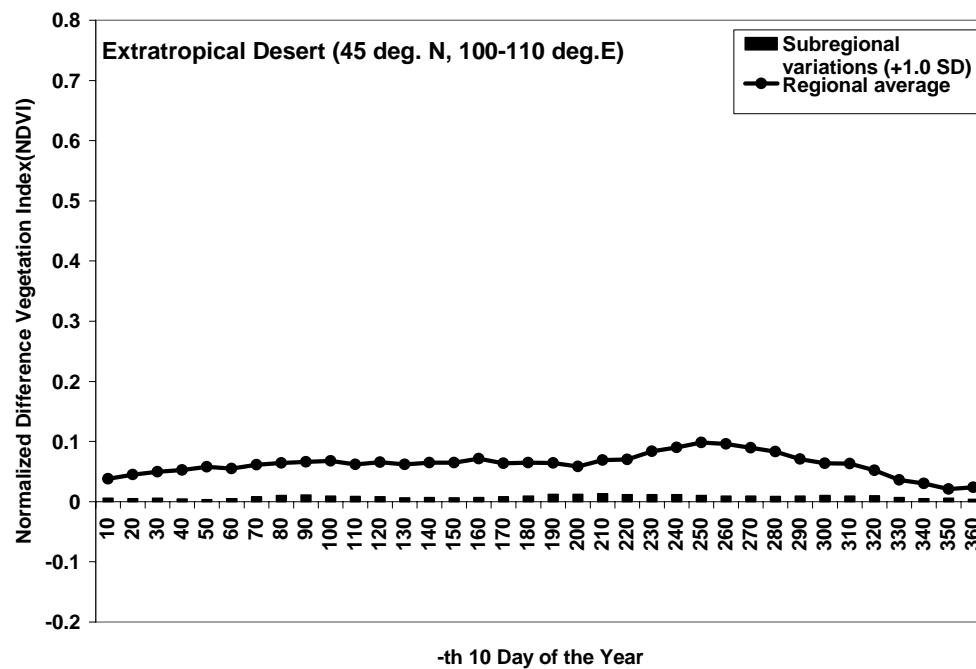
(c) Northeastern U.S. mixed forest



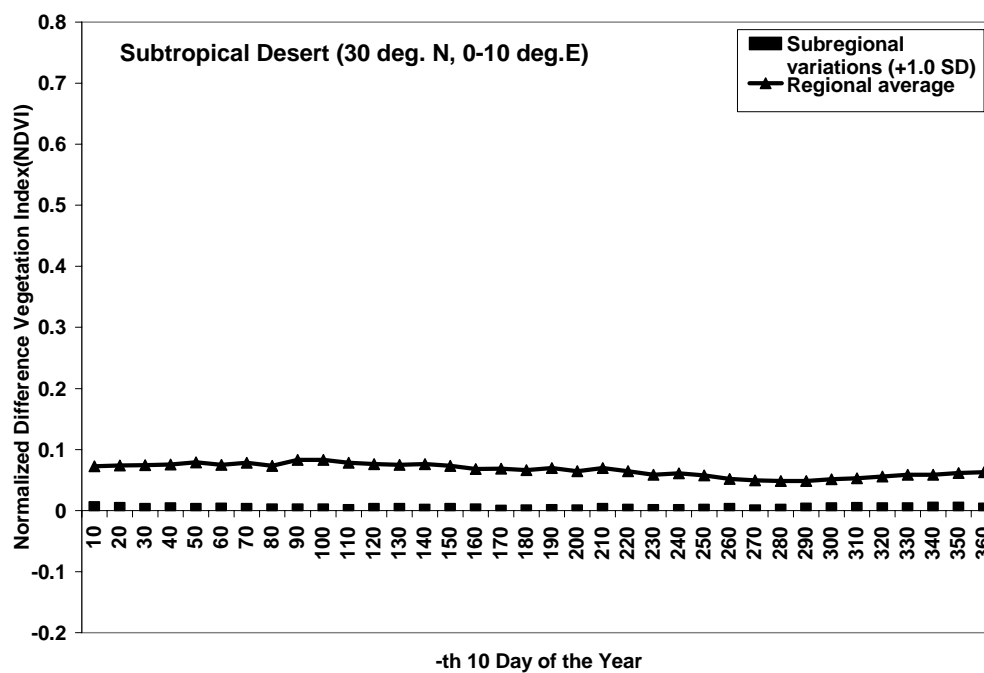
(d) Eastern U.S. deciduous forest



(e) Northern Chinese desert



## (f) Sahara desert



## (g) Indian monsoon savanna

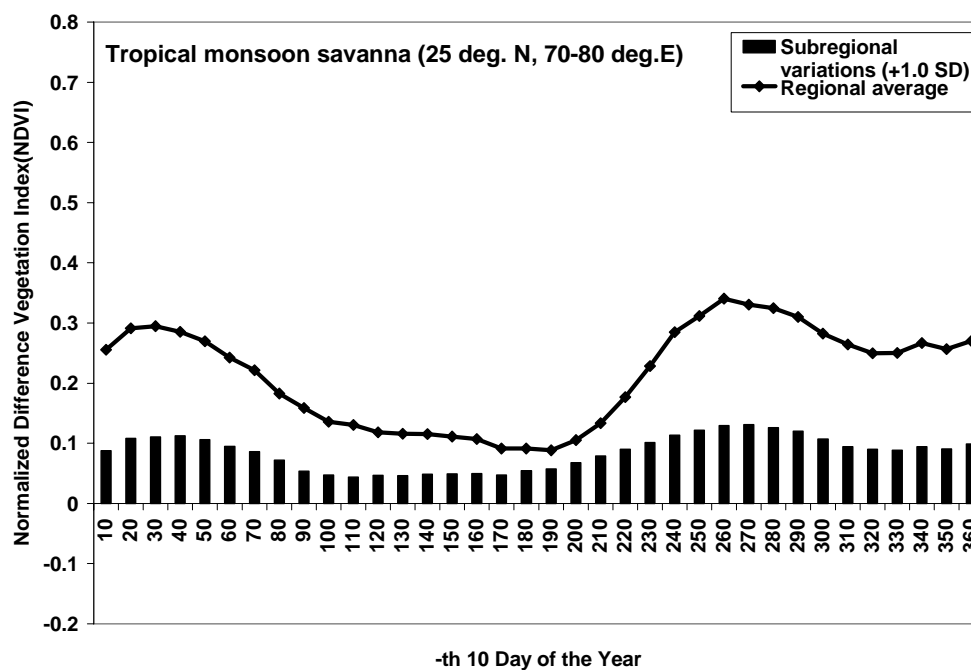


Figure 3.9. Intra-annual variability of the ten-day composite of NDVI by vegetation types (1982-2000): (a) tundra, (b) taiga, (c) mixed forest at mid-latitudes, (d) mid-latitude deciduous forest, (e) mid-latitude desert, (f) subtropical desert, and (g) tropical savanna.

## CHAPTER 4

### GEOGRAPHICAL THERMAL SEASONS IN THE NORTHERN HEMISPHERE

#### 4.1. Introduction

The spatially and temporally-varying climatological seasons derived from air temperature are called geographical thermal seasons. As reviewed in Chapter 2, there have only been a few studies that defined the floating thermal seasons on broad regional scales (Chang 1934; Jefferson 1938; Woś 1981). The threshold and methods used in them vary such that it is difficult to use them to define floating thermal seasons on a hemispheric scale. This chapter examines temporal and spatial characteristics of Northern Hemisphere thermal seasonal onsets and durations derived from NCEP/DOE reanalysis II 2m-temperature data for the period 1979-2005. As introduced in more detail in Chapter 3, four seasonal onsets and durations are extracted from the intra-annual progression curve of daily mean temperature for more than 9000 Gaussian grid cells covering the Northern Hemisphere. Eleven day moving averages are carried out to remove the small peaks and troughs in the curve so as to best determine seasonal threshold dates. The first or last dates when daily mean temperatures fall below 5°C and exceed 20°C are selected as the seasonal onset or end. Intervals between two continuing seasonal onset dates are defined as seasonal durations. These seasonal onset and duration records are extracted for each grid cell in each individual year.

The Northern Hemisphere seasonal onset and duration maps are constructed based on long term (1979-2005) average values of the seasonal data on the grid cell scale. In interpolating the grid cell data, the Inverse Distance Weighting (IDW) interpolation

algorithm in the Geostatistical Analyst of ArcGIS 9.2 is used. The variability and trends of seasonal onset date and duration are examined through analyses of standard deviation maps and time series for the study period. The spatial patterns of changes in seasonal onset and duration between the earlier and latter period are determined using the Mann-Whitney U-tests. This is a non-parametric probability test popularly used to examine the significance of differences between two groups of data (von Storch & Zwiers 2002).

The composition of this chapter is as follows: Section 4-2 depicts spatial patterns of long-term average seasonal onsets and durations on a hemispheric or regional scale such as zonal and latitudinal variations. In section 4-3 various Northern Hemisphere seasonal cycles and their spatial patterns are discussed. Section 4-4 illustrates inter-annual variability and spatio-temporal changes of seasonal onsets and durations for the period 1979-2005. Section 4.5 provides a summary and conclusion.

## **4.2. Climatologies of thermal seasonal onset and duration in the Northern Hemisphere**

### **Temporal and spatial ranges of hemispheric thermal seasons**

The latitudinal range of thermal spring onset progression is similar to that of thermal winter onset, but logically they progress into the opposite direction (Figure 4.1). Both the earliest thermal winter onset and the latest spring onset occur at 81°N around the Arctic Ocean in early August, while the latest thermal winter onset and the earliest thermal spring onset occur at 17°N over northern Africa in early February. The temporal range of thermal spring onset (Day 14-Day 212) is 31 days longer than that of thermal winter

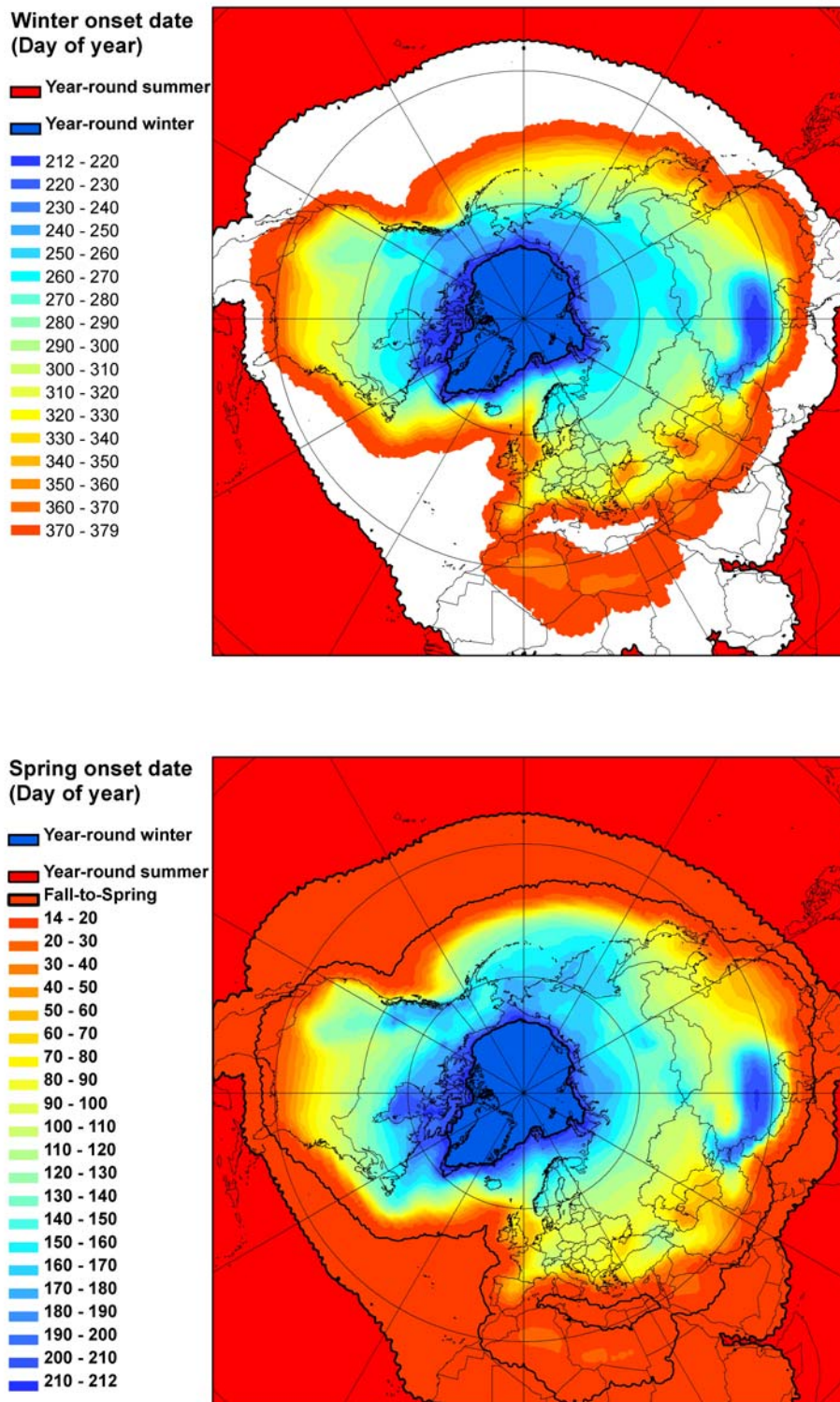


Figure 4.1. Spatial patterns of thermal winter onset (top) and thermal spring onset (bottom) in the Northern Hemisphere, 1979-2005

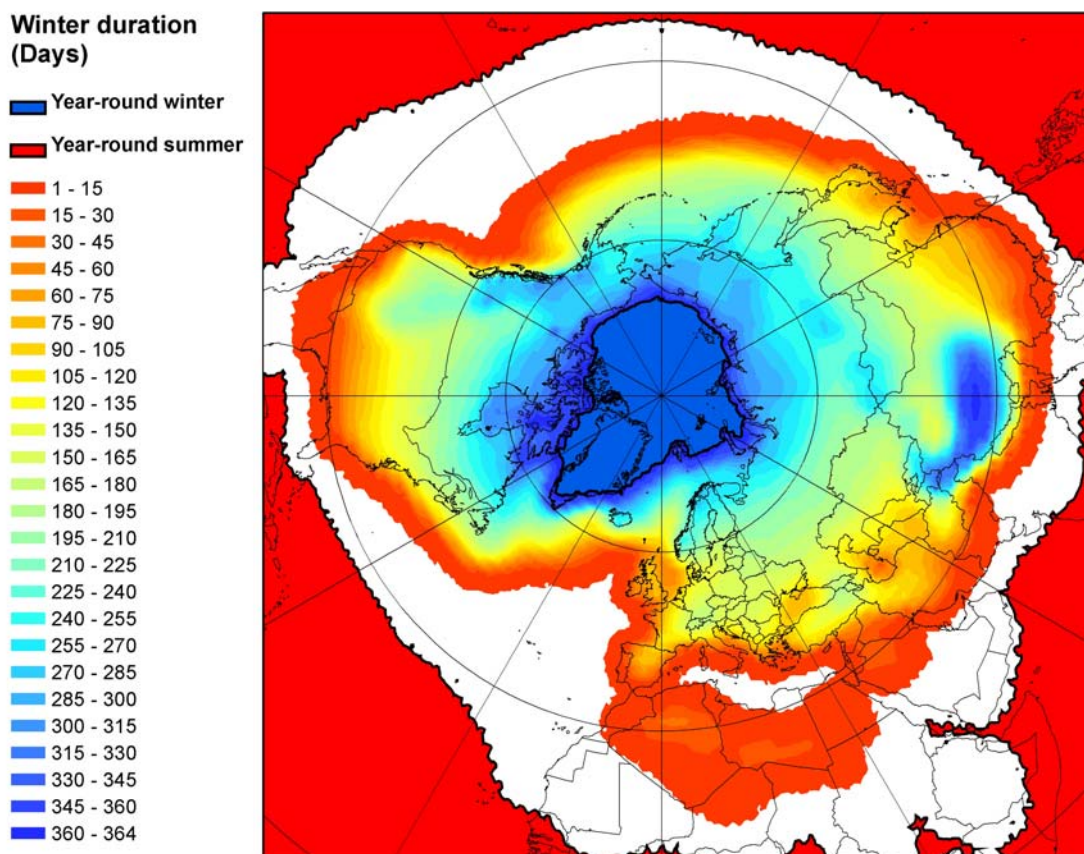


Figure 4.2. Spatial patterns of thermal winter duration in the Northern Hemisphere, 1979-2005

onset (Day 212 – Day 379). The thermal winter duration, which is the interval between the winter onset and the spring onset, varies from 1 day in the low latitude fringe to 365 days in the Arctic Ocean. The snow/ice albedo feedback may delay northward propagation of thermal spring onset. The high albedo of the snow pack diminishes the amount of solar radiation available to melt the snow. In contrast, the absorption and retention of solar energy by the Arctic Ocean during the ice/snow-free period delays the formation of cold air masses. Thus, the southward propagation of thermal winter onset

may be associated with the delay of cold air masses due to the thermal inertia of the Arctic Ocean.

Compared with oceans, the southern fringe of thermal winter progression is located further south over land masses (Figure 4.2). The southern fringe over land masses passes northern Mexico, northern Sahara Africa, northern Middle East, and southern China. In contrast, over oceans, it encompasses the coastal lines in North America to 45°N, in Europe to 55°N, and in northeastern Asia to 30°N. The latitudinal range of thermal winter duration over land masses is 2.5 times greater than that over the oceans. The southern fringe over oceans is 5-25° of latitude further north over eastern sides of oceans than over western sides. As a result, the zonal patterns of thermal winter and spring onsets are modified in the northeastern Pacific and Atlantic. The zonal patterns of thermal winter duration are elongated southward in these regions. The northern fringe of both the earliest winter onset and the latest spring onset surrounds Arctic coastlines and passes southern Greenland. In the Arctic Ocean above the fringe, thermal winter continues all the year round.

The spatial range of thermal seasonal duration is inversely associated with the progression speed of seasonal onset and offset (Figure 4.3). Thermal winter onset propagates southward at a rate of 3.0- 3.5 days/degree along central regions of land masses such as eastern Asia (110°E), western Asia (60°E), and North America (100°W). Northward propagation speeds of thermal spring onset are 3.4-4.1 days/degree over land masses. Hopkin's (1919) estimated that the bioclimatic seasonal progression of plants and animals in North America was 4 days/degree of latitude for both spring and winter onsets. This is similar to the progression of thermal spring found in this study, while the current

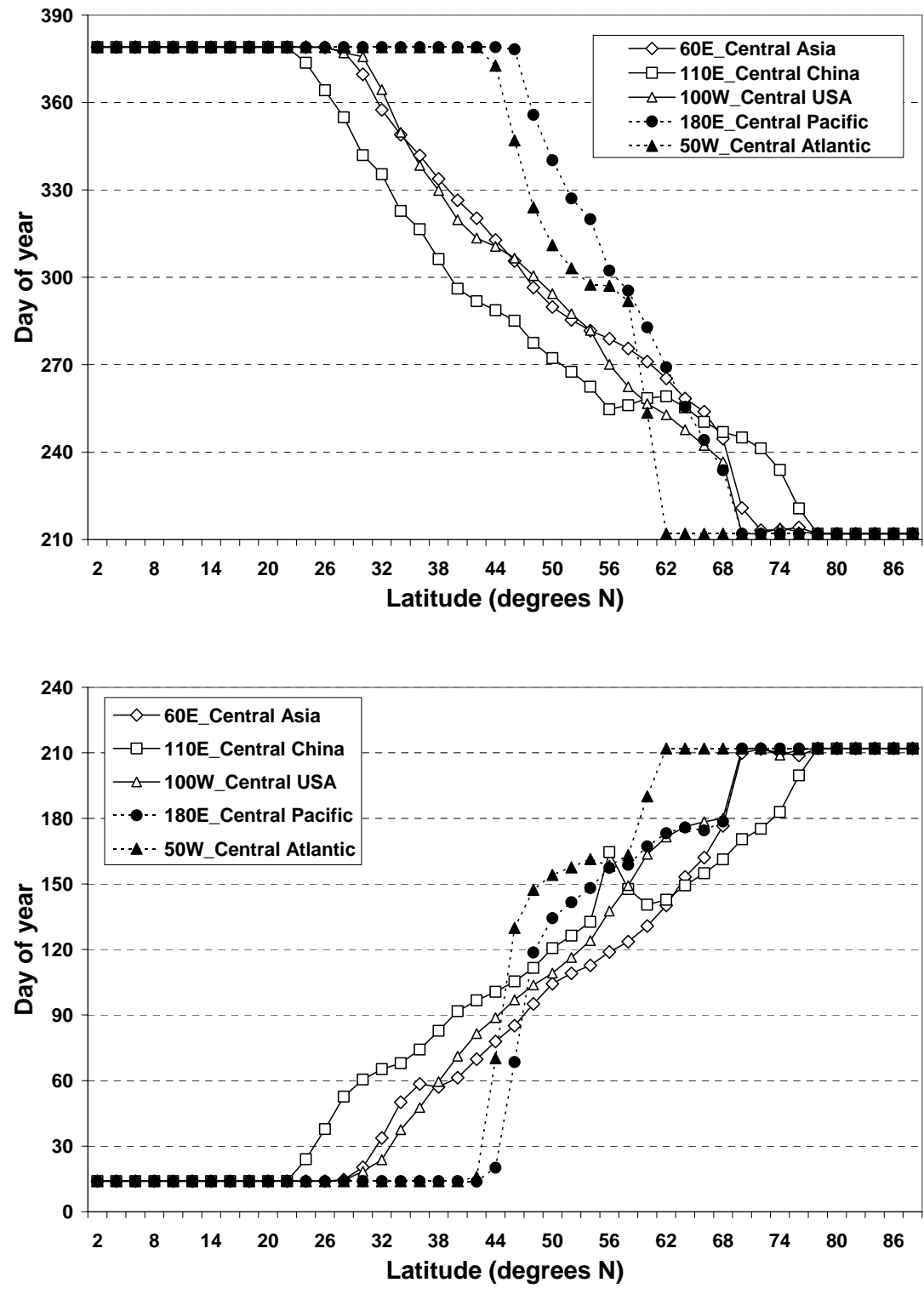


Figure 4.3. Latitudinal gradients of thermal winter onset (top) and thermal spring onset (bottom) dates over land masses (open symbols) and over oceans (filled symbols) in the Northern Hemisphere

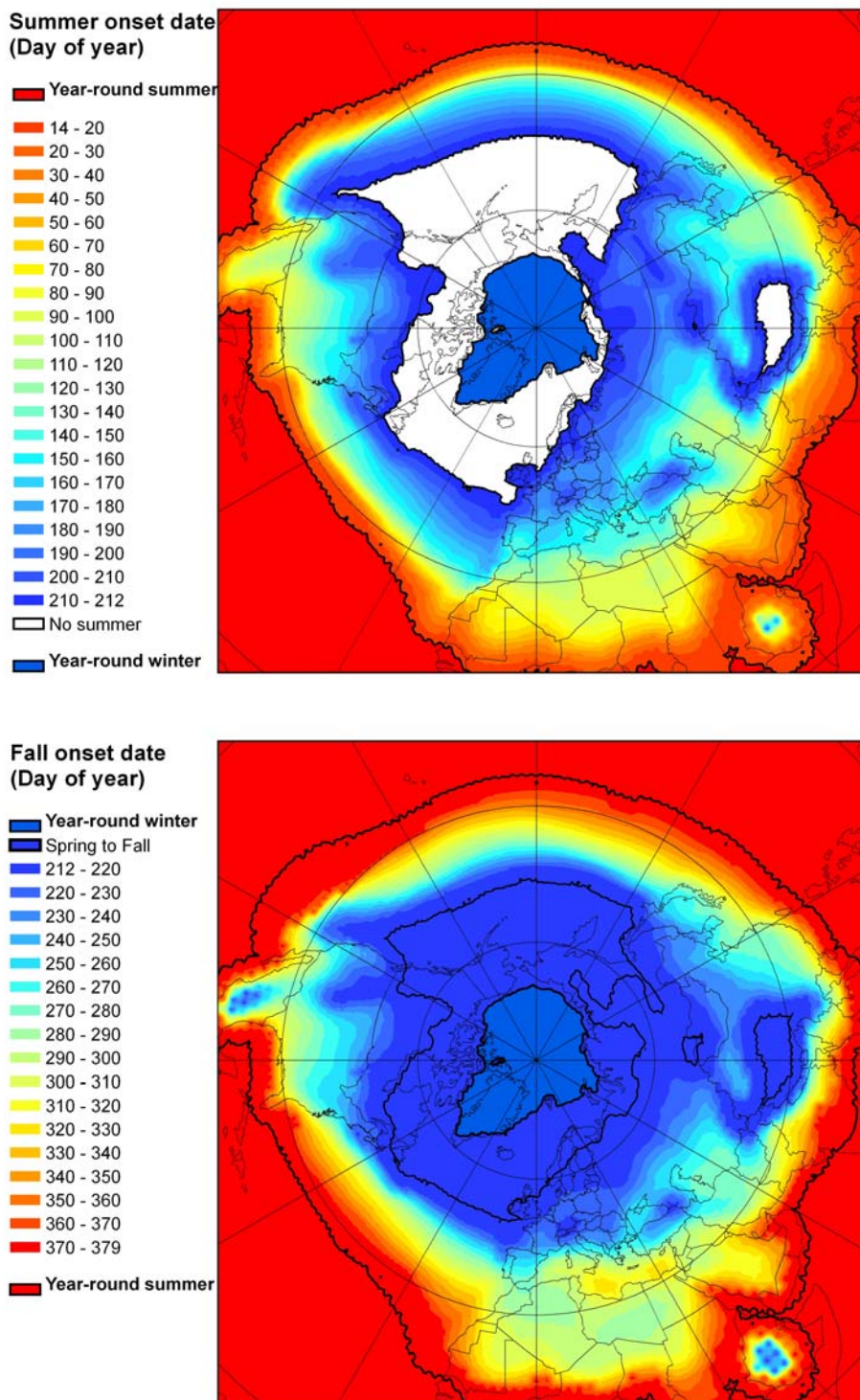


Figure 4.4. Spatial patterns of thermal summer onset (top) and thermal fall onset (bottom) dates in the Northern Hemisphere, 1979-2005

observed thermal winter onset progresses at a much faster speed than Hopkin's (1919) estimate. In contrast, the propagation speeds of both thermal winter onset and thermal spring onset over oceans are 1.7-2.0 times slower than over land masses. The progression speeds of thermal winter onset are 6.3-6.9 days/degree over the central Pacific (180°E) and the central Atlantic (50°W). Thermal spring onset propagates at a rate of 6.4 - 7.2days/degree over the oceans.

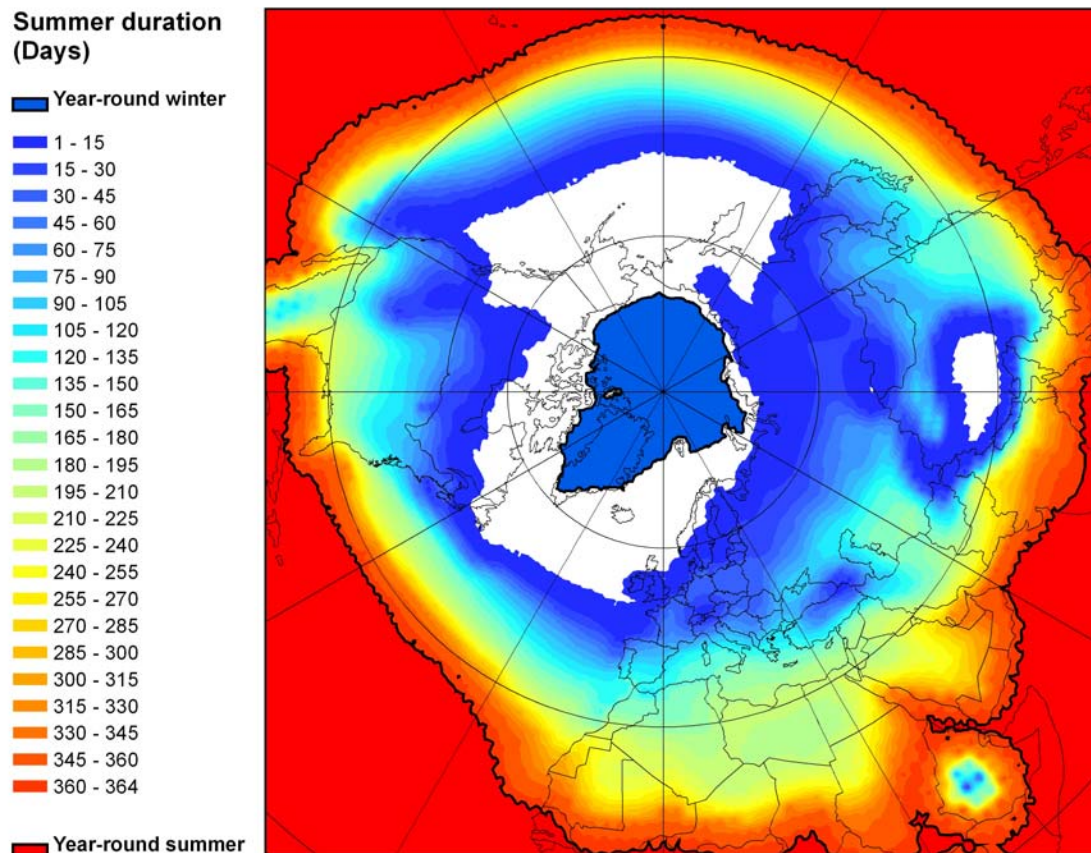


Figure 4.5. Spatial patterns of thermal summer duration in the Northern Hemisphere, 1979-2005

The spatial range of thermal summer onset progression is similar to that of thermal fall onset (Figure 4.4). The southern fringe where summer continues all the year round appears over low latitude oceans below 25°N, and over land masses it retreats more southward to 5°N in Africa, 6°N in North America, and 14°N in Asia (Figure 4.5). The boundary where both thermal summer onset and thermal fall onset is located further north over land masses than oceans. It is located at 71°N along the Arctic coastline in Eurasia and at 62°N across the southern regions of the Northwest Territories in Canada, while it is located at 42 °N over the Pacific and at 47°N over the Atlantic. The latitudinal range of thermal summer onset and thermal fall onset is 2.5 times greater over land masses than over oceans. The temporal range of thermal summer onset (Day 14 – Day 212) is longer than that of thermal fall onset. The summer is shorter by 15 days (between late July and early August) along the northern fringe of either thermal summer onset or thermal fall onset. These regions extend 16° of latitude further north over land masses than over oceans, while thermal summer onset, offset, and duration show more zonal patterns over oceans than over land masses.

Over oceans, the latitudinal progression speeds of both thermal summer onset and thermal fall onset are 1.7 times slower than those of thermal winter onset and thermal spring onset (Figure 4.6). The northward propagation speeds of thermal summer onset are 12.5-13.7 days/degree of latitude, and southward propagation speeds of thermal fall onset are 9.0-9.9 days/degree of latitude. In contrast, over land masses, the progression speeds of both thermal summer onset and thermal fall onset are similar to those of thermal winter onset and thermal spring onset. Thermal summer onset over land masses

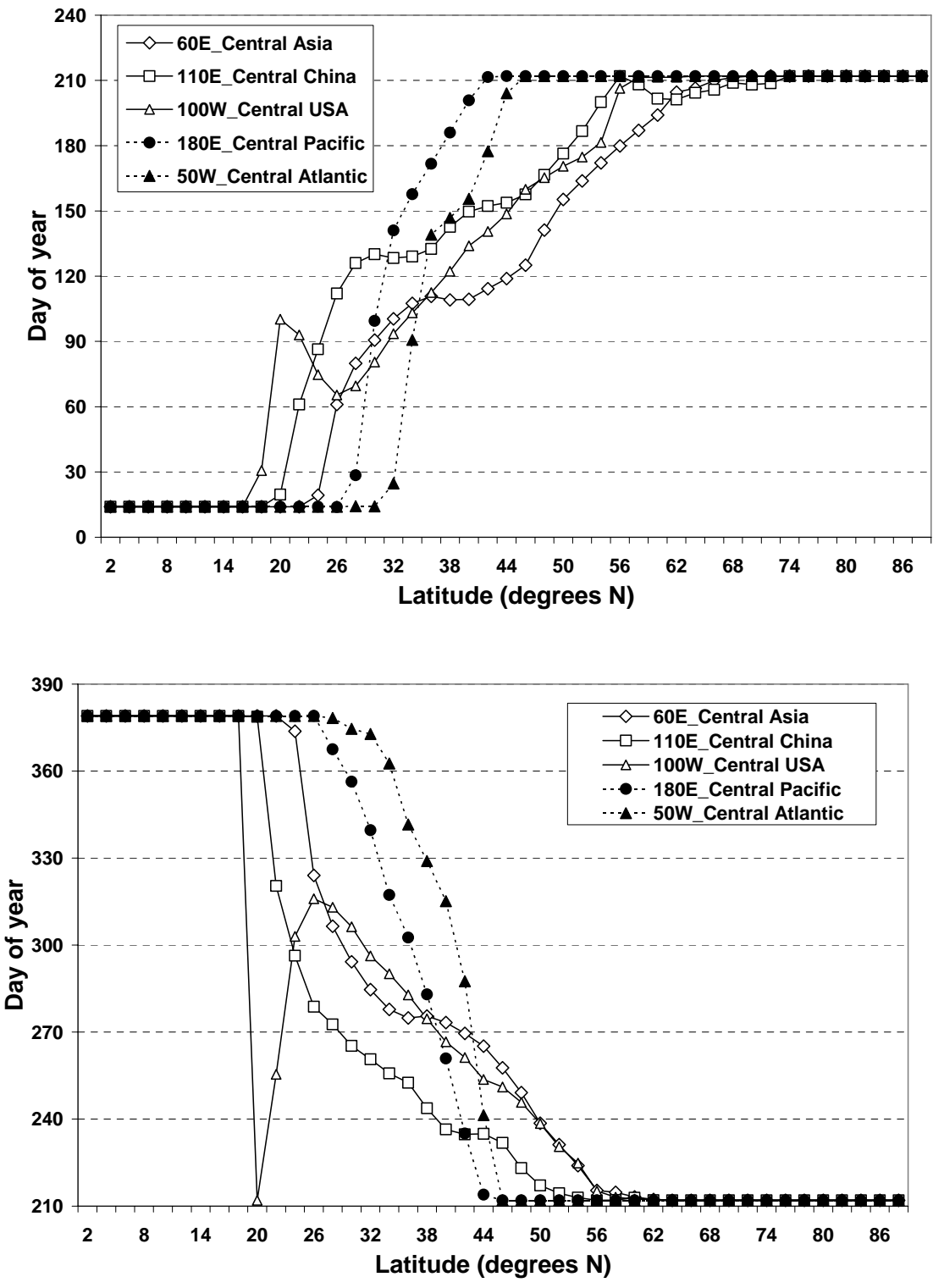


Figure 4.6. Latitudinal gradients of thermal summer onset (top) and thermal fall onset (bottom) dates over land masses (open symbols) and over the oceans (filled symbols) in the Northern Hemisphere

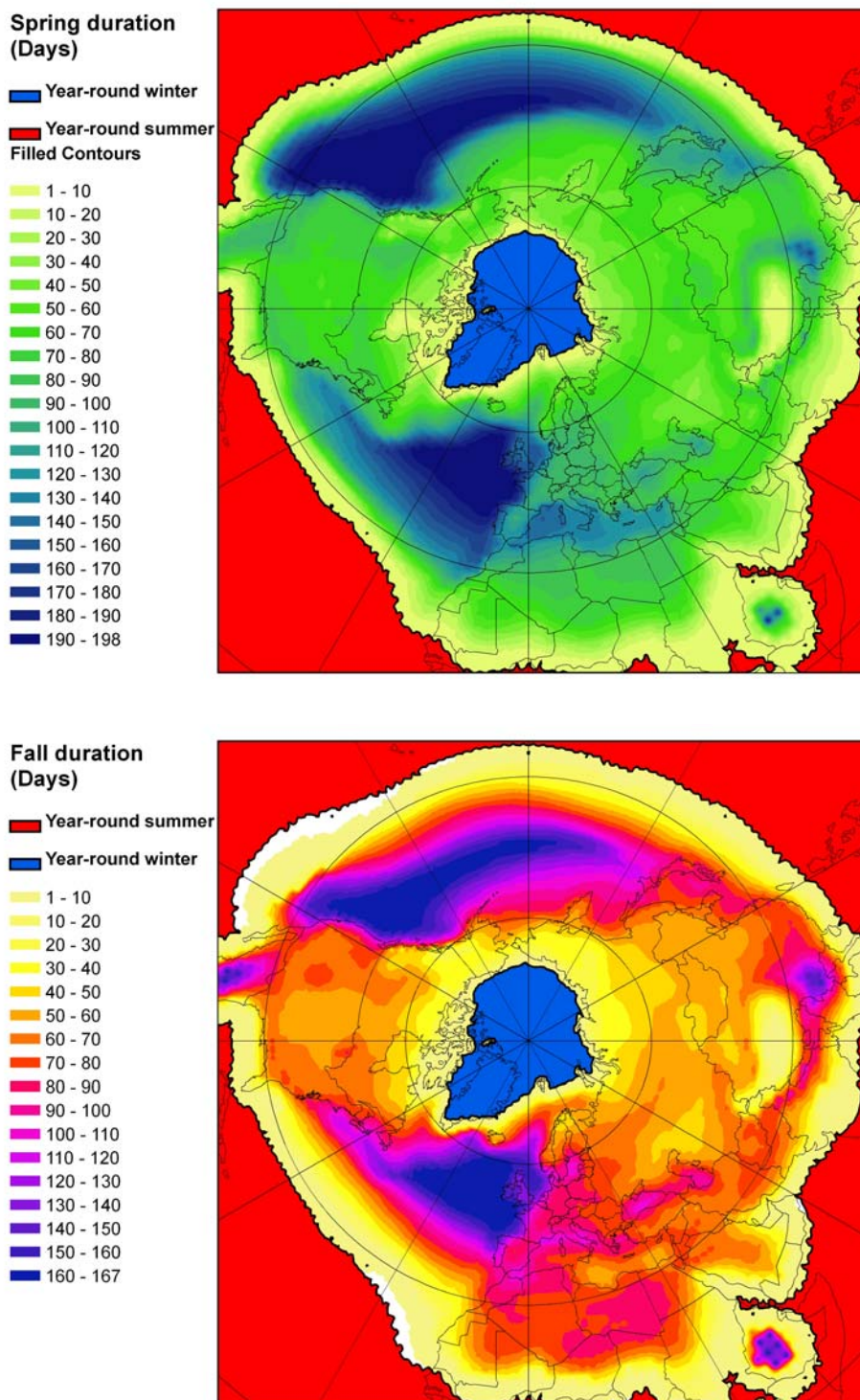


Figure 4.7. Spatial patterns of thermal spring duration (top) and thermal fall duration (bottom) in the Northern Hemisphere, 1979-2005

propagates northward at a rate of 3.6-4.8 days/degree of latitude, while the southward speed of thermal fall onset is 3.2-4.0 days/degree of latitude. The progression speed of thermal summer onset is 3.4 times faster over land masses than oceans. Similarly, the propagation speed of thermal fall onset over land masses is 2.7 times faster than that over oceans.

Thermal spring and thermal fall durations are longer over oceans than land masses at mid-latitudes (Figure 4.7). Over land masses, the thermal spring duration is less than 110 days, and thermal fall duration is less than 90 days. The longest thermal spring and thermal fall durations occur in the eastern Pacific (120-180°W, 26-52°N) and Atlantic (5-40°W 40-58°N). In these regions, thermal spring lasts for more than 180 days, and similarly thermal fall lasts for more than 160 days. The thermal spring and fall durations in the western side of the oceans are at least 50 days shorter than toward the east. In contrast, thermal spring and fall last for less than 10 days over land masses between 25-30°N as well as in Arctic tundra regions. Zonal patterns of thermal spring and fall are clearly evident over oceans, while over land masses the zonal patterns are not obvious.

### **Regional variations of thermal seasons**

Zonal patterns of thermal seasonal onset and duration are modified by regional static factors such as elevation, topography, and proximity to water bodies, as well as dynamical factors such as air masses and ocean currents. Over the Tibetan Plateau, the average elevation amounts to 4500m above seal level and the highest elevation exceeds 5000m. Similarly, the highest peak in the Himalayas exceeds 8800m. In these highland regions, spring onset is 120 days later (Figure 4.8), while the fall onset is 60 days earlier

compared with nearby lowlands in China. As a result, winter lasts for 240 days or more without thermal a summer period. This results in a 60-120 day spring-fall period (Figures 4.7). The Canadian Rockies are also free from the occurrence of thermal summer (Figure 4.5).

The impacts of high elevation are detected over highlands at low latitudes such as central Mexico at 22°N and Ethiopia in Africa at 8°N. For instance, fall onset over the highlands in central Ethiopia is 70-100 days earlier than in nearby low-elevated tropical regions (Figure 4.8). Over these tropical highlands, both spring and fall durations last for at least 90 days, whereas summer continues for more than 330 days over nearby tropical lowlands. Similarly, over highland areas in Mexico (elevations exceeding 2000m), the length of summer is 120-150 days, while over nearby low-elevation locations it is more than 300 days (Figure 4.5).

Lakes and proximity to oceans and seas are other factors that modify the zonal patterns of seasonal onsets and durations on regional scales. Winter onset dates around the Black Sea and the Caspian Sea are 40 days later and winter duration is 40-90 days shorter compared with neighboring inland areas (Figure 4.10). Over the Mediterranean Sea, winter does not occur, while winter is 10 days or less over northern Africa (Figure 4.2). Over Hudson Bay, winter lasts for more than 285 days, whereas at similar latitudes in the northeastern Atlantic, winter duration is less than 15 days. The relatively warm Gulf Stream waters that include the latter regions result in spring and fall durations that are 100 days longer than over landmasses at similar latitudes (Figure 4.7). In contrast, cold ocean currents such as California and Canary Currents result in no summer until south of 35-45°N over eastern Pacific and Atlantic oceans (Figures 4.5 and 4.9)

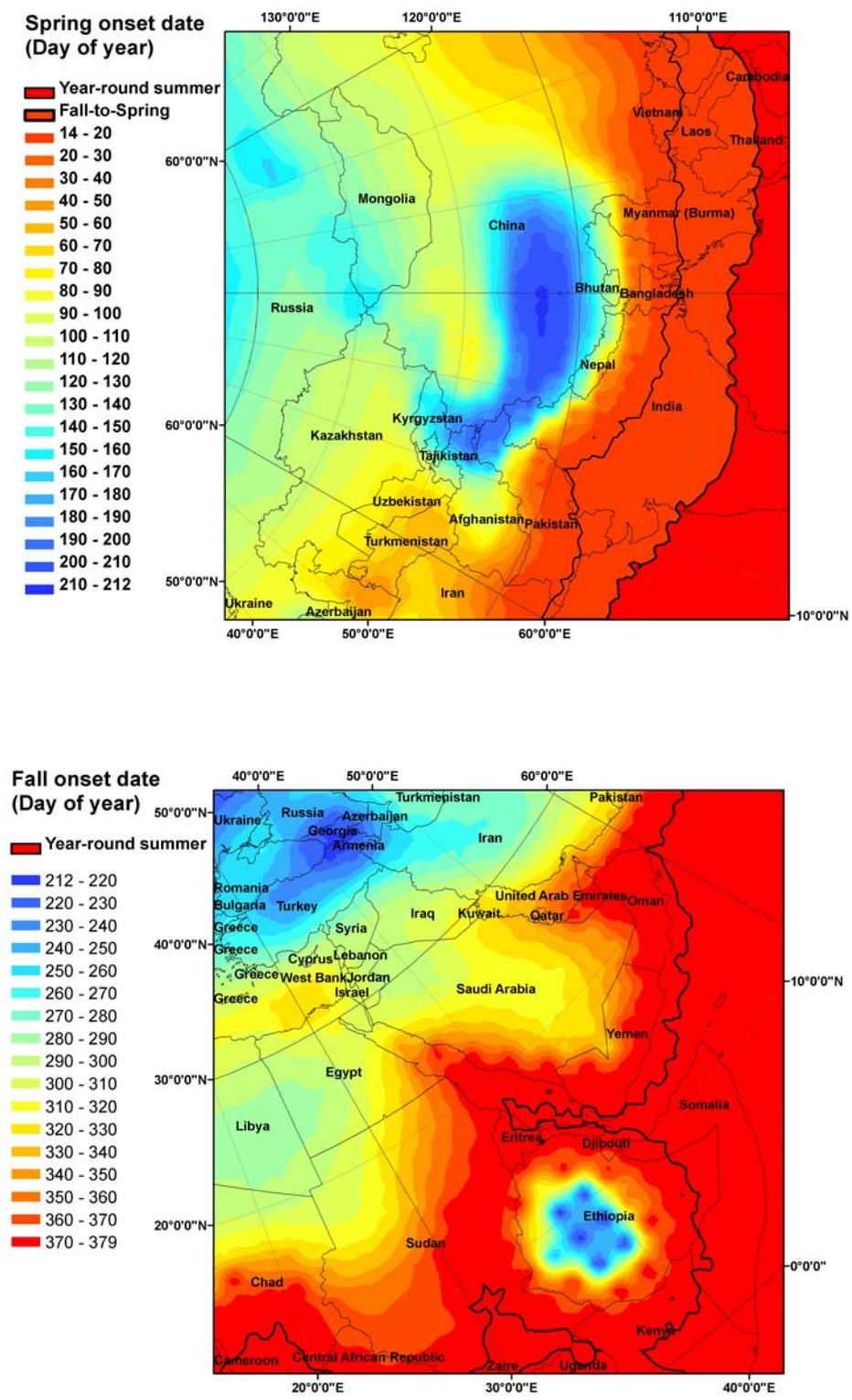


Figure 4.8. Impacts of high elevation on thermal spring onset in the Tibetan Plateau and the Himalayas (top) and thermal fall onset in central Ethiopia (bottom)

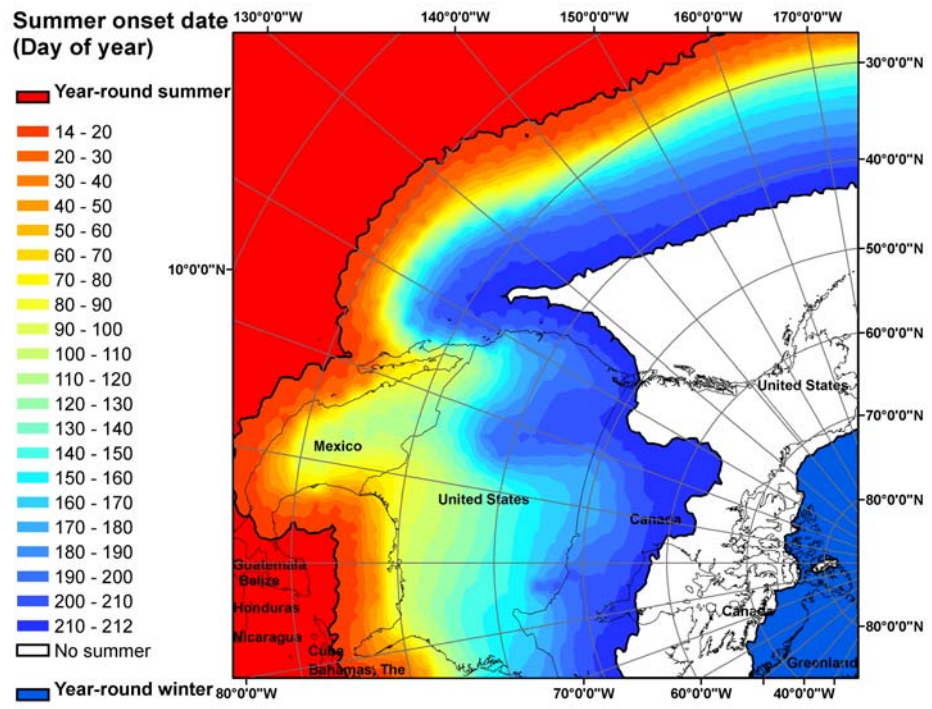


Figure 4.9. Impacts of the cold California Currents and the high elevation of the Rockies on thermal summer onset

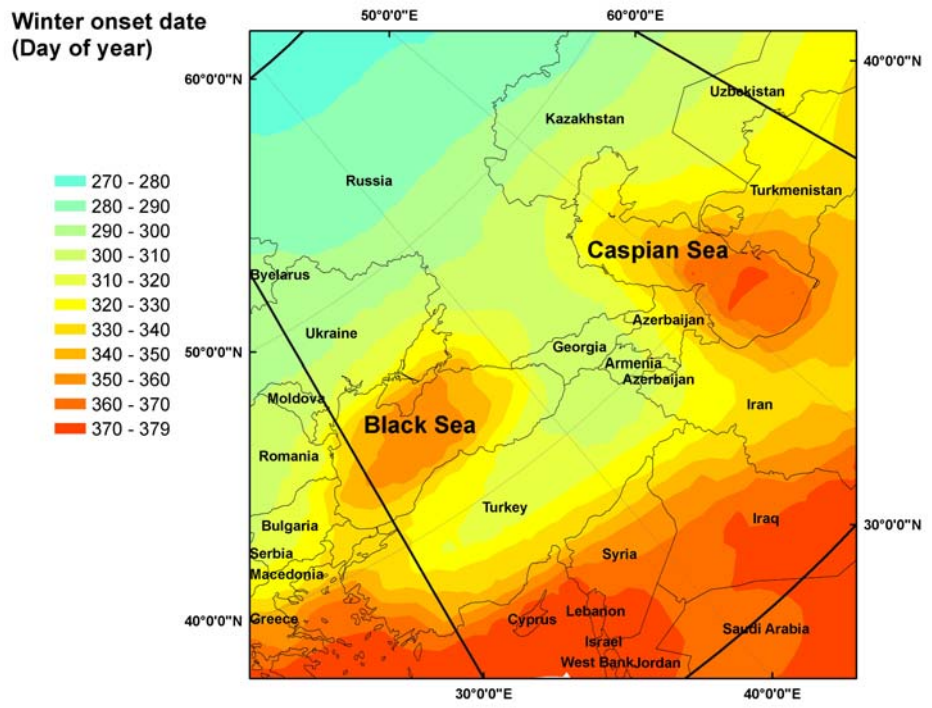


Figure 4.10. Impacts of water bodies on delay of thermal winter onset over the Black Sea and the Caspian Sea

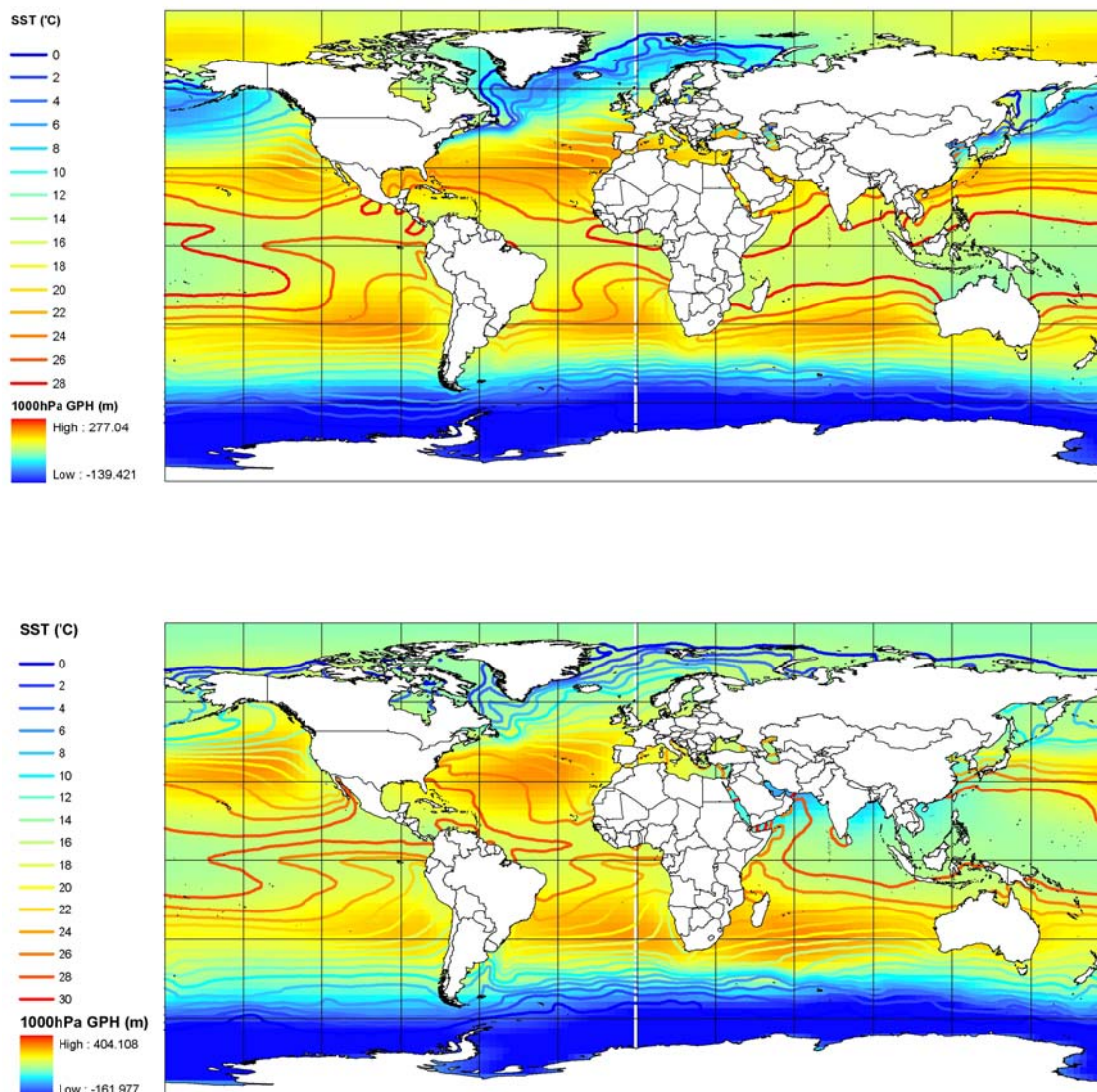


Figure 4.11. 1000hPa geopotential height (1979-2005) and sea surface temperature (1982-2005) during the meteorological winter (DJF) (top) and during the meteorological summer (JJA) (bottom)

In addition to static factors such as latitude, elevation, and surface condition, dynamical factors, including ocean currents or locations of quasi-stationary air masses, influence the spatial ranges of each thermal seasonal onset and duration. Figure 4.11 shows long-term average (1979-2005) 1000hPa geopotential heights (color solid line) and sea surface temperature (SST) (color shaded) during the cold period (DJF). Quasi-

stationary high pressure systems such as the Pacific High and Bermuda High are observed in the eastern side of the oceans. These dynamical factors extend the spatial range of winter-absent cycle toward the northeastern side of both oceans. In contrast, according to the maps for the hot period (JJA), cold ocean currents such as the California Current and Canary Current result in the positioning of the northern boundary of the summer-only cycle a 5-10° further south over the eastern side of both the Pacific and Atlantic oceans.

#### **4.3. Thermal seasonal cycles in the Northern Hemisphere**

Previous studies that define seasons presumed that four seasons repeat in the order of spring-summer-fall-winter year-to-year everywhere on the globe as a standard annual climate cycle. However, this study finds that there are seven different types of thermal seasonal cycles in the Northern Hemisphere (Table 4.1). They include winter-only, summer-absent, four-seasons, spring-fall-only, winter-absent, spring-summer-only, and summer-only. Latitude and surface condition determine the spatial patterns of each thermal seasonal cycle. The seven seasonal cycle regions form zonal patterns along similar latitudes between the Arctic Ocean and the tropics. However, their latitudinal ranges are not identical between land masses and oceans. Moreover, over oceans, all seven seasonal cycles are present, whereas over land masses, spring-fall-only cycle does not occur.

The winter-only cycle occurs within the Arctic Ocean above 72°N, and extends southward to 63°N over Greenland (Figure 4.12). The summer-absent cycle occurs in the northern Pacific and northern Atlantic (43°N-71°N) as well as across Canadian Pacific

Table 4.1. Types of thermal seasonal climate cycles in the Northern Hemisphere

Thermal seasonal cycles					Spatial ranges	
Types	Sp	Su	Fa	Wi	Oceans	Land masses
Winter-only				■	72°N ≤ latitude (Arctic Ocean)	63°N ≤ latitude ≤ 83°N (Greenland)
Summer-absent	■		■	■	43°N ≤ latitude ≤ 72°N (Northern Pacific and northern Atlantic)	50°N ≤ latitude ≤ 81°N (Canadian Pacific regions to Arctic islands) & 30°N ≤ latitude ≤ 35°N (Himalayas/Tibetan Plateau)
Four-seasons	■	■	■	■	20°N ≤ latitude ≤ 50°N (Along southern China Sea to northwestern Atlantic)	12°N ≤ latitude ≤ 72°N (northern Africa– Siberian tundra)
Spring-fall-only	■		■		130-137°W, 42-45°N, or 13-22°W, 50-55°N	
Winter-absent	■	■	■		13°N ≤ latitude ≤ 50°N (Pacific along Mexico to northeastern Atlantic)	0°N ≤ latitude ≤ 26°N (Eastern Africa, northern India, and southern Mexico)
Spring-summer-only	■	■			14°N ≤ latitude ≤ 27°N (Southeastern Pacific and southeastern Atlantic)	0°N ≤ latitude ≤ 12°N (Sahel Africa and southern Mexico)
Summer-only		■			latitude ≤ 25°N (Southern Atlantic and southern Pacific)	latitude ≤ 20°N (Yucatan Peninsula in Mexico and southern India)

regions, northern Canada, and the Canadian Arctic islands (50°N-81°N). They surround the winter-only region and extend southward over oceans than over land masses. The summer-absent cycle is also observed over the Himalayas and the Tibetan Plateau. The four-season cycle occurs over most of the middle and high latitude land masses, whereas over oceans, it is confined to the northwestern Pacific and Atlantic as well as off coastal regions adjacent to mid-latitude land masses. The spring-fall-only cycle is found over small areas of the northeastern Atlantic (13-22°W, 50-55°N) and Pacific (130-137°W, 42-45°N). The winter-absent cycle occurs along the central Pacific and the central Atlantic, as well as in Mexico and Sahel Africa. The summer-only cycle prevails over the tropical oceans below 25°N and over tropical land masses below 20°N.

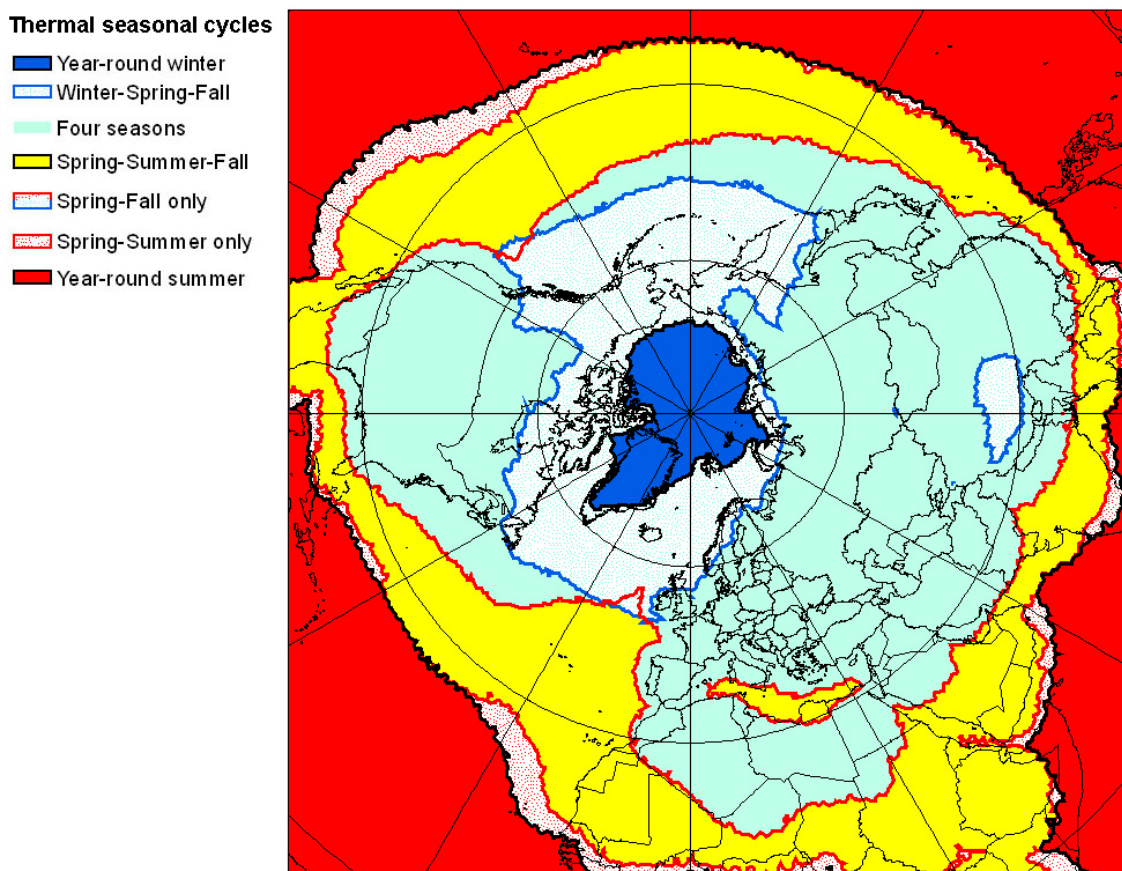


Figure 4.12. Spatial distribution of various thermal seasonal cycle types in the Northern Hemisphere.

#### 4.4. Inter-annual variability and temporal trends of thermal seasonal onsets and durations

The inter-annual variability of thermal winter and summer durations for the study period 1979-2005 is illustrated in standard deviation maps (Figure 4.13). High inter-annual variations of summer duration are observed over oceans along 30 °N, while winter duration is highly variable around fringes of the Arctic Ocean and along high mountain ridges at mid-latitudes. In these regions, the inter-annual variability of both winter and summer durations corresponds to  $\pm 25$  days. In contrast, inter-annual variability of

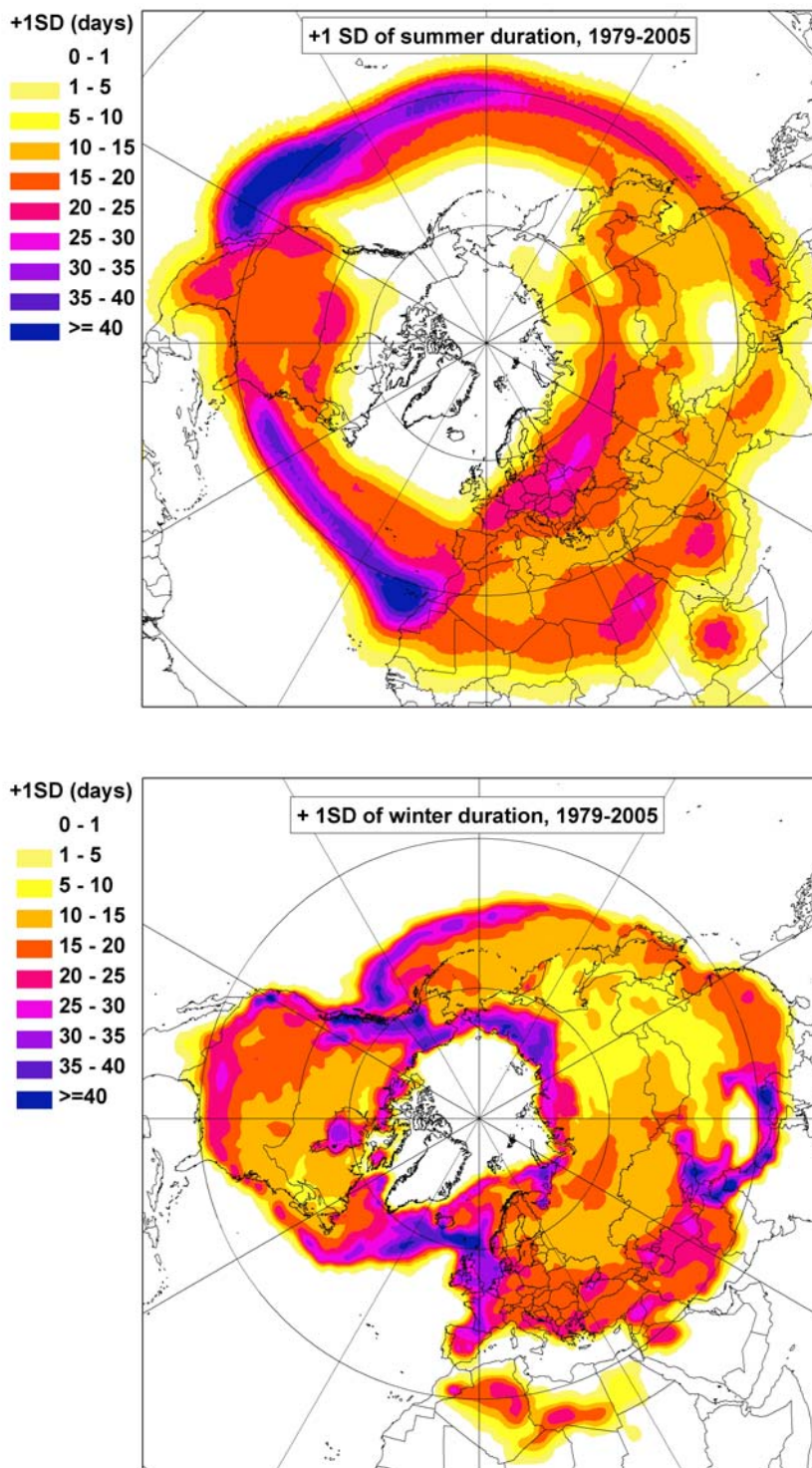


Figure 4.13. Inter-annual variability (one standard deviation) of the Northern Hemisphere averages of thermal summer (upper) and winter (bottom) durations, 1979-2005

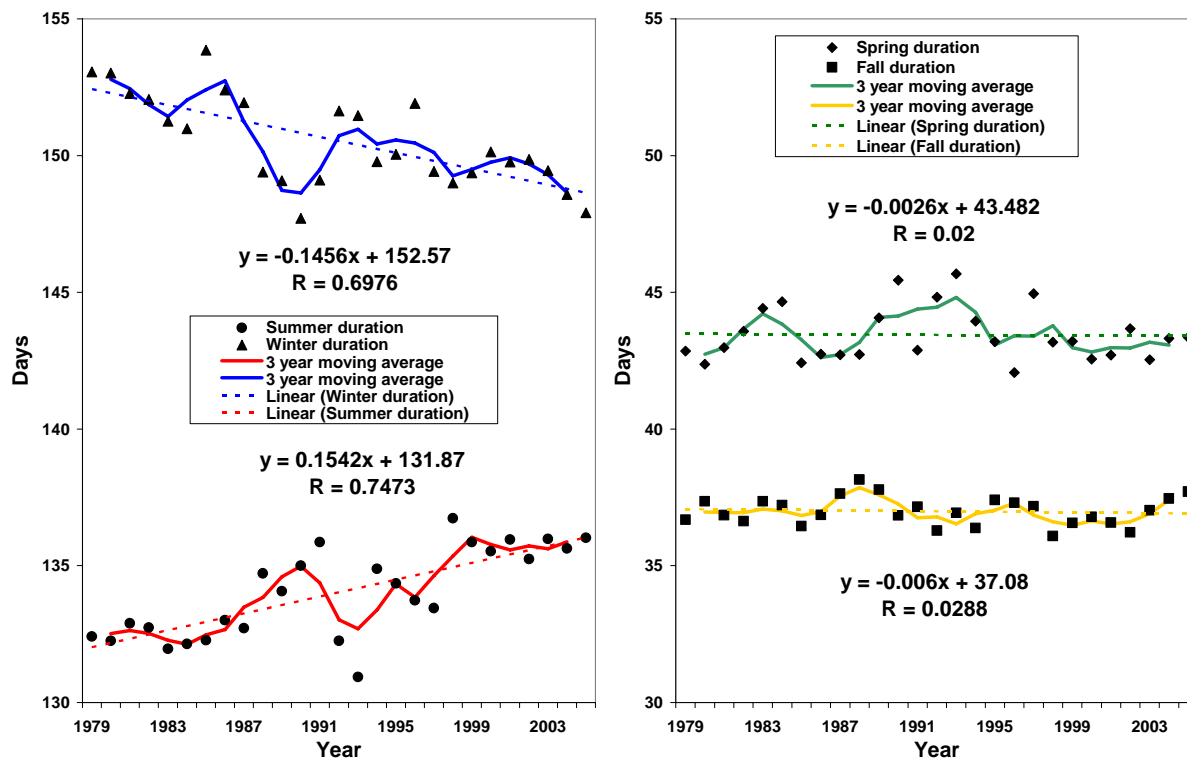


Figure 4.14. Fluctuations of the Northern Hemisphere average of the spatially-varying thermal summer and winter durations, 1979-2005

summer duration is less than 15 days at lower mid-latitudes in Eurasia and northern Africa, while the variability is low (10 days or less) in eastern Siberia and northern China.

Floating thermal seasonal onsets and durations at the grid cell scale are averaged and displayed as inter-annual time series to examine variability at a hemisphere scale (Figure 4.14). The averages of the observed summer and winter durations are greater than those of the spring and the fall. Winter duration has decreased by 3.9 days, while summer duration has increased by 4.2 days between 1979 and 2005. Spring and fall durations show small inter-annual fluctuations without any temporal trends.

To determine the inflection point year in the times series (Figure 4.14), Mann-Whitney U tests are performed. Significance level and z-value are calculated for the

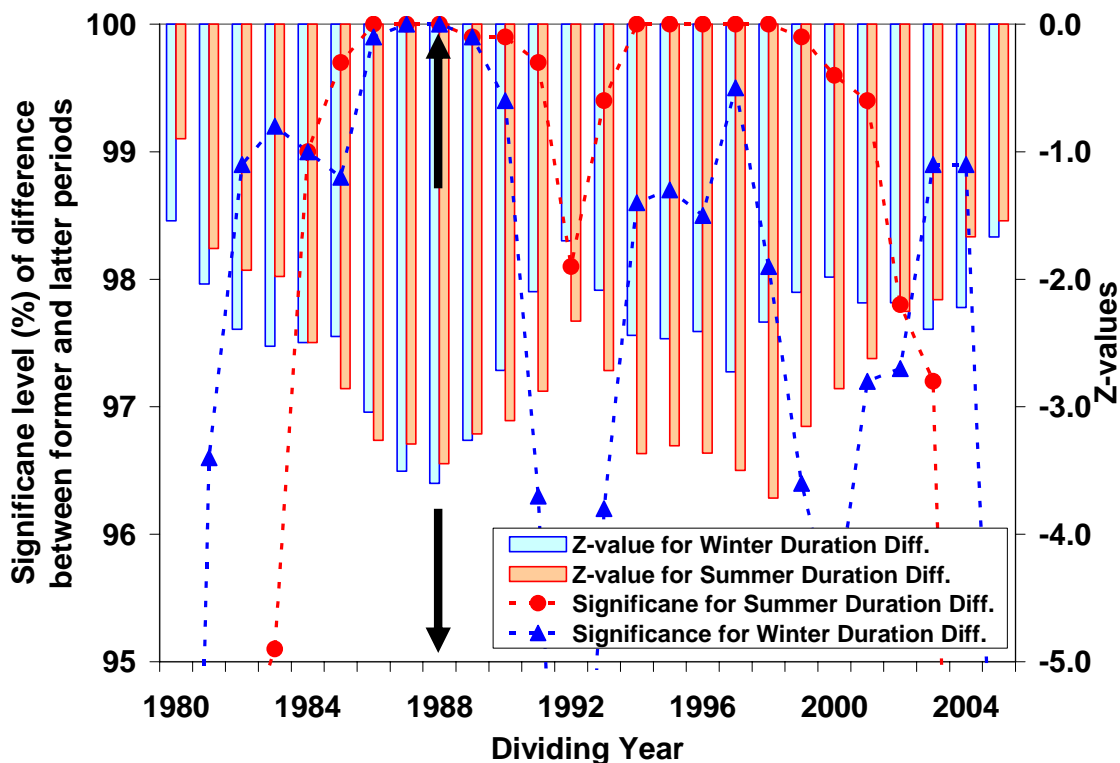


Figure 4.15. Variations of significance level and Z-value in the Mann-Whitney U-test which show statistical significance of differences in Northern Hemisphere averages of thermal winter and summer durations before and since each dividing year

differences in both thermal winter and summer durations between the earlier and the latter periods. Mann-Whitney U test graphs show that the highest significant differences (>99%) in both thermal seasonal durations are gained when two periods are divided based on 1986, 1987, 1988, 1989, and 1990 (Figure 4.15). Further analyses of Z-values indicate that 1988 is the most statistically significant inflection year in the 1979-2005 time series. Based on the inflection point year of 1988, differences of both thermal winter and summer durations between the pre-1988 years (1979-1987) and the post-1987 periods (1988-2005) are calculated for each grid cell. According to the interpolated difference maps, winter duration has decreased by 5-30 days across the Northern

Hemisphere, while summer duration has increased by 5-30 (Figures 4.16 and 4.18). In particular, over high elevation regions such as the Rockies, the Himalayas, and the Alps, 5-30 day reductions in winter duration are observed, while more than a 25 day extension in summer duration is identified near 30° N over the Atlantic and the Pacific.

Reductions of winter duration and extensions of summer duration are also observed over low-elevation regions. In Central Asia, and East Asia, as well as along the Arctic coastline, the length of the winter period has decreased by 5-15 days. Over oceans, there has been a reduction of 5-15 days in the northwestern Pacific and 20 days in the northern

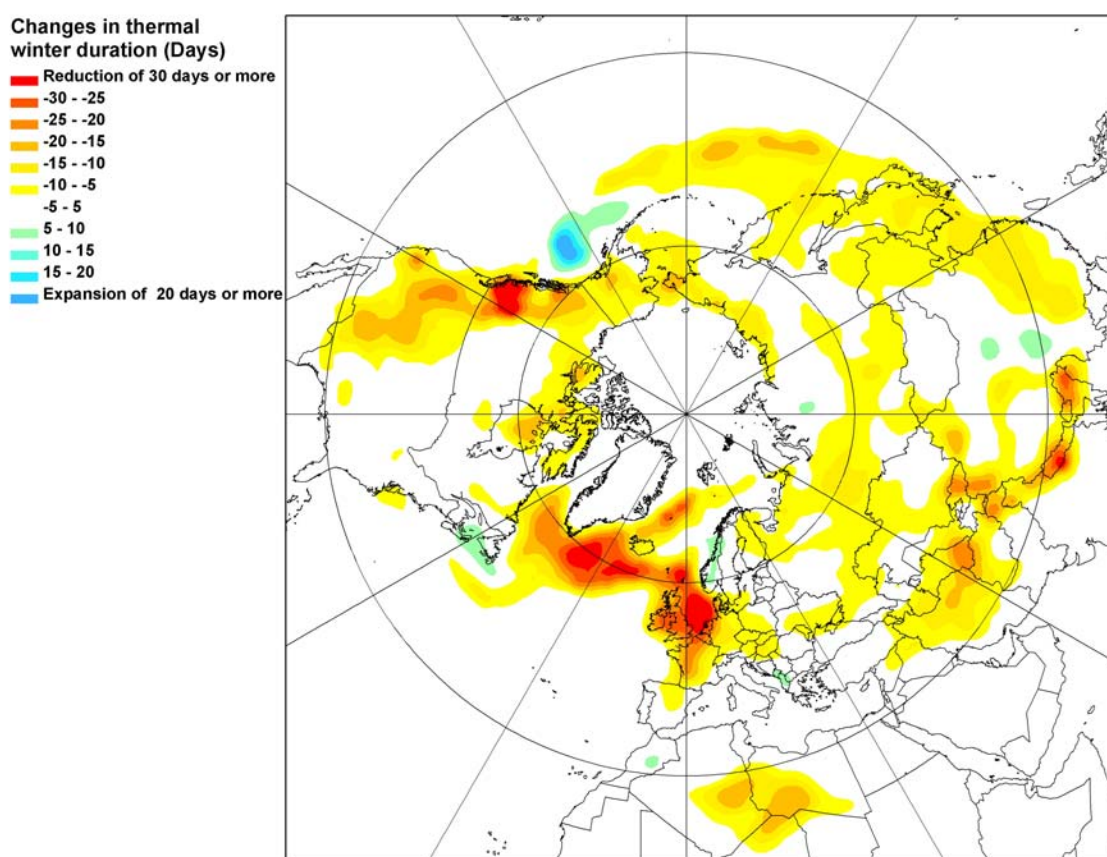


Figure 4.16. Changes in thermal winter duration between the pre-1988 years (1979-1987) and the post-1987 years (1988-2005)

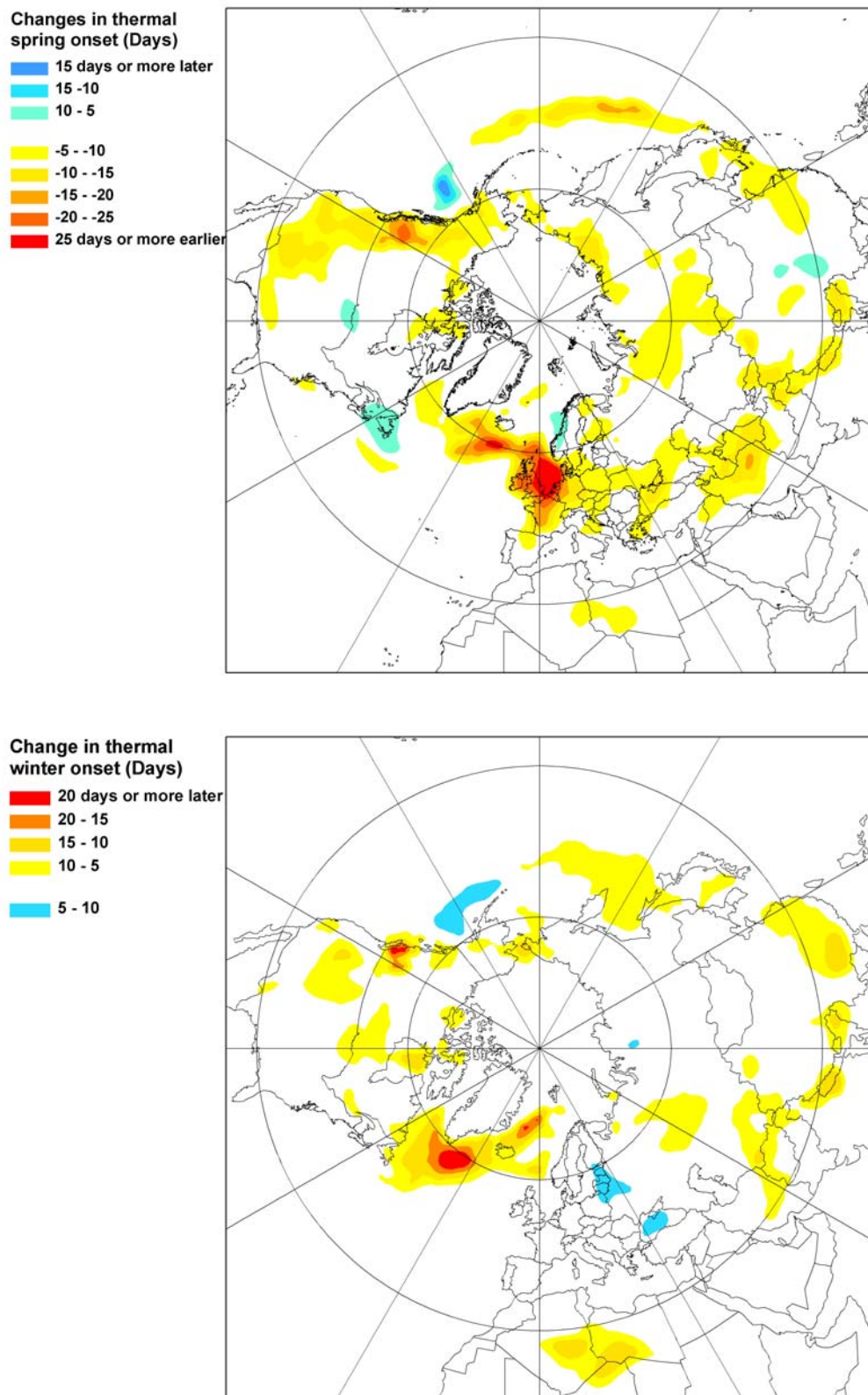


Figure 4.17. Changes in thermal spring onset (top) and thermal winter onset (bottom) between the pre-1988 (1979-1987) and post-1987 (1988-2005) periods

Atlantic. In contrast, increases in summer duration of 5-25 days are observed across Europe. Increases of 5-15 days are noted in the western United States, Mongolia, central China, northern India, and southwestern Siberia. At low latitudes, increases of 5-15 days occurred in northern Mexico and northern Africa including the highlands in Ethiopia. A shortened summer period of 5-10 days is detected in the southern United States and southwestern China.

The reduction of winter duration is more affected by advanced spring onset than by delayed winter onset (Figure 4.17). In North America, spring onset has advanced by 5-25

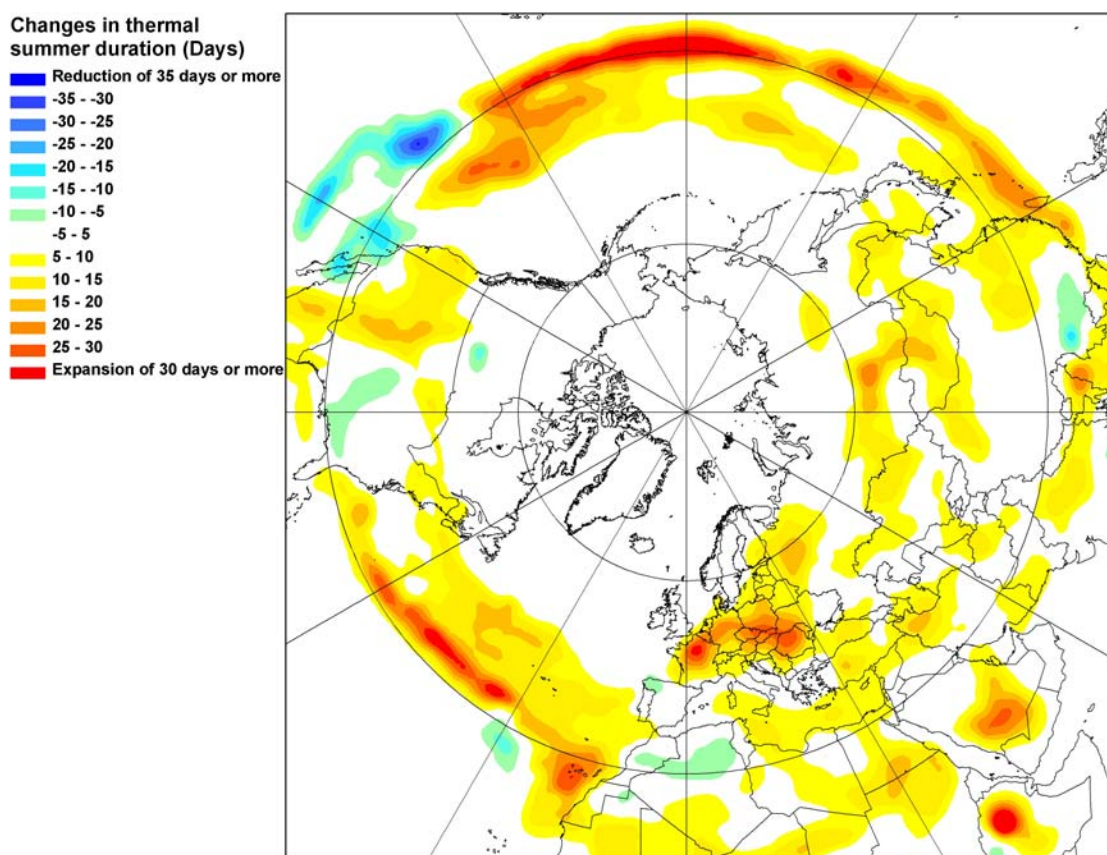


Figure 4.18. Changes in thermal summer duration between the pre-1988 (1979-1987) and the post-1987 (1988-2005) periods

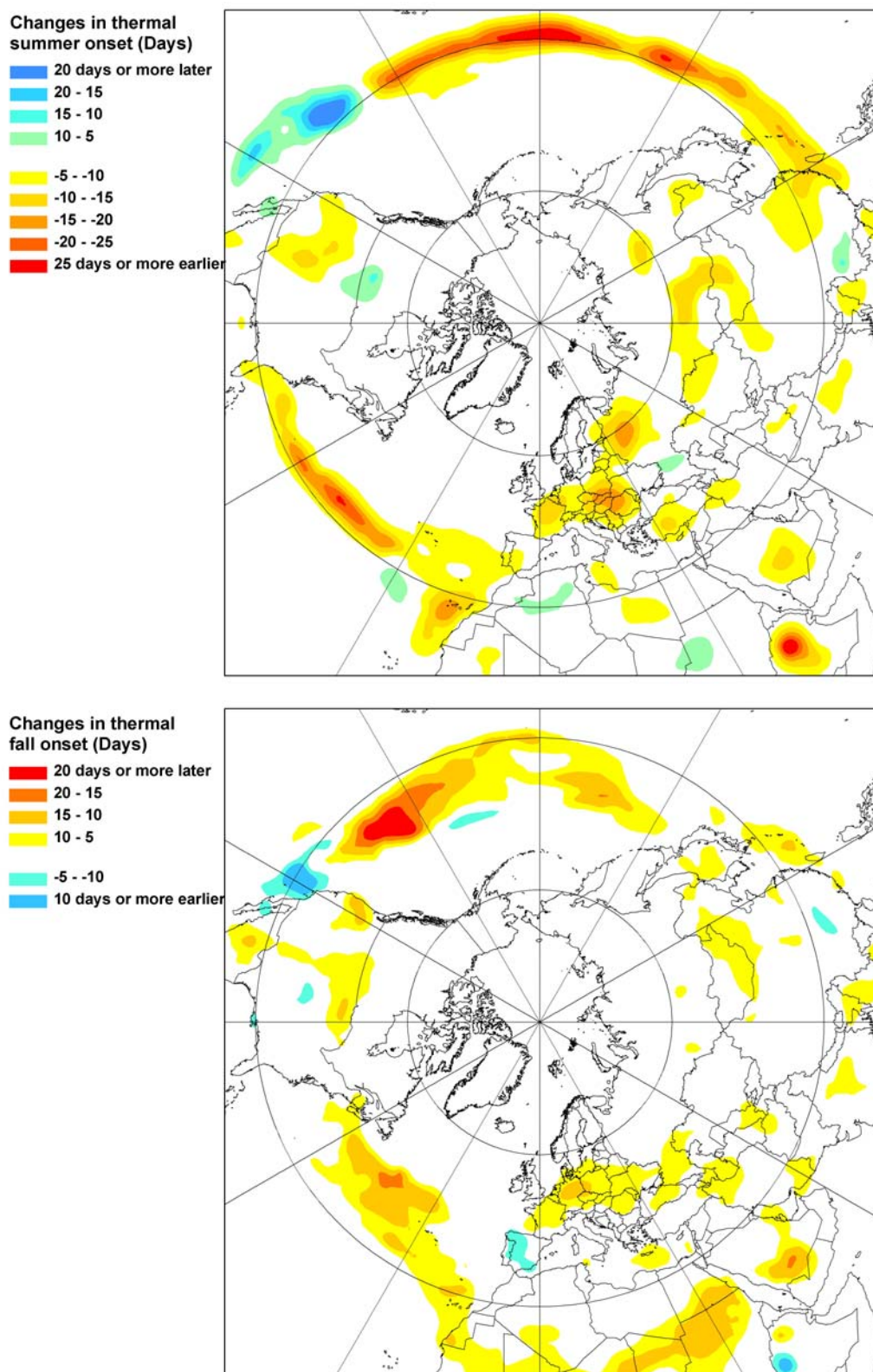


Figure 4.19. Changes in thermal summer onset (top) and thermal fall onset (bottom) between the pre-1988 (1979-1987) and post-1987 (1988-2005) periods

days along the Rockies, Alaska, and the Arctic coastline. Similarly, a 5-25 day earlier onset of thermal spring is identified across Europe. In particular, spring onset has advanced more than 25 days in the Black Sea region. Spring onset has become 5-15 days earlier over the Yangtze River basin in China, the Eastern Siberian Arctic coastline, the Himalayas, southern Siberia in eastern Asia, and around the Caspian Sea. In contrast, winter onset has been delayed by 5-10 days along the Rockies and the Himalayas, as well as in central China.

The extended summer period is attributable to advanced summer onset and delayed fall onset (Figure 4.19). The summer onset dates have advanced mainly in those regions where summer duration has increased. Along 30°N as well as across Europe, summer onset has advanced by 5-25 days. Changes in the fall onset are scattered over the central Pacific and the central Atlantic as well as northern Africa.

#### **4.5. Summary and conclusion**

This study is the first to define floating thermal seasonal onsets and durations on a hemispheric scale based on NCEP-DOE reanalysis II daily surface air temperature data. Spatial patterns and temporal changes of long-term average thermal seasons across the Northern Hemisphere were examined for the period 1979-2005.

The progression speed of thermal seasonal onsets is faster over land masses by the factor of 2-3 than over oceans and the spatial ranges of thermal seasonal progression is broader over land masses than over oceans. Thermal seasonal onsets advance or retreat at the rate of 3.3-3.9 days/degree of latitude over land mass, while the speeds over oceans

are 6.6-13.1 days/degree. In particular, thermal summer onset/offset (fall onset) progresses slower than winter onset/offset (spring onset) over oceans.

Seven different types of thermal seasonal cycles progress in different parts of the Northern Hemisphere. From the Arctic to the tropics, those cycles include winter-only, summer-absent, four-seasons, spring-fall-only, winter-absent, spring-summer-only, and summer-only. Their latitudinal ranges are not identical between land masses and oceans. Over land masses, the four-season cycle (spring-summer-fall-winter) prevails, while over oceans, summer-absent, spring-fall-only, and summer-only cycles predominantly occur.

Thermal winter duration has decreased by 5-30 days between 1979 and 2005, primarily due to earlier spring onsets. In contrast, summer duration has extended by 5-30 days, primarily due to advanced summer onset. The reduction in winter duration appeared along the Rockies, the Himalayas, and Arctic coastlines as well as in Europe, central Siberia, and Eastern Asia. Summer extension has occurred along 30°N over oceans and scattered regions over land masses.

Given the relatively short period of available data, any interpretation of changes in thermal seasonal onsets and durations must be limited. For instance, the accuracy of reanalysis data for regions where observations are scarce, as well as potential decadal scale fluctuations of the seasonal cycle, should be considered when climatology and changes of seasons are interpreted. To do that, future studies should include the following: 1) extended study in regions where long term data exist, 2) regional studies that further examine the impacts of altitude and surface conditions, and 3) empirical and model investigations of potential causative mechanisms for spatial and temporal variations.

## CHAPTER 5

### SNOW SEASONS IN THE NORTHERN HEMISPHERE

#### 5.1. Introduction

Snowfall is a marked seasonal phenomenon that characterizes cold winter seasons. Analyses of satellite imagery illustrate that snow cover is the cryospheric variable that is most sensitive to the seasonal progression of temperature. Precipitation usually falls as snow when air temperature is below the freezing point, while it falls as rain during warm periods. The fallen snow remains on the surface forming a cover across circumpolar regions unless it melts due to increases of temperature. On high mountain ridges such as the Himalayas, the Rockies, and the Andes, alpine glaciers are formed by snow accumulated over time. Snow cover fluctuates on hemispheric scales. For instance, its maximum extent approaches 47 million km<sup>2</sup> in January and February whereas in August it is reduced to 4 million km<sup>2</sup> in the Northern Hemisphere (Robinson & Frei 2000). Inter-annual variations of snow extent occur on a regional scale at the mid-latitudes and are associated with meridional oscillations in geopotential height fields (Frei & Robinson 1999).

Snow cover affects spatial patterns of thermal energy and hydrological resources on longer time scales than rainfall. High albedo of snow cover lowers surface air temperature by 4-8°C compared with snow-free areas (Dewey 1977; Baker et al. 1992; Leathers & Robinson 1993; Groisman et al. 1994). In addition, snow cover supplies a considerable amount of water to human society and ecosystems in spring. Agricultural regions adjacent to high mountains such as northern India have a high dependence on

melting snow (Bagla 2007). Thus, continued monitoring of changes in the timing of snow season onset and offset as well as the inter-annual variability of snow cover is needed. Several studies have examined lead-lag relationships between the timing of snow appearance/disappearance or duration and atmospheric conditions such as temperature (Leathers & Luff 1997), the Arctic Oscillation (Bamzai 2003), summer monsoon (Ye et al. 2003), and warm moisture advection (Shinoda et al. 2001; Ueda et al. 2003; Iijima et al. 2007).

A few studies have documented that hydrological spring signals such as the timing of spring peak streamflow have advanced during the recent 30-50 years in Canada (Burn, 1994; Zhang et al. 2001) and the United States (Cayan et al. 2001; Regonda et al. 2005; McCabe & Clark 2005; Stewart et al. 2005) along the Rockies and in the northeastern United States (Hodgkins et al. 2003; Cziknowsky & Fitzjarrald 2004; Hodgkins & Dudley 2006). These studies have also reported that the advanced seasonal onset of peak streamflow is attributable to earlier snow melting in spring. Consistently, other studies have also reported a reduction of the spring snow extent on continental or hemispheric scales (Groisman et al. 1994; Robinson et al. 1995; Robinson & Frei 2000; Brown 2000) in recent decades. Moreover, an earlier disappearance of last snow cover in spring in recent decades (Dye 2002) and subsequently an increase of snow-free days on continental scales (Bamzai 2003) have been documented. Furthermore, along regions where snow melt advanced, problems relevant to hydrological imbalance such as spring droughts and more frequent, intensive wildland fires have been reported (Westerling et al. 2006).

In this chapter the Northern Hemisphere snow season onset/offset and duration are defined based on snow cover data. Spatial patterns and temporal variability are examined

for the period 1967-2005. A weekly Northern Hemisphere snow cover data set provided by the Rutgers Global Snow Lab is employed to define snow seasons.

Section 5-2 introduces the definitions of snow seasons and spatial patterns of long-term average snow seasons. Section 5-3 depicts temporal variability and changes in snow seasons. Section 5-4 provides a summary and conclusion.

## **5.2. Progression of snow seasons in the Northern Hemisphere**

### **Definition of the Full Snow Season (FSS) and the Core Snow Season (CSS)**

Figure 5.1 illustrates the percentages of years with snow cover for at least one week between the 1967/1968 and 2004/2005 snow seasons. Circumpolar regions above 45°N are covered with snow for at least one week every year. In mid-latitude regions between 25°N and 45°N, the possibility of snow cover appearance during the cold period is less than 100%. In Eurasia, the possibility of snow cover appearance is less than 50% in western Europe, while in eastern Siberia snow cover appears every year. In the Tarim Basin of northwestern China, the possibility of snow season appearance is also reduced to 50% or less. In spite of high elevation of more than 4000m, the possibility of snow cover appearance over the Tibetan Plateau corresponds to less than 100%. In contrast, the possibility exceeds 75% in northeastern regions on Japanese islands. The possibility of snow cover appearance during the cold period is 100% along the Rockies as well as along The Himalaya Mountain ridge, even though they are located in the lower mid-latitude regions below 45°N. South of 25°N, snow cover does not appear during the cold period.

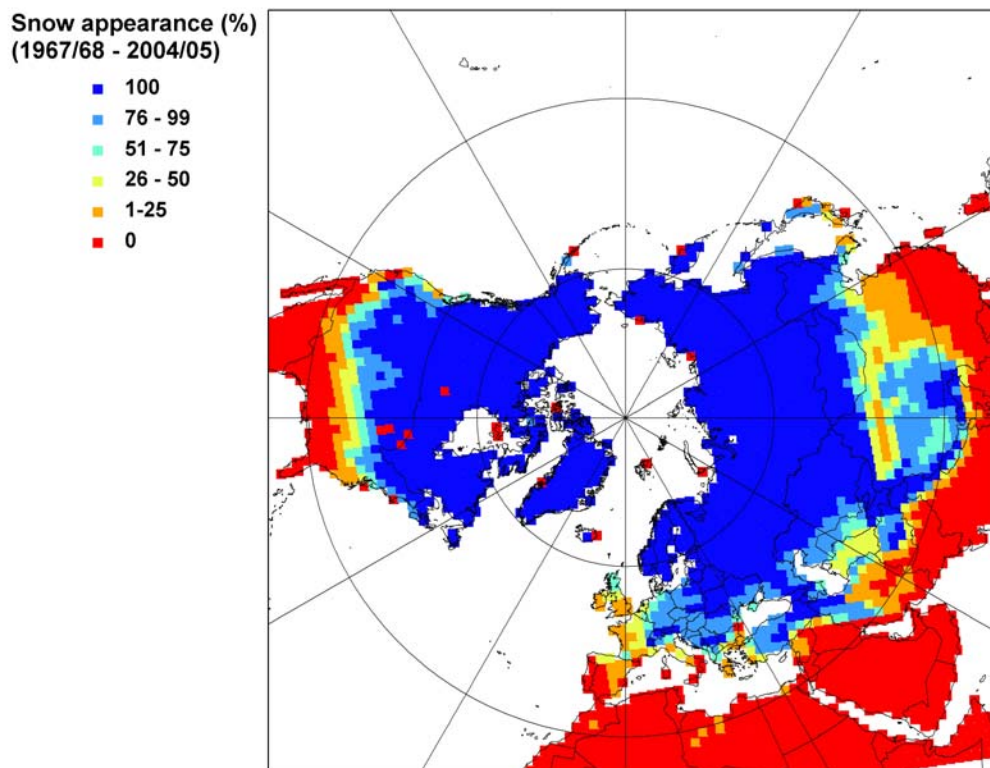


Figure 5.1. Percentage of years with snow cover for at least one week between 1967/1968 and 2004/2005 snow seasons

Snow cover does not always appear continuously during the cold period at high latitudes. Figure 5.2 exemplifies the temporal discontinuity of snow cover along 50°N during the 2004/2005 snow cover period. The horizontal axis indicates longitude along 50°N, and the vertical-axis shows the time between week 33 in 2004 and week 33 in 2005. Snow cover can melt (white cell) and reappear (black cell) in both transitional periods of the snow seasons. Considering these discontinuities, two snow seasons are defined in this study: Full Snow Season (FSS) and Core Snow Season (CSS). An interval between the First Appearance Date (FAD) and the Last Disappearance Date (LDD) of discontinuous snow cover event is the Full Snow Season (FSS). An interval between the

First snow-Covered Date (FCD) of the Longest-lasting continuous snow cover event and the First snow-Free Date (FFD) is defined as the Core Snow Season (CSS). CCS is defined only when snow cover last for more than two weeks around weeks 4-5 (late January-Early February).

$$\text{Full Snow Season (FSS)} = (52\text{weeks} - \text{FAD week} + \text{LDD week})$$

$$\text{Core Snow Season (FSS)} = (52\text{weeks} - \text{FCD week} + \text{FFD week}).$$

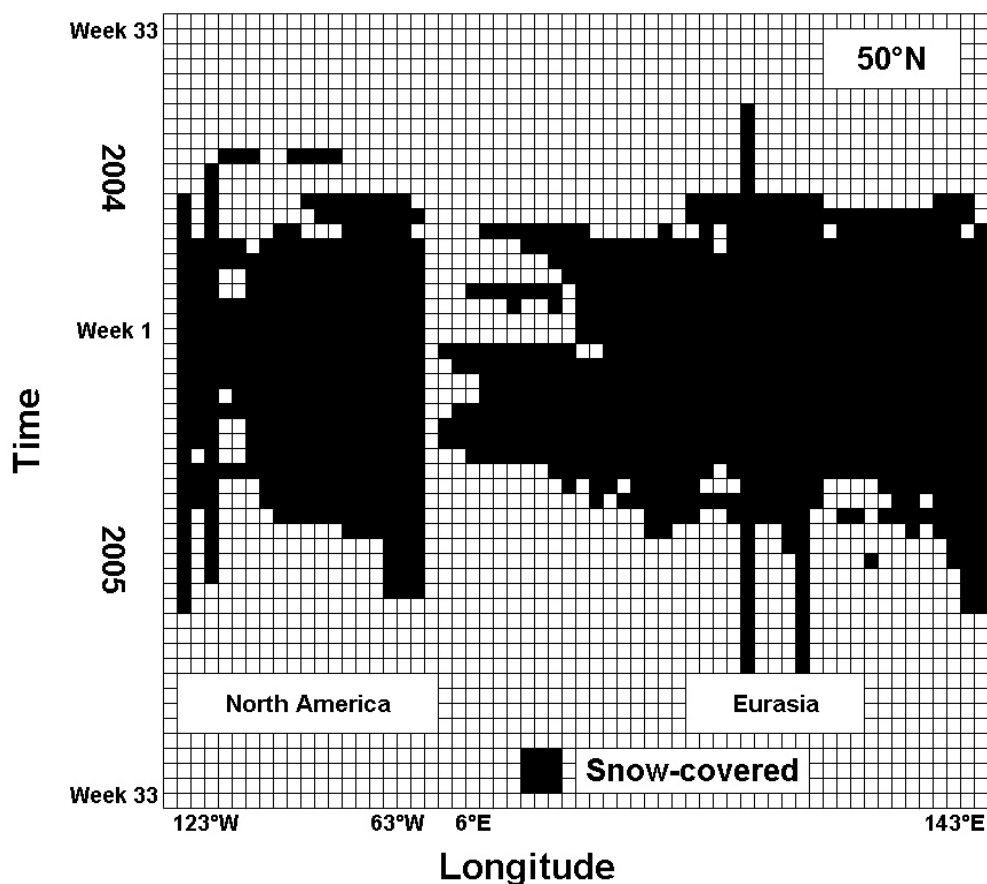


Figure 5.2. Temporal discontinuities of snow cover appearances detected along 50°N during the 2004/2005 cold period

Dye (2002) and Bamzai (2003) defined a Snow-Free Duration (SFD) based on the weeks of the last- and first-observed snow cover. In particular, the SFD used in Dye (2002) is the opposite of the FSS defined in this study. Dye (2002) examined the first- and last-observed snow cover only for high latitude regions where snow cover occurs every year and only for April-June and September-November. Comparatively, in this study, the first (February-July) and second (August-January) full half month periods of the year are regarded as the potential snow season period when the onset and end dates of the FSS or the CSS can occur. Consideration of the full half year periods makes it possible to examine the continuity and discontinuity of snow cover during the FSS or the CSS.

The first date of week 1 in weekly snow cover data varies year-to-year. To eliminate inter-annual differences of those dates, Dye (2002) adjusted the date for week 1 in the original data to the case that the first date of week 1 is the 1<sup>st</sup> of January. In this study, the snow season onset/offset dates extracted from snow cover data are adjusted to the case that the first week begins on the 1<sup>st</sup> of January, which can eliminate the 0-3 day potential bias originating from the adjustment of data.

In calculating a climatology for the period 1967-2005, the weeks with missing data such as weeks 27-30 in 1968, weeks 23-43 in 1969, and weeks 28-39 in 1971 are replaced by the averages from the rest of the years. The estimated values from the rest of the years affect only the data for Greenland and some highland regions such as the Himalayas. In contrast, the rest of the snow-covered regions are free from the impacts of these missing data periods. Thus, including the years 1968, 1969, and 1971 in calculating the climatology of snow seasons maximizes the data period without significant bias of the

long term trend. However, the data in these missing years are excluded from the time series analyses because the estimated average values during the missing data period can cause potential biases in examining long term trends of snow season onset/offset and duration.

### **Patterns of the Full Snow Season (FSS)**

Both the First Appearance Date (FAD) and the Last Disappearance Date (LDD) of snow cover in the Northern Hemisphere show zonal patterns (Figure 5.3). The earliest FAD occurs in Arctic regions in week 39 with the latest FAD in lower mid-latitude regions in week 55. Spatial patterns of the latest LDD are reversed and the propagation period of LDD (weeks 5-27) is 6 weeks longer compared with the FAD between the Arctic and lower mid-latitude regions. The difference indicates that snow melting events in the first half of the year propagate more slowly toward high latitudes than snow appearance events do toward low latitudes in the second half of the year. Combined spatial patterns of the FAD and LDD lead to a 9 month long FSS along the high mountain ranges such as the Himalayas as well as pan-Arctic areas above 60°N, while FSS is less than one month in low-elevated regions at 25-40°N (Figure 5.4).

Zonal patterns of the FAD and LDD are asymmetric in some areas. For instance, the isolines of both FAD and LDD are meridional along high mountain ridges such as the Himalayas and the Rockies. Over the Himalayas at 25-35°N, the FAD appears in weeks 35- 41 (September-October) which is 2-10 weeks earlier than the FAD in southern Siberia. Moreover, based on four divisions at every 90° of longitude, the FAD in eastern Siberia and western Canadian Arctic Alaska (60-70°N, 90-270°E) is 2-6 weeks earlier

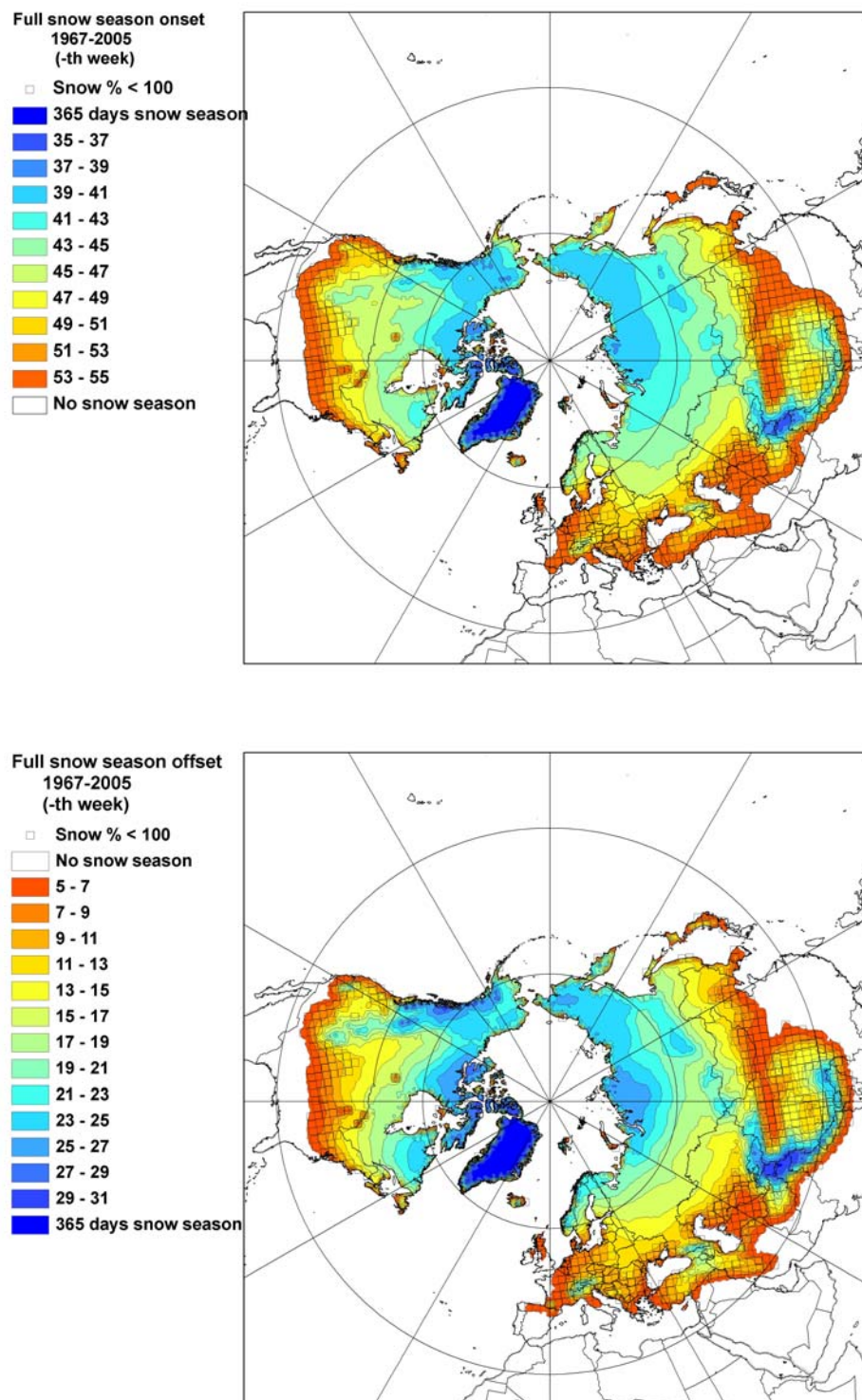


Figure 5.3. Long-term (1967-2005) average onset (FAD; top) and offset dates (LDD; bottom) of the Full Snow Season (FSS) in the Northern Hemisphere. The boxes denote the regions where percentage of snow seasons is less than 100% between 1967/1968 and 2004/2005 as shown in Figure 5.2.

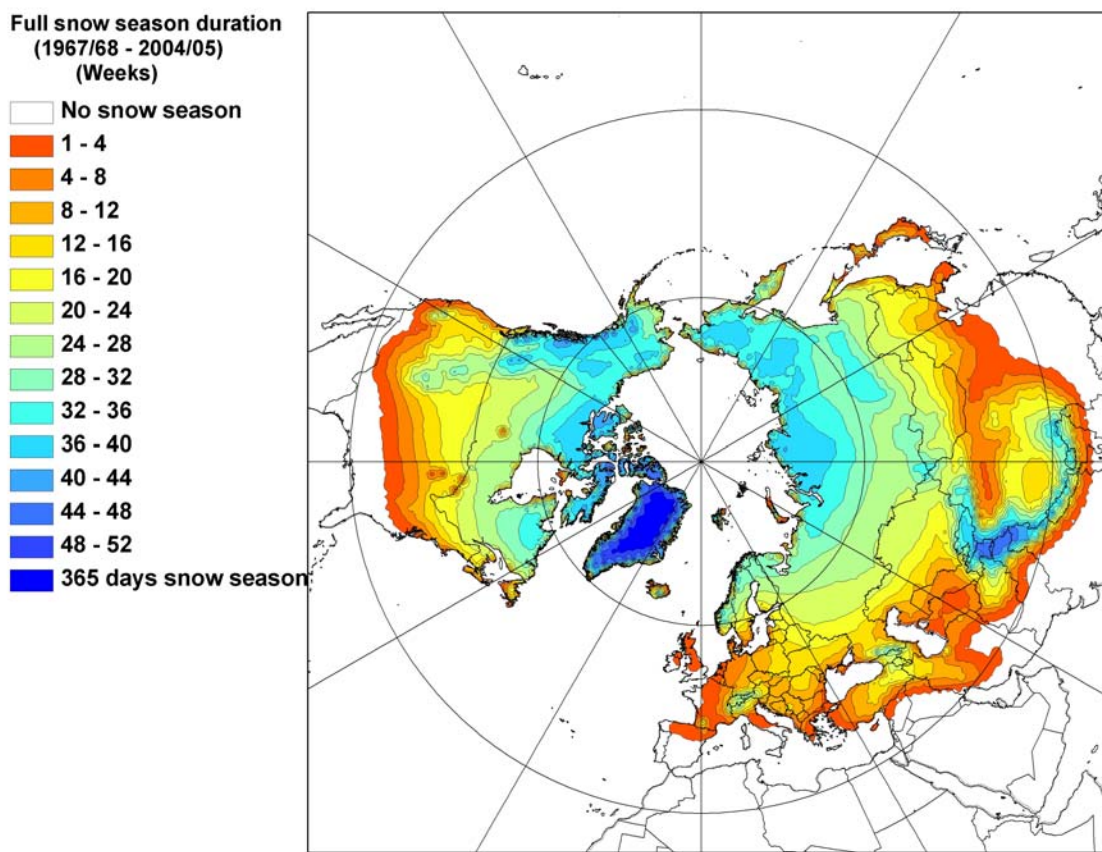


Figure 5.4. Long-term (1967/68-2004/05) average duration (weeks) of the Full Snow Season (FSS) in the Northern Hemisphere

than in Eastern North America and western Europe (60-70°N, 270-90°E). On regional scales, the FSS is also reduced over large lakes such as the Black Sea, and the Aral Sea.

Figures 5.5-5.6 illustrate the spatial patterns of extreme snow season records including the earliest FSS onset and the latest FSS offset at each location over the course of 1967/1968-2004/2005 snow seasons. The corresponding years of the selected values vary across the locations. The spatial range of the earliest FAD and the latest LDD extends 5° further south than the long-term average (Figures 5.5-5.6). The southern fringes of both the earliest FAD and the latest LDD appear from southern Iran and

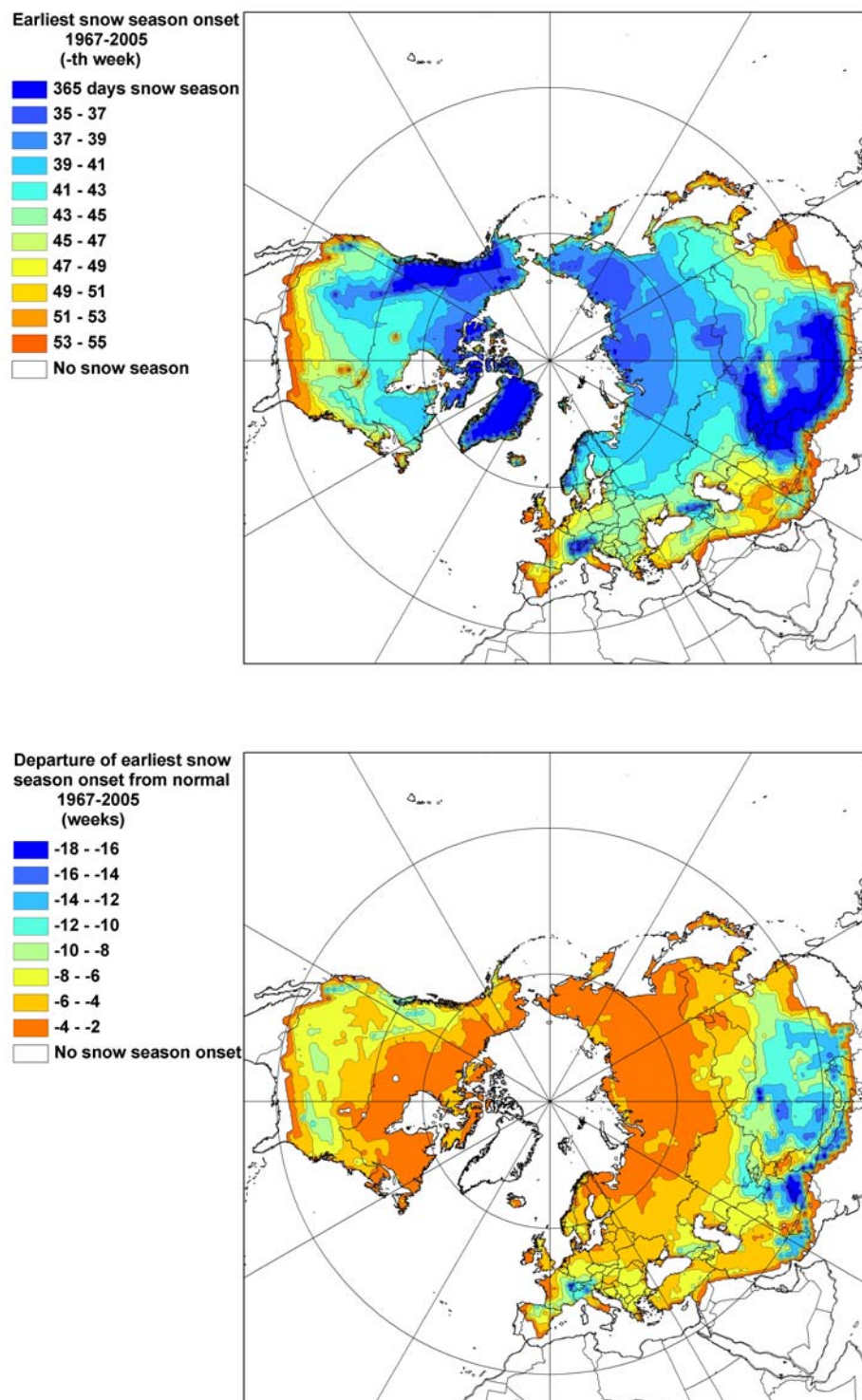


Figure 5.5. The earliest onset of the FSS (top) and its departure from normal (bottom) at different locations in the Northern Hemisphere during the 1967-2005 period. Extreme changes within high mountain areas should be considered too large. Details of this unrealistic result are provided in Chapter 3.

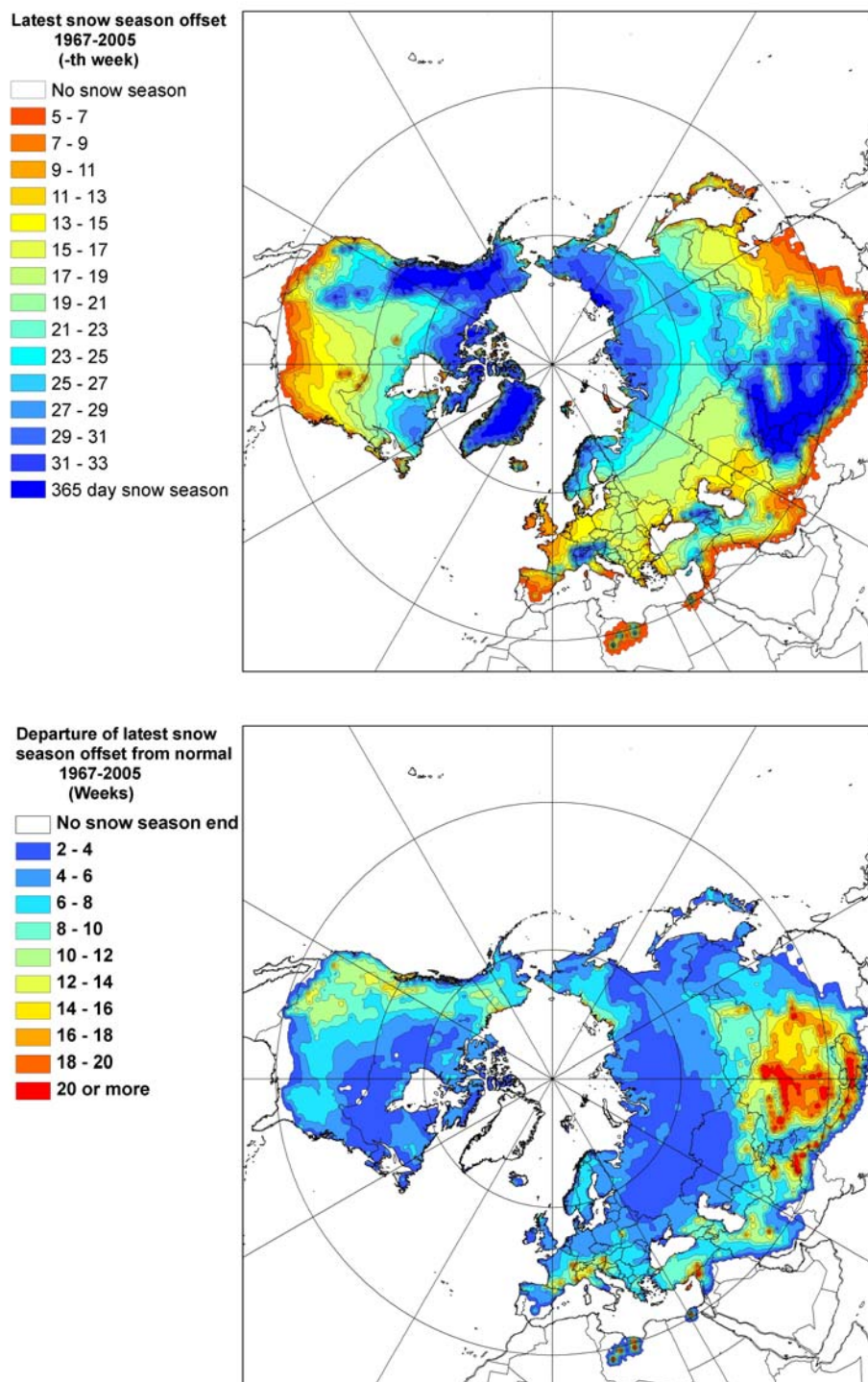


Figure 5.6. The latest offset of the FSS (top) and its departure from normal (bottom) at different locations in the Northern Hemisphere during the 1967-2005 period. Extreme changes within high mountain areas should be considered too large. Details of this unrealistic result are provided in Chapter 3.

northern Myanmar at 25°N to northern Mediterranean coastlines in Europe to 30°N in North America and East Asia. The earliest FAD is 2-16 weeks earlier compared with normal, while the latest LDD is 2-16 weeks later. Caution is needed to interpret unrealistic extreme departures of more than 14 weeks over the Himalayas and the Tibetan Plateau because there were snow charting problems in NOAA's pre-IMS era data set (Robinson & Estilow 2006). The magnitude of these extreme occurrences is smaller in pan-Arctic regions above 60°N than in low latitude regions. Arctic departures of both the earliest FAD and the latest LDD from normal are less than one month, while in mid-latitude regions ranging from 45°N to 60°N, the departure for both amounts to 4-10 weeks.

### **Patterns of the Core Snow Season (CSS)**

The Core Snow Season (CSS) is the period of the longest-lasting continuous snow cover extent around mid-winter (between late January and early February). In the Northern Hemisphere, the First snow-Covered Date of the longest-lasting snow cover event (FCD) occurs between weeks 43-55, while the First snow-Free Date after the longest-lasting snow cover event (FFD) occurs between weeks 5-31 (Figure 5.7). CSS duration ranges from 2 weeks (lower mid-latitude regions) to 44 weeks (Arctic) (Figure 5.8). The FCD period is 2.5 weeks shorter than the FFD interval. Both the earliest FCD and the latest FFD are observed on the Canadian Arctic islands, while both the southernmost latest FCD and the southernmost earliest FFD are found along the southern flank of the Himalayas. The CSS onset and offset in circumpolar regions progresses more rapidly than across southern fringe CSS regions.

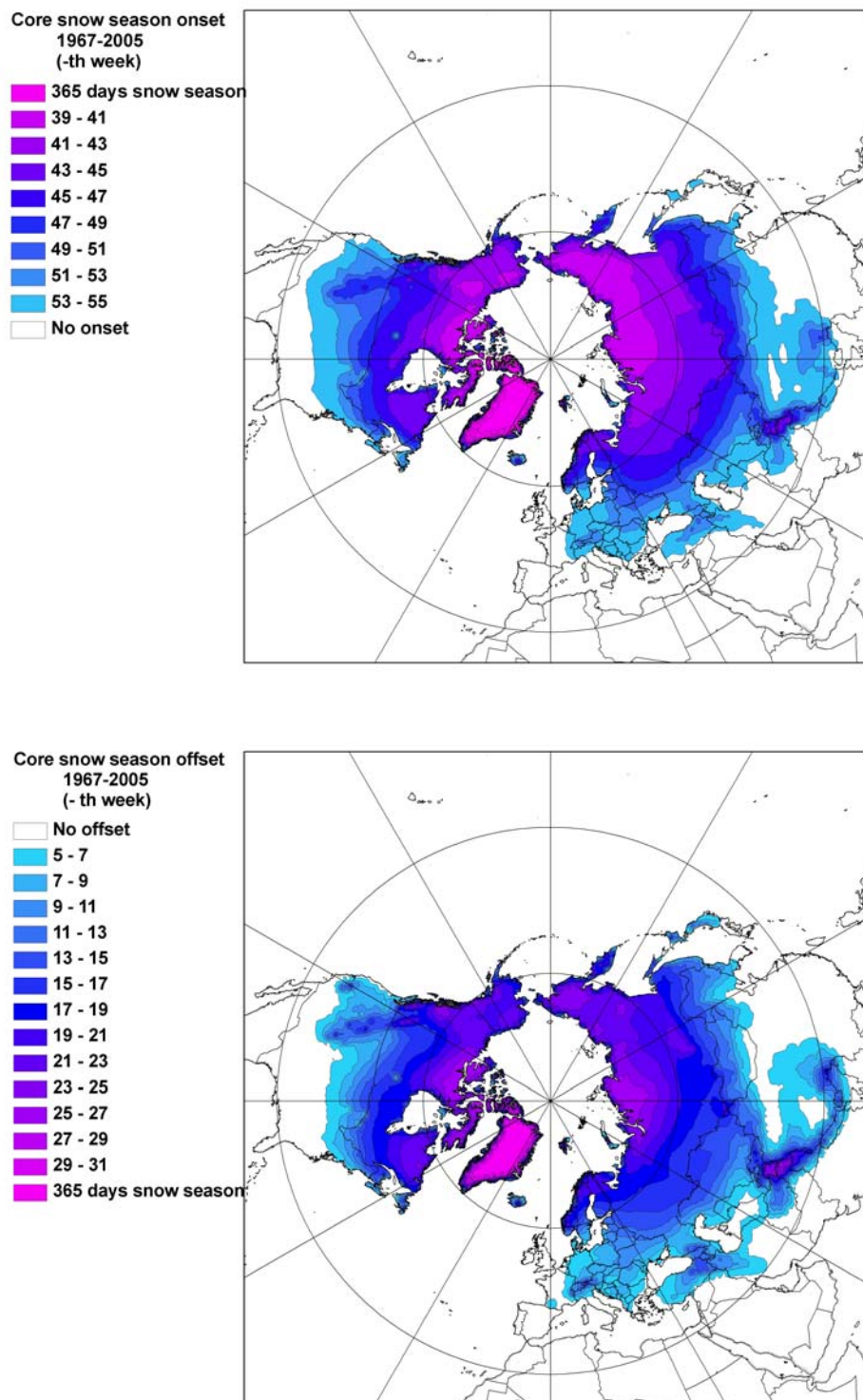


Figure 5.7. Long-term (1967-2005) average onset (FCD) and offset (FFD) of the Core Snow Season (CSS) in the Northern Hemisphere

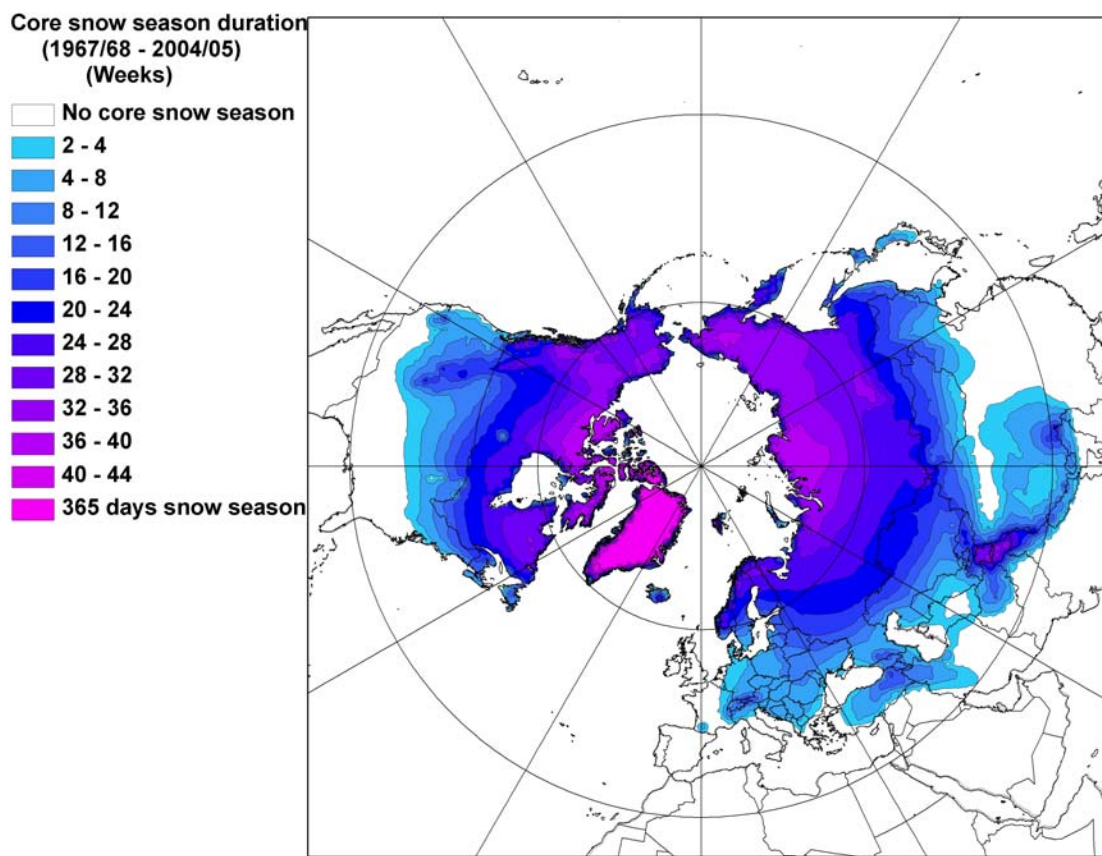


Figure 5.8. Long-term (1967-2005) average duration of the Core Snow Season (CSS) in the Northern Hemisphere

Over the Rockies, the Himalayas, and the Tibetan Plateau, the FCD appears 2-6 weeks earlier compared with nearby low elevation regions, but the FFD occurs 8 weeks or later (Figure 5.7). In eastern Siberia, the FCD is delayed by 2-4 weeks compared to western Siberia, while the FFD is advanced by 2-4 weeks in eastern Siberia. As a result, a CSS longer than 2 weeks does not occur in western Europe, while in northeast Asia adjacent to the Pacific, the CSS continues for 8-20 weeks (2-5 months). In North America, the CSS duration is 1-2 weeks longer along the Pacific coast than along the Atlantic coast. The CSS duration within the Great Plains corridor in western America is 1-2 weeks shorter than in eastern America.

In circumpolar regions above 50°N, the CSS onset (FCD) is 2 weeks later compared with the FSS onset (FAD), while there is no difference between the CSS offset (FFD) and the FSS offset (LDD) (Figures 5.3 and 5.7). In lower mid-latitude regions below 50°N, no obvious difference between the CSS onset (FCD) and the FSS onset (FAD) is detected, while the CSS offset (FFD) is 2 weeks earlier than the FSS offset (LDD). Moreover, the CSS duration in lower mid-latitude regions is 4-12 weeks shorter compared with the FSS duration, while there is no difference in circumpolar regions above 50°N (Figures 5.4 and 5.8). The longest CSS duration of 40 weeks is found in the central northernmost portions of both continents at 90°E and 90°W.

### **Relationships between the FSS and the CSS**

A comparison of Full Snow Seasons (FSS) and Core Snow Seasons (CSS) reveals six snow seasonal cycle zones clustered across the Northern Hemisphere (Figure 5.9). In Greenland, both CSS and FSS continue year round. In Siberia and Canada, the duration of FSS is similar to CSS. In particular, the difference between FSS and CSS is less than one week in circumpolar regions. In most mid-latitude regions and along high mountain ridges, the difference between FSS and CSS is two weeks or greater. Along the southern boundaries of the FSS zone, a CSS does not occur. A FSS usually does not occur below 35°N. However, snow cover is observed occasionally in the southeastern United States and central China.

The consistency of onsets and offsets between FSS and CSS at high latitudes is associated with two extreme cases of the intensity of solar radiation during the course of the year. The circumpolar regions is exposed to intense solar radiation for 24 hours

during the meteorological summer (June to August), whereas in the meteorological winter (December to February), the Arctic regions radiate only outgoing long wavelength energy in the absence of insolation. In high latitude regions, snow can remain on the surface under low air temperatures due to a negative net energy budget during polar winter. Thus, the onset of FSS is almost equivalent to the onset of CSS in this zone. During polar summer, solar radiation for 24 hours each day melts high latitude snow at a fast speed, making the offset of FSS similar to the offset of CSS. The differences between

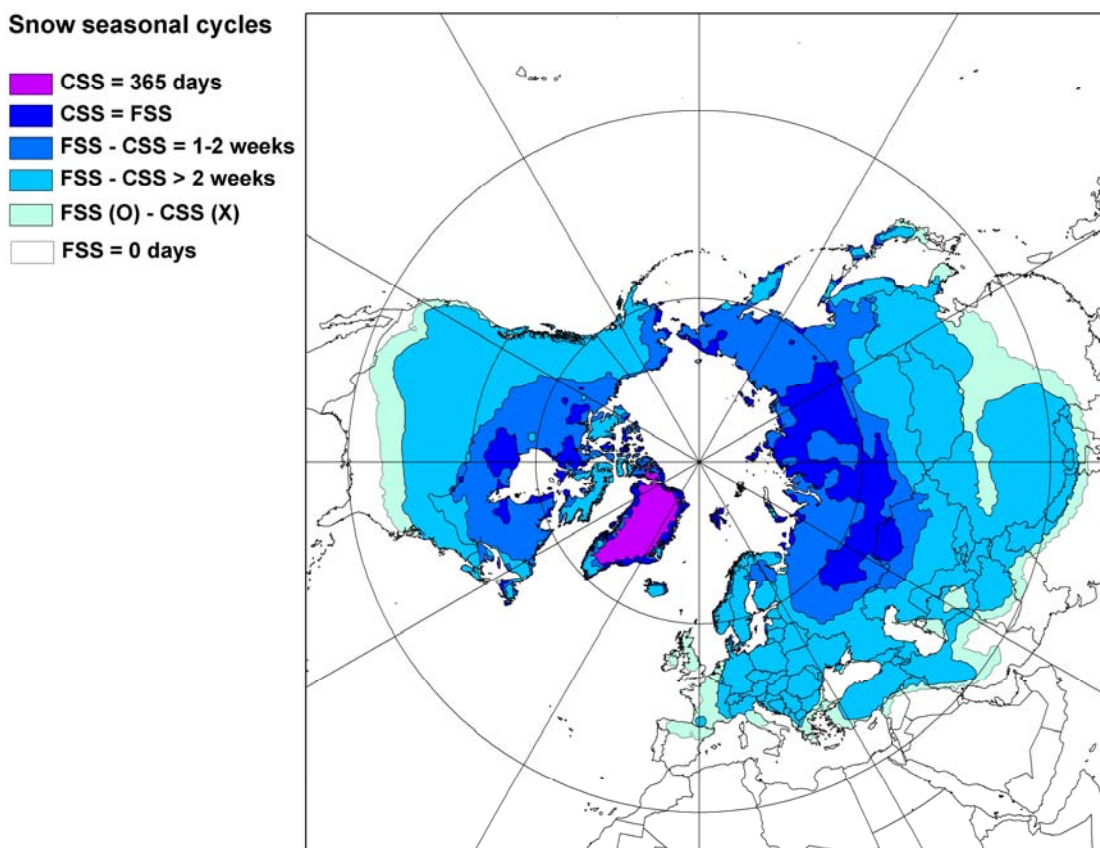


Figure 5.9 Snow seasonal cycle zones classified by relationships between Full Snow Season (FSS) and Core Snow Season (CSS) in the Northern Hemisphere, 1967-2005.

FSS and CSS durations increase at lower latitudes as snowfalls are more affected by day-to-day migrations of low pressure systems and local topography than by the zonal variation of insolation.

### **5.3. Inter-annual variations in snow season cycles**

#### **Trends of the Northern Hemisphere average FSS and CSS**

Northern Hemisphere averages of onset, end, and duration of both the Full Snow Season (FSS) and the Core Snow Season (CSS) are calculated to examine their long-term variability, including only those areas where each are recognized. Pre-1972 data are excluded in the examination of the time series due to the missing data for several weeks in 1968, 1969, and 1971. According to the long-term Northern Hemisphere average, FSS duration is 20.4 weeks (143 days), while the CSS duration is 3.4 weeks (24 days).

There have been changes in Northern Hemisphere average snow seasons in recent decades (Figures 5.10-5.12). The FSS duration has decreased at the rate of 0.7 week/decade (5.1 days/decade) (Figure 5.12). The decreasing trend of the FSS duration is more obvious between 1972/1973 - 1987/1988 compared with more recent years. The analyses of the Mann-Whitney U test show that the difference of the FSS between the former and the latter periods based on the year 1988 is the most statistically significant during the study period. The CSS duration does not show any noticeable increasing or decreasing trend between 1972 and 2005.

The reduction of the FSS duration is attributed to a persistent advance of the Last Disappearance Date (LDD) of snow cover (Figure 5.11). The FSS end (LDD) has

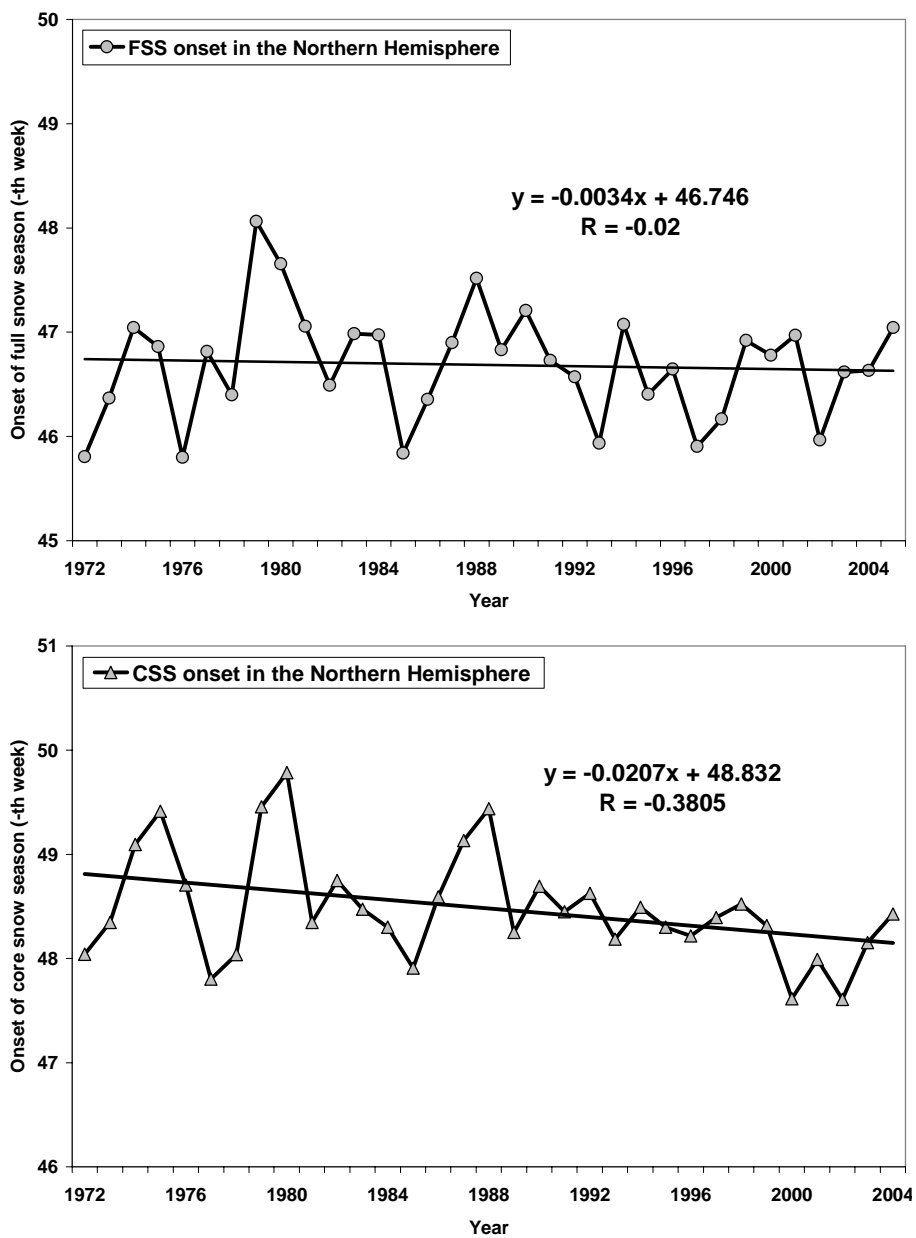


Figure 5.10. Inter-annual variations in the onsets of the Full Snow Season (FSS) and the Core Snow Season (CSS), 1972-2005

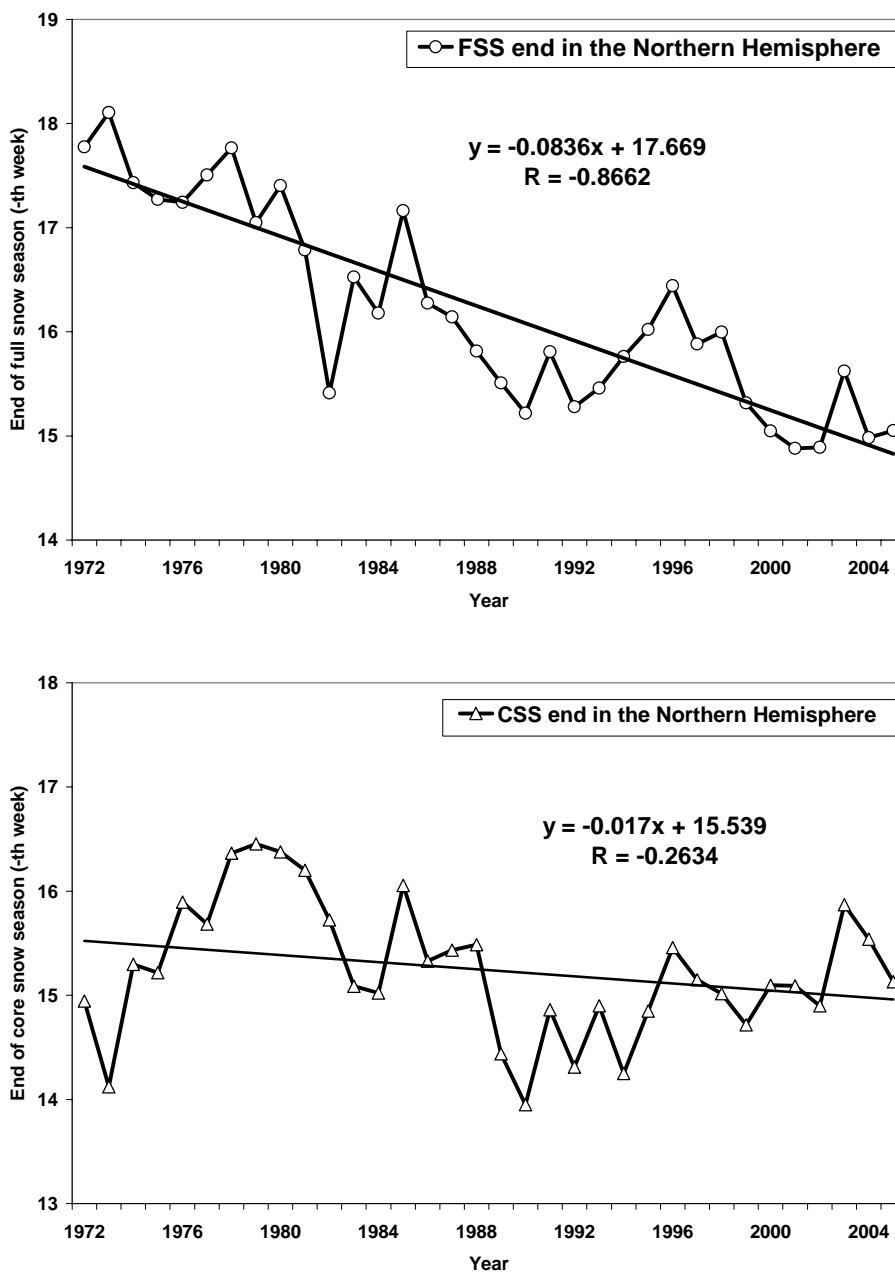


Figure 5.11. Inter-annual variations in the offsets of the Full Snow Season (FSS) and the Core Snow Season (CSS), 1972-2005

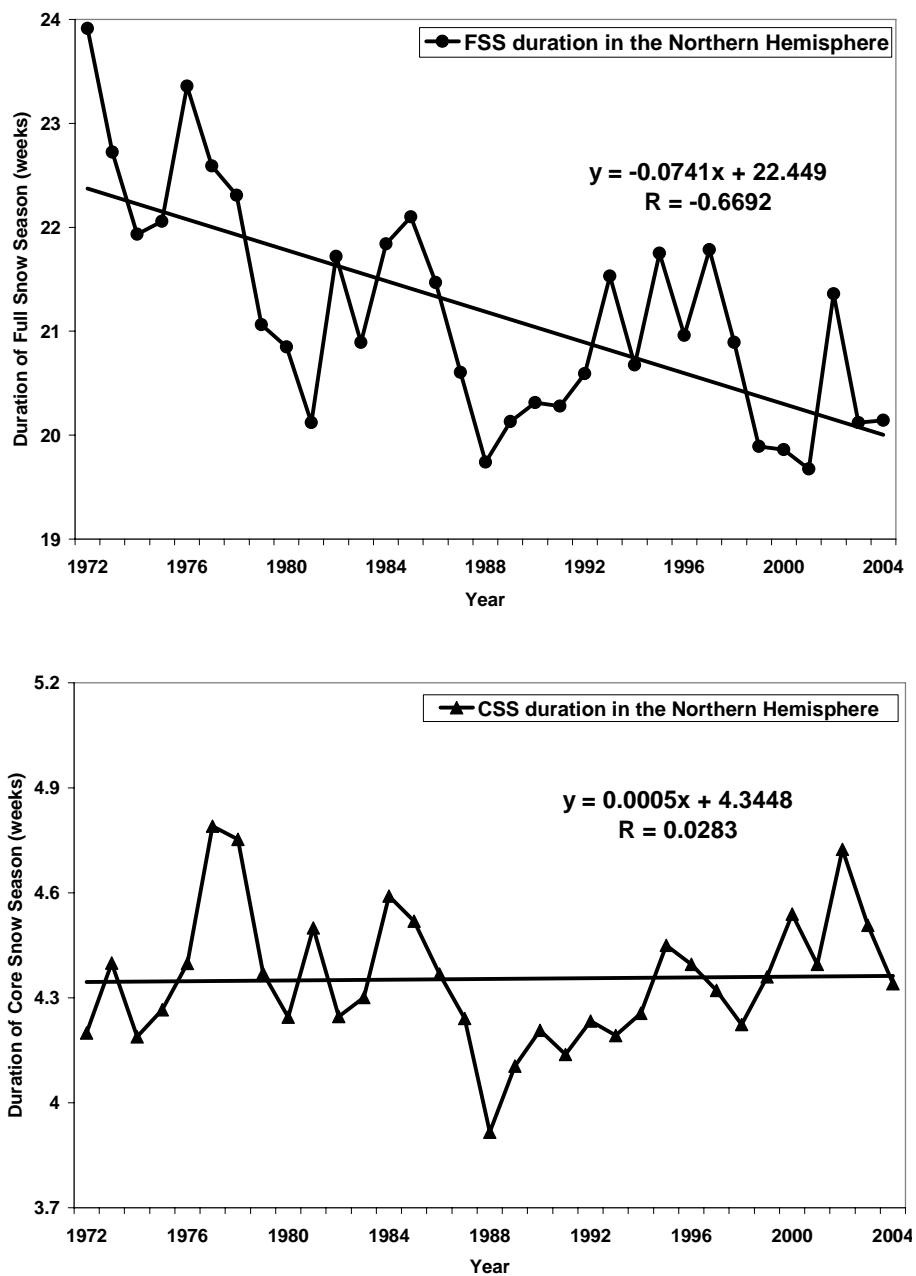


Figure 5.12. Inter-annual variations in the durations of the Full Snow Season (FSS) and the Core Snow Season (CSS), 1972-2005

advanced at the rate of -0.8 week/decade (-5.9 days/decade) during the study period. This rate is statistically significant ( $r = -0.87$ ). There is no noticeable trend in Northern Hemisphere average FSS onset dates (Figure 5.10). CSS onset and offset do not show any trend during the study period (Figures 5.10-5.11). Rather, the variability of CSS onset has decreased since the 1990s. There is a weak delay in the CSS offset in the early 1970s and between the late 1980s and the early 1990s. The overall inter-annual variation of the CSS duration is similar to that of the CSS end (Figures 5.11-5.12).

Pearson correlation coefficients amongst onsets, offsets, and durations of Northern Hemisphere average FSS and CSS show the most significant ( $\geq 99\%$ ) relationships in the FSS duration and the FSS end pair ( $r = 0.712$ ) and in the CSS duration and the CSS end pair ( $r = 0.712$ ) (Table 5.1). These statistics support the finding that the reduction of the FSS duration in recent decades has been the result of an earlier FSS end. They also support the fact that the inter-annual fluctuations of the CSS duration are more influenced by variations of the CSS end than by the CSS onset. Correlations between CSS duration and onset ( $r = -0.598$ ), and between FSS duration and onset are also significant ( $r = -$

Table 5.1. Pearson correlation coefficients ( $r$ ) amongst the Northern Hemisphere averaged snow season onsets, ends, and durations during the 1972/1973-2004/2005 period. CSS denotes the Core Snow Season, and FSS denotes the Full Snow Season

Snow seasons		CSS			FSS		
		Onset	End	Duration	Onset	End	Duration
CSS	Onset	1	0.137	-0.598**	-0.582**	0.240	-0.089
	End	0.137	1	0.712**	0.229	0.430*	0.258
	Duration	-0.598**	0.712**	1	-0.228	0.177	0.271
FSS	Onset	-0.582**	0.229	-0.228	1	-0.20	-0.540**
	End	0.240	0.430*	0.177	-0.020	1	0.712**
	Duration	-0.089	0.258	0.271	-0.540**	0.712**	1

\*\* Correlation is significant at the 0.01 level (2-tailed).

\* Correlation is significant at the 0.05 level (2-tailed).

0.540). Between the CSS and the FSS cycles, the FSS end and the CSS end show a significant correlation ( $r = 0.430$ ), while the FSS and the CSS onsets do not show any significant correlation. In other words, the FSS end date is advanced when the CSS end date is advanced, while there are no lead-lag relationships between the FSS and CSS onset dates on a hemispheric scale.

### **Changes in spatial patterns of the FSS and the CSS**

Differences in snow season onsets, ends, and durations between the early 16 years (1972-1987) and the later 16 years (1988-2003) are examined. The year 1988 is not only the middle point of the study period but also the inflection point in the Mann-Whitney U test that shows the most statistically-significant differences of the Northern Hemisphere FSS durations and ends between two periods. The pre-1988 period minus the post-1987 period values for each location are interpolated using the Inverse Distance Weighting algorithm in Geostatistical Analyst of ArcGIS 9.2.

The Full Snow Season onset (FAD) has advanced by 5-20 days in the post-1987 period in eastern Europe, northern China, and the Great Plains compared with the earlier period (Figure 5.13). In contrast, it has been delayed by 30 days or more over these high mountains such as the Himalayas and the Tibetan Plateau, but these changes may originate primarily from charting problems in the NOAA's pre-IMS era weekly snow extent data set (Robinson & Estilow 2006)

The FSS end (LDD) has advanced across most of the Northern Hemisphere, while the FAD shows both signals on regional scales (Figure 5.13). The magnitude of the earlier LDD in low elevation regions ranges from 5 days to 30 days. In Manchuria, Mongolia,

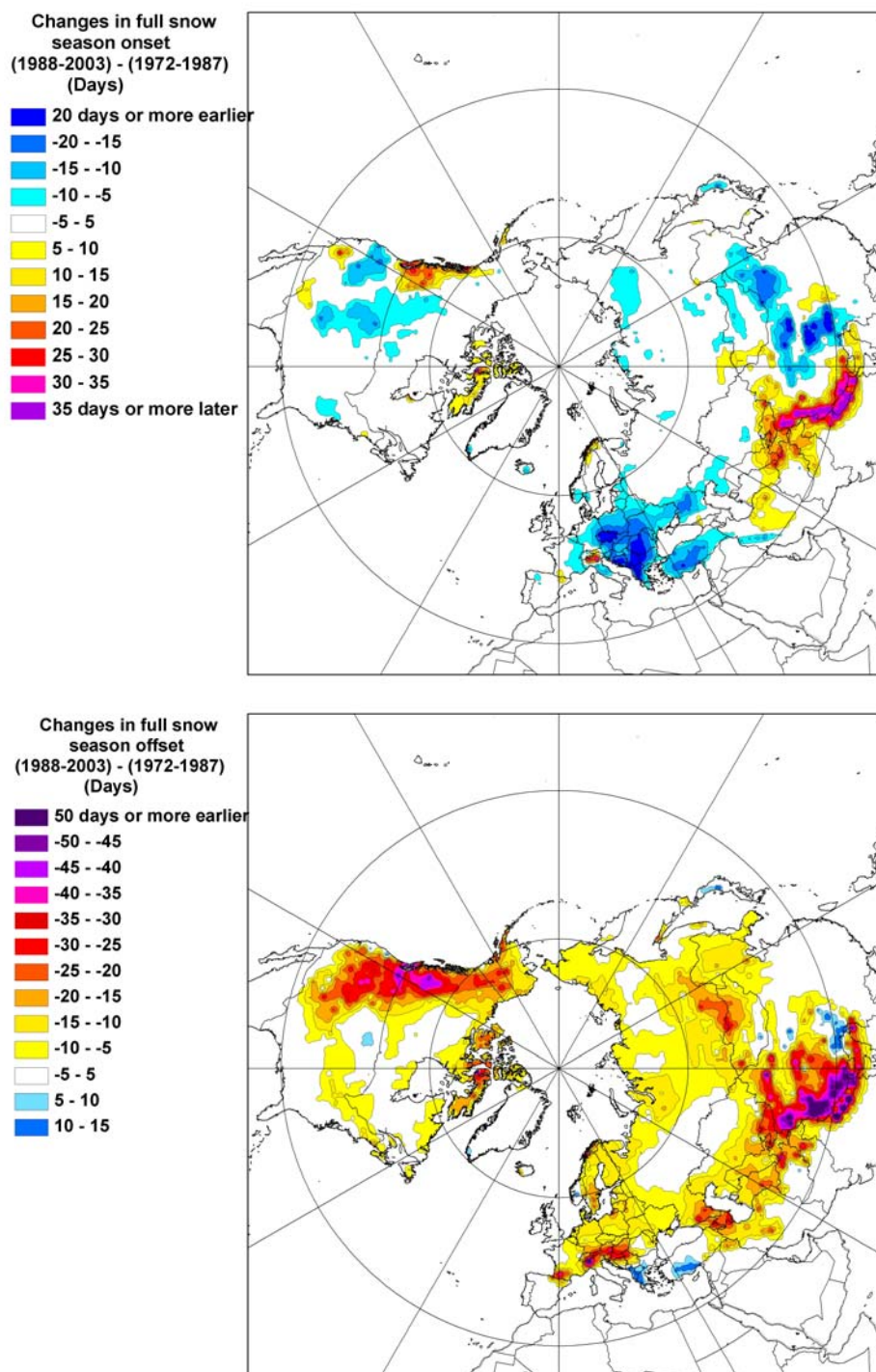


Figure 5.13. Changes (the post-1987 period minus the pre-1988 period) in the Full Snow Season (FSS) onset (top) and offset (bottom) in the Northern Hemisphere, 1972-2003. Extreme changes within high mountain areas should be considered too large. Details of this unrealistic result are provided in Chapter 3.

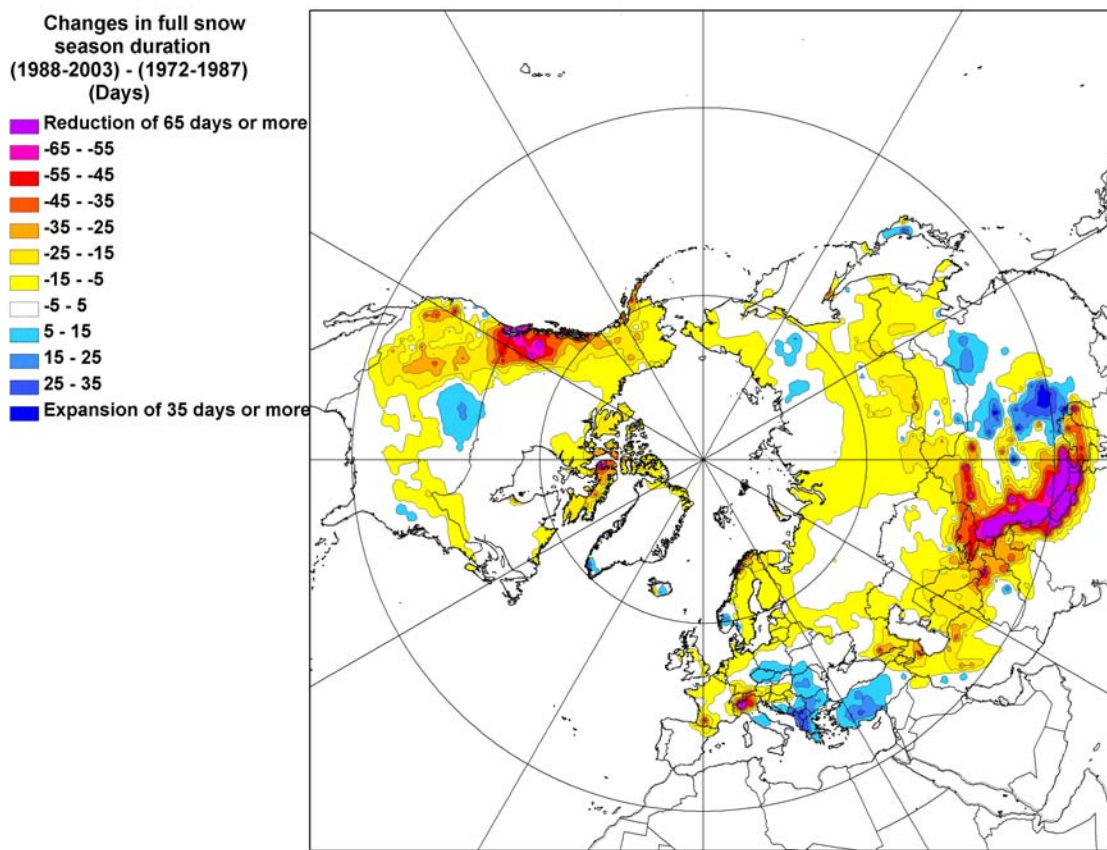


Figure 5.14. Changes (the post-1987 period minus the pre-1988 period) in the Full Snow Season (FSS) duration in the Northern Hemisphere, 1972/1973-2003/2004. Extreme changes within high mountain areas should be considered too large. Details of this unrealistic result are provided in Chapter 3.

Central Asia, and the Canadian Arctic Islands, the LDD has advanced by 5-25 days.

Within the Siberian Arctic and Europe above 60°N, the LDD has advanced by 5-15 days.

Similarly, the LDD has advanced by 5-15 days from New England to the central Great Plains. Along the Rockies, the LDD has advanced by 5-35 days.

The overall advance of the LDD across the Northern Hemisphere has led to a reduction of the Full Snow Season (FSS) in the post-1987 period (Figure 5.14). In circumpolar regions above 60°N, the FSS duration has reduced by 5-25 days. In mid-

latitude Eurasia, the FSS duration has decreased by 5-25 days. In mid-latitude North America, the FSS duration has decreased by 5-10 days along the New England-central Great Plains corridor in the United States and by 15-45 days along the Rockies. In spite of the overall patterns of reduced FSS duration across the Northern Hemisphere, the FSS duration has increased in southeastern Europe, northern China, and the northern Great Plains of the United States. In these regions, the FSS duration has expanded by 5-15 days due to the advances of onset.

Noticeable earlier offset (FCD) as well as weak earlier CSS onset (FFD) led to both increases and decreases of the CSS duration on regional scales in the Northern Hemisphere in the post-1987 period (Figures 5.15-5.16). A 5-15 day earlier FFD is found along the Rockies as well as 40-50°N in Eurasia, including Mongolia, northeastern China, and southeastern Europe. The FCD has been advanced by 15-40 days in northern and eastern Europe, around the Caspian Sea, and in the Tibetan Plateau. The FCD has also advanced by 5-15 days along the Rockies including Alaska, Canadian Arctic islands, central Siberia, northern Tibetan Plateau, as well as low elevation areas along 40-50°N in North America. In contrast, a 5-15 day later FFD is detected in the northern Great Plains in the United States, and the FCD has been delayed by 5-20 days in the western Himalayas and northeastern Canada.

These regional earlier CSS onsets and offsets led to complicated variations in direction and magnitude of the CSS duration across the Northern Hemisphere (Figure 5.16). The noticeable reduction of the CSS duration of 20 days or more is found in northern and eastern Europe and the Canadian Arctic islands. A 5-15 day decrease of CSS duration has occurred between 40-45°N and the southern Rockies, as well as in

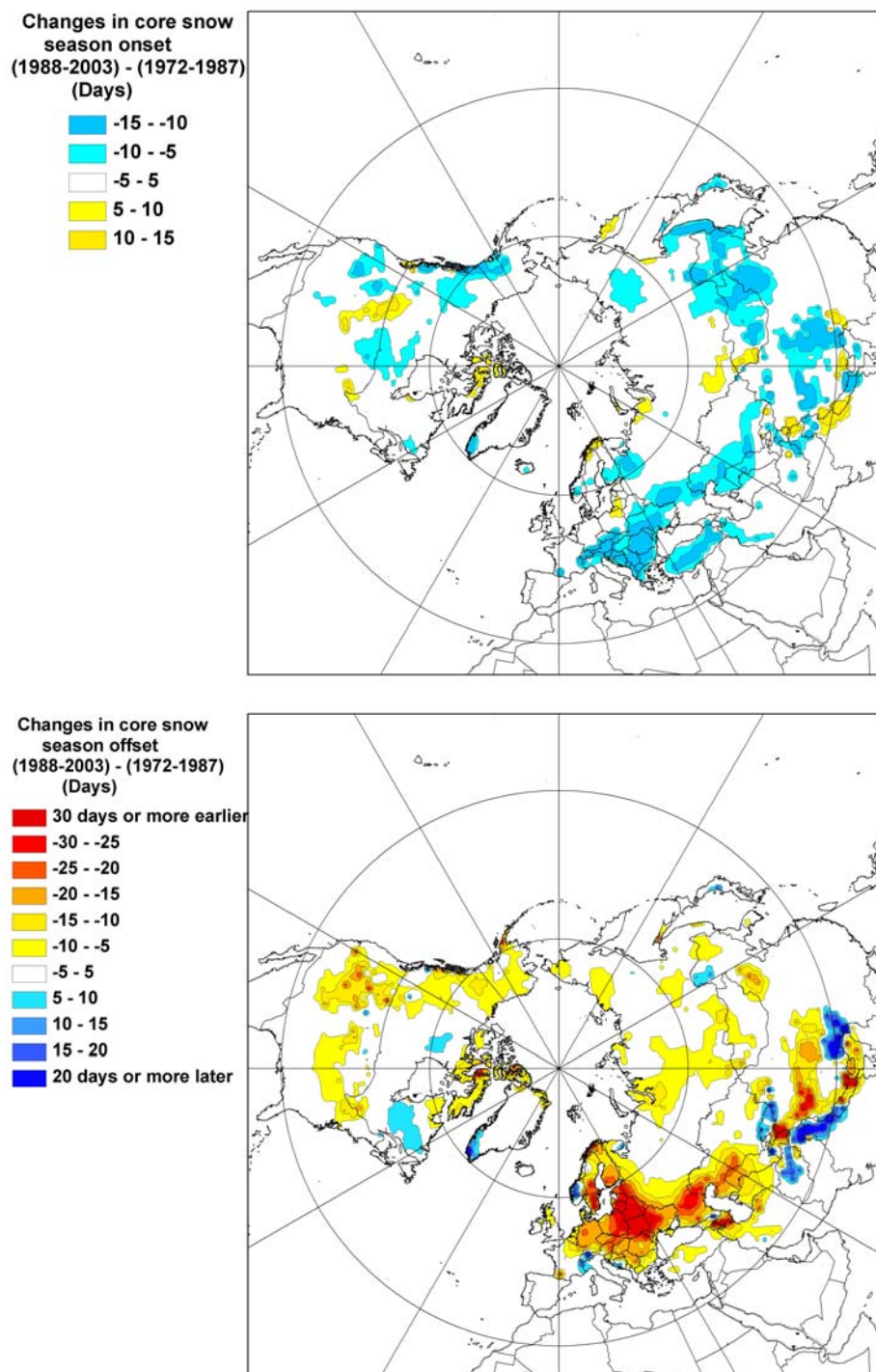


Figure 5.15. Changes (the post-1987 period minus the pre-1988 period) in the Core Snow Season (CSS) onset (top) and offset (bottom) in the Northern Hemisphere, 1972-2003

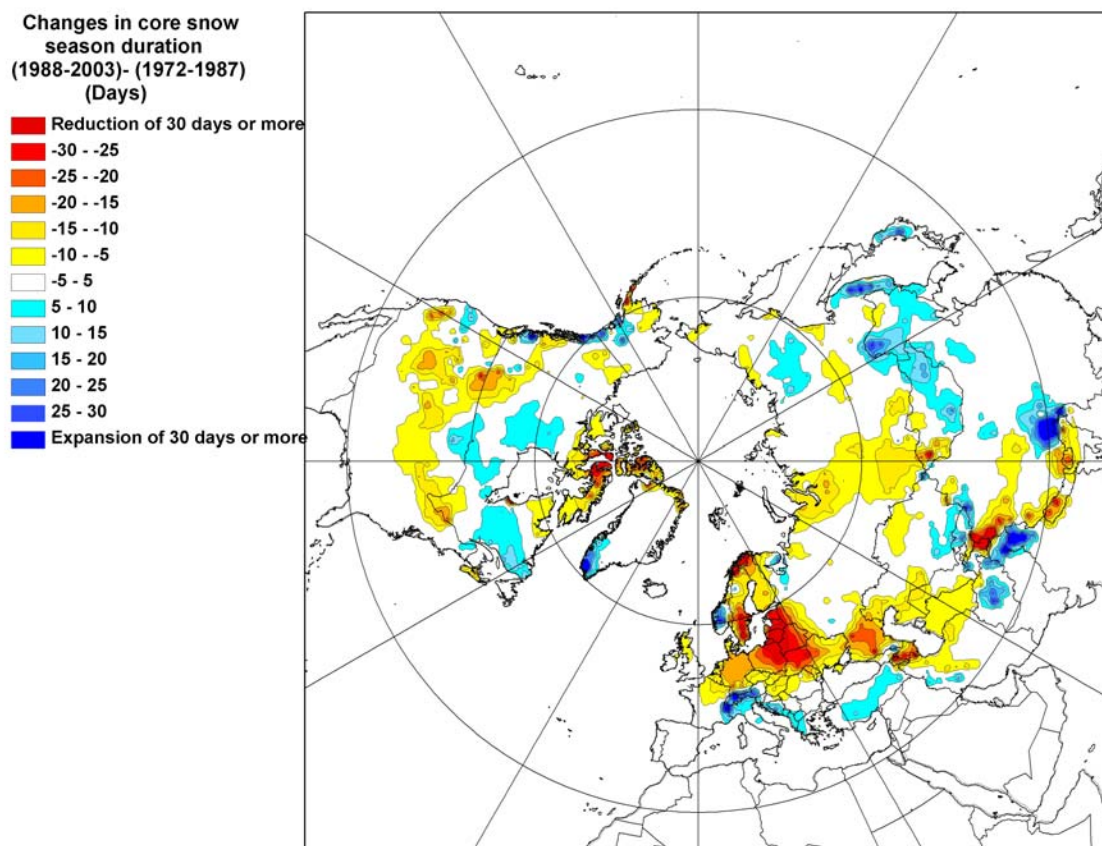


Figure 5.16. Changes (the post-1987 period minus the pre-1988 period) in the Core Snow Season (CSS) duration in the Northern Hemisphere, 1972/1973-2003/2004

central Siberia. In contrast, the CSS duration has increased by 10 days or more over the Canadian Pacific coast, the Mongolia-Manchuria corridor, eastern Tibetan Plateau, northern Pakistan, and southern Europe.

#### 5.4. Summary and conclusion

In this study, the Full Snow Season (FSS) and the Core Snow Season (CSS) were defined. Climatologies and temporal changes of both snow seasonal onsets/offsets and durations were examined for the period 1967-2005.

Progression periods of both FSS and CSS onsets are shorter than those of offsets, indicating that the northward retreat of the snow season front progresses slower than the southward advance. The contrast may be associated with different mechanisms between formation and melt of snow cover. Snow cover usually forms as low pressure systems migrate at low temperatures, whereas snow melt does not occur until a certain amount of solar energy has accumulated, suggesting a need to develop new indices such as snow melt degree days.

Six snow seasonal cycle zones are observed through an analysis of FSS and CSS durations: 1) 365 day snow zone, 2) FSS-CSS identical zone, 3) FSS-CSS similar zone, 4) longer FSS-shorter CSS zone, 5) FSS-only zone, and 6) 0 day snow zone. Above 50°N, the FSS-CSS identical or similar zones dominate. The consistency of FSS-CSS cycles at high latitude may be associated with the two extreme regimes of solar radiation during the course of the year: 24 hour sunshine during polar summer and no sunshine during polar winter.

The Northern Hemisphere average FSS duration has decreased at a rate of 0.7 week/decade (5.1days/decade) between 1972/1973 and 2004/2005, while there is no significant change in the CSS duration on a hemispheric scale. Changes in the FSS duration is attributed primarily to the earlier offset, which has advanced at a rate of -0.8

week/decade (-5.9 days/decade). The changes in FSS offset and duration occurred in the late 1980s.

The earlier offsets of both FSS have occurred on continental scales, while the earlier onsets are observed on regional scales. The earlier offset (5-25 days) and subsequently abbreviated duration (5-45 days) are observed in western Europe, East Asia, central Asia, as well as along the Rockies and the southwestern United States. The earlier onset and subsequently increased FSS/CSS duration are found in southeastern Europe, northern China, and the northern United States Great Plains.

The onset of CSS shows an earlier trend across the Northern Hemisphere continents in recent decades as the offset shows earlier trends on regional scales. Regional scale changes in both CSS onset and offset toward earlier times of the year resulted in mixed trends in CSS duration. Spatial patterns of earlier or later CSS onset/offset are identical to those of the FSS.

Examples of future study topics needed based on these results are 1) relationships between the positioning of snow progression front and upper atmospheric circulation such as circumpolar vortex and jet stream on a hemispheric scale, 2) mechanisms of earlier snow seasonal offsets, and 3) developments of snow season prediction models.

## CHAPTER 6

### VEGETATION SEASON AND CARBON DIOXIDE SEASON IN THE NORTHERN HEMISPHERE

#### 6.1. Introduction

Vegetation cover is an important indicator of seasonal progression. According to intra-annual variations of vegetation indices in satellite imagery, vegetation greenness sharply increases with the advent of spring, and vegetation growth continues into summer. In contrast, vegetation loses its vigor during the fall, and the intensity of greenness approaches the lowest stage with the arrival of winter. Hemispheric scale variations in spatial patterns of vegetation greenness are called green waves (Schwartz 1998). Among various vegetation indices derived from satellite imagery, the Normalized Difference Vegetation Index (NDVI) has most commonly been used to quantify vegetation greenness (Thorp & Tian 2004; Gitelson 2004; Pettorelli et al. 2005). From mid-latitudes to high latitudes, intra-annual time series of NDVI appear as bell-shaped curves with inflection points showing sudden increasing and decreasing times. The inflection points on both sides of the curves indicate the sudden greening-up of vegetation in the early spring and the green-down in the late fall. In this study, the timing of vegetation green-up and green-down are defined as the onset and offset of the vegetation season, respectively.

Long-term average atmospheric gases such as atmospheric carbon dioxide are homogeneously distributed in the lower troposphere on a global scale. However, intra-annual carbon dioxide shows seasonality as bell-shaped curves (Keeling et al. 1996) and its concentration also fluctuates spatially. Regional carbon dioxide cycles are affected by

the varying magnitude and seasonality of vegetation greenness with respect to latitude and altitude. For instance, Keeling et al (1996) revealed that the intra-annual amplitude of carbon dioxide concentration has been greater at high latitudes than at low latitudes. It is also known that carbon dioxide concentration is lower at high altitudes than at low altitudes. The composition ratio of carbon dioxide in the atmosphere has increased from pre-industrial 288ppm to 383ppm in 2007 due to anthropogenic emissions.

To date, the spatially and temporally varying vegetation season or atmospheric chemical season has rarely been studied on a global scale. Only a few studies examined temporal trends of spring phenological phenomena on continental or mid-latitude scales (Menzel & Fabian 1999; Schwartz et al. 2006). For example, Schwartz et al (2006) found through analyses of leaf burst dates of lilac (*Syringa*) phenology that spring onset has advanced at a rate of -1.2 days/decade across the Northern Hemisphere mid-latitude land masses for the period 1955-2002. However, the phenological data used in many earlier studies were collected at point observation sites that are not homogeneously distributed across study regions. The target species of observation also vary from region to region. Moreover, some current phenological data have urban heat island biases due to rapid urbanization of the sampling sites during the 20<sup>th</sup> century. Another shortcoming is that most phenological data, such as flowering and leaf sprouting, only detect spring onset. There is also an argument as to whether a phenology of a single species can be a representative indicator to determine climatological spring onset. Vegetation index data derived from satellite imagery have a global coverage in a consistent manner, quantifying greenness regardless of vegetation species. Therefore, satellite-based products such as

NDVI are more appropriate when examining the vegetation season on a global scale as opposed to using heterogeneous point observed phenological data.

Several studies have used satellite observed data to extract the spatially-varying vegetation season on a regional scale. For instance, the onset and duration of vegetation growing seasons in Mongolia (Lee et al. 2002; Yu et al. 2003, 2004), Scandinavia (Hogda et al. 2001; Karlsen et al. 2006) and the United States (White et al. 2002; Schwartz et al. 2002) were examined based on NDVI data derived from satellite imagery. In addition, regionally-averaged onset of vegetation season by latitude (Myneni 1997; Shabanov et al. 2002), by continent (Tucker et al. 2001), and by land cover types (Reed et al. 1994) were also studied based on NDVI data. Some of these studies suggested that spring onset dates have advanced in recent decades on a regional scale (Tucker et al, 2001; Shabanov et al, 2002).

None of these studies examined both the onset/offset and duration of spatially-varying vegetation season on a hemispheric scale. Furthermore, they did not examine whether changes in the seasonality of vegetation greenness occurred on a global scale in recent decades. In addition, the onset and offset of atmospheric chemical seasons such as carbon dioxide cycles, which are related to fluctuations of vegetation seasons, have not yet been defined. The purpose of this chapter is to define vegetation and carbon dioxide seasons in the Northern Hemisphere and examine recent temporal variability or spatial change in vegetation and carbon dioxide seasonal cycles.

Composites of ten-day maximum NDVI derived from NOAA AVHRR satellite visible and infrared imagery are employed to extract the onset and offset of vegetation season for the period 1982-2001. In the time series analyses, the vegetation season data in 1994 and

2001 are not used because the NDVI data set is incomplete. The NOAA AVHRR NDVI for the Northern Hemisphere consists of 32400  $1^{\circ} \times 1^{\circ}$  grid pixels. Onset and offset dates of vegetation season for each grid cell covering the Northern Hemisphere are defined and extracted from the intra-annual NDVI curves. Intervals between onset and offset dates are defined as the vegetation season. Corresponding dates to inflection points that show sudden increases or decreases of NDVI for each pixel in bell-shaped NDVI annual curves were chosen as the onset and offset timing of vegetation seasons. NDVI ideally varies between -1 and +1 (cf. overview in Chapter 3), but in reality, it seasonally fluctuates between a winter minimum -0.1 and a summer maximum +0.7 at mid-latitudes. The seasonal variations of NDVI in tropical and desert regions are more sensitive to the times of rainy or dry spells than to intra-annual temperature. The difference of monthly average NDVI values between July and December is less than 0.17 in tropical regions. Annual maximum NDVI is lower than 0.15 in desert regions. Thus, these two areas are excluded from this study. Elsewhere, vegetation season data are averaged across cells where the green season occurred 50% or more of the time during the study period. The interpolation of long-term averaged data is carried out using the Inverse Distance Weighting (IDW) algorithm of ArcGIS 9.2 Geostatistical Analyst.

In addition, daily carbon dioxide data observed at Point Barrow, Alaska ( $71.3^{\circ}\text{N}$ ,  $157.3^{\circ}\text{W}$ ) and Mauna Loa Observatory, Hawaii ( $19.5^{\circ}\text{N}$ ,  $155.6^{\circ}\text{W}$ ), are used to extract the onset and offset dates of biochemical seasons.

Section 6-2 introduces spatial patterns of long-term average onset/offset and duration of the vegetation season. Section 6-3 illustrates variations of the vegetation season with respect to latitude, longitude, and elevation. Section 6-4 provides a definition of the

carbon dioxide season. Section 6-5 describes changes in vegetation and carbon dioxide seasons. A summary and conclusion follows in section 6-6.

## 6.2. Spatial patterns of the vegetation season

According to maps of long-term averages (Figures 6.1-6.2), the vegetation season that is indicated by sudden green-up and green-down in annual NDVI time series occurs between lower mid-latitude vegetation regions and the Arctic tundra regions. In the

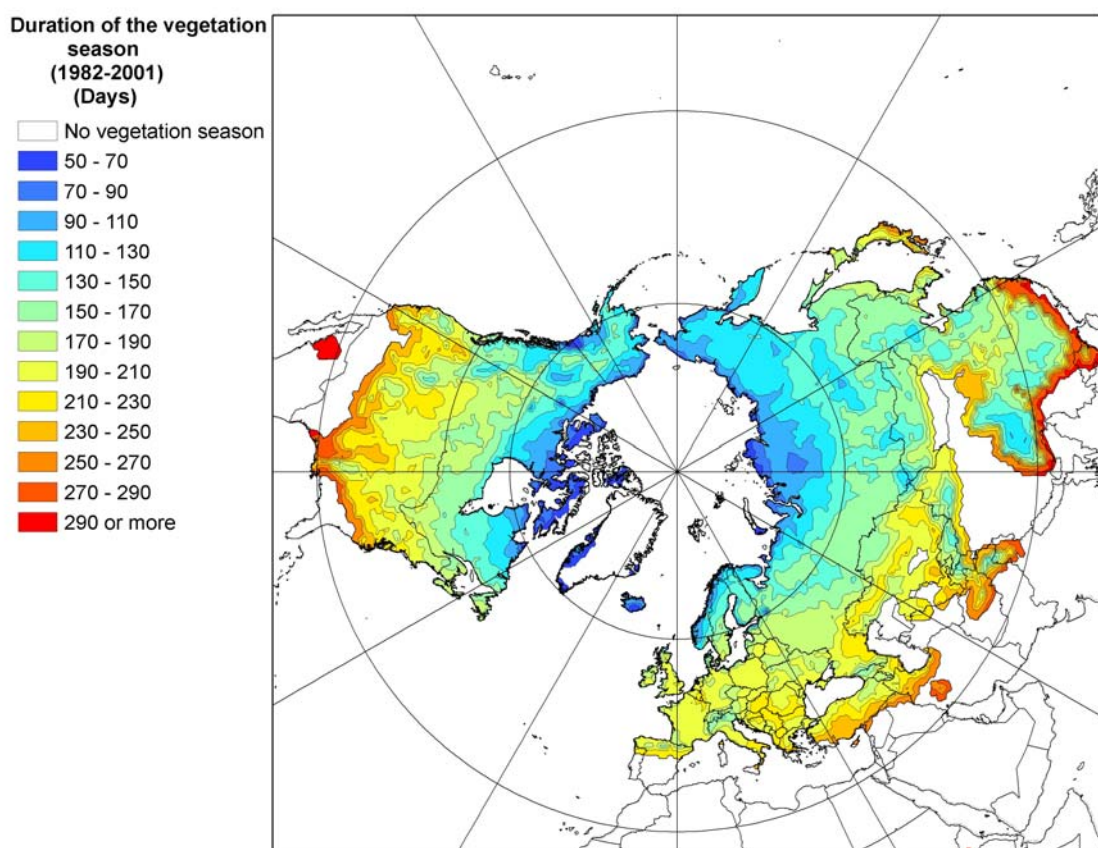


Figure 6.1. Duration of the vegetation season derived from NDVI data in the Northern Hemisphere, 1982-2001

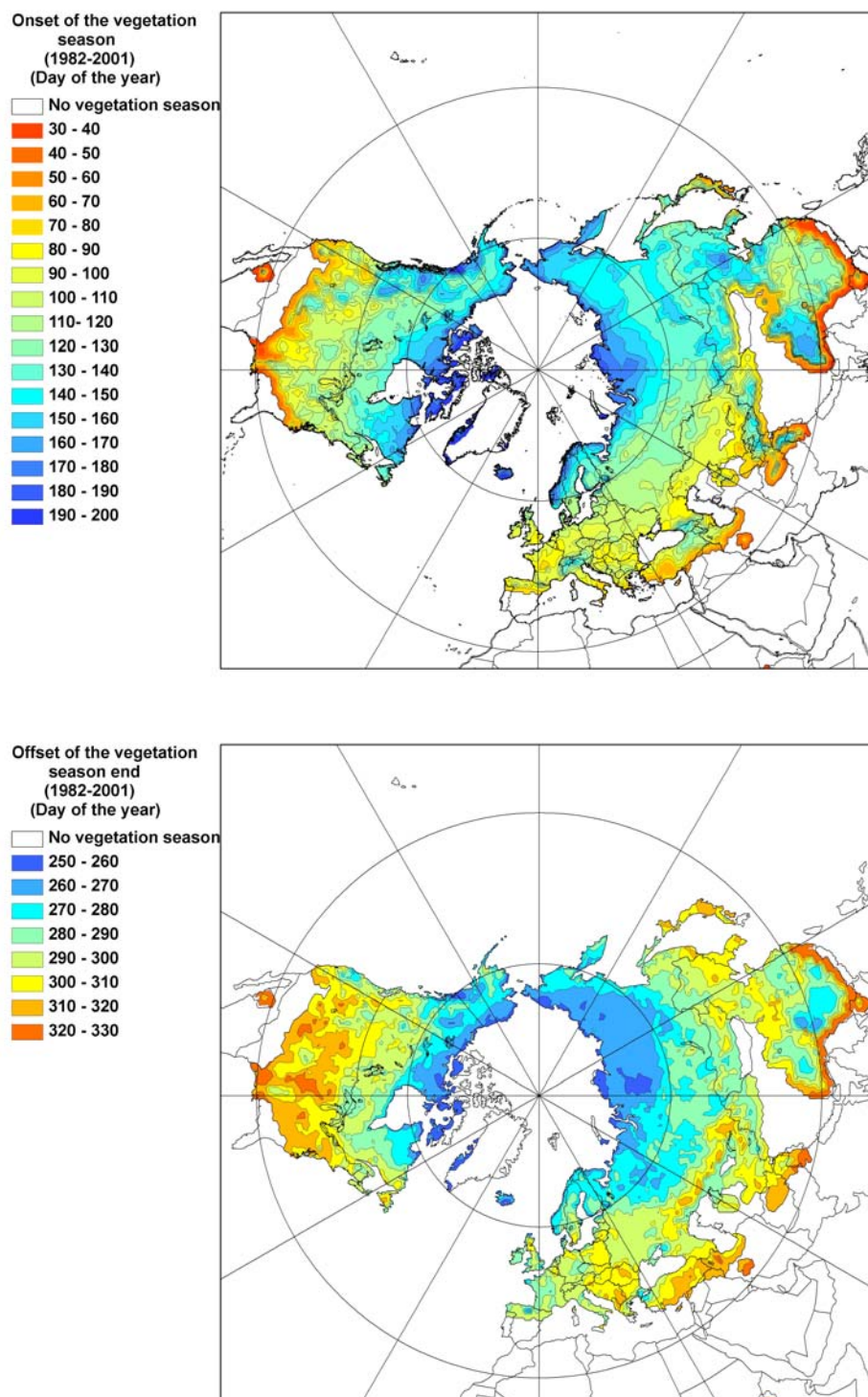


Figure 6.2. Onset (top) and offset (bottom) of the vegetation season derived from NDVI data in the Northern Hemisphere, 1982-2001

tropical region, NDVI seasonality is more affected by dry-wet periods than thermal seasonal cycles. Thus, there is no thermally-driven vegetation season in the tropical and desert regions.

The southern fringe of vegetation season onset appears in the range of 30-40°N in North America and Europe. In China, the southern fringe stretches southward to 22°N. The earliest onset occurs at the beginning of February and propagates toward high latitudes over the next 150 days with the onset at high latitudes from early June to early July. The offset of the vegetation season begins the earliest around the Arctic tundra regions in early September and propagates toward low latitudes within approximately 70 days, with the offset at low latitudes in late November. The duration of the vegetation season is 90-110 days in Arctic, while it extends for 250 days or more in southern boundary regions.

The onset/offset and duration of the vegetation season exhibit zonal patterns on a hemispheric scale. However, regionally, the zonal patterns are fragmented by types of vegetation as well as local physical settings such as high topography or proximity to water bodies (Figure 6.1). For example, the duration of vegetation season in the Great Plains is 10-30 days longer than in other regions at similar North American latitudes. In addition, the duration in northern China is 20-60 days shorter than in other regions of Eurasia and North America at the same latitude. In addition, the duration is reduced by 20-60 days at the elevations of 600-1500m compared with the low lands at similar latitudes. The vegetation season does not exist on the western Tibetan Plateau and the Himalayas at the elevations above 4000m due to persistently cold conditions.

### 6.3. Zonal, longitudinal, and vertical gradients of the vegetation season

Meridional profiles of onsets and offsets of the vegetation season along 110°E in Eastern Asia and 100°W in North America illustrate latitudinal gradients (Figures 6.3-6.4). At 110°E, where elevation is relatively homogenous at 320-740m, the onset progresses at the rate of 2.9 days/degree of latitude, while the offset propagates southward at 1.2 days/degree of latitude. Over the Great Plains (elevations under 500m), the onset gradient is similar to that of offset. The onset progresses northward at the rate of 2.1 days/degree of latitude, and the offset propagates southward at the rate of 2.1 days/degree of latitude. These rates indicate that the recently observed progressive onset and offset of the vegetation season is twice as rapid as that estimated by Hopkin's (1919). The duration of the vegetation season increases by 4 days/degree of latitude between the Arctic and southern regions where the vegetation season is observed. The latitudinal gradients are modified by regional factors such as elevation and vegetation type. For instance, latitudinal gradients are not evident in China and Mongolia due to the complex topography.

Longitudinal gradients of vegetation season exist over North America and Eurasia (Figures 6.5-6.6). For instance, the onset of the vegetation season is 40 days earlier in Europe compared with eastern Siberia and 20 days earlier in the Great Plains compared with the eastern United States. The offset is 10 days later in Europe compared with eastern Siberia and 20 days later in the Great Plains compared with the eastern United States. The eastward gradient between 0°E and 140°E in Eurasia is 3.7days/10 degrees of longitude (Figure 6.4). The onset is delayed toward eastern North America between 115°W and 65°W by 4.3 days/10 degrees of longitude. The gradient of the offset between

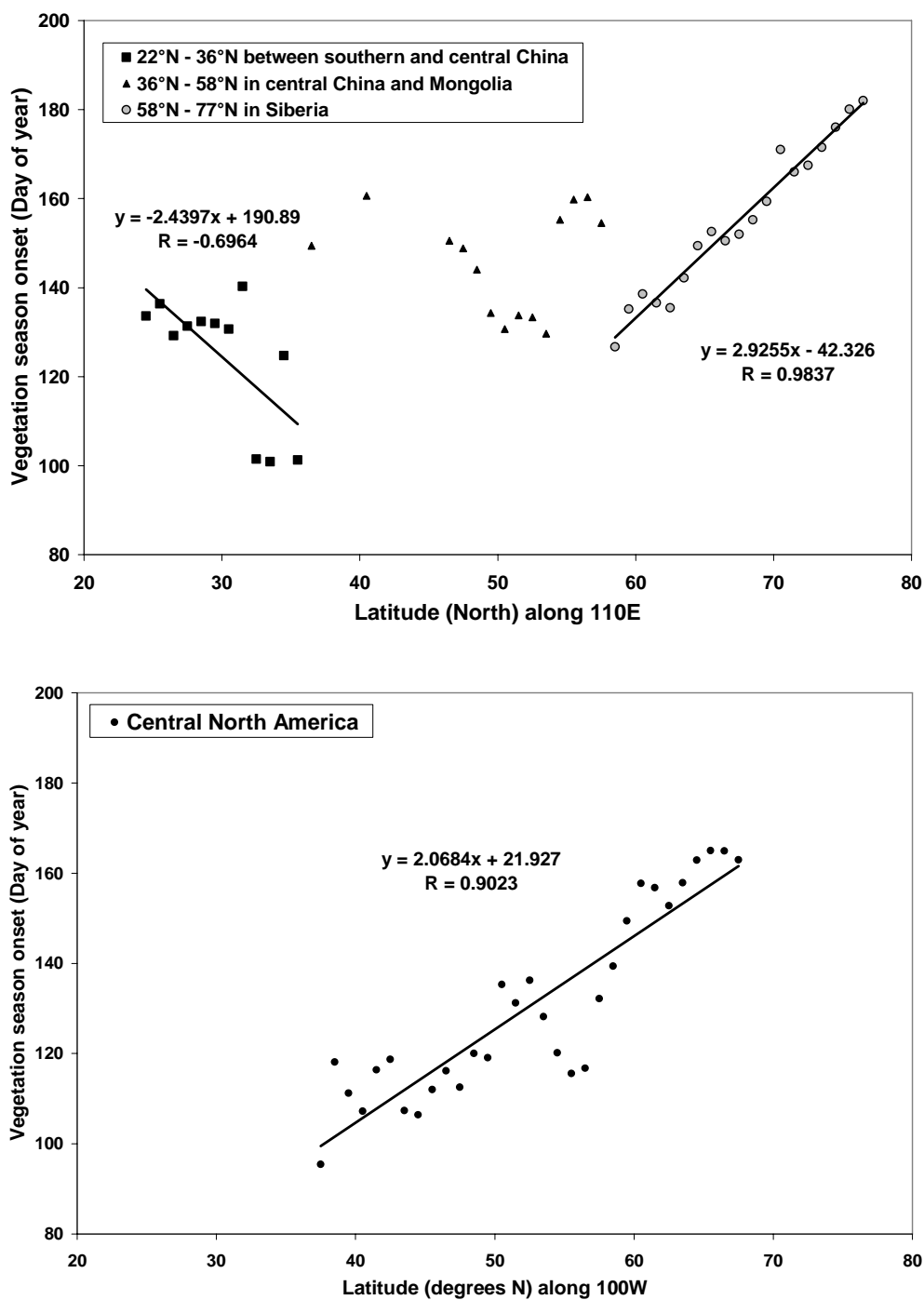


Figure 6.3. Latitudinal gradients of vegetation season onset in eastern Asia at 110°E (top) and in central North America at 100°W (bottom), 1982-2001

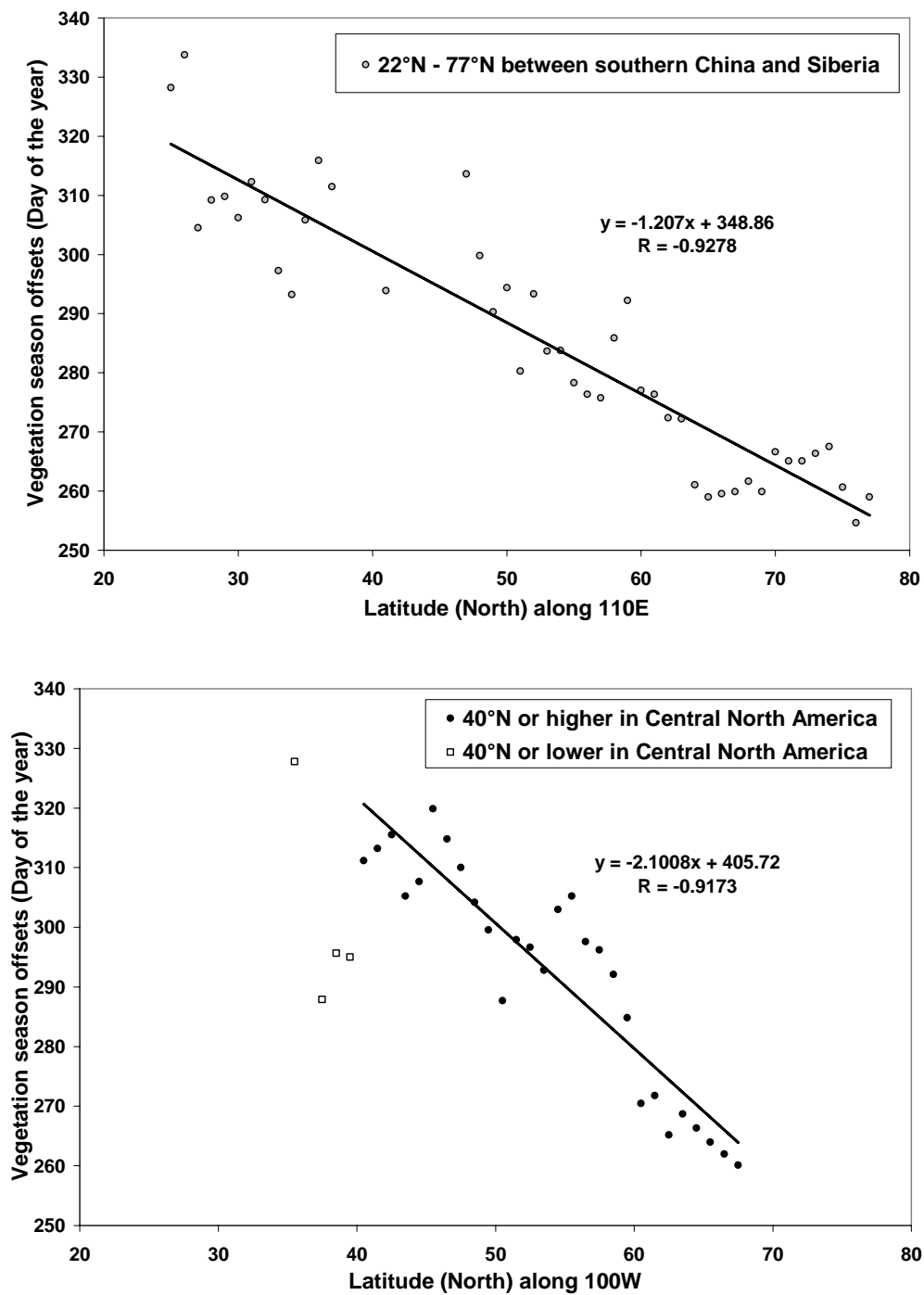


Figure 6.4. Latitudinal gradients of vegetation season offset in eastern Asia at 110°E (top) and in central North America at 100°W (bottom), 1982-2001

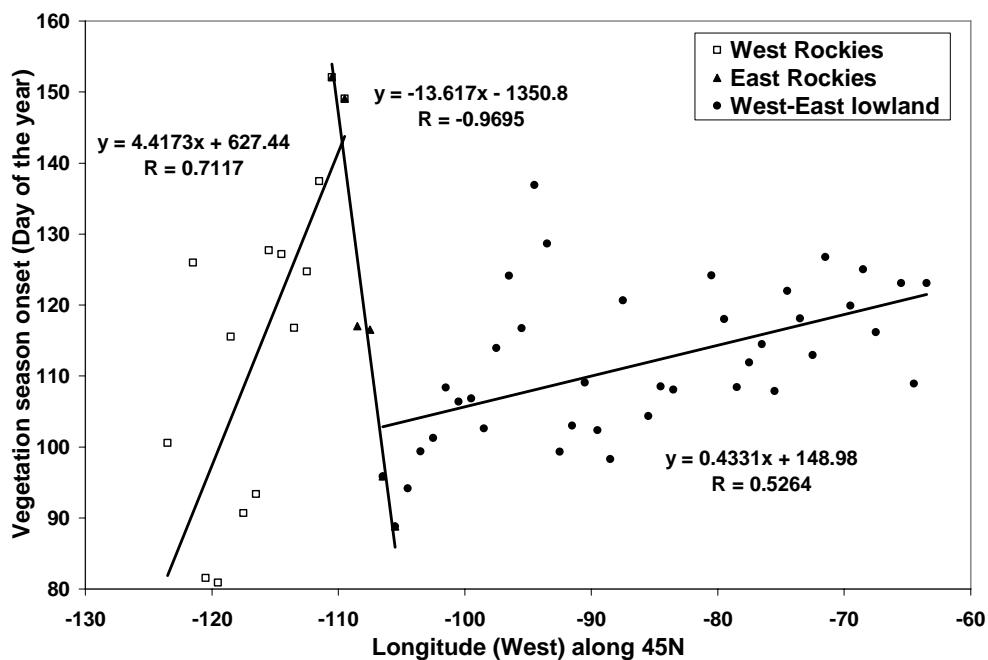
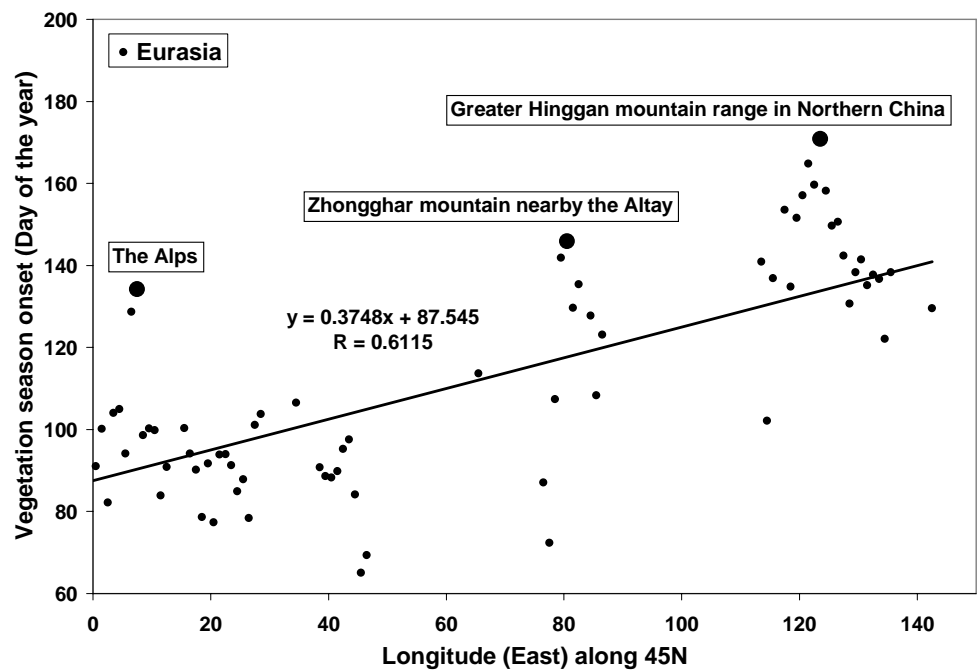


Figure 6.5. Zonal gradients of vegetation season onset in Eurasia (top) and in North America (bottom) along 45°N, 1982-2001

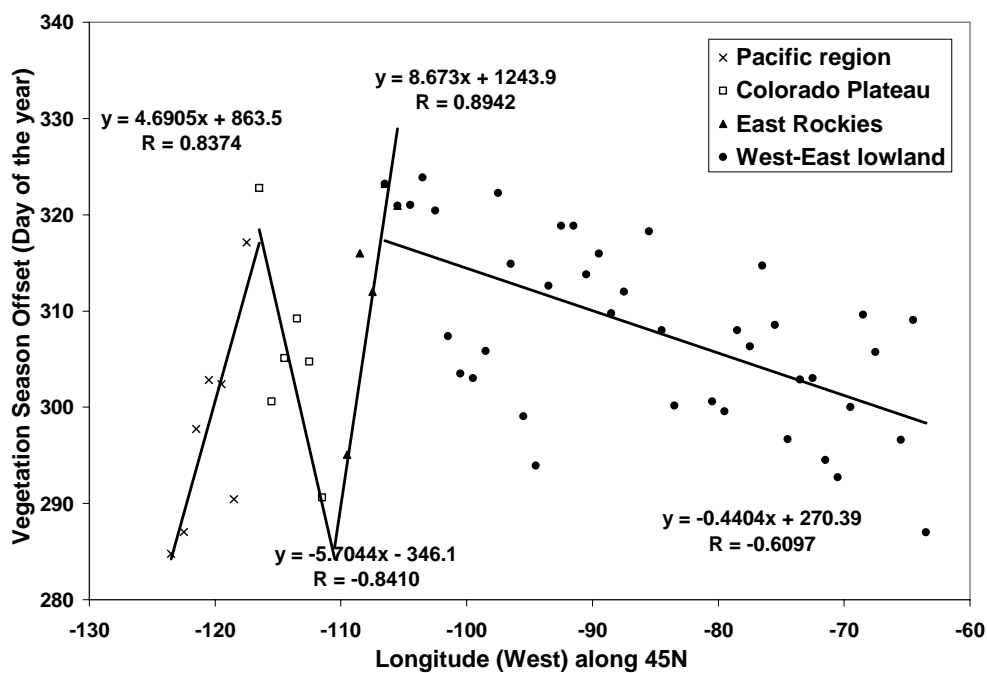
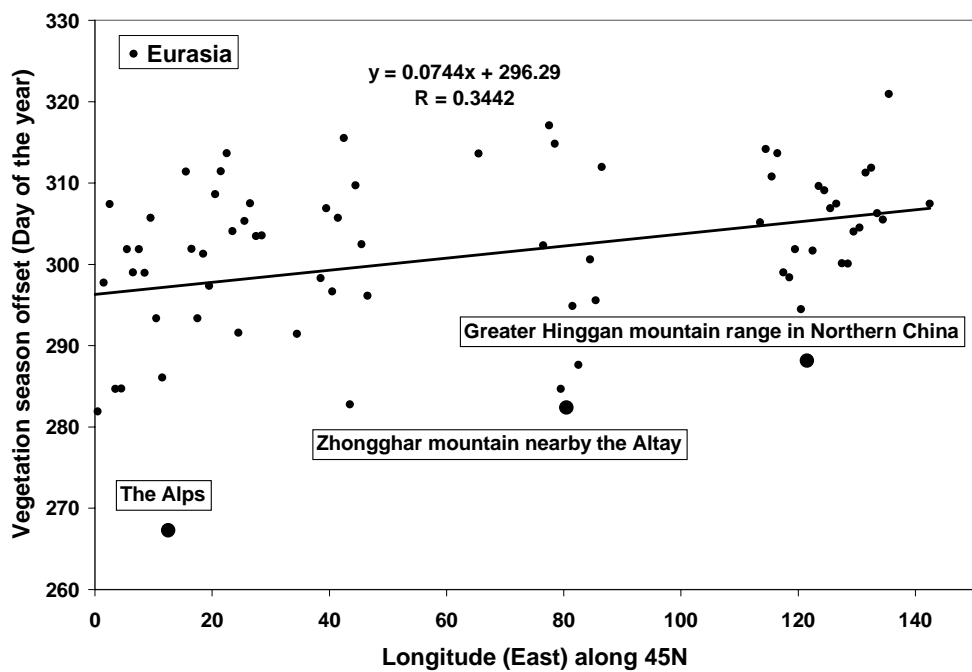


Figure 6.6. Zonal gradients of vegetation season offset in Eurasia (top) and in North America (bottom) along 45°N, 1982-2001

Europe and Eastern Asia is 0.7 days/10 degrees of longitude, while it is 4.4 days/10 degrees of longitude in North America.

Elevation plays an important role in causing vertical gradients of regional onsets and offsets. For instance, in the Rockies, the onset is delayed by approximately 3.5days/100m while the offset is advanced by 2 days/100m (Figures 6.5-6.6). As a result, the duration of the vegetation season over the highlands of the Rockies is about 110 days shorter than at lower elevations. This vertical progression of onset speed is similar to Hopkin's (1919) estimate (4days/400ft), whereas the propagation speed of the offset from high to low altitudes is faster than his estimate. Along 45°N in Eurasia, the vegetation season over high mountains such as the Alps, the Zongghar mountains, and the Greater Hinggang Mountains is also modified. Over these high mountains, the onset is 15-20 days later, while the offset is 20-30 days earlier compared to nearby lowlands.

#### **6.4. Defining the carbon dioxide season**

Intra-annual carbon dioxide concentration levels fluctuate as reverse bell-shaped curves because the gas is absorbed by vegetation through photosynthesis during the growing seasons and released into the atmosphere as vegetation lapses into dormancy each fall. In this study, the carbon dioxide season (CDS) is defined as the period free from the reduction of carbon dioxide by the photosynthesis of local vegetation. The onset and offset of CDS are selected based on inflection points in intra-annual variations of carbon dioxide. Long term (1974-2003) carbon dioxide data measured at Barrow, Alaska (71.3°N, 157.3°W) and at the Mauna Loa Laboratory in Hawaii (19.5°N, 155.6°W) are analyzed to understand variations of the CDS at low and high latitudes in

the Northern Hemisphere. As shown in the 2003 carbon dioxide time series data at Barrow Alaska (Figure 6.7), inter-daily carbon dioxide (black curve with square symbols) fluctuates with irregular peaks and troughs due to inter-daily air mass changes (Johnson & Kelley 1970). Therefore, 30 day moving averages are carried out twice to remove this daily noise. The double moving average method creates smooth curves (red curve), which helps detect inflection points. Then, second derivatives (blue curve) are calculated based on the smoothed curves. Again, 15 day moving averages between the corresponding date and 15 days earlier/later are subtracted to calculate the second derivatives to consider the persistence of intra-annual variations.

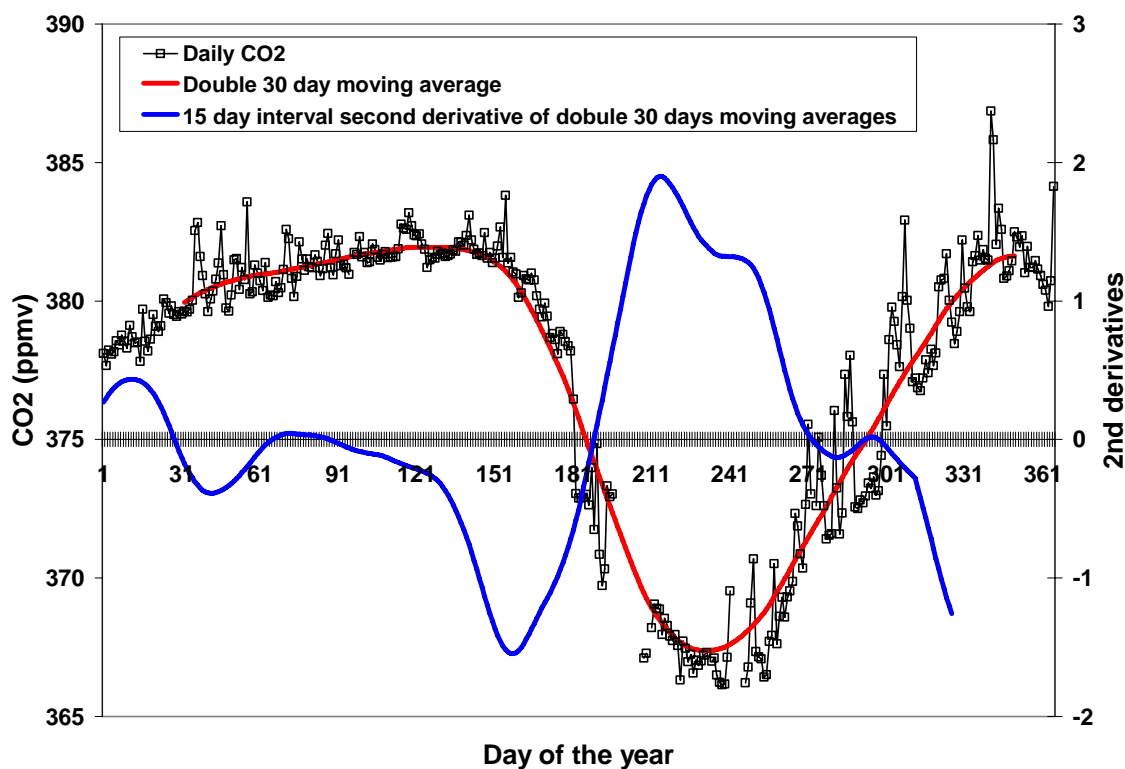


Figure 6.7. Time series of daily carbon dioxide, double moving average, and its second derivative in Barrow, Alaska in 2003

According to the double moving average curve (red curve) at Barrow in Figure 6.7, the maximum intra-annual carbon dioxide level is approached in early May. Carbon dioxide continues increasing until local vegetation absorbs the gas with its green-ups. The carbon dioxide level increases by 3ppm between January and May as the vegetation season propagates towards high latitudes. In other words, the magnitude of the carbon dioxide increased by anthropogenic activities during this period is greater than the capacity that forests at low and mid latitudes have to remove all of the increase from the atmosphere. In early June, the intra-annual curve decreases sharply with the onset of local vegetation green-up. Correspondingly, the second derivative also shows the lowest value because the change in carbon dioxide levels is maximized with the local green-up. Carbon dioxide at Barrow decreases more than 14ppm due to green-up of vegetation through photosynthesis between early June and late July. In particular, the difference (14-3= 9ppm) between January and late July indicates the magnitude of carbon dioxide that local vegetation green-up can reduce. The maximum capacity of the vegetation absorption of carbon dioxide through photosynthesis decreases in early July. The rate of the decrease is fast when local vegetation reduces the capacity of photosynthesis by falling leaves. The offset of the vegetation season lags between high and mid-latitudes; therefore, once annual leaves of vegetation fall, the carbon dioxide level is remotely affected by vegetation states at these latitudes. Photosynthesis of remote vegetation at lower latitudes continuously attenuates increases in carbon dioxide at high latitudes, even if the magnitude is not strong enough to make the level stable. As a result, the sign of second derivatives as shown in Figure 6.7 changes from positive to negative because the increase of carbon dioxide weakens with the advent of the offsets.

Based on these characteristics, the date with the lowest value in the curve of second derivatives between Day 50 and Day 210 is defined as the offset of the carbon dioxide season in this study. As discussed above, it is because the lowest second derivative indicates an inflection point that shows the fast decrease of carbon dioxide due to local photosynthesis. In contrast, the first date when the second derivative changes from a positive value to a negative value between Day 240 and Day 350 is defined as the onset of the carbon dioxide season. This date indicates the time when a sharp reduction in the absorption rate of carbon dioxide by local vegetation signals the advent of dormancy.

Table 6.1 summarizes the basic information about both observation sites and the extracted offsets/onsets of carbon dioxide seasons. The average offset of CSD for the study period is Day 165 (June 14) at Barrow and Day 145 (May 25) at Mauna Loa. Mauna Loa is located in tropical regions, but the offset of CSD exists there because the

Table 6.1. Stations, data, and onsets/offsets of carbon dioxide seasons analyzed in this study

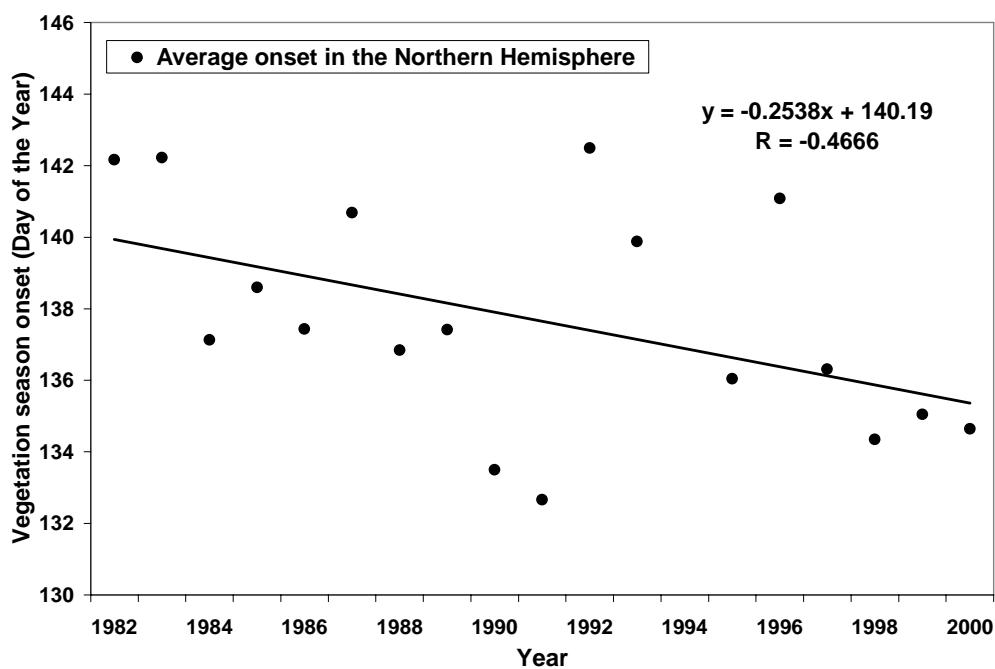
Station		Barrow, Alaska	Mauna Loa Observatory, Hawaii
Latitude		71.3°N	19.5°N
Longitude		155.6°W	157.3°W
Elevation (m) above msl		11	3397
Analyzed data period		1973-2003	1974-2004
Temporal scale		Daily	Daily
Offset	Average (day of the year)	165	145
	Standard deviation (days)	8	17
	Missing year	1987,2002	1975,1976,1984,1999
Onset	Average (day of the year)	277	317
	Standard deviation (days)	11	9
	Missing year	2002	1988,1992
Duration	Average (days)	253	193

elevation there is 3397 m above sea level. The average offset of CSD is Day 277 (October 4) in Barrow and Day 317 (November 13) in Mauna Loa. The average duration is 253 days in Barrow and 193 days in Mauna Loa, respectively. Standard deviations of onsets at both sites as well as offsets at Barrow are 8-11 days, while the standard deviation of offsets at Mauna Loa is 17 days.

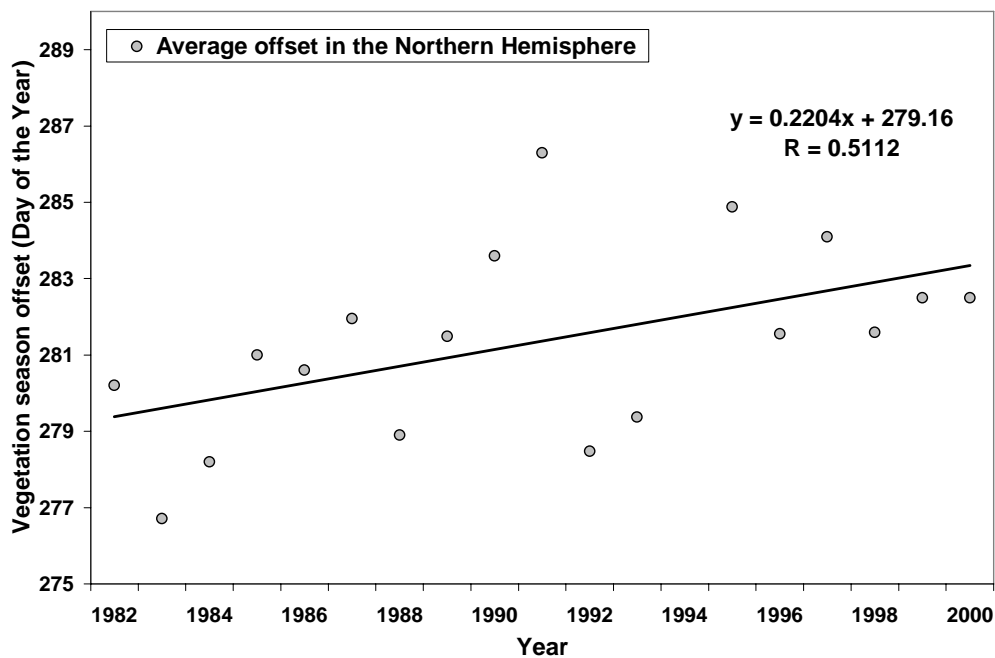
### 6.5. Changes in the vegetation and carbon dioxide seasons

In the Northern Hemisphere, the duration of the vegetation season has increased between 1982-2000 due to the advance of onset and delay of offset. Figure 6.8 illustrates the time series of the Northern Hemisphere averages of onsets, offsets, and durations across regions where the vegetation season occurs every year. According to linear

(a) Onset



## (b) Offset



## (c) Duration

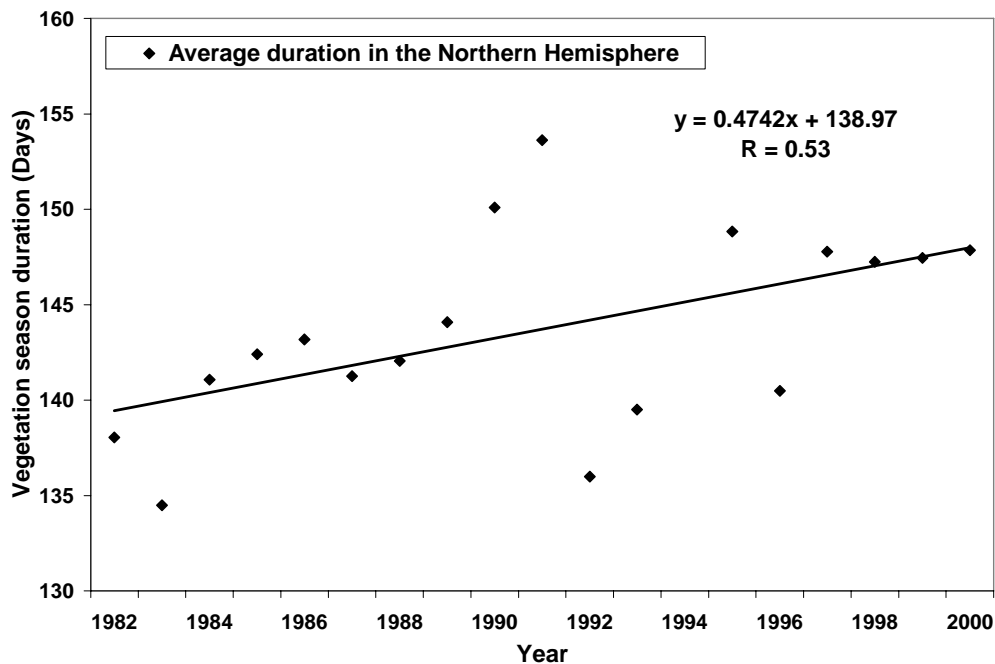


Figure 6.8. Trends of onset (a), offset (b), and duration (c) of spatially-averaged vegetation season in the Northern Hemisphere for the period 1982-2000

regression lines, the onset has advanced by 2.5 days/decade, while the offset has delayed by 2.2 day/decade. As a result, the duration of vegetation season has increased by 4.7 days/decade.

Figure 6.9 shows spatial patterns of these differences between the first five years (1982-1986) and the last five years (1996-2000) of observations. The onset of the vegetation season has advanced noticeably between 50°N and 60°N. Between Europe and Mongolia, the onset has advanced by 5-35 days. In highlands such as the Rockies and the western Tibetan Plateau, the onset has advanced by 5-15 days. In contrast, the onset is delayed in scattered regions of the eastern United States and northeastern China between 40°N and 50°N. In particular, the onset is delayed by 15 days or more along 40°N in the eastern United States. Offsets of the vegetation season in the most recent five year interval (1996-2000) were 3-35 days later in the corridor from the central United States to the southern Canadian Rockies as well as Alaska and northeastern China compared to the 1982-1986 year period. The most noticeable delays of more than 35 days are identified in the Great Plains. In contrast, the offset has advanced by 5-35 days in eastern and northwestern Canada and eastern Siberia. In particular, the offset has advanced by 35 days or more in eastern Canada. In Europe and western Siberia, the offset patterns are mixed, showing both decreasing and increasing trends on regional scales.

The offset of the carbon dioxide season (CDS) at Barrow has advanced at the rate of 5.9 days/decade for the period 1973-2003 (Figure 6.10). The Pearson correlation coefficient ( $r$ ) for the trend is -0.63, which is statistically significant. The offset of CDS at Mauna Loa shows an earlier trend at the rate of 4.9 days/decade, but it is not statistically significant because Pearson's  $r$  value is low (Figure 6.11). The onset of CDS at both

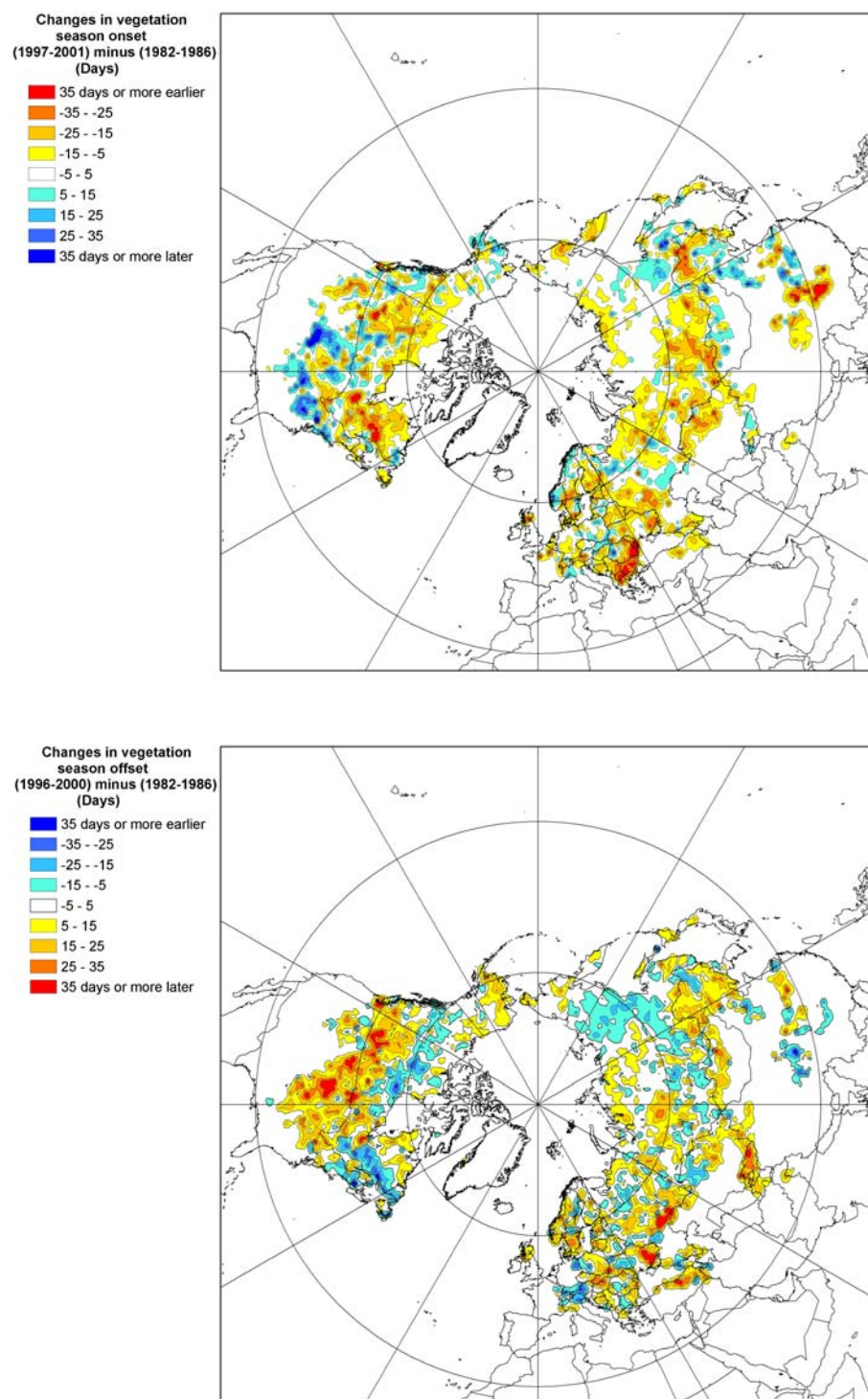


Figure 6.9. Changes in the onset (top) and offset (bottom) of vegetation season: Last five year (1996-2000) average minus first five year (1982-1986) average

locations shows a weak delay at the rate of approximately 2 days/decade, but statistically the rate is not significant.

The timing of the vegetation season has not changed at Barrow in recent decades, even though the onset of thermal spring and the offset of the Full Snow Season (FSS) have advanced 5-15 days in Alaska since the 1970s. Thus, it is speculated that a ten-day resolution of NDVI data used to define the vegetation season may not be enough to detect temporal changes of CDS which are less than 10 days. In addition, inconsistencies between carbon dioxide and the continental vegetation seasonal cycle may be associated with the oceanic carbon dioxide cycle. This cycle can lead or lag the timing of vegetation-driven carbon dioxide seasonal onset/offset at regional scales.

The Mauna Loa laboratory Hawaii is located at 3397m above sea level. Thus, onsets and offsets of the vegetation season in Hawaii with respect to elevation may exist at a local scale. For instance, the average of the offset of CDS at Mauna Loa is Day 153 (Early June), but inter-annual variability is high. It implies that the CDS at Mauna Loa is more affected by variability of local scale highland vegetation than the evergreen rainforest at low elevations.

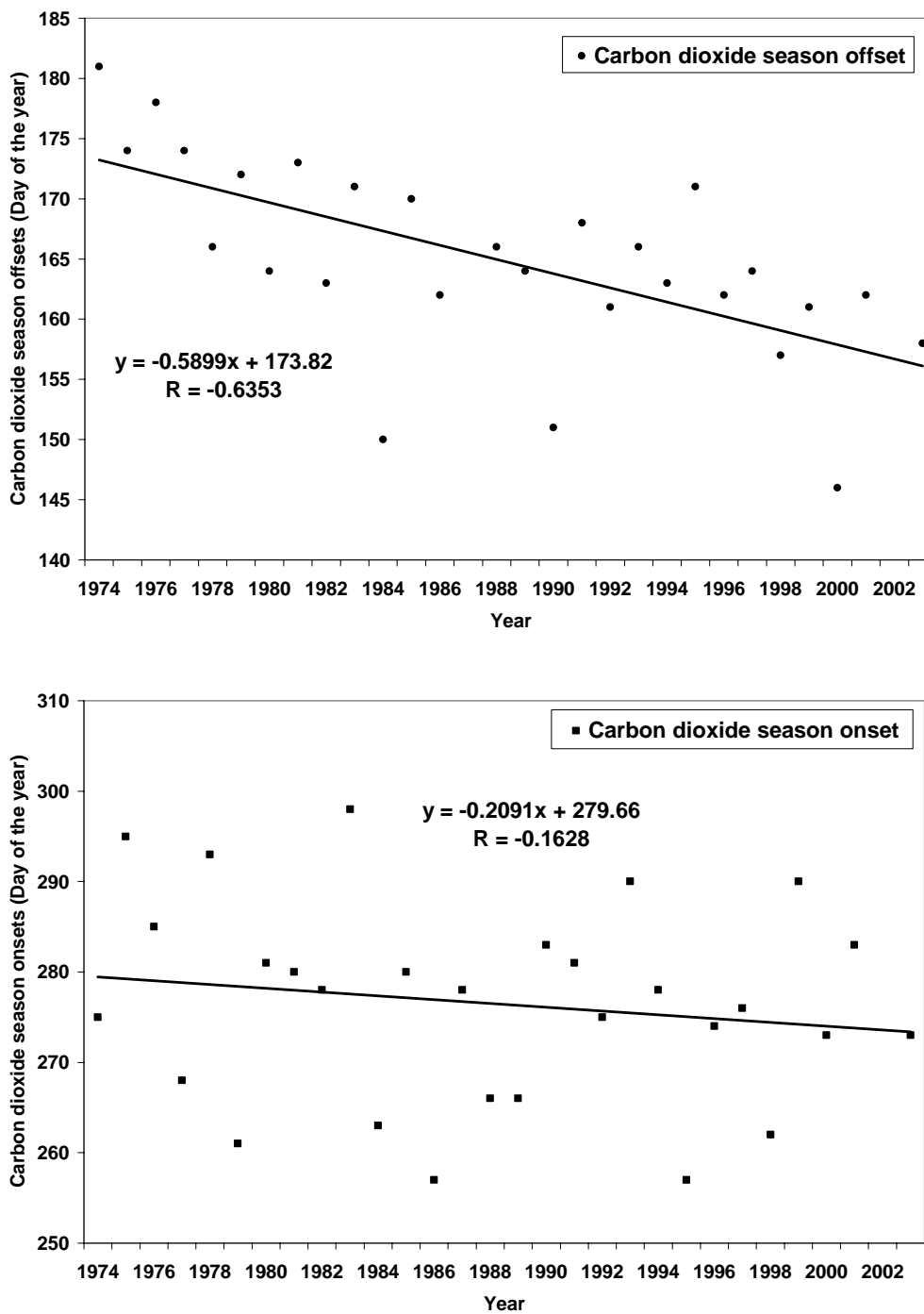


Figure 6.10. Inter-annual variations of the onset and offset of carbon dioxide season in Barrow, Alaska, 1974-2004

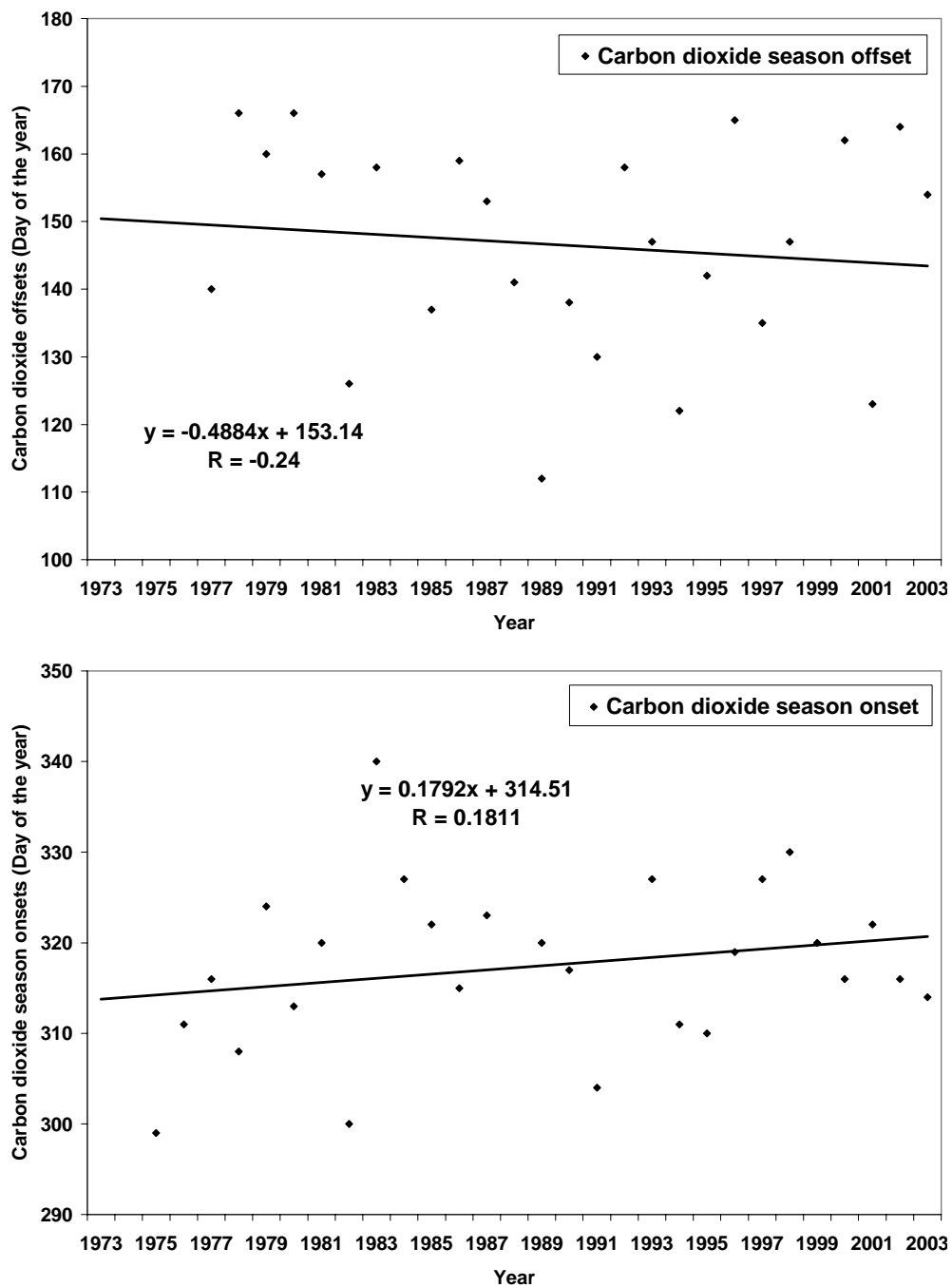


Figure 6.11. Inter-annual variations of the onset and offset of carbon dioxide season in Mauna Loa, Hawaii, 1973-2003

## 6.6. Summary and conclusion

Spatial patterns and temporal changes of the Northern Hemisphere vegetation season onset/offset and duration were examined between 1982 and 2001. Spatial differences, meridional, zonal, and vertical gradients, and potential trends were discussed. In addition, a definition of the carbon dioxide season was given, and changes in the onset/offset of this season at Barrow, Alaska and Mauna Loa, Hawaii were examined from 1974 to 2003. Major findings are summarized as follows:

The northward propagation of vegetation season onset is slower than the southward retreat of the offset. The onset period extends for 150 days from southern reaches in early February to the Arctic by early July, while the offset period lasts only 70 days from early September to late November. The onset propagates northward at a rate of 2.9 days/degree of latitude, while the offset retreats at -1.3 days/degree of latitude.

Zonal gradients of vegetation season onset/offset are found in both North America and Eurasia. At 45°N in North America, the onset is advanced over the Great Plains, while the offset is delayed. Zonal gradients of both onset and offset are approximately 7 days/10 degrees of longitude. At 45°N in Eurasia, the onset is delayed eastward by 3.7days/10 degrees of longitude.

The elevation also affects the onset/offset of the vegetation season. The onset in the Rockies is delayed at a rate of 3.5 days/100m, while the offset is advanced at a rate of 2.0 days/100m.

The onset of the vegetation season over the Northern Hemisphere has advanced by 2.5 days/decade, while the offset has delayed by 2.2 day/decade for the period 1982-2000. As

a result, the hemispheric average duration of the vegetation season has increased by 4.7 days/decade during the study period.

Changes in the vegetation season differ regionally in the late 1990s (1996-2000) compared to the early 1980s (1982-1986). An earlier onset is identified in coniferous taiga forest regions between 50°N and 60°N in the late 1990s, while the offset is delayed in the corridor from the central United States to southern Canadian Rockies. The offset is delayed by 35 days or more in the Great Plains grasslands, while the offset is advanced by 5-25 days in eastern Canada and eastern Siberia.

The offset of the carbon dioxide season in Barrow, Alaska has advanced by 5.9 days/decade for the period 1974-2004. However, trends of changes in the onset or offset are not statistically significant at Mauna Loa.

The results revealed in this study can be used to understand hemispheric scale patterns of vegetation and carbon dioxide seasons. The ten-day temporal resolution of NDVI data has limits when analyzing local or regional seasonality. Thus, future studies based on fine resolution data are needed. Furthermore, analyses of regional or local scale interactions between vegetation and atmospheric biochemical seasons such as carbon dioxide are needed.

## CHAPTER 7

### RELATIONSHIPS BETWEEN VARIOUS SEASONS AND SEASONAL PREDICTABILITY BASED ON ATMOSPHERIC CIRCULATION INDICES

#### 7.1. Introduction

The purpose of this chapter is to examine the similarity or dissimilarity of temporal and spatial patterns of the atmosphere, cryosphere, biosphere, and biochemical seasons as defined in previous chapters. Furthermore, statistical seasonal prediction models are developed based on linkages between seasons and atmospheric circulation indices such as the Arctic Oscillation (AO) and the El Niño Southern Oscillation (ENSO).

Pearson correlation analyses are carried out to examine relationships among various types of hemispheric average seasonal onsets and durations derived from temperature (Chapter 4), snow cover (Chapter 5), vegetation index, or atmospheric carbon dioxide concentration (Chapter 6). In addition, spatial patterns of long-term average onset and duration are compared amongst these various seasons using spatial overlapping techniques in GIS.

Canonical correlation analysis (CCA), which helps identify teleconnections between two gridded data sets of climate variables (Nicholls 1987), is used to develop statistical seasonal prediction models. In CCA, eigenvectors for gridded data such as spatially varying seasonal onset and duration data are depicted as spatial maps, while eigenvectors for temporal data such as monthly atmospheric circulation indices are illustrated as time series (von Storch & Zwiers 2002). Glahn (1968) was the first to discuss meteorological applications of CCA and the relationships of CCA to discriminant and multiple

regression analyses. Since then, CCA has been commonly used to forecast seasonal temperatures over North America (Barnston 1994; Shabbar & Barnston 1996; Mo 2003), Africa (Barnston et al. 1996; Ntale et al. 2003), Europe (Johansson et al. 1998; Friederichs & Hense 2003), and Asia (Hwang et al. 2001) using SST related to ENSO as a predictor.

For calculations of CCA, monthly atmospheric circulation indices are used as predictor variables and gridded onset or duration data of thermal seasons as predicted variables. Atmospheric circulation indices used in CCA include monthly Arctic Oscillation (AO), El Niño Southern Oscillation (ENSO), Northern Atlantic Oscillation (NAO), and Pacific North America pattern (PNA), each calculated by the NOAA Climate Diagnostic Center (NOAA 2006). To identify lead-lag relationships simultaneously, monthly average circulation data between July in the previous year and June in the corresponding year are used to predict thermal spring onset and thermal summer onset, while monthly circulation data between January and December in the corresponding year are used to predict thermal fall onset and thermal winter onset. The Climate Predictability Tool (CPT) developed by the International Research Institute for Climate and Society (IRI) at Columbia University is used to conduct the CCA. The CPT enables the rapid production of seasonal climate forecasts based on canonical correlation analysis or principal components analysis. Regional data showing statistically-significant relationships in the CCA analyses are subset to develop regional scale prediction models through simple linear regression analyses. SPSS 14.0 is employed in constructing the regression model and in calculating its statistical significance.

In section 7-2, spatial and temporal progression patterns of thermal, snow, vegetation, and carbon dioxide seasons are compared. In section 7-3, teleconnections of those seasonal onset or durations with various atmospheric circulation indices are discussed. Section 7-4 introduces statistical models for predicting thermal seasonal onsets and durations developed through canonical correlation and simple linear regression analyses. A summary and conclusion are given in section 7-5.

## **7.2. Comparison of thermal, snow, vegetation, and carbon dioxide seasons**

### **Correlations among hemispheric average onsets and durations**

Correlations amongst Northern Hemisphere average onsets, ends, and durations of thermal (Chapter 4), snow (Chapter 5), vegetation, and carbon dioxide (Chapter 6) seasons are calculated (Tables 7.1-7.4). Definitions of each seasonal onset and duration are provided in Chapters 4-6.

Table 7.1 summarizes Pearson correlation coefficients ( $r$ ) between thermal seasons and snow seasons for the period 1979-2005. The most statistically significant (>99%) correlation is found between the end of the Full Snow Season (FSS) and thermal spring onset ( $r= 0.732$ ). The Core Snow Season (CSS) shows a less significant correlation with thermal spring onset ( $r= 0.587$ ), indicating that thermal onsets are more associated with the FSS offset than the CSS offset. Similarly, thermal winter duration shows more statistically-significant correlation with the FSS ( $r= 0.731$ ) end than CSS ( $r= 0.517$ ) end. These correlations indicate that inter-annual variability of thermal winter duration is more affected by the end than the onset. It is also inferred that the last snow-covered event in late thermal winter is more associated with the arrival of thermal spring than the

Table 7.1. Pearson correlation coefficients ( $r$ ) between Northern Hemisphere average thermal seasons and snow seasons for the period 1979-2005; Full Snow Season (FSS), Core Snow Season (CSS), Onset (O), End (E), Duration (D), Spring (Sp), Summer (Su), Fall (Fa), and Winter (Wi)

1979-2005		Thermal seasons							
		Sp_O	Su_O	Fa_O	Wi_O	Sp_D	Su_D	Fa_D	Wi_D
Snow seasons	FSS O	0.148	-0.069	-0.084	0.126	-0.219	0.000	0.333	0.026
	FSS E	0.732**	0.436**	-0.651**	-0.554**	-0.326	-0.573**	0.092	0.731**
	FSS D	0.323	0.601**	-0.451*	-0.572**	0.249	-0.574**	-0.185	0.483*
	CSS O	0.249	0.152	-0.448**	-0.203	-0.107	-0.306	0.373	0.257
	CSS E	0.587**	0.289	-0.192	-0.294	-0.319	-0.264	-0.156	0.517*
	CSS D	0.285	0.116	0.194	-0.081	-0.179	0.024	-0.419*	0.221

\*\* Correlation is significant at the 0.01 level (2-tailed).

\* Correlation is significant at the 0.05 level (2-tailed).

disappearance of long-lasting snow cover in mid-winter. Thermal winter onset shows a statistically significant association with both the FSS end ( $r = -0.554$ ) and the FSS duration ( $r = -0.572$ ), but there is no significant correlation between thermal winter onset and CSS cycle, implying that the CSS duration is independent from inter-annual variations of thermal winter duration on a hemispheric scale.

Thermal summer onset shows significant positive correlations with the FSS end ( $r = 0.436$ ) and duration ( $r = 0.601$ ), whereas thermal fall onset shows significant negative correlations with the FSS end ( $r = -0.651$ ), FSS duration ( $r = -0.451$ ), and the CSS onset ( $r = -0.488$ ). Thermal summer duration shows statistically significant negative correlations with the FSS ( $r = -0.573$ ) end and duration ( $r = -0.574$ ). These results suggest that advances in FSS offset in recent decades may be associated with the extension of thermal summer durations. In contrast, thermal spring and fall durations do not show significant correlations with both snow season onset/offset. The CSS duration shows a significant correlation ( $r = -0.419$ ) with thermal fall duration.

Thermal seasons show several statistically-significant relationships with vegetation

Table 7.2. Pearson correlation coefficients ( $r$ ) between Northern Hemisphere average thermal seasons and vegetation season (V) for the period 1982-2001, or between thermal seasons and carbon dioxide (CO<sub>2</sub>) seasons at Barrow, Alaska (B) and at Mauna Loa, Hawaii (M) for the period 1979-2005; Onset (O), End (E), Duration (D), Spring (Sp), Summer (Su), Fall (Fa), Winter (Wi)

1982-2001 1979-2003		Thermal seasons							
		Sp O	Su O	Fa O	Wi O	Sp D	Su D	Fa D	Wi D
Vegetation seasons	V O	0.585**	0.739**	-0.809**	-0.689**	0.167	-0.824**	0.178	0.707**
	V E	-0.400	-0.604**	0.563*	0.489*	-0.200	0.630**	-0.051	-0.490*
CO <sub>2</sub> seasons	B E	0.405	0.248	-0.459*	-0.345	-0.162	-0.365	0.180	0.423*
	B O	-0.095	0.175	-0.058	-0.134	0.261	-0.134	-0.113	0.001
	M E	0.449*	0.261	-0.353	-0.443*	-0.223	-0.327	-0.149	0.501*
	M O	0.061	0.406*	-0.145	-0.135	0.319	-0.304	0.033	0.102

\*\* Correlation is significant at the 0.01 level (2-tailed).

\* Correlation is significant at the 0.05 level (2-tailed).

season or carbon dioxide season as summarized in Table 7.2. Four thermal seasonal onsets are associated with the onset of the vegetation season. The most significant correlation is found between thermal summer duration and vegetation season onset ( $r = -0.824$ ). The negative correlation indicates that thermal summer duration is shortened when the onset of the vegetation season is delayed. The end of the vegetation season is correlated with the onsets of thermal summer ( $r = -0.614$ ), thermal fall ( $r = 0.563$ ), and thermal winter ( $r = 0.489$ ), as well as durations of thermal summer ( $r = 0.630$ ) and thermal winter ( $r = -0.493$ ). These correlations suggest that the end of the vegetation season is delayed when the duration of the thermal summer increases.

In the case of correlations between thermal seasons and carbon dioxide season at Barrow, Alaska (71.3°N, 157.3°W; 11 m above msl) and Mauna Loa, Hawaii (19.5°N, 155.6°W; 3397 above msl), only thermal winter duration shows a significant positive correlation with the offset of carbon dioxide season at both locations, indicating that the earlier the end of the carbon dioxide season in spring, the shorter thermal winter gets. In other cases, only one location shows statistically-significant correlations. These results

Table 7.3. Pearson correlation coefficients (r) between Northern Hemisphere average vegetation season (V) and carbon dioxide (CO<sub>2</sub>) seasons at Barrow, Alaska (B) and at Mauna Loa, Hawaii (M) for the period 1979-2005; Onset (O) and End (E)

1982-2001		CO <sub>2</sub> seasons			
		B E	B O	M E	M O
Vegetation seasons	V O	0.311	0.158	0.417	0.209
	V E	-0.080	-0.135	-0.319	-0.536**

\*\* Correlation is significant at the 0.01 level (2-tailed).

\* Correlation is significant at the 0.05 level (2-tailed).

imply that absorption of carbon dioxide by vegetation in spring is a key factor associated with the duration of thermal winter season, while other thermal seasonal onsets and durations are independently associated with variations of carbon dioxide on a local scale rather than on a global scale. Similarly, hemispheric average onset and offset of the vegetation season are not significantly correlated with the carbon dioxide season (Table 7.3). Only the onset of the carbon dioxide season shows a negative correlation with the end of the vegetation season ( $r = -0.536$ ) at Mauna Loa, Hawaii.

Significant correlations are also identified between snow seasons and vegetation or carbon dioxide seasons (Table 7.4). The FSS duration is positively correlated with the

Table 7.4. Pearson correlation coefficients (r) between Northern Hemisphere average snow seasons and vegetation season (V) for the period 1982-2001, or between snow seasons and carbon dioxide (CO<sub>2</sub>) seasons at Barrow, Alaska (B) and at Mauna Loa, Hawaii (M) for the period 1979-2005; Full Snow Season (FSS), Core Snow Season (CSS), Onset (O), End (E), Duration (D), Spring (Sp), Summer (Su), Fall (Fa), Winter (Wi)

1982-2001 1974-2003		Snow seasons					
		FSS O	FSS E	FSS D	CSS O	CSS E	CSS D
Vegetation seasons	V O	-0.250	0.360	0.448*	0.219	0.151	-0.035
	V E	-0.163	-0.225	-0.129	-0.216	-0.107	0.058
CO <sub>2</sub> seasons	B E	-0.036	0.664**	0.496**	0.312	0.226	-0.036
	B O	-0.110	0.113	0.052	-0.010	-0.107	-0.009
	M E	0.067	0.414*	0.191	0.084	0.553**	0.368
	M O	0.022	-0.088	-0.180	-0.162	-0.176	-0.027

\*\* Correlation is significant at the 0.01 level (2-tailed).

\* Correlation is significant at the 0.05 level (2-tailed).

onset of the vegetation season ( $r= 0.448$ ) and the offset of the carbon dioxide season ( $r=0.496$ ) at Barrow. In contrast, the FSS offset is not correlated with the onset of the vegetation season, but has a significant positive correlation with the offset of the carbon dioxide season at both Barrow ( $r= 0.664$ ) and Mauna Loa ( $r= 0.414$ ). This suggests that the end of the carbon dioxide season is advanced when the end of the snow season is advanced on a hemispheric scale. Relationships between local carbon dioxide seasons and hemispheric average vegetation seasons are not clear. CSS variables do not show any significant correlations with vegetation or carbon dioxide seasons except for a positive correlation ( $r= 0.553$ ) between the end of carbon dioxide season at Mauna Loa and the end of CSS. Thus, FSS is more associated with vegetation or carbon dioxide season than CSS.

### **Spatial lead-lag relationships in the seasonal progression**

Temperature is considered as one of the important factors that affect intra-annual growth of vegetation. For instance, a  $5^{\circ}\text{C}$  daily mean temperature is commonly used to define the growing season (Menzel et al. 2003; Zheng et al. 2006). However, the comparison between thermal and vegetation seasonal progressions shows that temperature-vegetation relationships are not constant from one ecosystem to another (Figure 7.3). Both thermal spring onset ( $T_{\text{mean}} \geq 5^{\circ}\text{C}$ ) and vegetation season onset (increasing inflection point in NDVI time series) occur between Day 30 (February) and Day 180 (late June) over the Northern Hemisphere land masses (Figure 7.1).

At lower mid-latitudes, thermal spring onset isolines of Day 60-90 are located more northward than vegetation season onset zones of Day 60-90, implying that the onset of

the vegetation season progresses behind the onset of thermal spring by 30-60 days at lower mid-latitudes. For example, the onset of vegetation season follows 30-60 days after thermal spring season onset progresses in Manchuria. At mid-latitudes, between 40°N and 60°N, thermal spring onset dates are consistent with the vegetation season onset dates. Above 60°N such as Alaska and eastern Siberia, the onset of the vegetation season occurs before thermal spring arrives. For example, the vegetation seasonal onset lines of Day 120-150 are located at higher latitudes compared with thermal spring onset contour lines of Day 150.

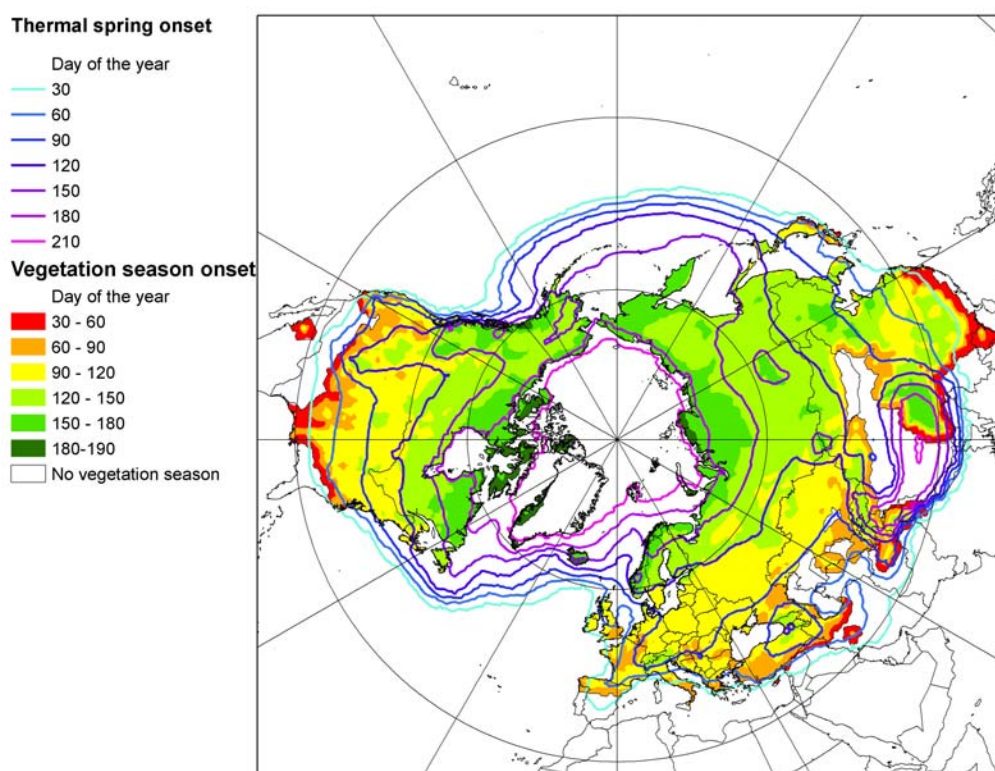


Figure 7.1. Comparison of long-term average thermal spring onset (1979-2005) with vegetation seasonal onset (1982-2001) in the Northern Hemisphere

The lead-lag spatial patterns between the offset of the vegetation season and thermal winter onset progressions are reversed. The offset of the vegetation season occurs within three months between mid-September and mid-December, while thermal winter onset occurs between Day 220 (mid August) and Day 370 (early January) (Figure 7.2). The offset of the vegetation season at high latitudes occurs 10-30 days after thermal winter onset progresses southward, whereas between 20°N and 35°N, the offset of the vegetation season occurs 10-30 days before the onset of thermal winter. For example, the progression line of Day 280 thermal winter onset appears in northeastern China, while the vegetation season offset line of Day 280 are located at high latitudes above 55°N.

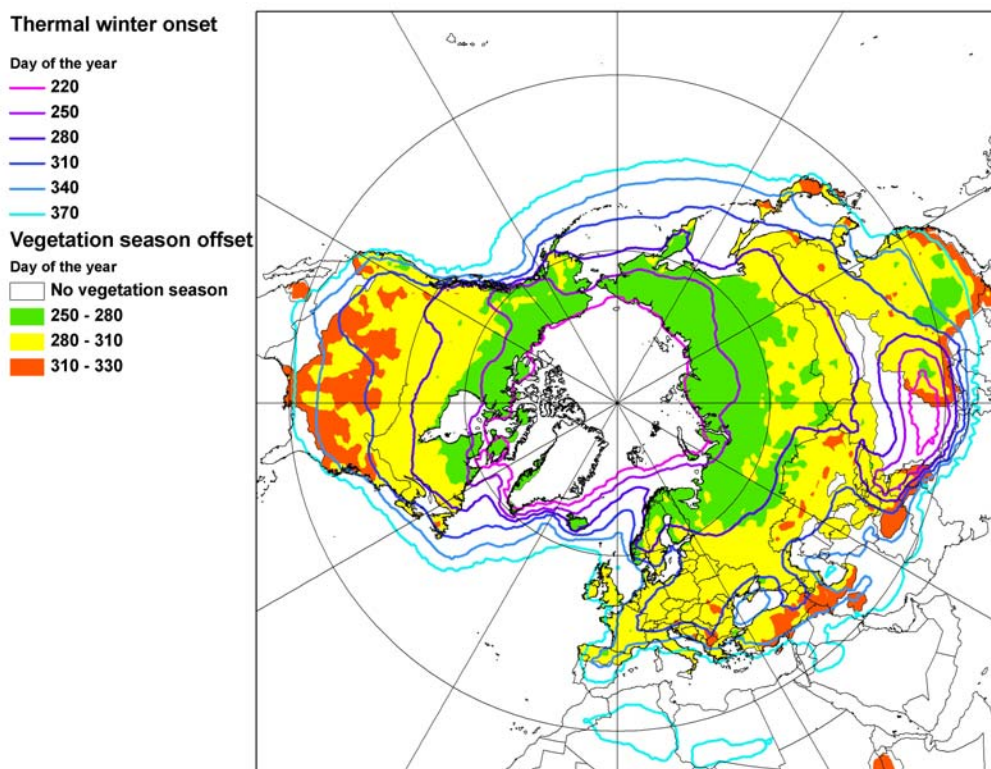


Figure 7.2. Comparison of long-term average thermal winter onset (1979-2005) with vegetation seasonal offset (1982-2001) in the Northern Hemisphere

Between 35-55°N, the offset of the vegetation season is coincident with thermal winter onset.

Differences exist between durations of vegetation and thermal growing seasons at high latitudes, high altitudes, and in the lower mid-latitudes (Figure 7.3). In the former two regions, the vegetation season lasts longer than the thermal growing season. The opposite occurs in the lower mid-latitudes. For instance, in southeastern United States, southern and western Europe, and eastern Asia, the vegetation season is shorter by at least 20 days than the thermal growing season.

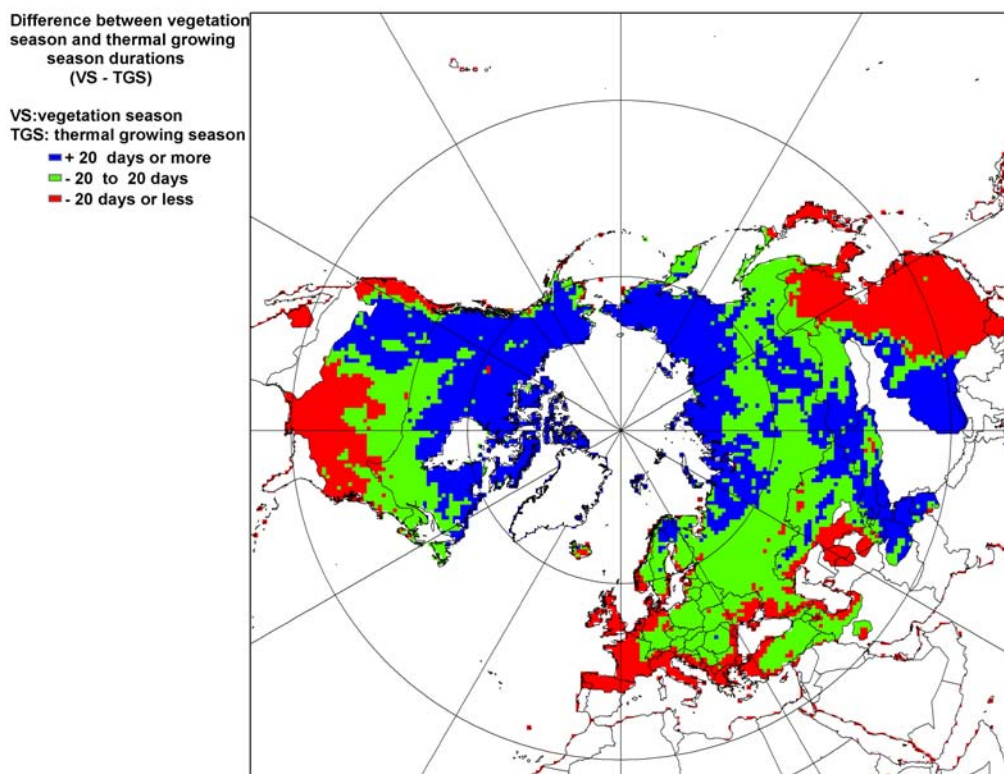


Figure 7.3. Differences between the vegetation season (1982-2001) and thermal growing season durations (1979-2005) in the Northern Hemisphere

These latitudinal inconsistencies indicate that the static threshold ( $T_{\text{mean}} \geq 5^{\circ}\text{C}$ ) used to define the thermal growing season is not appropriate to demarcate the actual vegetation season at all latitudes. The offset patterns between thermal and vegetation seasons suggest that high latitude or low latitude vegetation has evolved to prosper at conditions different from those found in the mid-latitudes. For instance, high latitude or high altitude ecosystems such as Arctic or alpine tundra are less sensitive to the occurrence of low temperature with the onset of thermal winter but more sensitive to the increase of solar radiation with the arrival of thermal spring compared with other zones or lower elevations. In contrast, low latitude vegetation is acclimatized to the warm climate, which makes it less sensitive to the arrivals of thermal spring but more sensitive to the occurrence of low temperature during the winter onset period. The use of accumulated degree days may be better than employing a static threshold of daily mean temperature to define vegetation growing seasons based on air temperature.

Vegetation seasonal zones are latitudinally asymmetrical in both North America and Eurasia (Figure 7.3). In North America, high elevation and topographical effects along the Rockies lead to a west-east gradient in both vegetation and thermal seasonal onsets. Similarly, 30-90 day differences in both thermal and vegetation seasonal onsets/offsets occur between Europe and East Asia. The west-east contrast in Eurasia may be associated with dynamical factors such as proximity to ocean and regional quasi-stationary pressure systems. For instance, the Bermuda high pressure system helps the mid-latitude westerly wind transport warm moist air over the warm Gulf Stream toward northern Europe. In contrast, the combined effects of the Siberian high and the Okhotsk low pressure systems allow the transport of high latitude cold air toward the mid-latitudes in East Asia.

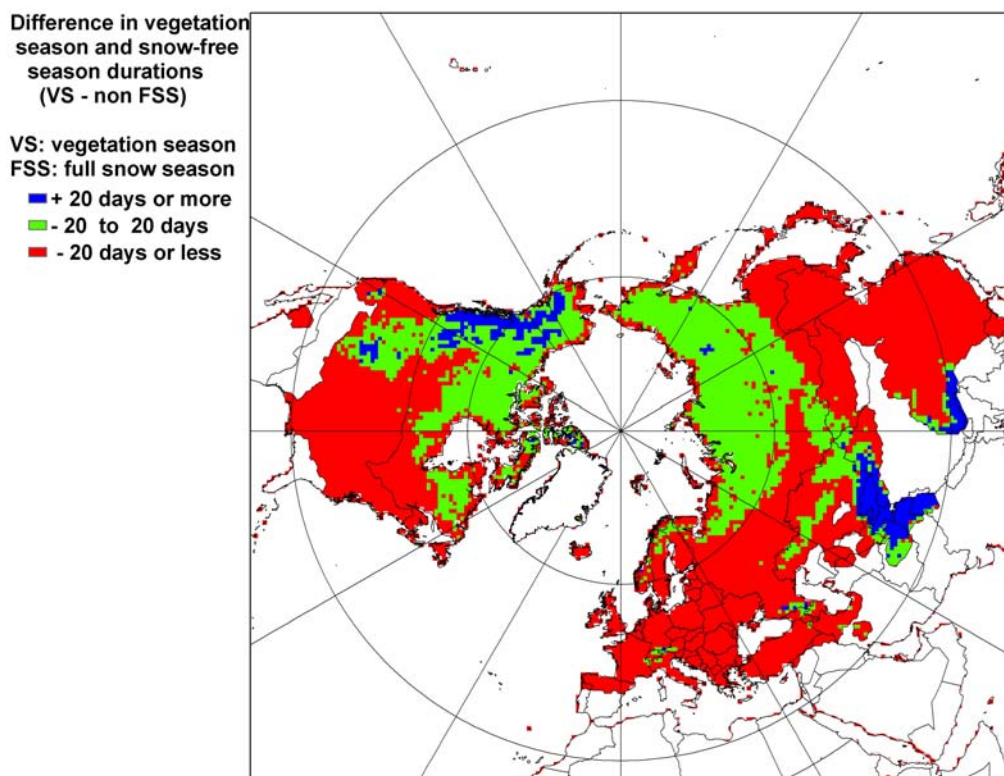


Figure 7.4. Differences between vegetation season (1982-2001) and non-Full Snow Season (non-FSS) durations (1967-2005) in the Northern Hemisphere

A comparison of vegetation season zones with snow-free (non-FSS) duration (Figure 7.4) finds patterns different than those observed in the comparison of vegetation-thermal season patterns. At high latitudes and high altitudes, the duration of the vegetation season is similar to that of the non-FSS season. In the polar region, the Core Snow Season (CSS) is similar to the Full Snow Season (FSS). In other words, the front of a green wave propagates along with snow melt line at high latitudes. Snow melt and vegetation green-up likely occur simultaneously because continuous solar radiation during the polar summer provide more energy per day compared with sunshine hours at low latitudes. In

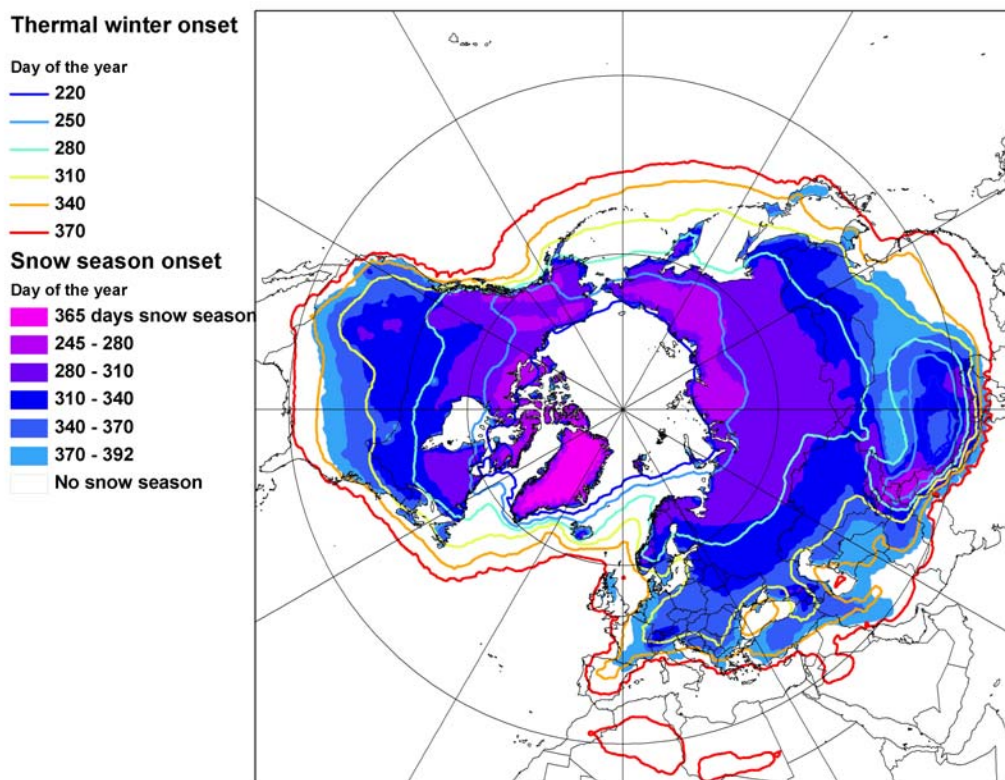


Figure 7.5. Comparison of long-term average thermal winter onset (1979-2005) with snow season onset (1967-2005) in the Northern Hemisphere

high elevation regions at mid-latitudes, the non-snow free season lasts longer than the vegetation season, suggesting that alpine vegetation at mid-latitudes is more sensitive to the occurrence of warmth with the arrival of spring than to occasional snowfall. In low land regions at mid-latitudes, the vegetation season is shorter than the snow-free season, indicating that mid-latitude vegetation is more sensitive to the occurrences of low temperature compared with vegetation at high latitudes or high altitudes.

The onset/offset of the Full Snow Season (FSS) also shows latitudinal differences from the progression patterns of thermal seasonal onset ( $T_{\text{mean}} \geq 5^{\circ}\text{C}$ ). The onset of the FSS begins 30-60 days later than the thermal winter onset (Figure 7.5). For example, the

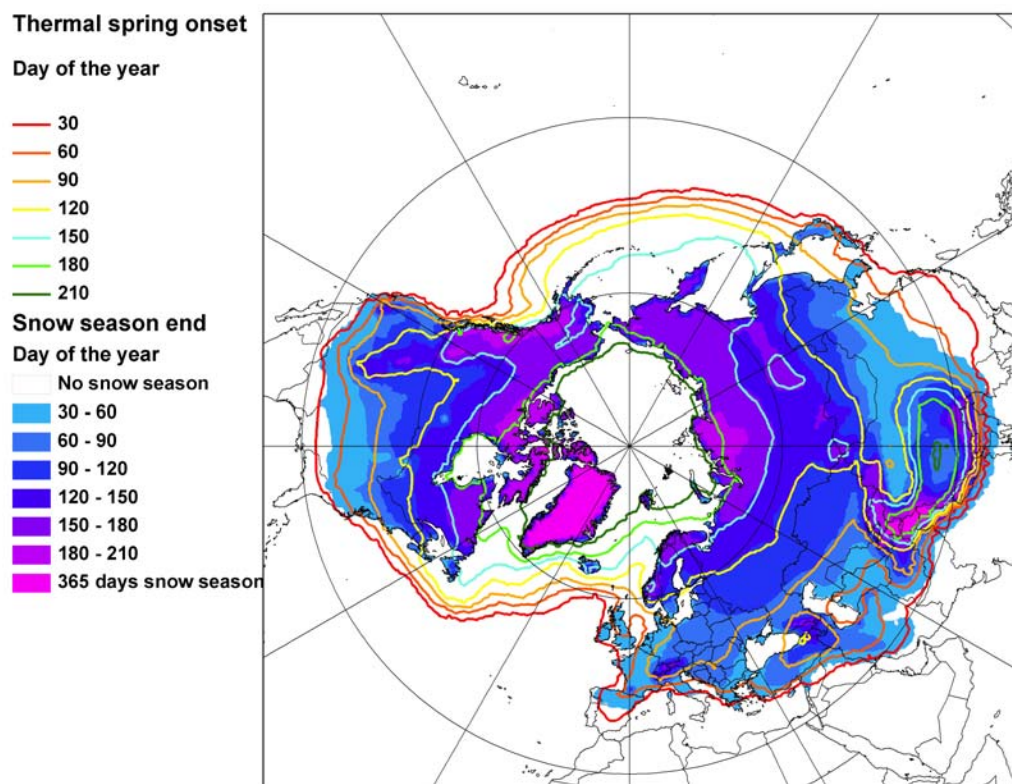


Figure 7.6. Comparison of long-term average thermal spring onset (1979-2005) with Full Snow Season (FSS) offset (1967-2005) in the Northern Hemisphere

FSS onset in northern Siberia occurs between Day 250 and Day 280, but the Day 280 line of thermal winter onset progresses more southward over southern Siberia. In contrast, the offset above  $45^{\circ}\text{N}$  consistently retreats northward with the progression of thermal spring onset, while at lower mid-latitudes below  $45^{\circ}\text{N}$ , thermal spring onset progresses 30 days after the FSS ends (Figure 7.6). For instance, thermal spring onset in central Mongolia progresses in Day 120, while the FSS offset occurs in Day 90. Intervals in zonal patterns of both thermal and snow seasonal onsets are wider in snow/thermal winter onsets than those offsets, indicating that both onsets progress faster than the offsets.

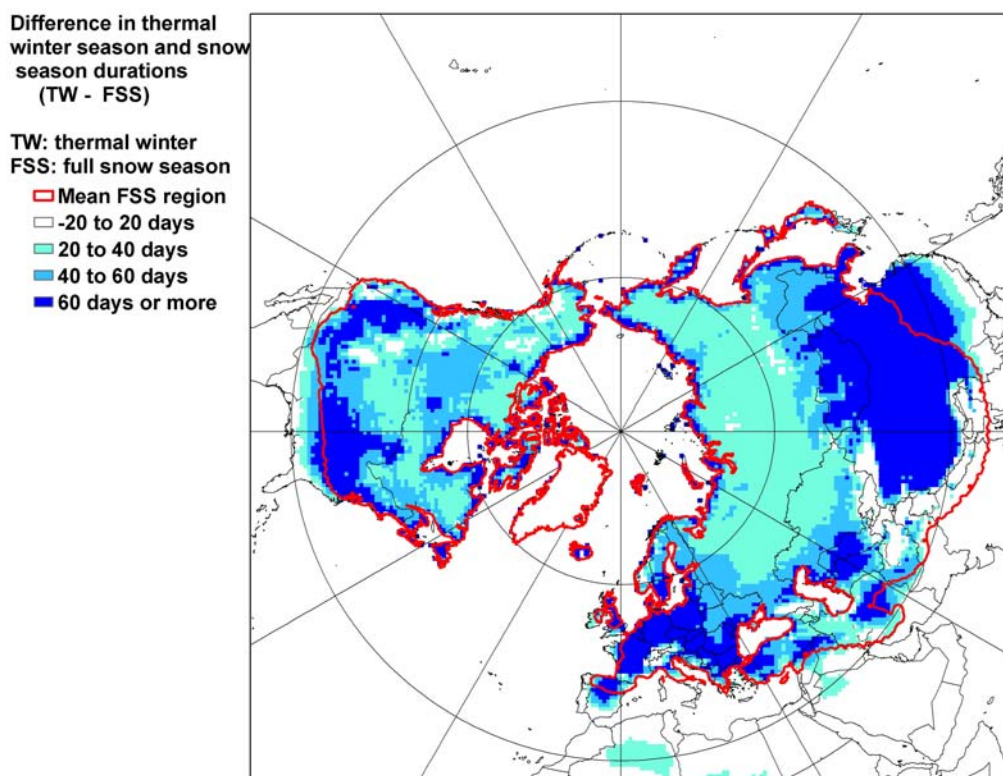


Figure 7.7. Differences between vegetation season (1982-2001) and non-Full Snow Season (non-FSS; 1967-2005) durations in the Northern Hemisphere

Differences between the thermal winter and FSS durations suggest four snow-thermal seasonal zones: 1) 365 day snow-winter zone, 2) snow-winter- equivalent zone, 3) snow-winter-different zone, and 4) snow-absent winter zone (Figure 7.7). A 365 day snow-winter zone is found in Greenland and along the Himalayas. A snow-winter equivalent zone is found in Greenland and along the Himalayas. A snow-winter equivalent zone is observed in semi-arid regions of central Asia. A snow-winter-different zone prevails across continents above 30°N with a greater difference at lower mid-latitudes. For instance, thermal winter lasts 20-40 days longer in Siberia than the FSS, and in northern China the difference is 60 days or more. A snow-absent winter zone is observed in the southeastern United States and China where occasional snow events occur. The

patterns of thermal winter-snow zones indicate that non-FSS duration is longer than thermal growing seasons across the Northern Hemisphere land masses.

### **7.3. Linkages of thermal seasonal onsets and durations with atmospheric circulation indices**

Pearson correlation coefficients are calculated to examine how atmospheric circulation may be associated with seasonal onsets and durations on a hemispheric scale (Tables 7.5-7.7). Table 7.5 summarizes the correlation between Northern Hemisphere average thermal seasons and monthly atmospheric circulation indices such as AO, NAO, PNA, and ENSO for the period 1979-2005. AO is a back and forth pattern of anomalies of atmospheric pressure between the Arctic and mid-latitudes (Thompson & Wallace 1998, 2000). NAO is an oscillatory pattern of winter atmospheric pressures in the Atlantic between the polar low around Iceland and subtropical high near Northwest Africa (Wallace & Gutzler 1981). PNA is the variation of atmospheric pressure between high and low latitudes of both the Pacific and North America (Wallace & Gutzler 1981). ENSO is a see-saw pattern of coupled pressure and SST between western and eastern equatorial Pacific regions (Troup 1965).

Thermal spring onset shows statistically significant (>99%) negative correlations with both AO and NAO between January and March, while thermal spring duration shows positive correlations with both AO and NAO between January and February. The eigenvector map of thermal spring onset from the canonical correlation analysis (CCA) further illustrates that these significant patterns are identified in Europe and East Asia. In the positive AO or NAO years, thermal spring onset has advanced, while thermal spring

duration has increased in these regions. To figure out their linkages, the AO of four highly positive (1989, 1990, 1993, and 2002) minus four negative (1979, 1980, 1985, and 1987) years for both thermal spring onset and 500hPa geopotential height (January-March) are superimposed (Figure 7.8). A positive phase of AO is characterized by higher pressures at mid-latitudes and a lower pressure over the Arctic Ocean. Large patches of 10-50 days earlier spring onsets are observed in Europe, East Asia, and the southwestern United States, where positive cores of the 500hPa geopotential height difference are

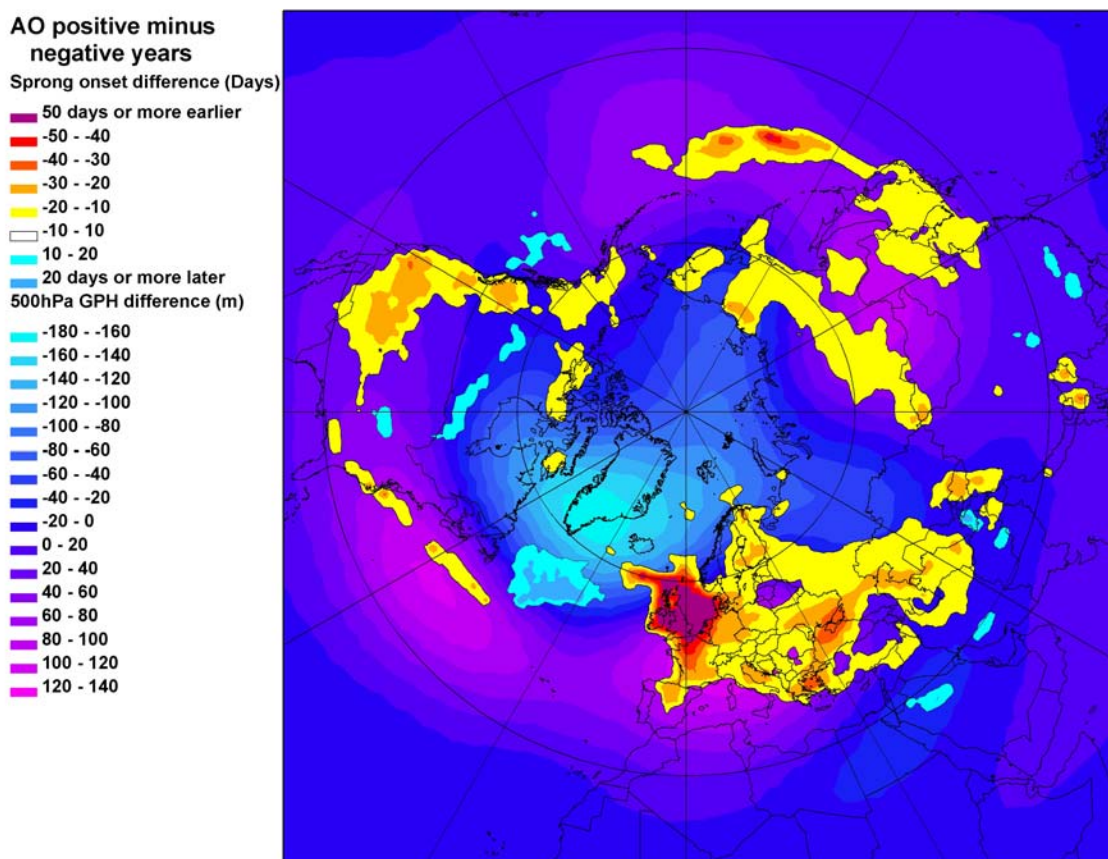


Figure 7.8. Differences in both thermal spring onset (red to blue) and 500hPa geopotential height (blue to purple) between AO positive and negative years. The differences denote the AO positive (1989, 1990, 1993, and 2002) minus and negative (1979, 1980, 1985, and 1987) years.

Table 7.5. Statistically-significant Pearson correlation coefficients (r) between thermal seasons and atmospheric circulation indices in the Northern Hemisphere for the period 1979-2005; Previous year (P), Spring (Sp), Summer (Su), Fall (Fa), Winter (Wi), Onset (O), Duration (D), Arctic Oscillation (AO), North Atlantic Oscillation (NAO), Pacific-North American pattern (PNA), and El Niño Southern Oscillation (ENSO)

Index	Month	Sp_D	Su_D	Fa_D	Wi_D	Sp_O	Su_O	Fa_O	Wi_O
AO	Jan	0.615**				-0.515**			
	Feb	0.427**				-0.511**			
	Mar	0.437**				-0.395**			
	May							0.402*	
	Sep			0.517**					
	Dec								0.390*
NAO	Jan	0.420*			-0.528**	-0.588**			
	Feb	0.394*			-0.446*	-0.526**			
	Mar	0.391*							
	Aug	0.455*							
PNA	P_Dec		0.407*				-0.398*		0.399*
	Apr			0.556*					
	May	0.416*	-0.450*				0.452*		
	Aug				-0.435**	-0.415**			
ENSO	Oct		0.424*				-0.511**		0.455*
	Nov						-0.387*		

\*\* Correlation is significant at the 0.01 level (2-tailed).

\* Correlation is significant at the 0.05 level (2-tailed).

found. The Arctic low pressure anomaly stays in southern Greenland, where a 10-20 day delay in thermal spring onset is detected. The mid-latitude ridges in Europe and East Asia modulate the Arctic trough in central Siberia and far-eastern Siberia, showing a meandering geopotential height anomaly train at mid-latitudes. The high pressure anomaly over these mid-latitude regions expands northward, driving cold storm tracks in that direction, whereas the Arctic low pressure anomaly keeps cold air over the polar region surrounded by a fast jet stream. Thus, it is concluded that the recent earlier thermal spring onset over Europe, East Asia, and the southwestern United States is associated with the Positive AO phase.

Pearson correlation analyses show that PNA in December of the previous year and May in the corresponding year has significant correlations with both thermal summer

onset and duration (Figure 7.5). Those correlation coefficients indicate that in the years of both negative December PNA and positive May PNA, thermal summer onset is delayed, and subsequently thermal summer duration shortens. According to the positive (1979, 1981, 1993, and 1997) minus negative (1987, 1998, 2003, and 2004) year map, these linkages are observed in the southwestern North America, northwestern Pacific, central Siberia, and northwestern Atlantic where negative pressure anomaly cores in the 500hPa

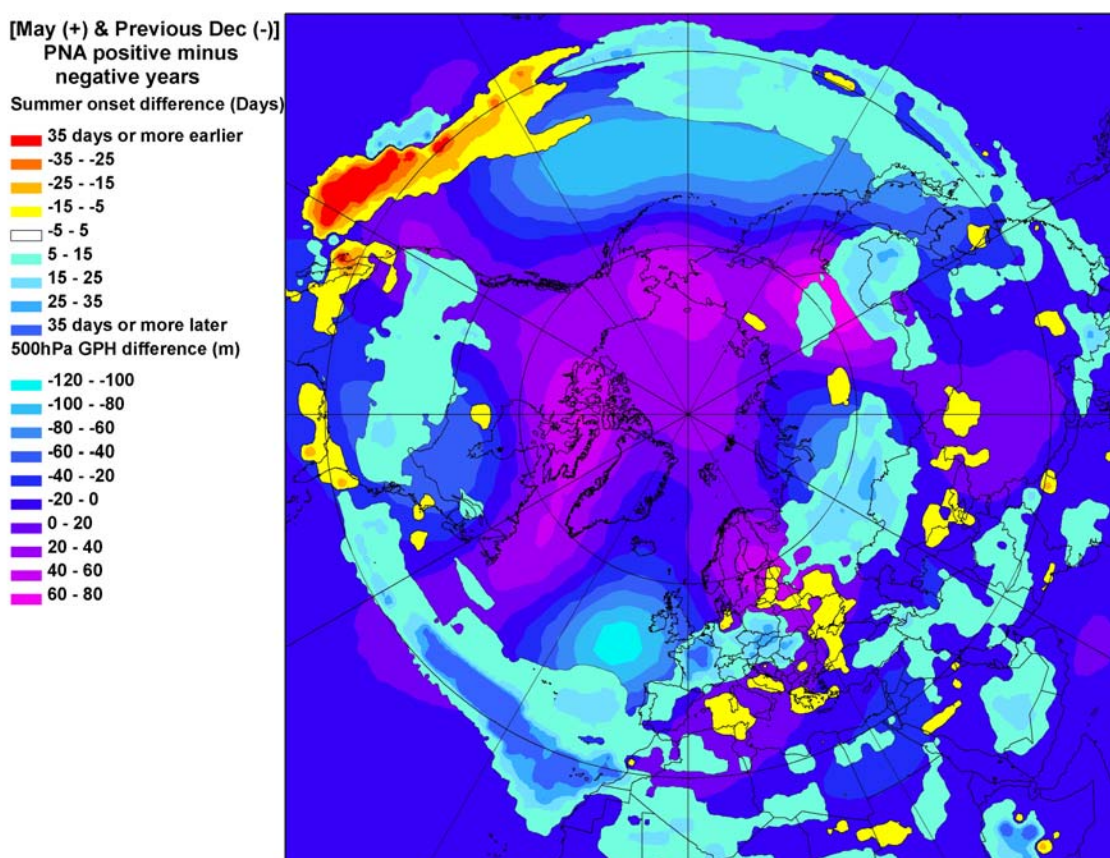


Figure 7.9. Differences in both thermal summer onset (red to blue) and 500hPa geopotential height (blue to purple) between positive and negative years of (May PNA - previous December PNA). The differences denote the positive (1979, 1981, 1993, and 1997) minus and negative (1987, 1998, 2003, and 2004) years.

Table 7.6. Statistically-significant Pearson correlation coefficients ( $r$ ) between snow seasons and atmospheric circulation indices in the Northern Hemisphere for the period 1972-2005; Previous year (P), Full Snow Season (FSS), Core Snow Season (CSS), Onset (O), End (E), Duration (D), Arctic Oscillation (AO), North Atlantic Oscillation (NAO), Pacific-North American pattern (PNA), and El Niño Southern Oscillation (ENSO)

Index	Month	FSS O	FSS E	FSS D	CSS O	CSS E	CSS D
AO	Jan					-0.458**	
	Mar	-0.356*					
	May				-0.362*		
	Aug					-0.429*	
	Dec						-0.571**
NAO	Jan					-0.379*	
	Feb		-0.479**			-0.486**	
	Dec	0.396*					-0.468**
PNA	P_Oct	0.382*				0.357*	
	P_Dec		-0.354*	-0.430*			
	Jan						0.372*
	Apr				0.401*		
	Jul					-0.362*	-0.485**
	Oct	0.384*			0.418*	0.471**	
ENSO	Jul	0.385*					

\*\* Correlation is significant at the 0.01 level (2-tailed).

\* Correlation is significant at the 0.05 level (2-tailed).

geopotential height fields are detected (Figure 7.9). Relationships between ENSO and thermal seasons are not clear except for a negative correlation between thermal summer onset or duration and ENSO between October and November.

Significant correlations between the snow seasons and atmospheric circulation indices are found during the cold period (October - April) (Table 7.6). The onsets of both the Full Snow (FSS) and Core Snow Seasons (CSS) are positively correlated with the October PNA, while the ends of both the FSS and CSS are negatively correlated with the February NAO. Moreover, the end of CSS shows a negative correlation with the January AO and NAO, while it shows a positive correlation with the October PNA. The CSS duration is correlated with the December AO or NAO. Relationships between the CSS or FSS offset and AO and NAO early in the year are consistent with the linkages between thermal

spring and the AO or NAO. They suggest that positive AO phases are associated with hemispheric scale variations in snow seasons such as the earlier onset and extended duration as it is associated with thermal winter seasons through fluctuations of dynamical atmospheric circulation.

The vegetation season shows statistically-significant correlations with the PNA and ENSO (Table 7.7). The June PNA is negatively correlated with the end of vegetation season and positively with the vegetation seasonal onset. In addition, November-December ENSO in the previous year is negatively correlated with the onset of vegetation season, indicating that a strong El Niño in early winter may be associated with the advance of vegetation seasonal onset. Positive phases of ENSO during November -

Table 7.7. Statistically-significant Pearson correlation coefficients (r) between vegetation (1982-2001) or carbon dioxide season (1974-2004) and atmospheric circulation indices in the Northern Hemisphere; Previous year (P), Vegetation season (V), Carbon dioxide season (CO<sub>2</sub>), Barrow, Alaska (B), Mauna Loa, Hawaii (M), Onset (O), End (E), Arctic Oscillation (AO), North Atlantic Oscillation (NAO), Pacific-North American pattern (PNA), and El Niño Southern Oscillation (ENSO)

Index	Month	V_O	V_E	CO <sub>2</sub> _B_O	CO <sub>2</sub> _B_E	CO <sub>2</sub> _M_O	CO <sub>2</sub> _M_E
AO	Apr						-0.395*
	May				-0.499**		
	Nov					-0.382*	
NAO	Sep					-0.435*	
PNA	P_Nov		-0.515*				
	Mar		-0.506*			0.543**	
	Apr					0.389*	
	Jun	0.663**	-0.600**				
	Sep		0.471*				
	Oct						0.526**
ENSO	P_Oct		0.473*				
	P_Nov	-0.447*					-0.392*
	P_Dec	-0.481*					-0.555**
	Jan		0.486*			-0.443*	
	Feb						-0.389*
	Mar					-0.497**	
	Dec						0.397*

\*\* Correlation is significant at the 0.01 level (2-tailed).

\* Correlation is significant at the 0.05 level (2-tailed).

December also show correlations with the carbon dioxide seasons in Mauna Loa. These patterns suggest winter ENSO-spring vegetation-carbon dioxide linkages in the central or eastern Pacific. The migration of the warm SST due to El Niño phases toward the eastern Pacific may affect the earlier vegetation seasonal onset and subsequently influence an earlier offset of carbon dioxide season in the central Pacific islands through earlier photosynthesis of vegetation.

#### **7.4. Development of seasonal prediction models**

According to correlations between Northern Hemisphere thermal seasons and atmospheric circulation indices (Table 7.5), significant correlations (>95%) are found between January-March AO or NAO and thermal spring onset, between January-February AO and thermal winter duration, and between October-November ENSO and thermal summer duration. For these combinations, canonical correlation analyses (CCA) are conducted to develop seasonal prediction models for regions where significant correlations with several monthly circulation indices in previous seasons are found. For the period 1979-2005, monthly circulation indices are used as predictor variables and the spatially- and temporally-varying thermal seasonal onset or duration data based on Gaussian grid cells as predictand variables. Monthly circulation indices between July in the previous year and June in the corresponding year are used to predict thermal spring and summer onsets or durations.

Table 7.8. Canonical correlation coefficients between thermal seasons and atmospheric circulation indices; Arctic Oscillation (AO), North Atlantic Oscillation (NAO), Pacific-North American pattern (PNA), and El Niño Southern Oscillation (ENSO)

Canonical correlations	Thermal Spring onset		Thermal spring duration		Thermal summer duration
	AO	NAO	AO	NAO	ENSO
1	0.854	0.725	0.845	0.588	0.602
2	0.566	0.366	0.390	0.494	0.480
3	0.132	0.060	0.348	0.254	0.405
4	0.096	0.030	0.175	0.103	0.019

Table 7.8 provides the canonical correlation coefficient for each combination of thermal seasons and atmospheric circulation indices. The most significant canonical correlations (CC) are found between monthly AO as predictor variables and northern hemisphere thermal spring onsets in the Gaussian grid cells. The first EOF mode accounts for 73% of the variance (CC= 0.854) between monthly AO and thermal spring onset across the Northern Hemisphere. Similarly, the CC of the first EOF mode in the CCA between monthly AO and thermal spring duration is 0.845. The CC of the first EOF mode between monthly ENSO and thermal summer durations is 0.602.

CCA results for the AO-spring onset pair and the ENSO-summer duration pair are provided in Figure 7.10. The first X EOF mode accounts for 22% of the variance among monthly AO indices. The first X EOF's monthly loadings of predictors are characterized by a high positive AO mode between January and March as illustrated in Figure 7.10(b). According to the first Y EOF's spatial loading in Figure 7.10(d), negative eigenvectors below -0.5 are identified in Europe and East Asia. Weak negative eigenvectors less than -0.3 are recognized along the Rockies in North America. This indicates that thermal spring onset is negatively correlated with positive AO between January and March in these areas. In other words, thermal spring onset in Europe and East Asia is advanced

**(a) X EOFs scree**

EOF mode	1	2	3	4
Variance (%)	21.7	15.8	14.1	10.3
Cumulative variance (%)	21.7	37.5	51.6	61.9

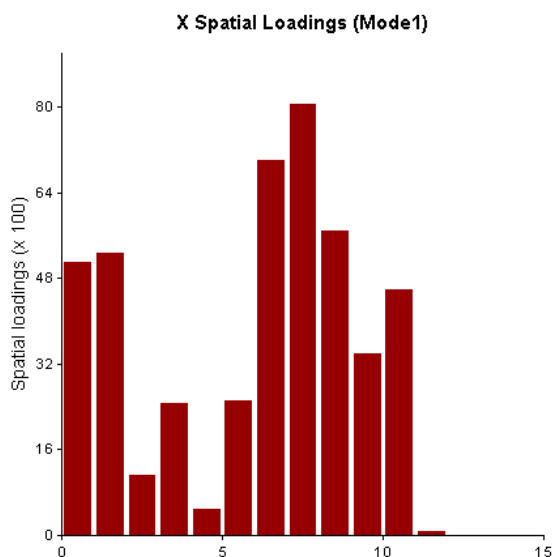
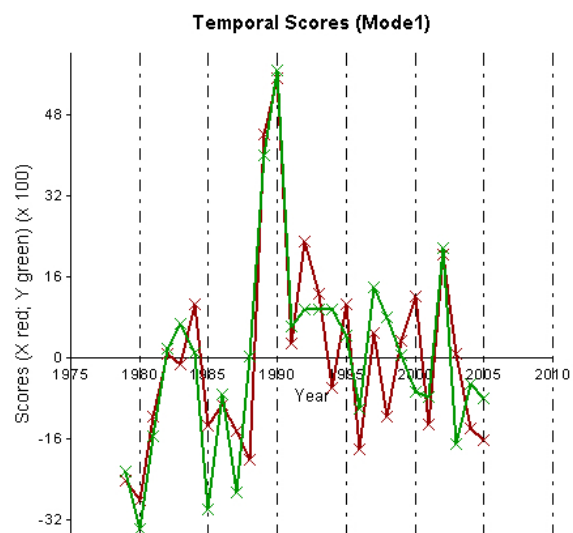
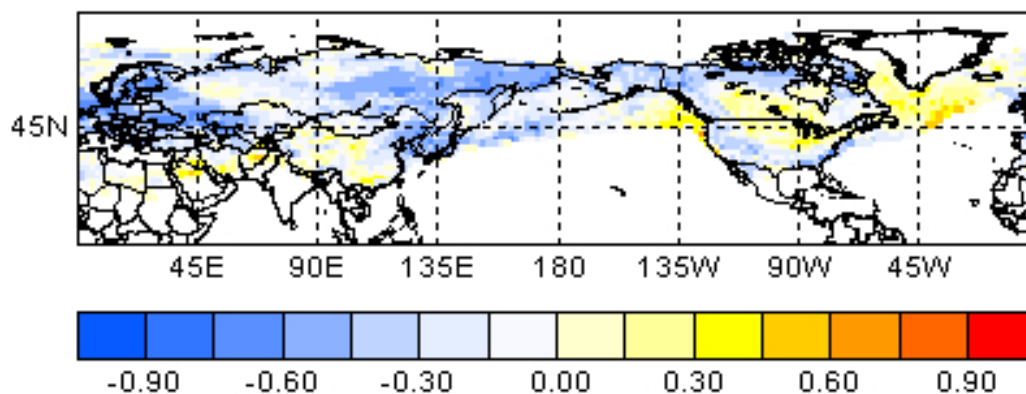
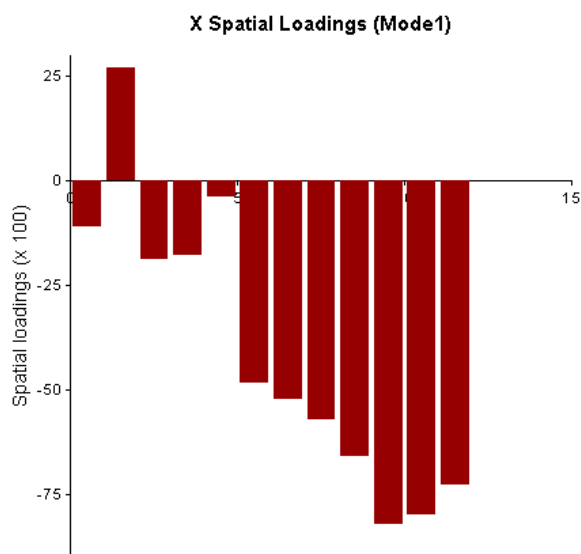
**(b) From July to June****(c)****(d)****Y Spatial Loadings (Mode1)**

Figure 7.10. X EOF scree (a), X spatial loadings (b), Temporal scores (c), and Y spatial loadings (d) of the first mode of canonical correlations ( $=0.854$ ) between Northern Hemisphere thermal spring onset (Y) and monthly Arctic Oscillation (AO) index from July in previous year to June in corresponding year (X) for the period 1979-2005

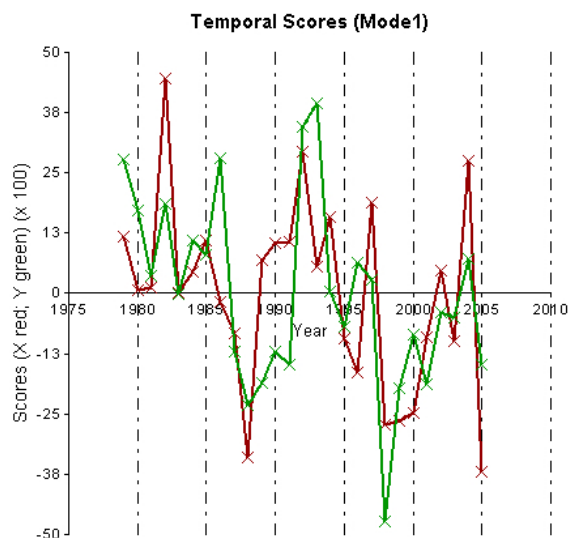
## (a) X EOFs scree

EOF mode	1	2	3	4
Variance (%)	45.9	24.4	8.9	6.9
Cumulative variance (%)	45.9	70.4	79.2	86.2

## (b) From January to December



## (c)



## (d)

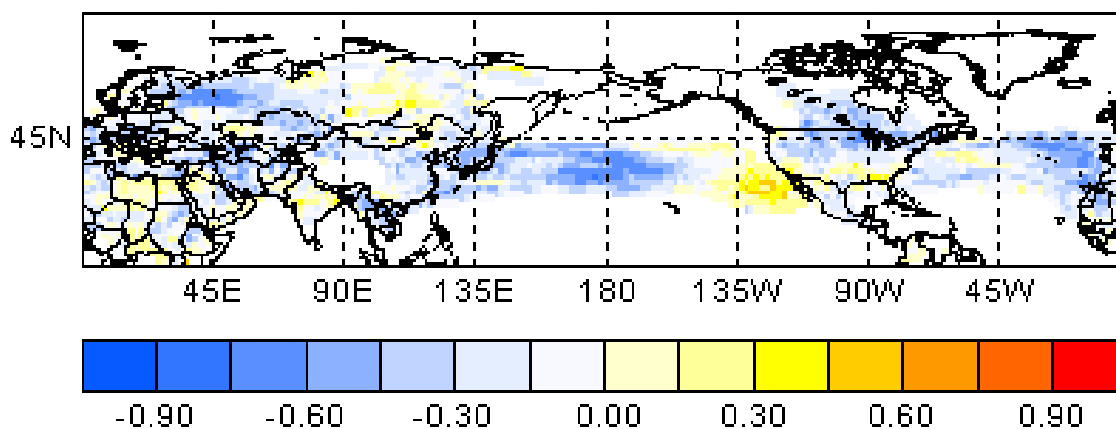
**Y Spatial Loadings (Mode1)**

Figure 7.11. X EOF scree (a), X spatial loadings (b), Temporal scores (c), and Y spatial loadings (d) of first mode of canonical correlations ( $=0.596$ ) between Northern Hemisphere thermal summer duration (Y) and monthly ENSO index from January to December (X) for the period 1979-2005

when the AO between January and March shows strong positive patterns. In positive winter AO years, both arctic low pressure and high pressure in northwestern Africa are intensified. The intensification of the AO modes results in a trough in western Siberia and a ridge in eastern Asia. It is inferred that the northward displacement of warm air at mid-latitudes may lead to advances of thermal spring onset in East Asia, while the intensification of high pressure in southern Europe results in advances of thermal spring onset in Europe. Temporal score graphs in Figure 7.10(c) illustrate inter-annual consistency of X-Y eigenvalues and their temporal fluctuations. The eigenvalues of AO and thermal spring onset show a shift from negative phase to positive phase between 1987 and 1989.

In the case of the monthly ENSO-summer duration pair, the first X EOF mode explains 46 % of the variance in temporal patterns of predicted variables presented in Figure 7.11(a). The first X EOF is characterized by a strong negative mode from January to December. Under the negative phase of the ENSO index, the CC of thermal summer duration in both the Pacific and Atlantic between 30°N and 40°N shows a negative phase below -0.5. This indicates that in La Niña years, thermal summer durations increase in these regions. However, according to the temporal scores of both sets of variables, the eigenvalues of the ENSO index show a decreasing trend during the study period.

Thermal spring onset and thermal summer duration prediction models are run for the regions where significant correlations are recognized in the CCA. Simple linear regression models, which use least squared deviations, are constructed using a calendar-based seasonal averaged atmospheric circulation index as an independent variable (X) and anomalies of thermal seasonal date as a dependent variable (Y). Specifically,

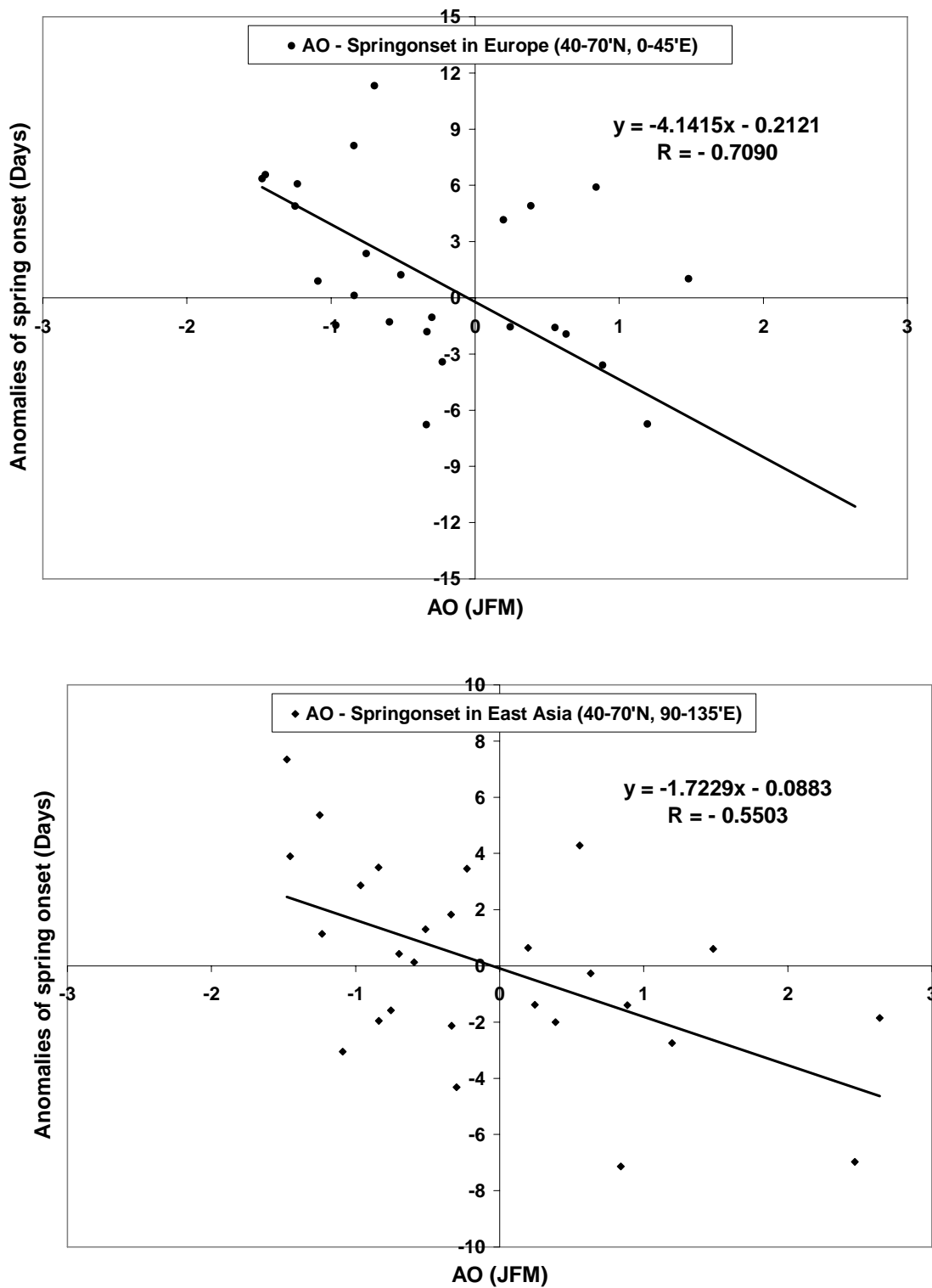


Figure 7.12. Simple linear regression models to predict thermal spring onset in Europe (top) and East Asia (bottom) based on the average AO index between January and March.

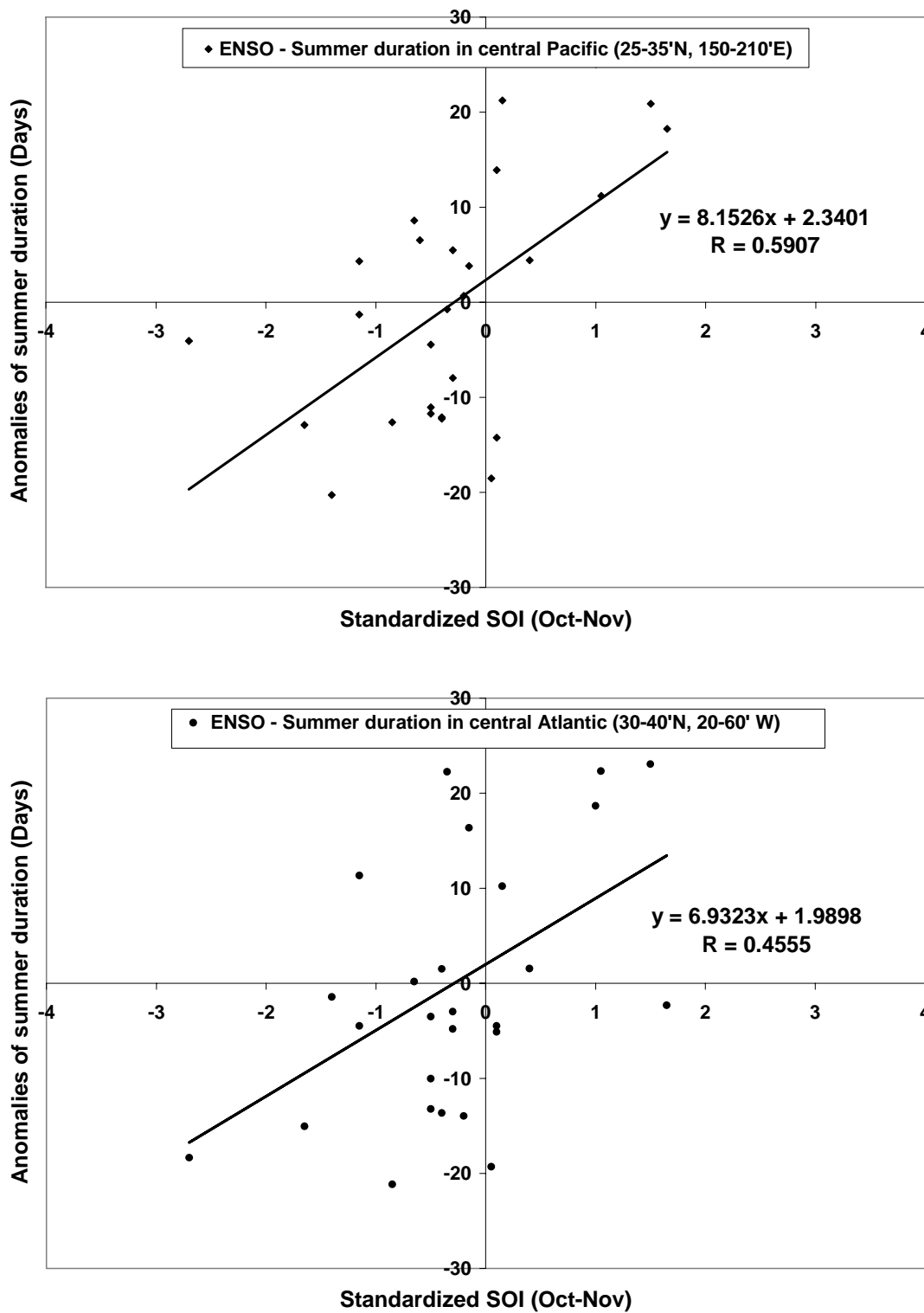


Figure 7.13. Simple linear regression models to predict thermal summer duration in central Pacific (top) and Atlantic (bottom) based on the average ENSO index between October and November.

regression models based on calendar month averaged AO and anomalies of regional average spring onset are constructed to predict departures of spring onset from long-term averages for Europe (40-70°N, 0-45°E) and East Asia (40-70°N, 90-135°E). Also, regression models to predict the departures of summer duration from long-term averages based on the ENSO index between October and November are constructed for the lower mid-latitude Pacific (25-35°N, 150-210°E) and Atlantic (30-40°N, 20-60°W). Over these oceanic regions, summer lasts until early January in the following year.

$$Y = a_0 + a_1 \times X$$

Figures 7.12-7.13 depict simple linear regression models for the prediction of spring onsets and summer durations, respectively. According to the models, a positive AO between January and March advances thermal spring onsets in both Eurasia and East Asia at the rate of -4.1 days per unit of AO and -1.7 days per unit of AO, respectively. Also, a positive ENSO between October and November leads to increases of thermal summer duration in the Pacific and Atlantic at the rate of 6.9-8.2 days per unit of standardized SOI.

## **7.5. Summary and conclusion**

Spatial and temporal patterns of onset/offset and duration of thermal, snow, vegetation and carbon dioxide seasons were compared across the Northern Hemisphere to investigate the consistency or lead/lag relationships associated with their seasonality. Statistically significant relationships between atmospheric circulation patterns and

various seasons were detected. Regional scale seasonal prediction models were developed based on the lead/lag relationships with atmospheric circulation indices.

Progressions of the vegetation seasonal onset/offset above 55°N and below 35°N are not consistent with that of thermal spring/winter onset. Compared with thermal seasonal onset, a 30-60 days earlier onset and 10-30 days later offset of the vegetation season above 55°N indicates that high latitude vegetation may be more sensitive to warming but less sensitive to cooling. The opposite patterns below 35°N indicates that low latitude vegetation may be more sensitive to cooling but less sensitive to warming. Thus it appears that the current temperature threshold (5°C) commonly used to define growing seasons should be modified depending on latitude.

The northward retreat of the Full Snow Seasonal offset above 45°N is consistent with the progression of thermal spring onset, but the offset at lower latitudes as well as the onset across the entire Northern Hemisphere land mass shows leads/lags of 30-60 days compared to thermal seasonal progression. The consistent zonal retreat of snow cover with thermal spring indicates that the latitudinal migration of high insolation may play an important role in the offset of the spring high latitude snow season.

The relationships of thermal, snow, and vegetation floating seasonal durations vary depending on latitude. At high latitudes, the durations of the vegetation and snow seasons are similar and are longer than the thermal growing season. At mid-latitudes, the durations of vegetation and thermal growing seasons are similar and are shorter than the non-Full Snow Season (non-FSS). At lower mid-latitudes, the vegetation season is shorter than the thermal growing season which is shorter than the non-FSS.

The AO and NAO between January and March are linked with thermal spring onset and duration in Europe, East Asia, and the southwestern United States. In positive AO or NAO years, spring onset is advanced, and subsequently spring duration increases in these regions. A positive ENSO during the winter leads to an advance of the Northern Hemisphere average vegetation seasonal onset as well as an offset of the carbon dioxide season at Mauna Loa, Hawaii.

Identifying such linkages permitted the development of regional scale seasonal prediction models. For instance, modeling revealed that a unit increase of the AO index advances spring onset by 4.1 days in Europe and 1.7 days in East Asia. Also, during an ENSO year, thermal summer duration over the central Pacific and Atlantic is extended 6.9-8.2 days per unit increases of the standardized SOI.

These findings contribute to an understanding of potential causes of observed earlier thermal spring onset and abbreviated thermal winter duration in Europe and East Asia, as well as the extension of summer duration along 30°N over the Pacific and Atlantic. Future studies are needed to develop seasonal prediction models based on other indicators such as local topography as well as synoptic atmospheric patterns.

## CHAPTER 8

### EXPLORING DIRECTIONS OF FUTURE CHANGES IN NORTHERN HEMISPHERE THERMAL SEASONS

#### 8.1. Introduction

The Intergovernmental Panel on Climate Change Third Assessment Report (IPCC, 2001) and Fourth Assessment Report (IPCC, 2007) summarize the prediction of future climate change based on the simulations of climate models. Future climate outlooks are produced based on six greenhouse gas emission scenarios: B1, B2, A1T, A1B, A1F1, and A2. Among those scenarios, A1B, which is characterized by a balanced emphasis on all energy sources, is an intermediate greenhouse gas emission scenario between B1 and A2. The B1 scenario is characterized by reductions in material intensity and the introduction of clean and resource efficient technologies, whereas A2 scenario is characterized by fragmented and slower technological changes than other storylines.

Multi-model ensemble means based on the A1B scenario predict that global mean surface air temperature will increase 2.7°C at the end of the 21<sup>st</sup> century (2080-2099) (IPCC 2007). Increases of temperature are projected to be more noticeable at high latitudes in meteorological winter (DJF), while in meteorological summer (JJA), increases of temperature will be greatest over mid-latitude land masses. Such warming is certain to lead to changes in thermal seasonal onsets and durations.

The purpose of this chapter is to examine changes in Northern Hemisphere thermal seasonal onset and duration at the end of the 21<sup>st</sup> century (2081-2100) based on (A1B)

compared with current (1981-2000) patterns. According to Reichler and Kim's (2007) model performance comparison, GFDL 2.1 is one of the most reliable climate models in simulating the observed climate during the 20<sup>th</sup> century. Thus, GFDL 2.1 2-m daily mean temperature output based on the A1B intermediate greenhouse gas emission scenario for the future (2081-2100) and on the modern times forcing for the current (1981-2000) are used in this evaluation. Thermal seasonal onset and duration are extracted from annual bell-shaped curves of daily mean temperature using the same method that is introduced in Chapter 4. That is, the period between the first and last dates below 5°C are defined as thermal winter duration, whereas 20°C is used to define thermal summer duration. The future (2081-2100) minus the current (1981-2000) thermal seasonal onsets and durations are compared with the current observed seasonal durations (1979-2005) derived earlier in this study using NCEP-DOE reanalysis II data.

In section 8-2, temporal trends and correlations of the Northern Hemisphere average thermal seasonal onsets and durations are discussed. In section 8-3, spatial patterns of changes in thermal seasonal onset and duration are described. Modeled and observed thermal seasonal durations for the current (1981-2000) period are compared in section 8.4. Results are summarized and conclusions drawn in section 8-5.

## **8.2. Temporal changes in thermal seasonal durations at the end of the 21<sup>st</sup> century**

Time series of the Northern Hemisphere average thermal seasonal durations for the current (1981-2000) and future (2081-2100) periods are illustrated in Figure 8.1. Thermal winter duration is predicted to be 13 days shorter at the end of the 21<sup>st</sup> century compared with the current period. Thermal summer duration is predicted to expand by 18 days. In

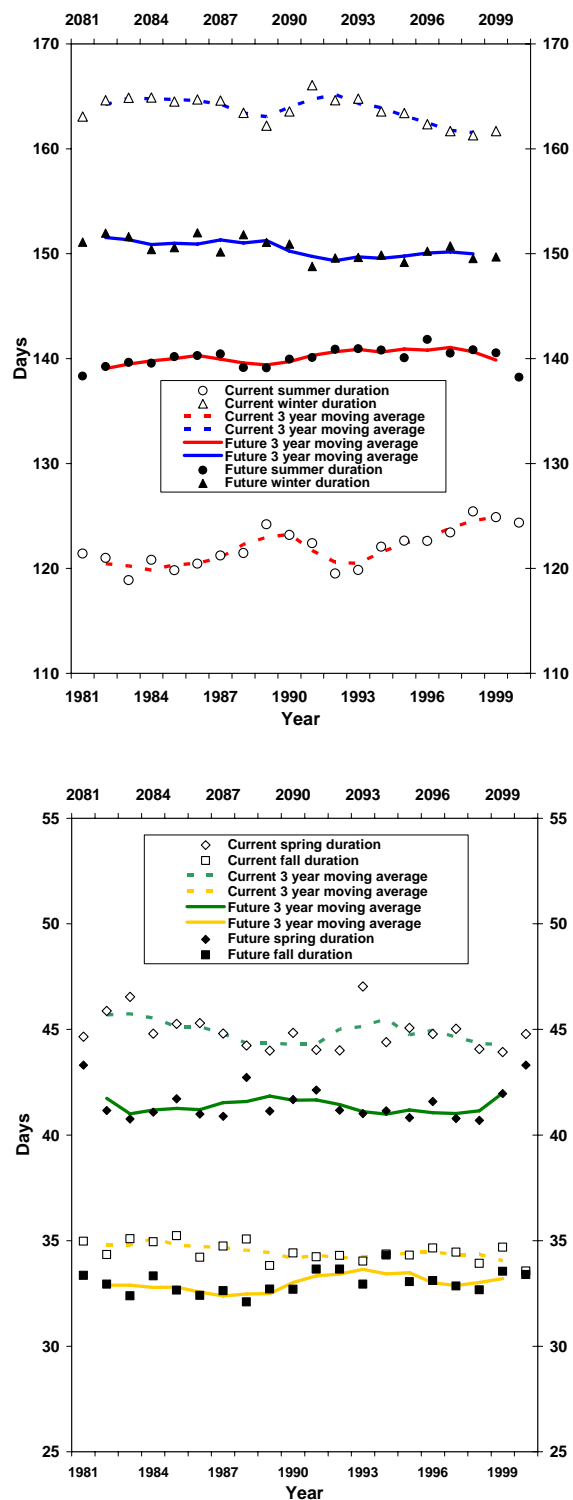


Figure 8.1. Time series of current (1981-2000) and future (2081-2100) Northern Hemisphere average thermal seasonal duration derived from the GFDL 2.1 model output surface air temperature data: summer and winter (a), and spring and fall (b)

Table 8.1. Changes in Northern Hemisphere average thermal seasonal onsets and durations between the current (1981-2000) and future (2081-2100) periods: onset (O), duration (D), spring (Sp), summer (Su), fall (Fa), and winter (Wi)

	Su D	Wi D	Sp D	Fa D	Sp O	Su O	Fa O	Wi O
Current (1981-2000)	122.0	163.7	44.9	34.5	102.2	147.1	269.1	303.5
Future (2081-2100)	140.0	150.5	41.5	33.0	95.2	136.7	276.7	309.7
Difference	18.0	-13.2	-3.4	-1.4	-7.0	-10.4	7.6	6.2

the future, summer will only be 10 days shorter than winter, whereas presently it is 40 days shorter. Spring and fall durations are projected to decrease by 3 days and 1 day, respectively. Thus, the future extension of summer duration will be due mainly to the reduction of winter duration but not abbreviated transitional seasons.

Hemispheric scale comparisons of future (2081-2100) thermal seasonal onsets and durations with the current (1981-2000) ones predict that the expansion of thermal summer duration will continue later in the 21<sup>st</sup> century primarily due to advances of thermal summer onset (Table 8.1). Thermal winter duration will also continue to shorten mainly due to an earlier spring onset.

Pearson correlation coefficients among the Northern Hemisphere average thermal seasonal onsets and durations derived from the climate model output temperature data for the future (2081-2100) and the current (1981-2000) are summarized in Table 8.2. Both current ( $r = -0.936$ ) and future ( $r = -0.965$ ) thermal summer durations show the most significant statistical correlations with thermal summer onset. Inter-annual variations of thermal summer onsets accounts for 87.6-93.1% of variations in summer durations for both current and future.

For the current period, thermal fall onset also shows a statistically significant correlation with thermal summer duration ( $r = -0.938$ ), while the correlation decreases in the case of the future thermal summer duration and thermal fall onset ( $r = 0.544$ ). It

Table 8.2. Pearson correlation coefficients (r) amongst Northern Hemisphere average thermal seasonal onsets and durations; Modeled future (2081-2100) and current (1979-2005) based on GFDL 2.1: onset (O), duration (D), spring (Sp), summer (Su), fall (Fa), and winter (Wi).

		Modeled future (2081-2100)						
Seasonality	Su_D	Wi_D	Sp_D	Fa_D	Sp_O	Su_O	Fa_O	Wi_O
Su_D	1							
Wi_D	-0.543*	1						
Sp_D	-0.595**	0.131	1					
Fa_D	0.137	-0.599**	0.180	1				
Sp_O	-0.391	0.330	-0.440	-0.470*	1			
Su_O	-0.936**	0.433	0.687**	-0.193	0.350	1		
Fa_O	0.544*	-0.427	-0.012	-0.079	-0.250	-0.215	1	
Wi_O	0.416	-0.751**	0.153	0.842**	-0.552*	-0.287	0.471*	1
		Modeled current (1981-2000)						
Seasonality	Su_D	Wi_D	Sp_D	Fa_D	Sp_O	Su_O	Fa_O	Wi_O
Su_D	1							
Wi_D	-0.784**	1						
Sp_D	-0.583**	0.401	1					
Fa_D	-0.504*	0.182	0.115	1				
Sp_O	-0.696**	0.540*	-0.122	0.410	1			
Su_O	-0.965**	0.713**	0.659**	0.397	0.666**	1		
Fa_O	0.938**	-0.787**	-0.420	-0.590**	-0.660**	-0.815**	1	
Wi_O	0.825**	-0.819**	-0.442	-0.064	-0.543*	-0.743**	0.843**	1

\*. Correlation is significant at the 0.05 level (2-tailed).

\*\*. Correlation is significant at the 0.01 level (2-tailed).

indicates that earlier thermal summer onset will be a more important factor to the extension of summer duration than the fall thermal onset in the future.

The current thermal winter duration shows high correlations with both thermal winter onset ( $r = -0.819$ ) and thermal spring onset ( $r = 0.540$ ) onsets, implying that current reductions in thermal winter duration are attributed to both the delayed winter onset and earlier spring onset. In contrast, there is no statistically significant correlation between thermal spring onset and thermal winter duration for the future period. Rather, future thermal winter onset shows statistically-significant correlations with thermal winter duration, indicating that future reductions in thermal winter duration will be more determined by delayed patterns in thermal winter onset than by variations in spring onset.

For both current and future periods, significant positive correlations are found between thermal summer onset and thermal spring duration ( $r = 0.659$  and  $0.687$ ), and between thermal fall onset and thermal winter onset ( $r = 0.801$  and  $0.471$ ). Significant negative correlations are identified between thermal winter onset and thermal spring onset ( $r = -0.543$  and  $-0.552$ ), between thermal summer duration and thermal winter duration ( $r = -0.784$  and  $-0.543$ ), and between thermal spring duration and thermal summer duration ( $r = -0.583$  and  $-0.595$ ). In the case of the correlation between thermal winter onset and fall duration, an increase of correlation significance level for the future period implies that inter-annual variations in future winter onsets are a key component that will lead to fluctuations of thermal fall duration as well as thermal winter duration on a hemispheric scale.

### **8.3. Spatial patterns of future changes in thermal summer and winter durations**

The differences of modeled seasonal durations between the current (1981-2000) and the future (2081-2100) are depicted spatially in Figures 8.2-8.3. The map illustrates that future summer duration will increase by 60 days or more along  $30^{\circ}\text{N}$  over the Pacific and the Atlantic oceans (Figure 8.2). At  $20\text{-}30^{\circ}\text{N}$  over land masses, thermal summer duration is predicted to increase by 40-70 days. As a result, over highlands in tropical regions such as central Ethiopia and northern Mexico, other seasons will shorten significantly or disappear altogether. This pattern indicates that the summer-only seasonal cycle zone will expand by 5-10 degrees of latitude northward. The systematic zonal changes in thermal summer duration indicate that in the future, low latitude atmospheric circulation such as the Hadley cell (Fu et al. 2006; Lu et al. 2007) will expand poleward earlier in the year. In particular,

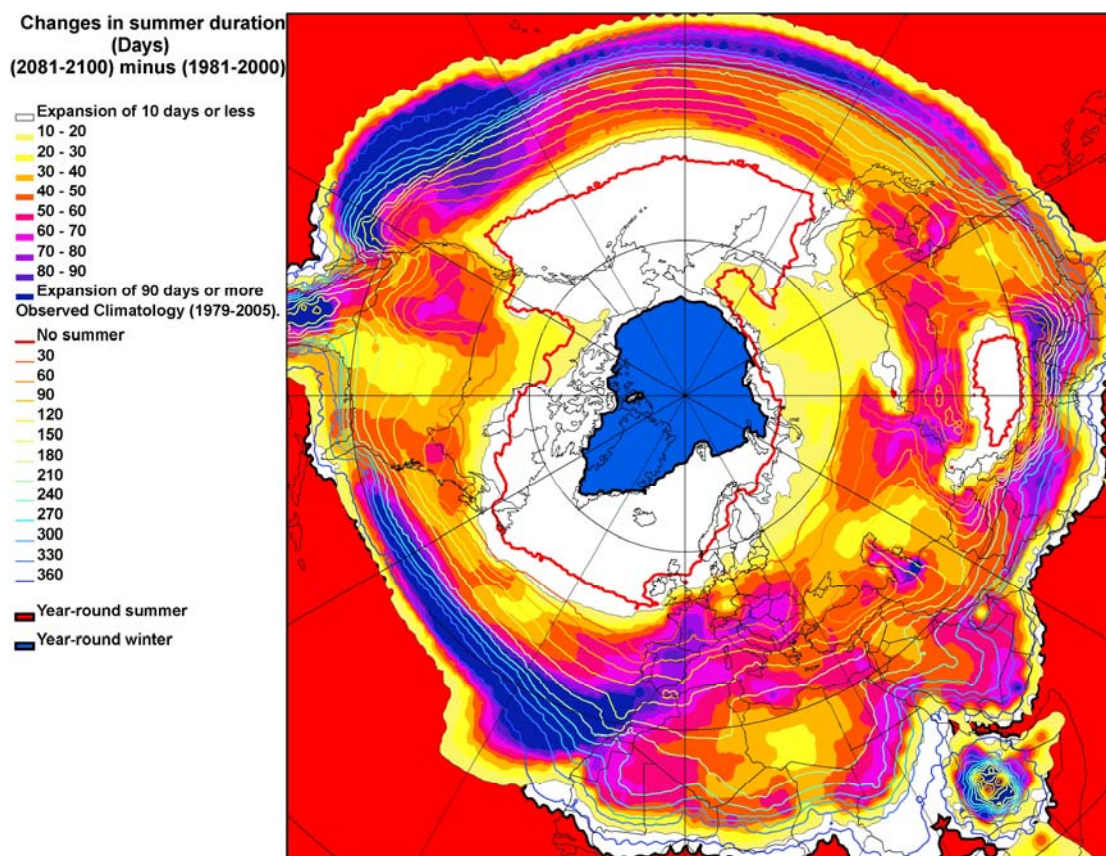


Figure 8.2. Current (1979-2005) observed climatology (color lines) and predicted future changes (colored shades) in thermal summer duration across the Northern Hemisphere. Changes are calculated from the future average (2081-2100) minus current average (1981-2000) extracted from GFDL 2.1 model output temperature data.

more noticeable cores of summer extension in the eastern ocean basins implies that quasi-stationary high pressure systems over oceans such as the Pacific high and the Bermuda high will intensify.

At mid-latitudes such as southern Europe, northern China, East Asia, the Rockies, increases in summer duration of 40-70 days are predicted to occur later this century. In contrast, in Arctic tundra regions, less than a 30 day extension in summer duration will occur in the future. Summer will not make it further north than is currently observed.

Figure 8.3 illustrates future (2081-2100) changes in thermal winter duration compared with the current (1981-2000). It is predicted that thermal winter duration will decrease across Northern Hemisphere land masses poleward of 30°N. The most noticeable reduction in thermal winter duration is predicted to occur over the northern Pacific and over the Tibetan Plateau. In these regions, winter duration will decrease by 30-90 days. In Europe, central Asia, the Hudson Bay, and the western Pacific along the eastern North American coastline, thermal winter duration will decrease by 30-60 days. Less than a 20

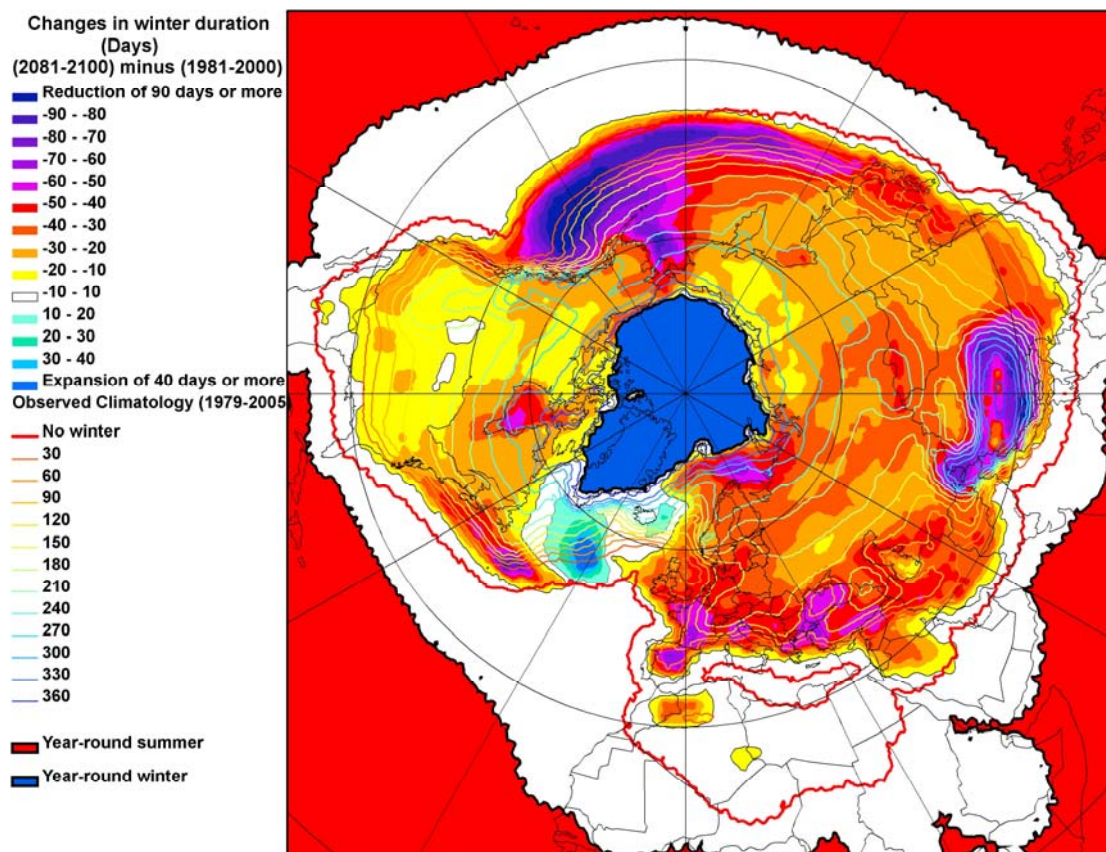


Figure 8.3. Current (1979-2005) observed climatology (color lines) and predicted future changes (colored shades) in thermal winter duration across the Northern Hemisphere. Changes are calculated from the future (2081-2100) average minus current (1981-2000) average extracted from GFDL 2.1 model output temperature data.

day reduction in thermal winter duration is predicted in the United States, western Canada, northeastern Siberia, and northern Africa. In the northern Atlantic, thermal winter duration is predicted to shorten by 10-30 days. The different phases of the winter duration changes, which are the northern Atlantic (+) / Europe (-) and the northern Pacific(-), suggest that a positive mode of the Arctic Oscillation (AO) may be associated with the future winter duration change pattern. In particular, the Aleutian low pressure system is predicted to weaken significantly in the future.

#### **8.4. Climate model performance in simulating thermal seasons**

Climate models are useful tools to understand the mechanisms of climate variability and to predict future climate change. To date, many efforts have been made to improve the performance of climate models through comparisons with observations. In this section, the performance of the GFDL 2.1 model in simulating thermal seasons is tested by comparing thermal seasonal durations derived from model output with those derived from observations for the period 1981-2000.

The differences between observed and modeled thermal summer and winter seasons are illustrated in Figure 8.4. It is observed that the GFDL 2.1 model underestimates thermal summer duration by 10-30 days across the Northern Hemisphere continents. Over oceans, the underestimation amounts to 90 days or more along 30°N over the Atlantic and along 27°N over the Pacific. In contrast, the model overestimates thermal winter duration by 10-30 days across the Northern Hemisphere continents. In the northern Pacific and Atlantic oceans, the overestimation exceeds 50 days. In the Canadian Arctic, the model shows an underestimate of 30 days or more.

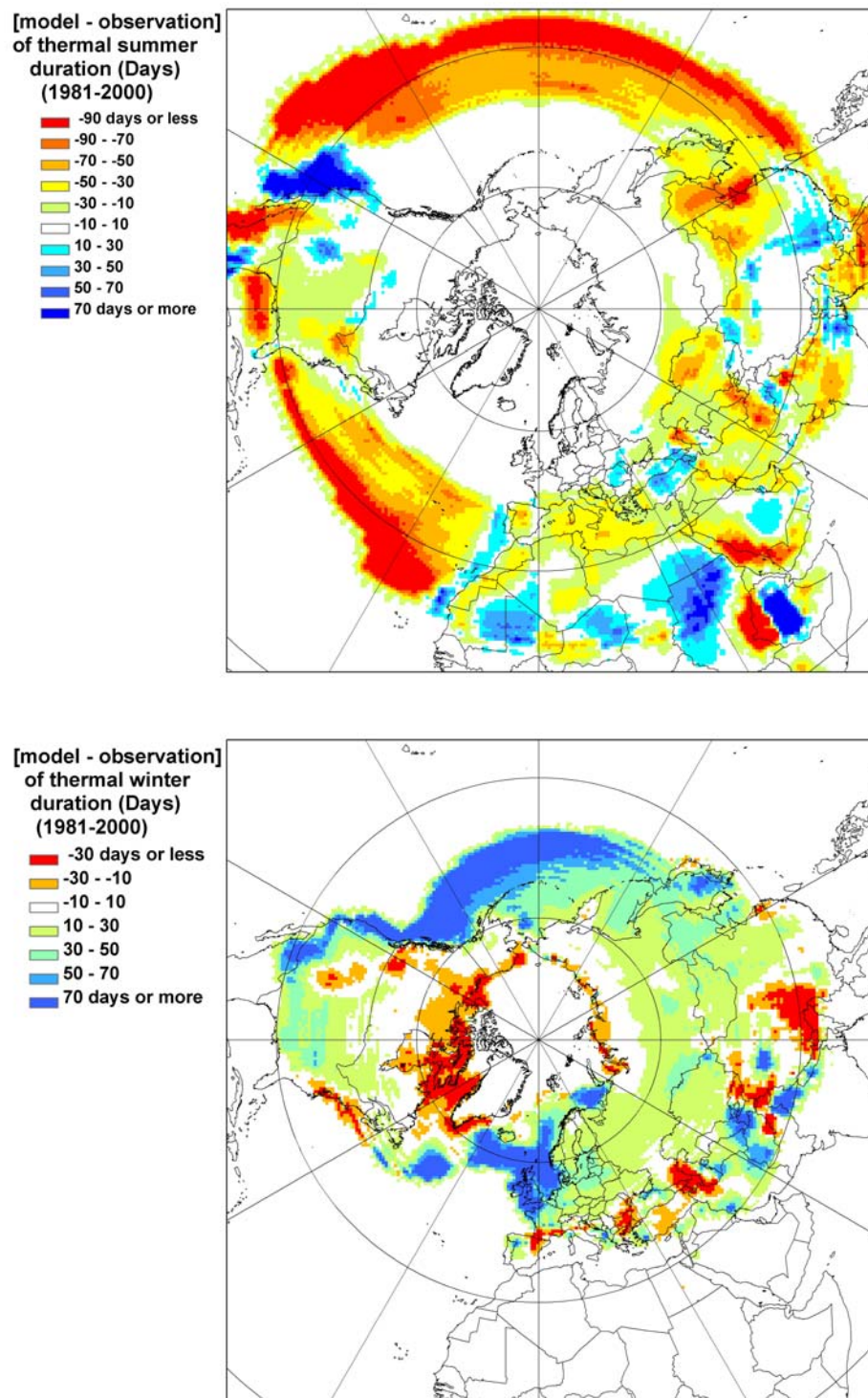


Figure 8.4. Differences (modeled-minus-observed) between modeled (GFDL 2.1) and observed (NCEP- DOE reanalysis II) thermal summer (top) and winter (bottom) durations, 1981-2000. Extreme caution is needed to interpret differences of more than 50 days over oceans. Refer to the text for details.

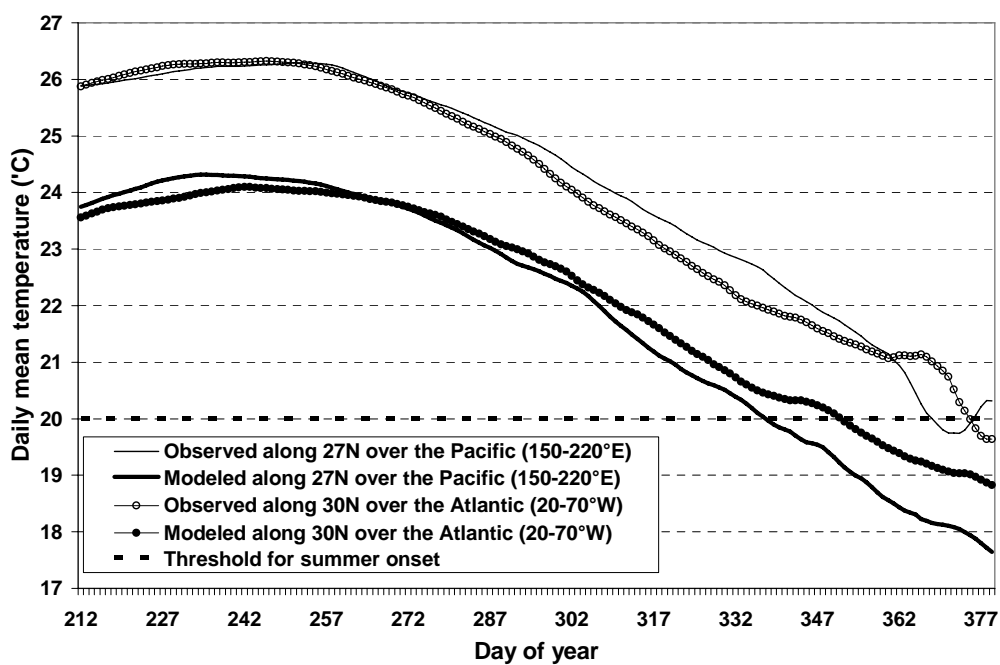
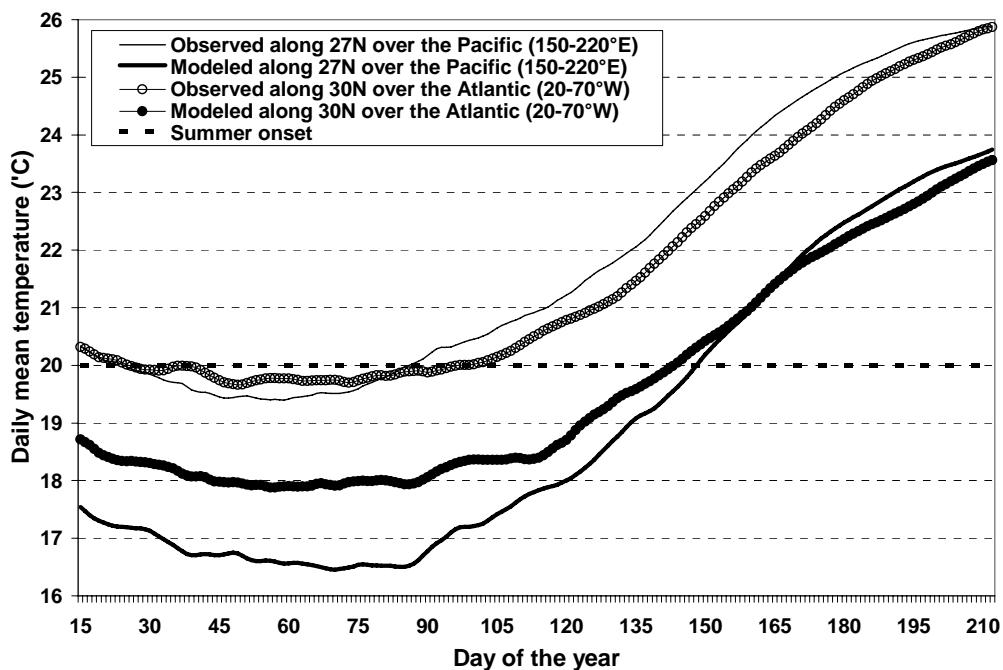


Figure 8.5. Comparison of modeled daily mean temperatures with observed daily mean temperature during the first half of the year (top) and during the second half of the year (bottom) for the current period (1981-2000) along 27°N over the Pacific and along 30°N over the Atlantic

These patterns indicate that the temperature modeled for the Northern Hemisphere continents is lower than the observed temperature. Figure 8.5 illustrates the example of the differences between modeled and observed daily temperature along 27°N over the Pacific and along 30°N over the Atlantic for the current period (1981-2000). A 20°C temperature base line represents the threshold for summer onset and offset. Summer duration decreases by more than 50 days over these regions due to the model underestimating temperature by 1.5-2.0°C. It is worth noting that this is a relatively constant offset, resulting in confidence that a comparison of differences of model output between the present and future periods has worth.

### **8.5. Summary and conclusion**

Future changes in thermal seasonal onsets and durations have been predicted by comparing the current (1981-2000) climatology with future (2081-2100) climatology, each derived from GFDL 2.1 model output 2-m temperatures. Temporal trends and spatial patterns of potential changes in future seasonal onsets and durations were examined. Major findings are as follows:

Hemispheric average thermal summer duration will increase by 18 days, while thermal winter duration will decrease by 13 days. Thermal spring and fall will show little change on a hemispheric scale.

Thermal summer duration will expand primarily due to earlier thermal summer onset. Similarly, the reduction in thermal winter duration will occur primarily due to earlier thermal spring onset.

A 60 day extension in thermal summer duration is predicted to occur along 30°N, suggesting that the Hadley cell may expand 5-10 degrees of latitude northward by the end of the 21<sup>st</sup> century. It is also suggested that over low latitude highlands such as northern Mexico and central Ethiopia, warming will lead to a significant reduction or the disappearance of other thermal seasons by the extension of thermal summer duration.

Thermal winter duration will be reduced by more than 40 days in the northern Pacific and Europe, and by 10-30 days in the northern Atlantic. This suggests an intensified positive mode of the Arctic Oscillation that may influence future changes in winter patterns in the Northern Hemisphere.

The comparison of modeled data with observed data reveals that the GFDL 2.1 model underestimates thermal summer durations but overestimates thermal winter durations, particularly over oceans due to underestimating daily mean temperature.

These predictions are based on one model (GFDL 2.1) and one greenhouse gas emission scenario (A1B). Future studies should include 1) single or multi-model ensemble data, 2) other greenhouse gas emission scenarios, and 3) other variables, including snow cover. Furthermore, detailed examinations of dynamical mechanisms as to how future changes in atmospheric circulation patterns such as Hadley cell, AO, and ENSO will influence the changes in seasonal onsets and durations are recommended.

## CHAPTER 9

### CONCLUSION AND FUTURE DIRECTIONS

This dissertation is the first study to define floating climatological seasons for temperature (1979-2005; 2081-2100), snow (1967-2005), vegetation (1982-2001), and carbon dioxide (1974-2003) on a hemispheric scale using multiple empirical and modeled variables. Climatological seasons defined in this dissertation show various dynamical characteristics, such as the geographic advance and retreat of seasons, which cannot be studied through static conventional fixed seasons such as three month meteorological seasons.

Climatologies of various floating seasonal onsets/offsets and durations were constructed and compared to examine the spatial relationships of seasonal progressions. Through an examination of seasonal onsets and durations, seven different types of thermal seasonal cycles were observed in the Northern Hemisphere, including winter-only, summer-absent, spring-fall-only, winter-absent, spring-summer-only, summer-only and all four seasons. An examination of Core Snow Season (CSS) to Full Snow Season (FSS) relationships found six snow seasonal zones, including 365 day snow zone, FSS-CSS identical zone, FSS-CSS similar zone, longer FSS-shorter CSS zone, FSS-only zone, and 0 day snow zone.

The progression speeds of dynamical seasonal onsets/offsets progress differ between ocean and land. The latitudinal progression of thermal seasons over oceans (6.6-13.1 days/degree) is slower compared to that over continents (3.3-3.9 days/degree) by a factor of 2-3, primarily due to the high oceanic heat capacity and thermal inertia. The southward

progressions of thermal fall and winter onsets, or the onset of snow seasons, are faster by 0.16 days/degree of latitude than the northward movement of thermal spring and summer or the offset of snow seasons. This pattern suggests that the time for the accumulation of solar energy to melt snow cover extends the seasonal progression period during the first half of the year, whereas the thermal inertia of the Arctic Ocean delays the formation of cold air masses and the ultimate southward propagation of thermal winter.

Comparisons of various floating seasonal onset/offset and duration patterns revealed that the relationships of three floating seasonal durations vary depending on latitude. At high latitudes, the duration of the vegetation season is similar to the duration of the snow season, but both seasons last longer than the thermal growing season. At mid-latitudes, the duration of vegetation seasons is similar to thermal growing seasons, but both seasonal durations are shorter than that of the non-Full Snow Season (non-FSS). At lower mid-latitudes, seasonal duration is longer in the order of non-FSS > thermal growing season > vegetation season. This pattern indicates that high latitude and low latitude vegetation may have different sensitivities to the arrivals of thermal and snow seasons, suggesting a need for the modification of temperature thresholds ( $T_{\text{mean}} \geq 5^{\circ}\text{C}$ ) currently used to define the growing seasons everywhere.

Time series of various seasonal onsets/offsets and durations show coherent changes amongst different variables in recent decades. Earlier thermal spring and vegetation seasonal (-3.1 days/decade over land) onsets as well as earlier snow (-5.9 days/decade over land) and carbon dioxide seasonal (-5.9 days/decade at Mauna Loa) offsets are noted. This demonstrates a 5-30 day reduction of thermal winter, snow, and carbon dioxide seasons as well as expansions of the vegetation season since the late 1980s, particularly

in western Europe, East Asia, and western North America. In contrast, thermal summer durations have expanded by 5-30 days, primarily due to earlier summer onset particularly along 30°N over oceans, suggesting changes in low latitude atmospheric circulation such as the Hadley cell.

Thermal season-atmospheric circulation relationships exhibit significant correlations between the positive Arctic Oscillation from January to March and earlier thermal spring onset in western Europe, East Asia, and western North America. Significant relationships were also observed between a positive El Niño Southern Oscillation (ENSO) and thermal summer duration in the central Pacific and Atlantic, and between the positive May - negative previous December Pacific North American pattern (PNA) and late summer onset in the southwestern North America, northwestern Pacific, central Siberia, and northwestern Atlantic. These lead/lag relationships suggest that changes in thermal winter and summer seasons are in part associated with oscillation patterns of hemispheric atmospheric circulation.

Anomaly cores of atmospheric pressure due to oscillations showed locational consistency with inter-annual fluctuations of regional seasonality. Thermal seasonal prediction models developed using these relationships showed a potential predictability of thermal spring onset (e.g. -4.1 day per unit of AO in Europe) and summer durations on a regional scale.

Analyses of changes in modern observations and climate model-derived thermal seasonal durations showed that the recently observed expansion of summer along 30°N over oceans as well as the reduction of winter over the continents will continue later in the 21<sup>st</sup> century. Models also find additional future regional changes in seasonal cycles,

such as the disappearance of spring and fall seasons in tropical highlands. The understanding of these current and future changes in seasonal onset and durations are critically important because changes in energy distribution patterns will lead to changes in the seasonal cycles of hydrological and biophysical interactions

This dissertation is the first study to address the hemispheric scale association of climatologies and temporal variations of seasonal onsets/offsets and durations with static factors, including latitude, altitude, topography effect, and surface condition, as well as dynamic factors such as ocean and atmospheric circulations. Among these, latitude and surface condition (continents versus oceans) are the two leading factors that determine zonal patterns of seasonal climatologies.

Examination of regional scale patterns revealed that other factors play roles as barriers (e.g. the Arctic Ocean for summer onset) or as contributors (e.g. elevation for winter onset). The role of some geographical factors varies depending on location. For instance, over high mountains in the tropics, spring and fall seasons occur due to elevation, whereas over high elevations at mid- to high latitudes, snow and thermal winter seasons are extended and the vegetation season reduced (e.g. 5.5 days/100m). Shadowing effects of high topography shorten thermal winter and snow season durations but extend the vegetation seasonal duration. At mid-latitudes, water bodies such as lakes shorten winter duration, whereas proximity to oceans extends the vegetation season. The cold ice/water in the Arctic Basin prevents the northward progression of warmer seasons.

It was also exemplified that dynamical factors such as ocean currents and quasi-stationary pressure systems also modify various seasonal progression patterns on regional scales. Air masses, such as the Bermuda and Siberian highs and the Aleutian low, as well

as ocean currents, including the warm Gulf Stream and cold California current, are associated with lead-lag patterns in seasonal cycles between the two ocean basins. Winter is shorter in the Atlantic than in the Pacific. Winter is shorter on the eastern side of each oceanic basin than on the western side.

Dynamical oscillations of hemispheric atmospheric circulation associated with AO and ENSO demonstrate potential linkages in inter-annual variability of thermal, snow, vegetation, and carbon dioxide seasonal onsets/offsets and durations over the Northern Hemisphere. A train of positive and negative anomaly cores in mid-troposphere geopotential height fields modulated by the large scale fluctuations of atmospheric circulation are associated with regional variations of seasonal onsets and durations. For instance, the positive AO phase between January and March forms positive pressure anomaly cores over Europe, East Asia, and the western United States, and a reduction of winter due to earlier thermal spring onset over these regions. This suggests that the transport of heat and energy poleward around these positive cores may advance spring onset. In addition, empirically observed and climate model simulated extensions in thermal summer durations along 30°N suggest that changes in general circulation such as the expansion of the Hadley cell may be associated with the zonal changes.

Earlier spring onset patterns along the Rockies are suggestive of other factors such as data noise as well as an anthropogenic impact. It may be possible that temperature re-analysis data and pre-IMS vs. IMS era snow extent data used in study may contain noise because they are based on small numbers of observations at poor resolution, particularly over high mountains. Latitudinal and altitudinal comparison of carbon dioxide seasonal onsets/offsets at Barrow and Mauna Loa with the vegetation seasonal cycle also suggests

that feedbacks between biosphere and geochemical cycles may be another potential driver in explaining the patterns along the high mountain ridges. Over high mountains, atmospheric carbon dioxide accumulates regionally because there is no vegetation that can absorb anthropogenic carbon dioxide, whereas at low elevations, the photosynthesis of vegetation actively sequesters atmospheric carbon waste in the growing seasons. Thus, the regionally enhanced greenhouse effect may intensify warming in the earlier times of the year due to the lack of interactions between the biosphere and atmosphere over the high mountains.

This dissertation opens many doors for future studies by providing the basis of the hemispheric-scale climatology and variability of floating climatological seasons. It should be expanded to cover the Southern Hemisphere. Downscaling to regional levels is also needed to facilitate studies of the long-term climatology of floating seasons back to the early 20<sup>th</sup> century. This may elucidate reasons for the variation of floating seasons in the context of climate change.

It would be exceedingly useful to add a third atmospheric dimension to studies using upper atmospheric variables such as circumpolar vortices, jet streams, and stratospheric variables. It will help to explain the three-dimensional mechanisms of seasonal progression.

Finally, global and regional modeling efforts are needed to fully understand the detailed feedbacks and physical mechanisms associated with the floating season results reported in this study. These should be carried out using multiple models and emission scenarios.

**CHAPTER 10****REFERENCES**

- Abbe, C., 1899: The duration of the growing season for 1898. *Monthly Weather Review*, 27, 255.
- Abdulla, S., 1999: Spring forward, fall back. *Nature@news*, 990304-7.
- Ahas, R., A. Aasa, S. Slim, and J. Roosaare, 2005: Seasonal indicators and seasons of Estonian landscapes. *Landscape Research*, 30, 173-191.
- Ahas, R., J. Jaagus, and A. Aasa, 2000: The phenological calendar of Estonia and its correlation with mean air temperature. *International Journal of Biometeorology*, 44, 159-166.
- Alexander, L.V., X. Zhang, T.C. Peterson, J. Caesar, B. Gleason, A.M.G. Klein Tank, M. Haylock, D. Collins, B. Trewin, F. Rahimzadeh, A. Tagipour, K. Rupa Kumar, J. Revadekar, G. Riffiths, L. Vincent, D.B. Stephenson, J. Burn, E. Aguilar, M. Brunet, M. Taylor, M. New, P. Zhai, M. Rusticucci, and J.L. Vazquez-Aguirre, 2006: Global observed changes in daily climate extremes of temperature and precipitation. *Journal of Geophysical Research*, 111, 1-22.
- Alpert, P., I. Osetinsky, B. Ziv, and H. Shafir, 2004: A new seasons definition based on classified daily synoptic systems: An example for the eastern Mediterranean. *International Journal of Climatology*, 24, 1013-1021.
- Alsop, T.J., 1989: The natural seasons of western Oregon and Washington. *Journal of Climate*, 2, 888-896.
- Argiriou, A.A., P. Kassomenos, and S.P. Lykoudis, 2004: On the methods for the delimitation of seasons. *Water, Air, and Soil Pollution: Focus*, 4, 65-74.
- Asrar, G., M. Fuchs, E.T. Kannemasu, and J. L. Hatfield, 1984: Estimating absorbed photosynthetic radiation and leaf area index from spectral reflectance in wheat. *Agronomy Journal*, 76, 300-306
- Badhwar, G.D., 1984: Use of Landsat-derived profile features for spring small-grains classification. *International Journal of Remote Sensing*, 5, 783-797.
- Badhwar, G.D., W.W. Austin, and J.G. Carnes, 1982: A semi-automatic technique for multitemporal classification of a given crop within a Landsat scene. *Pattern Recognition*, 15, 217-230.

- Bagla, P., 2007: Big melt threatens India's water. *ScienceNOW Daily News*, 112:1
- Baker, D.G., D.L. Ruschy, R.H. Skaggs, and D.B. Wall, 1992: Air temperature and radiation depressions associated with a snow cover. *Journal of Applied Meteorology*, 31, 247-254.
- Bamzai, A.S., 2003: Relationship between snow cover variability and Arctic Oscillation index on a hierarchy of time scales. *International Journal of Climatology*, 23, 131-142.
- Barnston A.G., 1994: Linear statistical short-term climate predictive skill in the Northern Hemisphere. *Journal of Climate*, 7, 1513-1564.
- Barnston A.G., W. Thiao, and V. Kumar, 1996: Long-lead forecasts of seasonal precipitation in Africa using CCA, *Weather and Forecasting*, 11, 506-520.
- Barriopedro, D., R. Garchia-Herrera, A.R. Lupo, and E. Hernandez, 2006: A climatology of Northern Hemisphere blocking, *Journal of Climate*, 19, 1042-1063
- Barry, R.G., and A.H. Perry, 1973: *Synoptic climatology: methods and applications*, Methuen&Co Ltd.
- Beaubien, E.G., and M. Hall-Beyer, 2003: Plant phenology in western Canada: Trends and links to the view from space. *Environmental Monitoring and Assessment*, 88, 419-429.
- Beaubien, E.G., and H.J. Freeland, 2000: Spring phenology trends in Alberta, Canada: links to ocean temperature. *International Journal of Biometeorology*, 44, 53-59.
- Belchansky, G.I., D.C. Douglas, and N.G. Platonov, 2004: Duration of the Arctic sea ice melt season: Regional and interannual variability, 1979-2001. *Journal of Climate*, 17, 67-80.
- Black, R.X., B.A. McDaniel, and W.A. Robinson, 2006: Stratosphere–troposphere coupling during spring onset. *Journal of Climate*, 19, 4891–4901.
- Blochman, L.E., 1925: A study of seasonal forecasting for California based on an analysis of past rainy seasons. *Monthly Weather Review*, 53, 489-493.
- Bogaert, J., L. Zhou, C.J. Tucker, R.B. Myneni, and R. Ceulemans, 2002: Evidence for a persistent and extensive greening trend in Eurasia inferred from satellite vegetation index data. *Journal of Geophysical Research*, 107, NO. D11, 119,10.1029/2001JD001075,2002.
- Brown, R.D., 2000: Northern Hemisphere snow cover variability and change, 1915–97. *Journal of Climate*, 13, 2339-2355.

- Bradka, J., 1966: Climatological seasons on the Northern Hemisphere. *Geophys Sb*, 262, 597-648.
- Brown, J.L., S.-H. Li, and N. Bhagabati, 1999: Long-term trend toward earlier breeding in an American bird: A response to global warming. *Proceedings of the National Academy of Sciences*, 96, 5565-5569.
- Bryson, R.A., and J.F. Lahey, 1958: *The march of seasons*, Final Report, NO-19-(604)-922, Department of Meteorology, University of Wisconsin, Madison.
- Burn, D.H., 1994: Hydrologic effects of climatic change in west-central Canada, *Journal of Hydrology*, 160, 53-70.
- Cannon, A.J., 2005: Defining climatological seasons using radially constrained clustering. *Geophysical Research Letters*, 32, L14706, doi:10.1029/2005LG023410, 2005.
- Cayan, D.R., S.A. Kammerdiener, M.D. Dettinger, J.M. Caprio, and D.H. Peterson, 2001: Changes in the onset of spring in the western United States. *Bulletin of the American Meteorological Society*, 82, 399-415.
- CDIAC, 2004, Atmospheric CO<sub>2</sub> from flask air samples at 10 sites in the SIO air sampling network, retrieved September 2007 from <http://cdiac.ornl.gov/trends/co2/sio-keel-flask/sio-keel-flask.html>.
- Chang, C.Y., 1946: Climate and man in China. *Annals of the Association of American Geographers*, 36, 44-74.
- Chang, P.K., 1934: The distribution of four seasons in China. *Acta Geogr Sinica*, 1, 19-56 (in Chinese)
- Cheng, S.Q., and L.S. Kalkstein, 1997: Determination of climatological seasons for the east coast for the US using an air mass-based classification. *Climate Research*, 8, 107-116.
- Choi, G., and W.T. Kwon, 2001: A shift of natural seasons' cycle and change of life temperature indices in South Korea during the 20<sup>th</sup> century. *Journal of Geography Education*, 45, 14-25 (in Korean).
- Choi, G., W.T. Kwon, and D.A. Robinson, 2006: Seasonal onset and duration in South Korea. *Journal of the Korean Geographical Society*, 41, 435-456 (in Korean).
- Comiso, J.C., 2003: Warming trends in the Arctic from clear sky satellite observations. *Journal of Climate*, 16, 3498-3510.
- Conrad, V., and L.W. Pollak, 1950: *Methods in Climatology*. 2<sup>nd</sup> eds. Cambridge, Mass.: Harvard University Press.

- Crick, H.Q.P., C. Dudley, D.E. Glue, and D.L. Thomson, 1997: UK birds are laying egg earlier. *Nature*, 388, 526.
- Crick, H.Q.P., and T.H. Sparks, 1999: Climate change related to egg-laying trends. *Nature*, 399, 423-424.
- Curry, J.A, W.B. Rossow, D. Randall, and J.L. Shramm, 1996: Overview of Arctic cloud and radiation characteristics. *Journal of Climate*, 9, 1731-1764
- Czikowsky, M.J., and D.R. Fitzjarrald, 2004: Evidence of seasonal changes in evapotranspiration in eastern U.S. hydrological records. *Journal of Hydrometeorology*, 5, 974-988.
- Defila, C., and B. Clot, 2001: Phytophenological trends in Switzerland. *International Journal of Bioclimatology*, 45, 203-207.
- Dewey, K.F., 1977: Daily maximum and minimum temperature forecasts and the influence of snow cover. *Monthly Weather Review*, 105, 1594-1597.
- D' Odorico, P., J. Yoo, and S. Jaeger, 2002: Changing seasons: An effect of the North Atlantic Oscillations? *Journal of Climate*, 15, 435-445.
- Dye, D.G., 2002: Variability and trends in the annual snow-cover cycles in Northern Hemisphere land areas. *Hydrological Processes*, 16, 3065-3077.
- Dzerdzeevskii, B.L., 1968: *Circulation mechanisms in the atmosphere of the Northern Hemisphere in the twentieth century*, Institute of Geography, Soviet Academy of Sciences, Moscow, R. Geodecke, Trans., BF., Berryman, Ed., University of Wisconsin.
- Emberlin, J., M. Detant, R. Gehrig, S. Jaeger, N. Nolard, and A. Rantio-letimaki, 2002: Responses in the start of the Betula (Birch) pollen seasons to recent changes in spring temperature across Europe. *International Journal of Biometeorology*, 46, 159-170.
- Emberlin, J., M. Smith, R. Close, and B. Adams-Groom, 2007: Changes in the pollen seasons of the early flowering trees *Alnus* spp. and *Corylus* spp. Worcester, United Kingdom, 1996-2005, *International Journal of Biometeorology*, 51, 181-191.
- Fischer, A., 1994: A model for the seasonal variations of vegetation indices in coarse resolution data and its inversion to extract crop parameters. *Remote Sensing of Environment*, 48, 220-230.
- Fitter, A.H., and R.S.R. Fitter, 2002: Rapid changes in flowering time in British plants. *Science*, 296, 1689-1691.

- Fitzjarrald, D.R., O.C. Acevedo, and K.E. Moore, 2001: Climatic consequences of leaf presence in the Eastern United States. *Journal of Climate*, 14, 598-614.
- Foster, J.L., 1989: The significance of the date of snow disappearance on the Arctic tundra as a possible, indicator of climatic change. *Arctic Alpine Research*, 21, 60-70.
- Foster, J.L., J.W. Winchester, and E.G. Dutton, 1992: The date of snow disappearance on the Arctic tundra as determined from satellite, meteorological station and radiometric in situ observations. *IEEE Transactions on Geoscience and Remote Sensing*, 30, 793-798.
- Frei, A., and D.A. Robinson, 1999: Northern Hemisphere snow extent: Regional variability 1972-1994. *International Journal of Climatology*, 19, 1535-1560.
- Friederichs, P., and A. Hense, 2003: Statistical inference in canonical correlation analyses exemplified by the influence of North Atlantic SST on European climate. *Journal of Climate*, 16, 522-534.
- Fu, Q., C.M. Johanson, J.M. Wallace, and T. Reichler, 2006: Enhanced mid-latitude tropospheric warming in satellite measurements. *Science*, 312, 1179.
- Gitelson, A.A., 2004: Wide dynamic range vegetation index for remote quantification of biophysical characteristics of vegetation. *Journal of Plant Physiology*, 161, 165-173.
- Glahn, H.R., 1968: Canonical correlation and its relationship to discriminant analysis and multiple regression. *Journal of the Atmospheric Sciences*, 25, 23-31.
- Gordon, H.R., J.W. Brown, and R.H. Evans, 1988: Exact Rayleigh scattering calculations for use with the Nimbus-7 Coastal Zone Color Scanner. *Applied Optics*, 27, 862-871.
- Green, M.C., R.G. Flocchini, and L.O. Myrup, 1993: Use of temporal principal components analysis to determine seasonal periods. *Journal of Applied Meteorology*, 32, 986-995.
- Groisman, P.Y., T.R. Karl, R.W. Knight, and G.L. Stenchikov, 1994: Changes of snow cover, temperature, and radiative heat balance over the Northern Hemisphere. *Journal of Climate*, 7, 1633-1656.
- Haque, M.A., and M. Lal, 1991: Diagnosis of satellite-derived outgoing long wave radiation in relation to rainfall in India. *Meteorology and Atmospheric Physics*, 45, 1-13.
- Hartley, S., and D.A. Robinson, 2000: A shift in winter season timing in the northern plains of the USA as indicated by temporal analysis of heating degree days. *International Journal of Climatology*, 20, 365-379.

- Hartshorne, R., 1938: Six standard seasons for the year. *Annals of the Association of American Geographers*, 28, 165-178.
- Hayhoe, K., C.P. Wake, T.G. Huntington, L. Luo, M.D. Schwartz, J. Sheffield, E. Wood, B. Anderson, J. Bradbury, A. DeGaetano, T.J. Troyand, and D. Wolfe, 2006: Past and future changes in climate and hydrological indicators in the US Northeast. *Climate Dynamics*, 28, 381-407.
- Hess, M., 1965: Pietra klimatyczne w Polskich Karpatach Zachodnich, *Zesz. Nauk. UJ. Prace Geograficzne*, 11, 267 (in Polish).
- Ho, C.H., E.J. Lee, I. Lee, and S.J. Jeong, 2006: Earlier spring in Seoul, Korea. *International Journal of Climatology*, 26, 2117-2127.
- Hodgkins, G.A., and R.W. Dudley, 2006: Changes in the timing of winter-spring streamflows in eastern North America, 1913-2002. *Geophysical Research Letters*, 33, L06402, doi:10.1029/2005GL025593,2006.
- Hodgkins, G.A., R.W. Dudley, and T.G. Huntington, 2003: Changes in the timing of high river flows in New England over the 20th Century. *Journal of Hydrology*, 278, 244–252.
- Hogda, K.A., S.R. Karlson, and I. Solheim, 2001: Climatic change impact on growing season in Fennoscandia studied by a time series of NOAA AVHRR NDVI data. *Geoscience and Remote Sensing Symposium, 2001. IGARSS '01. IEEE 2001 International*, 3, 1338-1340.
- Holben, B.N., 1986: Characteristics of maximum-value composite images from temporal AVHRR data. *International Journal of Remote Sensing*, 7, 1417-1434.
- Hopkins, A.D., 1919: Periodical events and natural laws as guides to agricultural research and practice. *Monthly weather review*, 47, 5-39
- Hwang, S.O., J.K.E. Schemm, A.G. Barnston, and W.T. Kwon, 2001: Long-lead seasonal forecast skill in far eastern Asia using canonical correlation analysis. *Journal of Climate*, 14, 3005-3016.
- Iijima, Y., K. Masuda , and T. Ohata , 2007: Snow disappearance in eastern Siberia and its relationship to atmospheric influences. *International Journal of Climatology*, 27, 169-177.
- Inoue, T., and J. Matsumoto, 2003: Seasonal and secular variations of sunshine duration and natural seasons in Japan. *International Journal of Climatology*, 23, 1219-1234

- Inouye, D.W., B. Barr, K.B. Armitage, and B.D. Inouye, 2000: Climate change is affecting altitudinal migrants and hibernating species, *Proceedings of the National Academy of Sciences*, 97, 1630-1633.
- IPCC, 2001: *Climate Change 2001: The Scientific Basis. Contribution of Working Group I to the Third Assessment Report of the Intergovernmental Panel on Climate Change* [Houghton, J.T., Y. Ding, D.J. Griggs, M. Noguer, P.J. van der Linden, X. Dai, K. Maskell, and C.A. Johnson (eds.)]. Cambridge University Press, Cambridge, United Kingdom and New York, NY, USA.
- IPCC, 2007: *Climate Change 2007: The Physical Science Basis. Contribution of Working Group I to the Fourth Assessment Report of the Intergovernmental Panel on Climate Change* [Solomon, S., D. Qin, M. Manning, Z. Chen, M. Marquis, K.B. Averyt, M. Tignor and H.L. Miller (eds.)]. Cambridge University Press, Cambridge, United Kingdom and New York, NY, USA.
- Ivanova, K., J.Y. Harrington, J. Verlinde, E.E. Clothiaux, and C.P. Bahrmann, 2004: Objective criterion to distinguish seasons in Arctic climate. *Proceedings of the 14<sup>th</sup> Atmospheric Radiation Measurement Science Team Meeting*, Albuquerque, NM.
- Jaggus, J., 2006: Climatic changes in Estonia during the second half of the 20<sup>th</sup> century in relationship with changes in large-scale atmospheric circulation. *Theoretical and Applied Climatology*, 83, 77-88.
- Jaagus J., and R. Ahas, 2000: Space-time variations of climatic seasons and their correlation with the phenological development of nature in Estonia. *Climate Research*, 15, 207-219.
- Jaagus, J., J. Truu, R. Ahas, and A. Aasa, 2003: Spatial and temporal variability of climatic seasons on the East European plain in relation to large-scale atmospheric circulation. *Climate Research*, 23, 111-129.
- Jastrzebowski, W., 1829: O rozprawie pt. O odmianach powietrza i fizycznych porach roku w naszym klimacie, *Pamiętnik Umiejetnosci*, 1, 69-82.
- Jefferson, M., 1938: Standard seasons. *Annals of the Association of American Geographers*, 28, 1-12.
- Jia, G.J., H.E. Epstein, and D.A. Walker, 2004: Controls over intra-seasonal dynamics of AVHRR NDVI for the Arctic tundra in northern Alaska. *International Journal of Remote Sensing*, 25, 1547-1564.
- Johansson, Å., A.G. Barnston, S. Saha, and H. van den Doo, 1998: On the level and origin of seasonal forecast skill in northern Europe. *Journal of the Atmospheric Sciences*, 55, 103-127.

- Johnson, P.L., and J.J. Kelley Jr., 1970: Dynamics of Carbon Dioxide and Productivity in an Arctic Biosphere. *Ecology*, 51, 73-80.
- Justice, C.O., J.R.G. Townshend, B.N. Holben, and C.J. Tucker, 1985: Analysis of the phenology of global vegetation using meteorological satellite data. *International Journal of Remote Sensing*, 8, 1271-318.
- Kalnay, E., M. Kanamitsu, R. Kistler, W. Collins, D. Deaven, L. Gandin, M. Iredell, S. Saha, G. White, J. Woollen, Y. Zhu, A. Leetmaa, B. Reynolds, M. Chelliah, W. Ebisuzaki, W. Higgins, J. Janowiak, K.C. Mo, C. Ropelewski, J. Wang, R. Jenne, and D. Joseph, 1996: The NCEP/NCAR 40-year reanalysis project. *Bulletin of the American Meteorological Society*, 77, 437-471.
- Kalnicky, R.A., 1987: Seasons, singularities, and climatic changes over the mid-latitudes of the northern hemisphere during 1899-1969. *Journal of Climate and Applied Meteorology*, 26, 1496-1510.
- Karlsen, S.R., A. Elvebakk, K.A. Høgda, and B. Johansen, 2006: Satellite-based mapping of the growing season and bioclimatic zones in Fennoscandia. *Global Ecology and Biogeography*, 15, 416-430.
- Kaufmann, R.K., L. Zhou, Y. Knyzikhin, N.V. Shabanov, R.B. Myneni, and C.J. Tucker, 2000: Effect of orbital drift and sensor changes on the time series of AVHRR vegetation index data. *IEEE Transactions on Geoscience and Remote Sensing*, 38, 2584-2597.
- Kawamura, T., 1973: The natural seasons of monsoon Asia, *Water Resources of monsoon Aisa* edited by Yoshino M.M. and K. Kinshoin, Tokyo, 227-244 (in Japanese).
- Keeling, C.D., J.F.S. Chin, and T.P. Whorf, 1996: Increased activity of northern vegetation inferred from atmospheric CO<sub>2</sub> measurements. *Nature*, 382, 146-149.
- Kira, T., 1949: *Forest zones of Japan*. Technological Association of Forestry Tokyo, Japan.
- Klinkowitz, J., 1998: *Vonnegut in fact: The public spokespersonship of personal fiction*, University of South Carolina Press.
- Kożuchowski, K., and J. Degirmendžić, 2005: Contemporary changes of climate in Poland: Trends and variation in thermal and solar conditions related to plant vegetation. *Polish Journal of Ecology*, 53, 283-297.
- Krishnamurti, T.N., S.O. Han, and V. Misra, 1995: Prediction of the dry and wet spell of the Australian monsoon. *International Journal of Climatology*, 15, 753-771.

- Kwaśniewska, E., and J. Pereyma, 2004: Thermal seasons in Hornsund. *Problems of Polar Climatology*, 14, 157-169 (in Polish).
- Lamb, H.H., 1950: Types and spells of weather around the year in the British Isles. *Quaternary Journal of Royal Meteorological Society*, 76, 393-438.
- Lamb, H.H., 1972: *Climate: Present, past, and future-fundamentals and climate now*, Methuen&Co LTD.
- Leathers, D.J., and B.J. Luff, 1997: Characteristics of snow cover duration across the northeast United States of America. *International Journal of Climatology*, 17, 1535-1547.
- Leathers, D.J., and D.A., Robinson, 1993: The association between extremes in North American snow cover extent and United States temperatures. *Journal of Climate*, 6, 1345-1355.
- Lee, B.S., 1979: A study of natural seasons in Korea. *Journal of the Korean Geographical Society*, 14, 1-11 (in Korean).
- Lee, R., F. Yu, K.P. Price, J. Ellis, and P. Shi, 2002: Evaluating vegetation phenological patterns in inner Mongolia using NDVI time-series analysis. *International Journal of Remote Sensing*, 23, 2505-2512.
- Levick, R.B.M., 1949: Fifty years of English weather, *Weather*, 4, 206-211.
- Lloyd, D., 1990: A phenological classification of terrestrial vegetation cover using shortwave vegetation index imagery. *International Journal of Remote Sensing*, 11, 2269-2279.
- Lu, J., G.A. Vecchi, and T. Reichler, 2007: Expansion of the Hadley Cell under the global warming. *Geophysical Research Letters*, 34, L06805, doi:10.1029/2006GL028443.
- Maejima, I., 1967: Natural seasons and weather singularities in Japan. *Geographical Reports of Tokyo Metropolitan University*, 2, 77-103.
- Makowiec, M., 1983: Wyznaczenie termicznych pór roku. *Prz. Geof.*, 28, 209-220 (In Polish).
- Markevičienė, I., 1996: Changes of seasonal limits and duration in Lithuania during the last 200 years. *The Geographical Yearbook*, 29, 146-159 (in Lithuanian).
- Markon, C.J., M.D. Fleming, and E.F. Binnian, 1995: Characteristics of vegetation phenology over the Alaskan landscape using AVHRR time-series data. *Polar Record*, 31, 179-190.

- McCabe, G.J., and M.P. Clark, 2005: Trends and variability in snowmelt runoff in the western United States. *Journal of Hydrometeorology*, 6, 476-482.
- McPeters, R.D., A.J. Krueger, P.K. Bhartia, J.R. Herman, A. Oaks, Z. Ahmad, R.P. Cebula, B.M. Schlesinger, T. Swissler, S.L. Taylor, O. Torres, and C.G. Wellemeyer, 1993: *Nimbus-7 Total Ozone Mapping Spectrometer (TOMS) Data Products User's Guide*, NASA Reference Publication 1323.
- Menzel, A., 2000: Trends in phenological phases in Europe between 1951 and 1996. *International Journal of Biometeorology*, 44, 76-81.
- Menzel, A., N. Estrella, and P. Fabian, 2001: Spatial and temporal variability of the phenological seasons in Germany from 1951 to 1996. *Global Change Biology*, 7, 657-666
- Menzel, A., and P. Fabian, 1999: Growing season extended in Europe. *Nature*, 397, 659.
- Menzel, A., and P. Fabian, 2001: Climate change and the phenology of European trees and shrubs. *Impacts of Climate Change on Wildfire*, Green R, Harley M, Spalding M, Zöckler eds., RSPB:Cambridge.
- Menzel, A., G. Jakobi, R. Ahas, H. Scheifinger, and N. Estrella, 2003: Variations of the climatological growing season (1951-2000) in Germany compared with other countries. *International Journal of Climatology*, 23, 793-812.
- Menzel, A., and V. Dose, 2005: Analysis of long-term time-series of beginning of flowering by Bayesian function estimation. *Meteorologische Zeitschrift*, 14, 429-434.
- Menzel, A., 2005: A 500 year pheno-climatological view on the 2003 heatwave in Europe assessed by grape harvest dates. *Meteorologische Zeitschrift*, 14, 75-77.
- Merecki, R., 1914: *Klimatologia Ziemi polskiej*. Warszawa, J.Coty.
- Mo, K.C., 2003: Ensemble canonical correlation prediction of surface temperature over the United States. *Journal of Climate*, 16, 1665-1683.
- Mooley, D.A., 1971: Independence of monthly and bimonthly rainfall over southeast Asia during the summer monsoon season. *Monthly Weather Review*, 99, 532-536.
- Moon, S.E., and H.H. Um, 1980: The divisions of the natural seasons of Korea. *Journal of the Korean Meteorological Society*, 16, 45-54.
- Myneni, R.B., C.D. Keeling, C.J. Tucker, G. Asrar, and R.R. Nemani, 1997: Increased plant growth in the northern high latitudes from 1981-1991. *Nature*, 386, 698-702.

- NASA, 2006, December 16: GES DISC DAAC data guide: NOAA/NASA Pathfinder AVHRR land data sets, retrieved September 2007 from [http://disc.sci.gsfc.nasa.gov/guides/GSFC/guide/avhrr\\_dataset.gd.shtml](http://disc.sci.gsfc.nasa.gov/guides/GSFC/guide/avhrr_dataset.gd.shtml).
- Neil, K., and W. Jianguo, 2006: Effects urbanization on plant flowering phenology: A review. *Urban Ecosystem*, 9, 243-257.
- NGDC, 1993: *ETOPO5 5-minute gridded elevations/bathymetry for the world*, Data announcement 93-MGG-01, National Geophysical Data Center, Boulder.
- Nicholls, N., 1987: The use of canonical correlation to study teleconnections, *Monthly Weather Review*, 115, 393-399.
- NOAA, 2002, November 5: NCEP/NCAR reanalysis project (CDAS), retrieved September 2007 from <http://www.cpc.ncep.noaa.gov/products/wesley/reanalysis.html#problem>.
- NOAA, 2006, August 16: AO, AAO, NAO, PNA, retrieved September 2007 from [http://www.cpc.noaa.gov/products/precip/CWlink/daily\\_ao\\_index/teleconnections.shtml](http://www.cpc.noaa.gov/products/precip/CWlink/daily_ao_index/teleconnections.shtml)
- NOAA, 2007a: Create a monthly/seasonal mean time series from the dataset, retrieved September 2007 from <http://www.cdc.noaa.gov/cgi-bin/Timeseries/timeseries1.pl>.
- NOAA, 2007b: North America climate extremes monitoring, retrieved September 2007 from <http://www.ncdc.noaa.gov/nacem/nacem.html>.
- Ntale, H.K., T.Y. Gan, and D. Mwale, 2003: Prediction of east African seasonal rainfall using simplex canonical correlation analysis. *Journal of Climate*, 16, 2105-2112.
- Oh, J.H., T. Kim, S.H. Lee, S.K. Min, and W.T. Kwon, 2004: Regional climate simulation for Korea using dynamic downscaling and statistical adjustment. *Journal of the Meteorological Society of Japan*, 82, 1629-1643.
- Palecki, M.A., 1994: The onset of spring in the eastern United States during the 20<sup>th</sup> century, *Proceedings of the American Meteorological Society meeting*, 23-28.
- Paluš, M., D. Novotná, and P. Tichavský, 2005: Shift of seasons at the European mid-latitudes: Natural fluctuations correlated with the North Atlantic Oscillation. *Geophysical Research Letters*, 32, L12805, doi:10.1029/2005GL022838, 2005.
- Parmesan, C., 2006: Ecological and evolutionary responses to recent climate change. *Annual Review of Ecology, Evolution, and Systematics*, 37, 637-669.
- Parmesan, C., and G. Yohe, 2003: A globally coherent fingerprint of climate change impacts across natural systems. *Nature*, 421, 37-42.

- Pempaitė, I., 1997: Dates of permanent passages of average day temperature (PPAT) above and below 0°C and 15°C and duration of climatic-thermal seasons in the Lithuanian territory in 1961-1990. *The Geographical Yearbook*, 30, 154-160 (in Lithuanian).
- Pennisi, E., 2007: Endangered species: US. weighs protection for polar bears. *Science*, 315, 25.
- Peñuelas, J., and I. Filella, 2001: Responses to a warming world. *Science*, 294,793–794.
- Pettorelli, N., J.O. Vik, A. Mysterud, J.-M. Gaillard, C.J. Tucker, and N.C. Stenseth, 2005: Using the satellite-derived NDVI to assess ecological responses to environmental change. *Trends in Ecology and Evolution*, 20, 503-510.
- Pielke, R.A., M. Garstang, C. Lindsey, and J. Gusdorf, 1987: Use of a synoptic classification scheme to define seasons. *Theoretical and Applied Climatology*, 38, 57-68.
- Piotrowicz, K., 1996: Thermal characterization of winters in the 20<sup>th</sup> century in Kraków. *Geographia Polonica*, 67, 77-88.
- Piotrowicz, K., 2000: The ways of defining seasons. *Przeglad Zagadinen Naukowych*, 45, 261-278 (in Polish).
- Piotrowicz, K., 2002-2003: Thermal conditions of winters in Cracow in the period 1792-2002. *Folia Geographica*, 33-34, 67-87 (in Polish).
- Ramsay, B.H., 1998: The interactive multisensor snow and ice mapping system. *Hydrological Processes*, 12, 1537-1546.
- Randerson, J.T., M.V. Thompson, T.J. Conway, I.Y. Fung, and C.B. Field, 1997: The contribution of terrestrial sources and sinks to trends in the seasonal cycle of atmospheric carbon dioxide. *Global Biogeochemical Cycles*, 11, 535-560.
- Rapp, J., and C.-D. Schönwiese, 1994: Thermal seasons as an illustrative description of climatic trends. *Meteorol Zeitschrift*, 3, 91–94 (in German).
- Reed, B.C., J. F. Brown, D. VanderZee, T.R. Loveland, J.W. Merchant, and D.O. Ohlen, 1994: Measuring phenological variability from satellite imagery. *Journal of Vegetation Science*, 5, 703-714.
- Regonda, S.K., B. Rajagopalan, M. Clark, and J. Pitlick, 2005: Seasonal cycle shifts in hydroclimatology over the western United States. *Journal of Climate*, 18, 372-384.
- Reichler, T., and J. Kim, 2007: How well do coupled models simulate today's climate? *Bulletin of the American Meteorological Society* (in press).

- Robertson, C., 1922: Flower seasons, *the Scientific Monthly*, 14, 201-203.
- Robinson, D.A., 1993: Hemispheric snow cover from satellites. *Annals of Glaciology*, 17, 367-371.
- Robinson, D.A., K.F. Dewey, and R.R. Heim, 1993: Global snow cover monitoring: an update. *Bulletin of the American Meteorological Society*, 74, 1689-1696.
- Robinson, D.A., and T. Estilow, 2006: An improved hemispheric snow cover extent climate data record. *Proceedings of the Eastern Snow Conference 63rd Annual Meeting*, Newark, DE, 33.
- Robinson, D.A., A. Frei, and M.C. Serreze, 1995: Recent variations and regional relationships in Northern Hemisphere snow cover. *Annals of Glaciology*, 21, 71-76.
- Robinson D.A., and A. Frei, 2000: Seasonal variability of Northern Hemisphere snow extent using visible satellite data. *The Professional Geographer*, 52, 307-315.
- Romer, E., 1904: Klimat ziem polskich. [W:] *Polska, obrazy i opisy*, 1, 6-12. (in Polish).
- Romer, E., 1949: Okresy gospodarca w Polsce. *Prace Wroclawskiego Towarzystwa Naukowego*, Seria B, nr 20 (in Polish).
- Root, T.L., J.T. Price, K.R. Hall, S.H. Schneider, C. Rosenzweig, and J.A., Pounds, 2003: Fingerprints of global warming on wild animals and plants. *Nature*, 421, 57-60.
- Roy, D.B., and J. Asher, 2003: Spatial trends in the sighting dates of British butterflies. *International Journal of Biometeorology*, 47, 188-192.
- Roy, D.B., and T.H. Sparks, 2000: Phenology of British butterflies and climate change. *Global Change Biology*, 6, 407-416.
- Schwartz, M.D., 1998: Green-wave phenology, *Nature*, 394, 839-840.
- Schwartz, M.D., R. Ahas, and A. Aasa, 2006: Onset of spring starting earlier across the Northern Hemisphere. *Global Change Biology*, 12, 343-351.
- Schwartz, M.D., and X. Chen, 2002: Examining the onset of spring in China. *Climate Research*, 21, 157-164.
- Schwartz, M.D., B.C. Reed, and M.A. White, 2002: Assessing satellite-derived start-of-season measures in the conterminous USA. *International Journal of Climatology*, 22, 1793-1805.

- Schwartz, M.D., and B.E. Reiter, 2000: Changes in North American spring. *International Journal of Climatology*, 19, 929-932.
- Scheifinger, H., A. Menzel, E. Koch, and C. Peter, 2003: Trends of spring time frost events and phenological dates in central Europe. *Theoretical and Applied Climatology*, 74, 41-51.
- Scheifinger, H., A. Menzel, E. Koch, C. Peter, and R. Ahas, 2002: Atmospheric mechanisms governing the spatial and temporal variability of phenological phases in central Europe. *International Journal of Climatology*, 22, 1739-1755.
- Schröder, W., G. Schmidt, and J. Hasenclever, 2006: Geostatistical analysis of data on air temperature and plant phenology from Baden-Württemberg (Germany) as a basis for regional scaled models of climate change. *Environmental Monitoring and Assessment*, 120, 27-43.
- Shabanov, N.V., L. Zhou, Y. Knyazikhin, R.B. Myneni, and C.J. Tucker, 2002: Analysis of interannual changes in northern vegetation activity observed in AVHRR data from 1981 to 1994. *IEEE Transactions on Geoscience and Remote Sensing*, 40, 115-130.
- Shabbar, A., and A.G. Barnston, 1996: Skill of seasonal climate forecasts in Canada using canonical correlation analysis. *Monthly Weather Review*, 124, 2370-2385.
- Shinoda, M., H. Utsugi, and W. Morishima, 2001: Spring snow-disappearance timing and its possible influence on temperature fields over central Eurasia. *Journal of the Meteorological Society of Japan*, 79, 37-59.
- Soanes, C., and A. Stevenson, 2005: *Oxford Dictionary of English*. Oxford University Press.
- Sparks, T.H., and P.D. Carey, 1995: an analysis of the Marsham phenological records, 1736-1947. *Journal of Ecology*, 83, 321-329.
- Sparks, T.H., E.P. Jeffree, and C.E. Jeffree, 2000: An examination of the relationship between flowering times and temperature at the national scale using long-term phenological records from the UK. *International Journal of Biometeorology*, 44, 82-87.
- Sparks, T.H., and A. Menzel, 2002: Observed changes in seasons: An overview. *International Journal of Climatology*, 22, 1715-1725.
- Stankūnavičius, G., and E. Rimkus, 1998: The first and the last snowfall in Lithuania in cold seasons. *The Geographical Yearbook*, 31, 34-45.
- Stewart, I.T., D.R. Cayan, and M.D. Dettinger, 2005: Changes toward earlier streamflow timing across western North America. *Journal of Climate*, 18, 1136-1155.

- Stirling, I., N.J. Lunn, and J. Iacozza, 1999: Long-term trends in the population ecology of polar bears in western Hudson Bay in relation to climate change. *Arctic*, 52, 294-306.
- Stone, R.S., E.G. Dutton, J.M. Harris, and D. Longenecker, 2002: Earlier spring snow melt in northern Alaska as an indicator of climate change. *Journal of Geophysical Research*, 107, D10, 4089, 10.1029/2000jd000286,2002.
- Takahashi, K., 1942: Dynamic climatology of Japan. *Journal of Meteorological Society of Japan*, 20, 171-181 (in Japanese).
- Tao, F., M.Yokozawa, Y. Xu, Y. Hayashi, and Z. Zhang, 2006: Climate changes and trends in phenology and yields of field crops in China, 1981–2000. *Agricultural and Forest Meteorology*, 138, 82-92.
- Terjung, W.H., 1968: World patterns of the distribution of the monthly comfort index. *International Journal of Biometeorology*, 12, 119-151.
- Thompson, D.W.J., and J.M. Wallace, 1998: The Arctic Oscillation signature in the wintertime geopotential height and temperature fields. *Geophysical Research Letters*, 25, 1297-1300.
- Thompson, D.W.J., and J.M. Wallace, 2000: Annular modes in the extratropical circulation. Part I: Month-to-Month Variability, *Journal of Climate*, 13, 1000-1016
- Thórhallsdóttir, T.E., 1998: Flowering phenology in the central highland of Iceland and implications for climatic warming in the Arctic. *Oecologia*, 114, 43-49.
- Thorp, K.R. and L.F. Tian, 2004: A review on remote sensing of weeds in agriculture. *Precision Agriculture*, 5, 477–508.
- Trenberth, K.E., 1983: What are the seasons? *Bulletin of the American Meteorological Society*, 64:1276-1282.
- Tromp, S.W., 1980: *Biometeorology: the impact of the weather and climate on humans and their environment*, Heyden press.
- Troup, A.J., 1965: The Southern Oscillation. *The Quarterly Journal of the Royal Meteorological Society*, 91, 490–506.
- Tucker, C.J., D.A. Slayback, J.E. Pinzon, S.O. Los, R.B. Myneni, and M.G. Taylor, 2001: Higher northern latitude normalized difference vegetation index and growing season trends from 1982-1999. *International Journal of Biometeorology*, 45, 184-190.
- Tuller, S.E., 1975: What are standard seasons in Canada? *Canadian Geographical Journal*, 90, 36-43.

- Tuller, S.E., 1977: Summer and winter patterns of human climate in New Zealand. *New Zealand Geographer*, 33, 4-14
- Tuller, S.E., 1990: Standard seasons. *International Journal of Biometeorology*, 34, 181-188.
- Tveito, O.E., E.J. Førland, R. Heino, I. Hanssen-Bauer, H. Alexandersson, B. Dahlström, A. Drebs, C. Kern-Hansen, T. Jónsson, E. Vaarby-Laursen, and Y. Westman, 2000: *Nordic temperature maps*, DNMI Report 09/2000 KLIMA, Oslo, Norway.
- Tyson, P.D., 1981: Atmospheric circulation variations and the occurrence of extended wet and dry spells over southern Africa. *International Journal of Climatology*, 1, 115 - 130.
- Ueda, H., M. Shinoda, and H. Kamahori, 2003: Spring northward retreat of Eurasian snow cover relevant to seasonal and interannual variations of atmospheric circulation. *International Journal of Climatology*, 23, 615-629.
- van Vliet, A.J.H., and M.D. Schwartz, 2002: Editorial: phenology and climate - the timing of life cycle events as indicators of climatic variability and change. *International Journal of Climatology*, 22, 1713-1714.
- Vincent, L.A., T.C. Peterson, V.R. Barros, M.B. Marino, M. Rusticucci, G. Carrasco, E. Ramirez, L.M. Alves, T. Ambrizzi, M.A. Berlato, A.M. Grimm, J.A. Marengo, L. Molion, D.F. Moncunill, E. Rebello, Y.M.T. Anunciação, J. Quintana, J.L. Santos, J. Baez, G. Coronel, J. Garcia, I. Trebejo, M. Bidegain, M.R. Haylock, and D. Karoly, 2005: Observed trends in indices of daily temperature extremes in South America 1960-2000. *Journal of Climate*, 18, 5011-5023.
- Visher, S.S., 1943: The seasons' arrivals and lengths. *Annals of the Association of American Geographers*, 33, 129-134.
- Visher, S.S., 1944: When American seasons begin, *the Scientific Monthly*, 59, 363-369.
- Visher, S.S., 1947: Precipitation seasons in the United States. *Geographical Review*, 37, 106-111.
- Visher, S.S., 1949: American dry seasons: Their intensity and frequency. *Ecology*, 30, 365-370.
- Visher, S.S., 1950a: Wet seasons in the United States: How wet and how frequent. *Ecology*, 31, 292-303.
- Visher, S.S., 1950b: High temperatures and the seasonal distribution of precipitation and some ecological consequences or correlations. *American Midland Naturalist*, 44, 478-487.

- von Storch, H., and F.W. Zwiers, 2002: *Statistical analysis in climate research*, Cambridge University Press, Cambridge.
- Wallace, J.M., and D.S. Gutzler, 1981: Teleconnections in the geopotential height field during the Northern Hemisphere winter. *Monthly Weather Review*, 109, 784–812.
- Walsh, J.E., and W.L. Chapman, 1998: Arctic-cloud-radiation-temperature associations in observational data and atmospheric reanalyses. *Journal of Climate*, 11, 3030-3045.
- Walther, G.-R., E. Post, P. Convey, A. Menzel, C. Parmesan, T.J.C. Beebee, J.-M. Fromentin, O. Hoegh-Guldberg, and F. Bairlein, 2002: Ecological responses to recent climate change. *Nature*, 416, 389-395.
- Westerling, A.L., H.G. Hidalgo, D.R. Cayan, and T.W. Swetnam, 2006: Warming and earlier spring increase western U.S. forest wildfire activity. *Science*, 313, 940-943.
- Weston, S.T., 2006: *Interannual trends in the radiation climatology of the Canadian high Arctic*, Master's thesis, Simon Fraser University.
- White, M.A., R.R. Nemani, P.E. Thornton, and S.W. Running, 2002: Satellite evidence of phenological differences between urban areas and rural areas of the eastern United States deciduous broadleaf forest. *Ecosystems*, 5, 260-273.
- White, W.P., 1925: when does winter come? *Science*, 62, 286.
- Wiig, Ø., 2005: Are polar bears threatened? *Science*, 309, 1814-1815.
- Wiszniewski, W., 1959: Some remarks concerning meteorological seasons of the year in Poland from the point of view of the normal temperatures. *Acta Geophysica Polonica*, 7, 467-475.
- Wiszniewski, W., 1960: Kilka uwag o meteorologicznych porach roku w Polsce w swietle srednich wieloletnich wartosci temperatur. *Prz. Geof.*, 5, 31-39 (in Polish).
- Woś, A., 1981: The seasonal structure of the climate of selected areas. *Quaestiones Geographicae*, 7, 135-146.
- Xu, S., and Gao Y., 1962, Natural seasons of China, In *Some problems on the monsoon in East Asia* ed. by Y. Gao, Peking, 88-103.
- Ye, D., Y. Jiang, and W. Dong, 2003: The northward shift of climatic belts in China during the last 50 years and the corresponding seasonal response. *Advances in Atmospheric Sciences*, 20, 959-967.

- Yoshino, M.M., and K. Kai, 1977: The divisions and characteristics of the natural seasons of Japan, *Geographical Review of Japan*, 50, 635-651 (in Japanese).
- Yu, F., K.P. Price, J. Ellis, and D. Kastens, 2004: Satellite observations of the seasonal vegetation growth in central Asia: 1982–90. *Photogrammetric Engineering and Remote Sensing*, 70, 461–469.
- Yu, F., K.P. Price, J. Ellis, and P. Shi, 2003: Response of seasonal vegetation development to climatic variations in eastern central Asia. *Remote Sensing of Environment*, 87, 42-54.
- Zhang, X., K.D. Harvey, W.D. Hogg, and T.R. Yuzyk, 2001: Trends in Canadian streamflow. *Water Resources Research*, 37, 987-999.
- Zhao, T., M.D. and Schwartz, 2003: Examining the onset of spring in Wisconsin. *Climate Research*, 24, 59-70.
- Zheng, J., Q. Ge, Z. Hao, and W.C. Wang, 2006: Spring phenophases in recent decades over eastern China and its possible link to climate changes. *Climatic change*, 77, 449-462.

## CURRICULUM VITAE

### GWANGYONG CHOI

#### Education

- 1999            B.A. Geography Education, Department of Geography Education, Seoul National University, Seoul, Republic of Korea.
- 2002            M.A. Geography (Climatology), Department of Geography Education, Seoul National University, Seoul, Republic of Korea (Thesis: The Geography of Bioclimatic Heat Stress in South Korea: 1973-1998).
- 2007            Ph.D. Geography (Climatology), Department of Geography, Rutgers The State University of New Jersey, New Brunswick, NJ, United States (Dissertation: Climatology and Variability of Northern Hemisphere Seasons).

#### Principal occupations

- 2000-2001      Departmental Administrator, Geography Education, Department of Geography Education, Seoul National University, Seoul, Republic of Korea.
- 2002, 2004      Researcher, Climate Research Lab., Meteorological Research Institute, Korea Meteorological Administration, Republic of Korea.
- 2003-2007      Teaching Assistant, Department of Geography, Rutgers The State University of New Jersey, New Brunswick, NJ, United States.
- 2003-2007      Instructor, Department of Geography & Department of Geology, Rutgers The State University of New Jersey, New Brunswick & Newark, NJ, United States.

#### Publications

- 2000            Choi, G., J.-N. Choi, and J.W. Kim, 2000: The temporal variations of summer temperature in central area of Korea during the 20<sup>th</sup> century. *Journal of Korean Geographical Society*, 35(4), 519-528.
- 2001            Choi, G., and W.-T. Kwon, 2001: Shift of natural seasons' cycle and

- change of life temperature indices in South Korea during the 20<sup>th</sup> Century. *Journal of Geography Education*, 45, 14-25.
- 2002 Choi, G., and C.S. Kang, 2002: Spatial distribution of winter daytime and nighttime apparent temperature in South Korea. *Journal of the Korean Geographical Society*, 37(3), 237-246.
- 2002 Choi, G., J. Choi, J.W. Kim, and S.W. Son, 2002: The climatology of perceived sultriness in South Korea. *Journal of the Korean Geographical Society*, 37(4), 385-402.
- 2005 Choi, G., J. Choi, and H.-J. Kwon, 2005: Impacts of high apparent temperature on the increase of summertime disease-related mortality in Seoul, 1991-2000. *Journal of Preventive Medicine and Public Health*, 38(3), 283-290.
- 2005 Choi, G., and W.-T. Kwon, 2005: Temporal and spatial patterns of tropical night phenomenon in South Korea. *Journal of the Korean Geographical Society*, 40(6), 730-747.
- 2006 Choi, G., J. Kim, and M.-S. Won, 2006: Spatial patterns and temporal variability of the Haines Index related to the wildland fire growth potential over the Korean Peninsula. *Journal of the Korean Geographical Society*, 41(2), 168-187.
- 2006 Choi, G., W.-T. Kwon, and D.A. Robinson, 2006: Seasonal onset and duration in South Korea. *Journal of the Korean Geographical Society*, 41(4), 435-456.
- 2006 Choi, G. 2006: A definition of Korean heat waves and their spatio-temporal patterns. *Journal of the Korean Geographical Society*, 41(5), 527-544.